ISSN 1007-9327 (print)
ISSN 2219-2840 (online)

World Journal of *Gastroenterology*

World J Gastroenterol 2024 January 14; 30(2): 115-198

Published by Baishideng Publishing Group Inc

World Journal of Gastroenterology

Contents

Weekly Volume 30 Number 2 January 14, 2024

World Journal of Gastroenterology

Weekly Volume 30 Number 2 January 14, 2024

Contents

NAME OF JOURNAL
World Journal of Gastroenterology

ISSN
ISSN 1007-9327 (print) ISSN 2219-2840 (online)

LAUNCH DATE
October 1, 1995

FREQUENCY
Weekly

EDITORS-IN-CHIEF
Andrzej S Tarnawski

EXECUTIVE ASSOCIATE EDITORS-IN-CHIEF
Xian-Jun Yu (Pancreatic Oncology), Jian-Gao Fan (Chronic Liver Disease), Hou-Bao Liu (Biliary Tract Disease)

EDITORIAL BOARD MEMBERS
http://www.wjgnet.com/1007-9327/editorialboard.htm

PUBLICATION DATE
January 14, 2024

COPYRIGHT
© 2024 Baishideng Publishing Group Inc

PUBLISHING PARTNER
Shanghai Pancreatic Cancer Institute and Pancreatic Cancer Institute, Fudan University
Biliary Tract Disease Institute, Fudan University

INSTRUCTIONS TO AUTHORS
https://www.wjgnet.com/bpg/gerinfo/204

GUIDELINES FOR ETHICS DOCUMENTS
https://www.wjgnet.com/bpg/GerInfo/287

GUIDELINES FOR NON-NATIVE SPEAKERS OF ENGLISH
https://www.wjgnet.com/bpg/gerinfo/240

PUBLICATION ETHICS
https://www.wjgnet.com/bpg/GerInfo/288

PUBLICATION MISCONDUCT
https://www.wjgnet.com/bpg/gerinfo/208

POLICY OF CO-AUTHORS
https://www.wjgnet.com/bpg/GerInfo/310

ARTICLE PROCESSING CHARGE
https://www.wjgnet.com/bpg/gerinfo/242

STEPS FOR SUBMITTING MANUSCRIPTS
https://www.wjgnet.com/bpg/GerInfo/239

ONLINE SUBMISSION
https://www.f6publishing.com

PUBLISHING PARTNER's OFFICIAL WEBSITE
https://www.shca.org.cn
https://www.zs-hospital.sh.cn

World Journal of Gastroenterology

Submit a Manuscript: https://www.f6publishing.com

World J Gastroenterol 2024 January 14; 30(2): 115-127

DOI: 10.3748/wjg.v30.i2.115

ISSN 1007-9327 (print) ISSN 2219-2840 (online)

REVIEW

Small nucleolar RNA and its potential role in the oncogenesis and development of colorectal cancer

Yang-Zheng Lan, Zheng Wu, Wen-Jia Chen, Ze-Xuan Fang, Xin-Ning Yu, Hua-Tao Wu, Jing Liu

Specialty type: Gastroenterology and hepatology

Provenance and peer review: Invited article; Externally peer reviewed.

Peer-review model: Single blind

Peer-review report's scientific quality classification

Grade A (Excellent): 0
Grade B (Very good): B
Grade C (Good): 0
Grade D (Fair): 0
Grade E (Poor): 0

P-Reviewer: Teramoto-Matsubara OT, Mexico

Received: November 20, 2023
Peer-review started: November 20, 2023
First decision: December 11, 2023
Revised: December 21, 2023
Accepted: December 28, 2023
Article in press: December 28, 2023
Published online: January 14, 2024

Yang-Zheng Lan, Zheng Wu, Wen-Jia Chen, Ze-Xuan Fang, Jing Liu, The Breast Center, Cancer Hospital of Shantou University Medical College, Shantou 515041, Guangdong Province, China

Xin-Ning Yu, Hua-Tao Wu, Department of General Surgery, The First Affiliated Hospital of Shantou University Medical College, Shantou 515041, Guangdong Province, China

Corresponding author: Jing Liu, MD, PhD, Academic Research, Associate Professor, Research Scientist, Senior Scientist, The Breast Center, Cancer Hospital of Shantou University Medical College, No. 22 Xinling Road, Shantou 515041, Guangdong Province, China.
jliu12@stu.edu.cn

Abstract

Small nucleolar RNAs (snoRNAs) represent a class of non-coding RNAs that play pivotal roles in post-transcriptional RNA processing and modification, thereby contributing significantly to the maintenance of cellular functions related to protein synthesis. SnoRNAs have been discovered to possess the ability to influence cell fate and alter disease progression, holding immense potential in controlling human diseases. It is suggested that the dysregulation of snoRNAs in cancer exhibits differential expression across various cancer types, stages, metastasis, treatment response and/or prognosis in patients. On the other hand, colorectal cancer (CRC), a prevalent malignancy of the digestive system, is characterized by high incidence and mortality rates, ranking as the third most common cancer type. Recent research indicates that snoRNA dysregulation is associated with CRC, as snoRNA expression significantly differs between normal and cancerous conditions. Consequently, assessing snoRNA expression level and function holds promise for the prognosis and diagnosis of CRC. Nevertheless, current comprehension of the potential roles of snoRNAs in CRC remains limited. This review offers a comprehensive survey of the aberrant regulation of snoRNAs in CRC, providing valuable insights into the discovery of novel biomarkers, therapeutic targets, and potential tools for the diagnosis and treatment of CRC and furnishing critical cues for advancing research into CRC and the judicious selection of therapeutic targets.

Key Words: Small nucleolar RNAs; Colorectal cancer; Dysregulation; Biomarker

Core Tip: Small nucleolar RNAs (snoRNAs) play vital roles in post-transcriptional RNA processing, influencing the cell fate and diverse disease progression. Dysregulated snoRNAs in various cancers, including colorectal cancer (CRC), show promise for improving prognosis and diagnosis. Despite this potential, understanding of snoRNAs' roles in CRC remains limited, warranting further research into their precise functions.

Citation: Lan YZ, Wu Z, Chen WJ, Fang ZX, Yu XN, Wu HT, Liu J. Small nucleolar RNA and its potential role in the oncogenesis and development of colorectal cancer. *World J Gastroenterol* 2024; 30(2): 115-127
URL: https://www.wjgnet.com/1007-9327/full/v30/i2/115.htm
DOI: https://dx.doi.org/10.3748/wjg.v30.i2.115

INTRODUCTION

For many years, small nucleolar RNAs (snoRNAs) have been considered one of the prime examples of non-coding RNAs (ncRNAs). They are small RNA molecules, typically consisting of 60 to 300 nucleotides, primarily located within the nucleolus of the cell[1,2]. The discovery of snoRNAs traces back to the late 1960s when researchers identified a group of distinct low-molecular-weight RNAs in the nucleoplasm and nucleolus of HeLa cells, in length ranging from 100 to 180 base pairs[3]. However, due to technological limitations of the time, the exact nature and precise locations of these small RNAs remained largely unknown. It wasn't until 1976 that scientists first identified a unique RNA in the cell nucleus, later named snoRNA U3[4], sparking further investigations into snoRNAs.

With the continuous development and application of transcription inhibitors and dynamic labeling techniques, snoRNAs were gradually confirmed to be stable products transcribed by RNA Polymerase II. In the study of mammals, frogs, and other organisms, researchers progressively unveiled the structural features of snoRNA expression, particularly variations like U3, revealing their close association with ribosomal RNA (rRNA)[1,5,6]. Then novel strategies and technologies for analyzing snoRNAs emerged from studies of mRNA splicing[7]. Since then, extensive research has illuminated snoRNA's primary role in modifying rRNA, which is its pivotal function to guarantee the proper assembly and functioning of ribosomes, the cellular machinery responsible for protein synthesis. Moreover, snoRNAs play a fundamental role in upholding cellular functions related to protein synthesis by actively engaging in the post-transcriptional processing and modification of various RNA molecules[8,9].

However, investigations into the potential roles of snoRNAs in cancer began with a study reporting significant downregulation of snoRNA in meningiomas when compared to normal brain tissue[10]. Recent research has also shown differential expression of snoRNAs in various cancers, such as breast cancer and non-small cell lung cancer (NSCLC), in clinical samples and cell lines, indicating their potential diagnostic and prognostic value[11,12]. These findings underscore the differential expression of snoRNAs in healthy and tumor tissues as well as body fluids, suggesting that snoRNAs might have a broader role as major gene regulatory factors at both the transcriptional and epigenetic levels[13]. Aberrant snoRNA expression has been identified as a hallmark of tumorigenesis, suggesting that these RNAs play a more complex and diverse role in cellular gene regulation[14,15]. Furthermore, changes in snoRNA function and expression levels have been linked to various diseases, particularly cancers[16], highlighting the active and expanding research field exploring the roles of snoRNAs in disease onset and progression.

Colorectal cancer (CRC) is a global health concern, has emerged as the leading cause of digestive system cancer-related deaths, ranking third in new cancer cases and cancer-related deaths, posing a significant threat to human health and quality of life[17,18]. Patients with early-stage CRC often lack noticeable symptoms, with unspecific manifestations such as constipation, diarrhea, rectal bleeding, abdominal pain, fatigue, and weight loss emerging as the disease progresses [19]. Unfortunately, these symptoms typically become apparent only in advanced stages, contributing to a dismal 5-year survival rate of approximately 14% for late-stage CRC patients. Shockingly, around 25% of CRC patients present with metastasis at the time of diagnosis[20]. Furthermore, roughly 50% of treated patients eventually experience metastasis during their lifetime[21,22]. The high mortality rate among CRC patients can be attributed primarily to its significant heterogeneity and proclivity for metastasis. The inherent characteristic poses a significant challenge to early diagnosis and treatment, because patients with CRC can be effectively cured if detected and treated in its early stages. Hence, early detection significantly reduces the mortality associated with CRC[23].

Until now, numerous established diagnostic approaches have contributed to the early management of CRC, thus enhancing patient prognosis. These methodologies encompass screening procedures such as fecal occult blood tests, fecal immunochemical tests, and fecal DNA testing[24]. Additionally, colonoscopies permit the direct sampling of irregular tissues or polyps[25]. Furthermore, blood-based biomarkers, such as carcinoembryonic antigen (CEA) and circulating tumor DNA, have emerged as non-invasive CRC screening techniques, with limitations regarding sensitivity and specificity[26,27]. Additionally, fecal DNA testing lacks comprehensive validation. Furthermore, concerns of a practical nature arise, including the risks associated with invasive colonoscopies, substantial financial outlays, and the need for skilled endoscopists, as well as patient compliance[28]. Hence, the development of innovative and efficient CRC diagnostic biomarkers holds paramount importance in facilitating early detection and mitigating CRC-related mortality. Researchers have identified leukocyte immunoglobulin-like receptor B2 (LILRB2) protein as a distinctive marker of CRC regarding diagnosis and therapeutics, facilitating early screening and precision treatment[29]. It is also shown that the combined assessment of the methylation status of SEPT9, SDC2, and ALX4 in plasma has the potential to enhance the

sensitivity of CRC detection[30]. Recent research has shed light on the significant association between snoRNA and CRC, delving into the potential role of snoRNAs in the onset and progression of CRC[31]. Aberrant expression or function of snoRNAs may be associated with the development and progression of CRC, which provides new clues for further research into the pathogenesis and treatment of CRC[2,32]. This article purposed to review the role and mechanisms of snoRNAs in the progression of CRC and explore their clinical applications in the diagnosis and prognosis of CRC.

DESCRIPTON OF SNORNA

Basic structure and biological function of snoRNA

SnoRNAs are a class of small ncRNAs with lengths ranging from 60 to 300 nucleotides, primarily named due to their localization within the nucleolus and typically playing a crucial role in the modification, maturation, and stability of rRNA by forming complexes with small nucleolar ribonucleoproteins (snoRNPs)[1,7]. Similar to other ncRNAs, snoRNAs lack translation functionality, but what sets them apart is their specific nucleotide sequences and spatial structures[33]. Based on distinct nucleotide motifs and secondary structures, snoRNAs are primarily categorized into C/D box snoRNAs and H/ACA box snoRNAs[34,35]. C/D box snoRNAs guide the 2′-O-methylation of specific nucleotides in the target RNA molecule by binding with four core proteins, namely nucleolar protein 56 (NOP56), NOP58, small nuclear ribonucleoprotein 13 (SNU13), and a methyltransferase fibrillarin (FBL)[36,37], while H/ACA box snoRNAs associated with conserved proteins glycine arginine-rich protein 1 (GAR1), non-histone chromosome protein 2 (NHP2), NOP10, and dyskeratosis congenita 1 (DKC1) guide the conversion of specific uridine nucleotides to pseudouridine[38].

C/D box snoRNAs (SNORDs) are typically 60 nt to 90 nt long and consist of two concise sequence elements, the C box (5′RUGAUGA3′) situated at the 5′ end and the D box (5′CUGA3′) located at the 3′ end. They contain internal structures similar to the C and D boxes, referred to as box C′ and box D′, respectively, with 4-6 nucleotides of reverse complementary sequences at both ends, forming a single hairpin structure[39]. SNORDs act as recognition sites for specific proteins such as NOP56, NOP58, SNU13, and FBL. When these proteins directly bind to SNORDs, they form a scaffold-like structure, enabling interactions with other proteins to execute various biological functions[40]. SNORDs are crucial for maintaining the structural stability of snoRNAs and their localization within the nucleolus, involving in the splicing and processing of rRNA precursors[41]. Most SNORDs contain an upstream segment of more than 21 nucleotides in the C/D box region, referred to as antisense snoRNA[42]. This segment has the ability to bind to target RNA through complementary base pairing. Antisense snoRNAs act as guide RNAs, directing the methylation of specific 2′-O-hydroxyl positions on target molecules, thereby facilitating 2′-O ribose methylation modifications at specific sites on rRNA[43].

H/ACA box snoRNAs (SNORAs) range from 120 nt to 140 nt and exhibit a typical secondary structure known as the "hairpin-hinge-hairpin-tail" structure. The hinge region consists of a single-stranded nucleic acid segment that acts as a bridge connecting two hairpin structures and both the hinge and tail regions contain conserved sequence elements known as the H box (5′ANANNA3′) and ACA box, respectively, with the ACA box usually located at the third nucleotides upstream from the 3′ end[44,45]. Due to the presence of the H box and ACA box, SNORAs can form a double-hairpin structure, and within the pseudouridine pockets of these hairpins, there exists antisense snoRNA that binds to specific sites on target molecules[46]. When antisense snoRNA associates with core proteins, such as GAR1, NHP2, NOP10, and DKC1, it forms a homologous snoRNP complex, guiding the pseudouridylation modification of target RNA [47]. In essence, the majority of SNORAs guide the pseudouridylation modification of specific sites within eukaryotic rRNA and snRNA, converting uridine into pseudouridine[48]. It is revealed that mammalian SNORAs share a similar H/ACA motif with human telomerase RNA, suggesting that H/ACA-like structural domains may be associated with cell proliferation[49,50].

Additionally, small Cajal body-associated RNAs (scaRNAs) are more variable in length, representing a specific subset of snoRNAs[51]. ScaRNAs play critical roles within the Cajal bodies, small membraneless subcompartments in the cell nucleus, and are involved in regulating the modification of snRNAs and post-transcriptional regulation of RNA. Structurally, scaRNAs are similar to snoRNAs, and some scaRNAs contain both C/D box and H/ACA box sequences [52]. Moreover, it has been identified a connection between dysregulated scaRNAs and the progression of certain cancers, including CRC. Notably, SCARNA12[53], SCARNA15[54], and SCARNA22[31] have been observed to have increased expression levels in CRC cell lines and clinical CRC tissue samples. However, there remains a limited understanding of their specific biological functions and the underlying molecular mechanisms within the context of CRC.

SnoRNAs participate in various biological processes, including the processing of rRNA[55], regulation of RNA splicing and translation[56], as well as responses to oxidative stress[57]. In essence, these post-transcriptional modifications are crucial for the production of efficient and accurate ribosomes, to maintain the intricate cellular functions associated with protein synthesis[58]. Over the past two decades, the understanding of the cellular functions of snoRNAs has significantly expanded, including the production of other regulatory RNAs involved in the regulation of gene expression (*e.g.*, the production of piRNAs[59], the production of miRNAs by shearing of snoRNAs[60,61]), the modulation of mRNA abundance[62], and the regulation of translational efficiency[63]. There have been reports of orphan snoRNAs, but their functions and target actions remain unclear[64]. Therefore, traditional snoRNA classifications may not comprehensively encompass all the functions of snoRNAs (Figure 1).

Pathological importance of snoRNA

In normal physiological processes, snoRNAs stably exist by forming snoRNPs through interactions with specific proteins, and they subsequently participate in 2′-O-methylation or pseudouridylation of rRNA[35]. With the completion of the human genome sequencing and the advancement of high-throughput sequencing in the early 21st century, coupled with

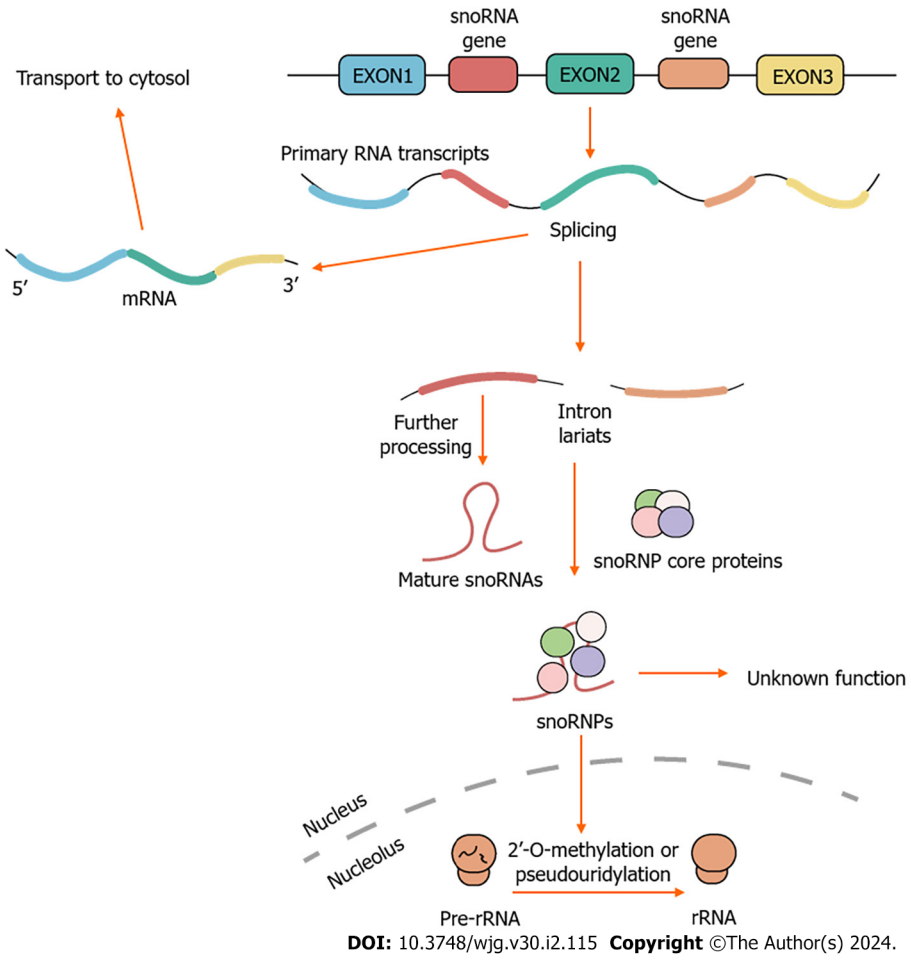

DOI: 10.3748/wjg.v30.i2.115

Figure 1 Biosynthesis of small nucleolar RNAs. snoRNA: Small nucleolar RNA; snoRNP: Small nucleolar ribonucleoprotein; rRNA: Ribosomal RNA.

the deepening research in nucleic acids and proteomics, an increasing number of snoRNAs associated with diseases have been discovered. Currently, the focus of research is to gain a deeper understanding of the functions of snoRNAs under both normal and pathological conditions[65].

The first report of snoRNAs' role in human diseases came with Prader-Willi syndrome, suggesting that snoRNA may have an important role in human diseases[66,67]. Subsequently, abnormal snoRNA expression has been reported in various human diseases, including congenital heart defects[68], neurodegenerative disorders[69], and cancers[70]. Researchers have observed a significant and pronounced alteration in the expression of snoRNAs in myocardial tissue affected by Tetralogy of Fallot, compared to healthy control myocardium, suggesting that snoRNA dysregulation might have an impact on development[68]. In mammals, especially in humans, approximately 90% of snoRNAs are encoded within introns, often associated with genes related to ribosome biogenesis[71]. This co-localization implies a coordinated expression designed to facilitate their collaborative functions.

Furthermore, it is revealed that SNORD113-1 suppresses the development of hepatocellular carcinoma (HCC). Compared to adjacent non-cancerous tissue, the expression of SNORD113-1 is significantly downregulated in HCC. Moreover, the decreased SNORD113-1 level is notably associated with adverse patient survival outcomes, indicating that SNORD113-1 plays an anti-cancer role in HCC as a potential diagnostic and therapeutic target for this condition[72]. Additionally, functionally aberrant snoRNAs may play a role in the onset and progression of malignant tumors in humans. For instance, SNORA42 has been shown to act as an oncogene in lung tumorigenesis[73]. Furthermore, snoRNAs (SNORD15A, SNORD15B, SNORD22, SNORD17, and SNORD87) and snoRNPs are frequently overexpressed in both mouse and human breast cancer and prostate cancer, demonstrating their association with tumorigenicity and highlighting the significant role of snoRNAs in regulating cancer biology[74].

As snoRNAs can be detected in both plasma and serum reliably, their levels in blood indicate various disease states and correlate with clinical pathological features, highlighting their applicability as potential disease biomarkers[31]. For instance, the expression level of SNORD33 in plasma was found to be correlated with the effectiveness of platinum-based drugs in patients with metastatic triple-negative breast cancer (TNBC), indicating that SNORD33's expression holds promise as a potential biomarker for predicting the efficacy of platinum drugs in TNBC patients[75]. Furthermore, the elevated expression of SNORD52 in HCC is closely associated with poor clinical prognosis, which promotes HCC development by upregulating CDK1, thus enhancing the stability of the CDK1 protein, indicating that targeting the Upf1/SNORD52/CDK1 pathway has therapeutic potential for HCC treatment[76]. In addition, SNORA38B exhibits high expression in NSCLC tissues and cell lines, correlating with unfavorable prognosis. SNORA38B acts as an oncogene in

NSCLC, in part, by directly binding to E2F1 and regulating the GAB2/AKT/mTOR pathway[77].

To sum up, in the process of tumorigenesis, ribosomes, which serve as molecular factories for protein biosynthesis, are typically highly activated to meet the heightened raw material demands of proliferating cancer cells. SnoRNAs play the critical role in the maturation of ribosomes[5,6]. Consequently, alterations in snoRNA expression may have an extensive impact on the mechanisms of cancer development and pathological processes. However, current reports are primarily centered around snoRNA screening and validating their associations with diseases, with an incomplete understanding of their mechanisms, especially their roles in cellular signal transduction pathways.

PROGRESS OF SNORNA IN CRC

CRC is one of the most prevalent cancers in humans[19]. Currently, advances in cancer prevention, early detection, and treatment have led to a decrease in mortality rates associated with CRC. However, the 5-year survival rate for this disease still remains relatively low[78]. Despite the utilization of advanced therapeutic approaches including surgical resection, chemotherapy, and radiotherapy, there hasn't been a notable improvement in the mortality rate of CRC patients, due to the resemblance of early-stage CRC to non-malignant intestinal conditions, a scarcity of distinctive symptoms, and the consequent delayed diagnoses[79]. Consequently, the absence of efficacious molecular biomarkers for early detection remains a substantial challenge in addressing CRC. Increasing evidence suggests that snoRNAs serve as key regulators of gene expression and RNA modification[58]. Defects in the functions of these molecules have become markers of tumorigenesis and cancer development[74]. Differential expression of snoRNAs in CRC may hold diagnostic and prognostic value[80,81]. Therefore, a comprehensive understanding of the mechanisms by which aberrant snoRNAs contribute to the development of CRC is imperative and the involvement of snoRNAs in the progression of CRC is gaining importance as a reliable molecular biomarker (Table 1). It has the potential to greatly enhance early clinical diagnosis and improve prognosis for CRC patients.

H/ACA box snoRNAs

SNORA21: SNORA21 is a type of H/ACA box snoRNA with a length of 132 nt and its host gene is RPL23. Next-generation sequencing results have suggested that SNORA21 could be a potential early detection and prognostic biomarker for NSCLC[93]. Whereafter, Yoshida *et al*[84] observed an upregulation in the expression levels of SNORA21 in both colorectal adenomas and CRC through a series of *in vitro* and *in vivo* experiments. Using CRISPR/Cas9-mediated manipulation of SNORA21 expression, they demonstrated its regulatory influence on multiple cancer-associated pathways, resulting in reduced cell proliferation and diminished invasion and migration capabilities. In summary, this substantiates the oncogenic function of SNORA21 in CRC, wherein it modulates the cell cycle, consequently inducing alterations in cell proliferation and tumor invasion. Furthermore, SNORA21 has demonstrated the capacity to stimulate the proliferation of CRC cells by influencing pivotal cancer-related pathways, including the Hippo and Wnt signaling pathways, and heightened levels of SNORA21 have exhibited a correlation with distant metastasis in the context of CRC. These findings underscore the pivotal role that snoRNAs may play in cancer biology and suggest SNORA21 as a potential target for CRC therapy[84].

SNORA24: SNORA24, a type of H/ACA box snoRNA, exhibits a length of 131 nt and originates from the host gene SNHG8. It is shown that SNORA24 is downregulated in HCC, and may be a tumor suppressor gene[94]. However, research indicates that SNORA24 is markedly upregulated in various cancers, including CRC. Overexpression of SNORA24 promotes cell proliferation and the growth of xenograft tumors by regulating the cell cycle process, particularly by facilitating the G1/S phase transition. Additionally, silencing SNORA24 induces substantial apoptosis within cells and modulates the stability of p53 protein through the proteasome degradation pathway[95]. These findings elucidate the mechanism by which SNORA24 exerts its oncogenic influence in CRC, in a p53-dependent manner, underscoring its potential utility as a biomarker and therapeutic target for patients with CRC[85].

SNORA42: SNORA42 belongs to the H/ACA box snoRNA, with a length of 134 nt, and its locus is TTC6. Research indicates that SNORA42 is highly expressed in NSCLC tissues and has been experimentally verified for its oncogenic function[73]. Soon, the study from another group suggests that SNORA24 may function as an oncogene in CRC, as its overexpression leads to enhanced cell proliferation, migration, invasion, anoikis resistance, as well as tumorigenicity. Notably, heightened SNORA42 expression levels have been linked to distant metastasis and unfavorable prognosis in individuals afflicted with CRC. Furthermore, available data indicates that the expression of SNORA42 can be used to identify high-risk patients with stage II CRC. Consequently, utilizing SNORA42 expression as a molecular biomarker holds promise in identifying high-risk CRC patients, particularly those with stage II CRC, for postoperative adjuvant therapy to improve prognosis[31].

SNORA71A: SNORA71A is a H/ACA box snoRNA with a total length of 134 nt, located at the genomic locus AL080249.26, and its host gene is SNHG17. The transcription of SNORA71A appears to be synchronized with that of SNHG17. It has been reported that SNHG17 exhibits upregulation in CRC tissues, implying a potential upregulation of SNORA71A in CRC as well[96]. Researchers conducted a comprehensive analysis of snoRNA expression profiles in CRC utilizing small RNA sequencing technology. The investigation revealed a substantial upregulation of SNORA71A in CRC tissues and cells. Furthermore, SNORA71A expression displayed a significant correlation with TNM staging and lymph node metastasis. It demonstrates both high sensitivity and specificity, making it a promising candidate as a biomarker for CRC. SNORA71A seems to play a role within the NF-κB signaling pathway and Toll-like receptor signaling pathway in

Table 1 Functions of small nucleolar RNAs in colorectal cancers

snoRNA	Type	Modification site	Length (nt)	Host gene	Expression	Mechanism	Potential functions	Ref.
SNORA5C	H/ACA	18S:U1238; 18S:U1625	137	TBRG4	Up-regulation	Unknown	Promote proliferation, and colony formation	[82]
SNORA15	H/ACA	18S:U1367	133	CCT6A	Up-regulation	Unknown	Exert the oncogenic effect	[83]
SNORA21	H/ACA	28S:U4401; 28S:U4270	132	RPL23	Up-regulation	Hippo signaling pathway, and Wnt signaling	Promote cell proliferation, and enhances tumor invasiveness	[84]
SNORA23	H/ACA	28S:U3737; 28S:U4331	189	IPO7	Up-regulation	Unknown	Unproved	[54]
SNORA24	H/ACA	18S:U863; 18S:U609	131	SNHG8	Up-regulation	P53	Promote G1/S phase transition, and cell proliferation	[54, 85]
SNORA41	H/ACA	18S:U1643	132	EEF1B2	Up-regulation	Unknown	Exert the oncogenic effect	[83]
SNORA42	H/ACA	18S:U572; 18S:U109	134	TTC6	Up-regulation	Unknown	Enhance cell proliferation, migration, invasion, anoikis resistance, and tumorigenicity	[31]
SNORA71A	H/ACA	18S:U406	138	SNHG17	Up-regulation	LBP, NF-kappaB, Toll-like receptor	Promote cell proliferation, migration and invasion	[54]
SNORD1C	C/D	28S:G4362	78	SNHG16	Up-regulation	Wnt/β-catenin pathway	Promote cell proliferation, migration, invasion and enhance cancer cell stemness	[86, 87]
SNORD12B	C/D	28S:G3878	91	ZFAS1	Up-regulation	Unknown	Promote tumorigenesis, proliferation, and metastasis	[88]
SNORD12C	C/D	28S:G3878	89	ZFAS1	Up-regulation	ZFAS1-NOP58-SNORD12C/78-EIF4A3/LAMC2	Promote cell proliferation	[13, 89]
SNORD14E	C/D	Unknown	85	HSPA8	Up-regulation	Unknown	Unproved	[89]
SNORD15B	C/D	28S:A3764	146	RPS3	Up-regulation	Unknown	Promote proliferation, and colony formation	[82]
SNORD17	C/D	28S:U3797	237	SNX5	Up-regulation	Unknown	Unproved	[89]
SNORD33	C/D	18S:U1326	83	RPL13A	Down-regulation	Unknown	Suppress cell anchorage	[83]
SNORD44	C/D	18S:A166	63	GAS5	Down-regulation	Caspase dependent pathway, PI3K/Akt	Inhibit tumor growth, and induce apoptosis	[90]
SNORD48	C/D	28S:C2279	64	SNHG32	Up-regulation	Unknown	Unproved	[82]
SNORD50A	C/D	28S:C2848; 28S:G2863	75	SNHG5	Down-regulation	Methylation of 28S rRNA gene, k-Ras	Promote tumor growth	[91]
SNORD50B	C/D	Unknown	70	SNHG5	Down-regulation	Methylation of 28S rRNA gene, k-Ras	Promote tumor growth	[91]
SNORD57	C/D	18S:A99	72	NOP56	Up-regulation	Unknown	Unproved	[92]
SNORD67	C/D	U6:C60	111	CKAP5	Up-regulation	Unknown	Unproved	[89]
SNORD76	C/D	28S:A2350	80	GAS5	Up-regulation	Unknown	Unproved	[31]
SNORD78	C/D	28S:G4593	65	GAS5	Up-regulation	ZFAS1-NOP58-SNORD12C/78-EIF4A3/LAMC2	Promote cell proliferation	[13, 31]
SNORD126	C/D	Unknown	77	CCNB1IP1	Up-regulation	PI3K/Akt	Promote cell growth	[65]
SCARNA12	scaRNA	U5:U46	270	PHB2	Up-regulation	PI3K/Akt	Promote proliferation and tumorigenicity	[53]

SCARNA15	scaRNA	U2:U37	127	SNHG21	Up-regulation	Unknown	Unproved	[54]
SCARNA22	scaRNA	Unknown	125	NSD2	Up-regulation	Unknown	Unproved	[31]

snoRNA: Small nucleolar RNA; scaRNA: Small Cajal body-associated RNAs; SNORDs: C/D box snoRNAs.

CRC, suggesting its involvement in the initiation and progression of CRC. And SNORA71A may be necessary for effective proliferation, migration, and invasion of CRC cells, as the results show that cell proliferation, migration, and invasion are significantly inhibited when SNORA71A is knocked down. These findings indicate the potential crucial role of SNORA71A in the malignant transformation, progression, or metastasis of CRC[54].

Other H/ACA box snoRNAs: In addition to the H/ACA box snoRNAs discussed above, there are several other H/ACA box snoRNAs that are closely associated with CRC. For instance, SNORA5C has been linked to promoting the proliferative potential of CRC cells[82], while SNORA15 and SNORA41 have been implicated in the potential oncogenic effects in CRC[83]. Besides SNOR71A, Zhang *et al*[54] also reported the high abundance of SNORA23 related to CRC, without function evaluation. However, the specific molecular mechanisms and biological functions of these snoRNAs require further investigation.

C/D box snoRNAs

SNORD1C: SNORD1C is a C/D box snoRNA with a length of 78 nt, and its host gene is SNHG16. It is well-known that ALDH1$^+$ tumor cells are typically characterized by heightened proliferation rates, enhanced self-renewal capabilities, and an increased potential for tumor formation *in vivo*, factors closely linked to cancer recurrence. Mannoor *et al*[97] found that SNORD1C exhibits elevated levels in ALDH1$^+$ NSCLC cells in comparison to ALDH1$^-$ NSCLC cells, indicating the driving role of SNORD1C in NSCLC[97,98]. However, the precise role of SNORD1C in CRC remains a subject of ongoing investigation. Researchers have observed significant upregulation of SNORD1C in the serum of CRC patients, and this upregulation is associated with low tissue differentiation and high CEA expression. Therefore, the elevated expression of SNORD1C is closely linked to poor outcomes and prognosis in CRC patients[86]. Furthermore, subsequent studies found that knocking down SNORD1C in CRC cell lines led to reduced cell proliferation, colony formation, migration, and invasion, as well as promoting apoptosis. Besides, SNORD1C has been proved to augment cancer cell stemness within the context of CRC, acting through the Wnt/β-catenin pathway. In summary, the suppression of SNORD1C is shown to reduce Wnt/β-catenin pathway expression. These alterations collectively lead to reduced resistance to chemotherapy, ultimately hampering the progression of CRC, which strongly suggests the clinical potential of targeting this specific snoRNA in the treatment of CRC[87].

SNORD12B: SNORD12B is a type of C/D box snoRNA with a length of 91nt and it is hosted by the gene ZFAS1. To explore factors associated with tumor progression and metastasis, Xu *et al*[88] examined the role of noncoding RNAs in CRC and discovered 32 differentially expressed snoRNAs in metastatic and late-stage CRC tissues, with SNORD12B exhibiting significant upregulation compared to normal samples. Through correlation analysis, they found a significant correlation between SNORD12B and the expression of miRNAs and mRNAs, suggesting its potential role in regulating the expression of other RNAs. Interestingly, the upregulation of SNORD12B was positively associated with hypoxia, tumor metastasis, and upregulated genes in the pentose phosphate pathway, while it was negatively correlated with the expression of tumor suppressor genes. These findings imply that SNORD12B may be involved in diverse aspects related to the tumor occurrence, proliferation, and metastasis[88]. Additionally, its host gene, ZFAS1 is also involved in various human malignancies and associated with many aspects of carcinogenesis, including proliferation, invasion, metastasis, apoptosis, cell cycle regulation, and drug resistance. Besides, SNORD12, and SNORD12C, hosted by ZFAS1, has been also significantly overexpressed in various human malignant tumors, including CRC. This suggests the potential close association between ZFAS1 and its hosted snoRNAs, such as SNORD12B, potentially playing a pivotal role in the malignant evolution, progression, or metastasis of CRC[99].

SNORD44: SNORD44 is a C/D box snoRNA, with a length of 63 nt, located within the exon of the GAS5 gene[100]. Researchers assessed the expression levels of SNORD44 and GAS5 in CRC tissues using qRT-PCR and evaluated their correlation *via* Pearson correlation analysis. It is observed that both SNORD44 and GAS5 were expressed at low levels in CRC tissues compared to control samples. Additionally, a positive correlation between the expression of SNORD44 and GAS5 in tumor samples was detected. The SNORD44 did not regulate the expression of its host gene, GAS5, and vice versa. The researchers engineered an oncolytic adenovirus (SPDD-UG) to overexpress SNORD44 and GAS5, and demonstrated that SNORD44 and GAS5 exhibited anti-tumor effects in CRC cells, inhibiting cancer growth and inducing apoptosis[90]. It is indicated that SNORD44 exhibited downregulated expression in CRC tissues, and overexpressing SNORD44 inhibited the growth of CRC cells, suggesting that SNORD44 may function as a tumor suppressor in CRC and providing a promising direction for potential CRC therapeutic strategies.

SNORD57: SNORD57 is a C/D box snoRNA with a length of 72 nt, its host gene is NOP56, and its derivative piRNA piR-54265 found in the 5′ end fragment of SNORD57. It is suggested that serum piR-54265 could serve as a biomarker for early detection and clinical monitoring of CRC[101,102]. After detecting SNORD57 and its derivative piRNA piR-54265 in

the serum of CRC patients, it is evident that SNORD57 exhibits a higher abundance in serum, thus rendering it a promising non-invasive biomarker for the early detection and clinical monitoring of CRC[92].

SNORD50A/B: SNORD50A, originating from the host gene SNHG5, is a C/D box snoRNA with a length of 75 nt. Similarly, SNORD50B, also derived from the host gene SNHG5, is a C/D box snoRNA with a length of 70 nt. Through a comparative analysis of tumor genomes and normal genomes, researchers have identified that the deletion frequency of SNORD50A and SNORD50B genes in various common cancers, including CRC, ranges from 10% to 40%. This deletion has been correlated with decreased survival rates in patients. It has been observed that SNORD50A and SNORD50B binds to K-Ras and inhibits K-Ras oncogenic function in various tumor types. Subsequent experiments have revealed that the absence of SNORD50A and SNORD50B in tumors augments the activities of K-Ras and its associated signaling pathway and an increased risk of tumorigenesis. These research findings suggest a potential synergistic interaction between mutations in the KRAS gene and the deletion of SNORD50A and SNORD50B in cancer[103]. Notably, KRAS plays a crucial role in the development, signaling, and proliferation of CRC. Mutations in the KRAS gene result in the permanent activation of the K-Ras protein, which is pivotal for tumor growth and heterogeneity[104]. Therefore, the loss of SNORD50A and SNORD50B may play a significant role in the pathogenesis of CRC, at least partially through interacting with KRAS gene mutations to promote tumorigenesis and progression, providing valuable insights into the mechanisms of CRC and offer new targets for potential therapeutic strategies.

SNORD12C/78: SNORD12C, arising from the host gene ZFAS1, is a C/D box snoRNA with a length of 89 nt. And SNORD78, originating from the host gene GAS5, is a C/D box snoRNA with a length of 65 nt. It is reported that SNORD12C/78 participate in a novel signaling pathway, ZFAS1-NOP58-SNORD12C/78-EIF4A3/LAMC2 axis, influencing the development and progression of CRC. This sheds light on new molecular mechanisms that underlie the regulation of CRC initiation and pathogenesis by ZFAS1. ZFAS1 assumes a critical oncogenic role in CRC, with its expression and function are indispensable for the development and maintenance of CRC cells and tissues. Mechanically, ZFAS1 recruits NOP58 as a scaffold protein to maintain the methylation function of SNORD12C and SNORD78, thereby facilitating the activities of SNORD12C and SNORD78 mediated 28S rRNA 2′-O-methylation at specific sites. This leads substantially heightened stability and translational activity of downstream target genes, such as EIF4A3, and LAMC2, ultimately fostering the proliferation of colon cancer cells. Inhibition of SNORD12C or SNORD78 results in diminished 2′-O-methylation modifications under the regulation of ZFAS1, thereby suppressing the stability and translational activity of downstream target genes. Thus, this unveils fresh possibilities for the potential application of snoRNA and cellular 2′-O-methylation-dependent translation networks in the prevention and treatment of CRC[13].

Other C/D box snoRNAs: In addition to the C/D box snoRNAs discussed above, several other C/D box snoRNAs have been show a close correlation with diverse characteristics of CRC. The elevated expression of SNORD15B[82] and SNORD126[65] has found to be associated with the proliferative potential of CRC cells. Conversely, reduced expression of SNORD33 can inhibit the anchoring function of CRC cells[83]. However, the potential roles of SNORD14E[89], SNORD17 [89], SNORD48[82], SNORD67[89], SNORD76[31], and others in CRC remain unclear, requiring further investigation to uncover their precise molecular mechanisms and biological functions.

CLINICAL PERSPECTIVES

CRC is a disease characterized by a multitude of genetic and epigenetic features[105,106], with its onset attributable to various intrinsic and extrinsic factors, including the accumulation of genetic mutations, susceptibility alleles associated with family history, and chronic or sustained inflammation[107]. Based on the source of mutations, CRC can be categorized into three types, sporadic (70%), hereditary (5%), and familial (25%). The pathogenic mechanisms leading to this condition may involve three types, namely chromosomal instability, microsatellite instability, and CpG island methylator phenotype[108,109]. While the molecular mechanisms of CRC have been extensively studied, there are still many details that remain unclear.

One of the primary reasons for the poor 5-year overall survival rate in CRC is late detection, missing the window for effective treatment[17]. Early diagnosis is the critical means of reducing mortality in CRC patients, and biomarker detection plays a pivotal role in early diagnosis[78]. Recently, the emergence of liquid biopsy techniques has brought new hope for early disease diagnosis. This method allows the detection of nucleic acids, peptides, proteins, and intact tumor cells in bodily fluids. Minimally invasive techniques like liquid biopsy are preferred for diagnosing and assessing patient prognosis, significantly improving clinical management in cancer patients[110,111]. SnoRNAs, due to their location within the nucleolus, are typically unaffected by hemolysis and remain relatively stable in the bloodstream as they form complexes with specific proteins. The application of high-quality microarrays and high-throughput sequencing has unequivocally demonstrated differential snoRNA expression in clinical samples and cell lines, implying diagnostic and prognostic potential in CRC[54,92]. While mounting evidence supports the functional role of snoRNAs in CRC development and their potential as biomarkers, there remains a paucity of research on their clinical significance and functional roles in CRC progression. Overall, snoRNAs possess advantages such as non-invasiveness, high sensitivity, and specificity, rendering them ideal biomarkers for early cancer screening and diagnosis in the current context. Moreover, they may exhibit functions akin to non-invasive biomarkers, resembling miRNAs[112,113].

Currently, the treatment for CRC primarily involves surgery, adjuvant chemotherapy, radiation therapy, and immunotherapy[21]. Given their abundance and detectability in both solid tumors and blood, snoRNAs may emerge as central

targets in cancer therapy[16]. Although current understanding of the molecular mechanisms of snoRNAs in tumorigenesis remains limited, some of their characteristics make them ideal candidates for therapeutic interventions[114]. For instance, studies indicate that manipulating snoRNA expression, both *in vitro* and *in vivo*, can enhance the tumorigenic and invasive properties of CRC, suggesting that targeting snoRNA expression represents a novel approach for CRC prevention and treatment[31,84]. Furthermore, snoRNAs involved in transcriptional gene silencing pathways may offer high therapeutic benefits[115]. Moreover, certain snoRNAs seem to have the potential for protein binding or dependence on secondary structures, providing a novel means of therapeutic intervention[116], while oncolytic adenovirus vectors have gained extensive use in cancer therapy[117]. The vectors exhibit selective infectivity towards tumor cells, leading to oncolysis while causing minimal toxicity to normal tissues[118,119]. Some investigations have explored the deployment of oncolytic adenovirus vectors for delivering snoRNAs and their host genes for cancer treatment, demonstrating selective replicability and potential cytotoxicity in cancer cells[90].

Nonetheless, the primary obstacle to implementing snoRNA-based therapeutic strategies in cancer patients primarily arises from a dearth of understanding regarding their functional roles in tumorigenesis and their specific downstream gene targets or pathways. As technological limitations are surmounted, snoRNAs may emerge as potential targets for treatment. While this field appears to be in its nascent stages, it should be currently witnessing the potential of snoRNAs in cancer therapy. In the near future, it is useful to harness their potential successfully.

CONCLUSION

An increasing body of research on snoRNAs in CRC has expanded the understanding of their molecular mechanisms and biological processes[2]. Specifically, the dysregulation of snoRNA function appears to be closely associated with the onset and development of CRC[31]. However, the functional roles of the majority of snoRNAs in CRC remain uncertain. Their roles in cell signaling pathways, molecular mechanisms, and regulation, require further clarification, and more research is needed to delve into the snoRNAs present in CRC and their respective targets. As the knowledge of novel snoRNA functions deepens, research based on snoRNAs has the potential to reshape the landscape of tumor biology and genetics, possibly uncovering new pathways that drive CRC.

In summary, the study of snoRNAs in the context of CRC is a continually expanding field, and future discoveries may provide deeper insights into the disease, utilizing snoRNAs as therapeutic targets, as well as diagnostic and prognostic markers. Current literature underscores the role of snoRNA dysregulation in promoting CRC, emphasizing the significance of snoRNA regulation in CRC biology and clinical outcomes. Therefore, understanding the roles of snoRNAs may enhance our comprehension of CRC and potentially harness the robust potential of snoRNAs in the clinical diagnosis and treatment of CRC in the future.

FOOTNOTES

Author contributions: Liu J and Lan YZ designed this study; Lan YZ, Wu Z, Chen WJ, and Fang ZX searched the publication; Lan YZ, Wu Z, Chen WJ, Fang ZX, Yu XN, Wu HT, and Liu J interpreted the results, constructed the structure of the review, and prepared the tables; Lan YZ prepared the draft of the manuscript; Lan YZ and Wu Z prepared the figures; Liu J revised the manuscript critically; and all authors have read and approve the final manuscript.

Supported by the National Natural Science Foundation of China, No. 82273457; Guangdong Basic and Applied Basic Research Foundation, No. 2021A1515012180 and No. 2023A1515012762; Special Grant for Key Area Programs of Guangdong Department of Education, No. 2021ZDZX2040; and Science and Technology Special Project of Guangdong Province, No. 210715216902829.

Conflict-of-interest statement: All the authors report no relevant conflicts of interest for this article.

Country/Territory of origin: China

ORCID number: Yang-Zheng Lan 0009-0000-4241-228X; Zheng Wu 0000-0002-1393-7586; Wen-Jia Chen 0000-0001-7157-3242; Ze-Xuan Fang 0000-0002-6100-9012; Xin-Ning Yu 0009-0003-4658-4275; Hua-Tao Wu 0000-0002-1640-6094; Jing Liu 0000-0002-7483-4572.

S-Editor: Chen YL
L-Editor: A
P-Editor: Yu HG

REFERENCES

1 **Maxwell ES**, Fournier MJ. The small nucleolar RNAs. *Annu Rev Biochem* 1995; **64**: 897-934 [PMID: 7574504 DOI: 10.1146/annurev.bi.64.070195.004341]

2 **Zhang X**, Wang C, Xia S, Xiao F, Peng J, Gao Y, Yu F, Chen X. The emerging role of snoRNAs in human disease. *Genes Dis* 2023; **10**: 2064-2081 [PMID: 37492704 DOI: 10.1016/j.gendis.2022.11.018]

3 **Weinberg RA**, Penman S. Small molecular weight monodisperse nuclear RNA. *J Mol Biol* 1968; **38**: 289-304 [PMID: 5718554 DOI: 10.1016/0022-2836(68)90387-2]

4 **Zieve G**, Penman S. Small RNA species of the HeLa cell: metabolism and subcellular localization. *Cell* 1976; **8**: 19-31 [PMID: 954090 DOI: 10.1016/0092-8674(76)90181-1]

5 **Kedersha NL**, Rome LH. Isolation and characterization of a novel ribonucleoprotein particle: large structures contain a single species of small RNA. *J Cell Biol* 1986; **103**: 699-709 [PMID: 2943744 DOI: 10.1083/jcb.103.3.699]

6 **Lübben B**, Marshallsay C, Rottmann N, Lührmann R. Isolation of U3 snoRNP from CHO cells: a novel 55 kDa protein binds to the central part of U3 snoRNA. *Nucleic Acids Res* 1993; **21**: 5377-5385 [PMID: 8265352 DOI: 10.1093/nar/21.23.5377]

7 **Tollervey D**. A yeast small nuclear RNA is required for normal processing of pre-ribosomal RNA. *EMBO J* 1987; **6**: 4169-4175 [PMID: 3327689 DOI: 10.1002/j.1460-2075.1987.tb02763.x]

8 **Ni J**, Tien AL, Fournier MJ. Small nucleolar RNAs direct site-specific synthesis of pseudouridine in ribosomal RNA. *Cell* 1997; **89**: 565-573 [PMID: 9160748 DOI: 10.1016/s0092-8674(00)80238-x]

9 **Matera AG**, Terns RM, Terns MP. Non-coding RNAs: lessons from the small nuclear and small nucleolar RNAs. *Nat Rev Mol Cell Biol* 2007; **8**: 209-220 [PMID: 17318225 DOI: 10.1038/nrm2124]

10 **Chang LS**, Lin SY, Lieu AS, Wu TL. Differential expression of human 5S snoRNA genes. *Biochem Biophys Res Commun* 2002; **299**: 196-200 [PMID: 12437969 DOI: 10.1016/s0006-291x(02)02623-2]

11 **Schulten HJ**, Bangash M, Karim S, Dallol A, Hussein D, Merdad A, Al-Thoubaity FK, Al-Maghrabi J, Jamal A, Al-Ghamdi F, Choudhry H, Baeesa SS, Chaudhary AG, Al-Qahtani MH. Comprehensive molecular biomarker identification in breast cancer brain metastases. *J Transl Med* 2017; **15**: 269 [PMID: 29287594 DOI: 10.1186/s12967-017-1370-x]

12 **Liao J**, Yu L, Mei Y, Guarnera M, Shen J, Li R, Liu Z, Jiang F. Small nucleolar RNA signatures as biomarkers for non-small-cell lung cancer. *Mol Cancer* 2010; **9**: 198 [PMID: 20663213 DOI: 10.1186/1476-4598-9-198]

13 **Wu H**, Qin W, Lu S, Wang X, Zhang J, Sun T, Hu X, Li Y, Chen Q, Wang Y, Zhao H, Piao H, Zhang R, Wei M. Long noncoding RNA ZFAS1 promoting small nucleolar RNA-mediated 2'-O-methylation *via* NOP58 recruitment in colorectal cancer. *Mol Cancer* 2020; **19**: 95 [PMID: 32443980 DOI: 10.1186/s12943-020-01201-w]

14 **Deogharia M**, Majumder M. Guide snoRNAs: Drivers or Passengers in Human Disease? *Biology (Basel)* 2018; **8** [PMID: 30577491 DOI: 10.3390/biology8010001]

15 **Dsouza VL**, Adiga D, Sriharikrishnaa S, Suresh PS, Chatterjee A, Kabekkodu SP. Small nucleolar RNA and its potential role in breast cancer - A comprehensive review. *Biochim Biophys Acta Rev Cancer* 2021; **1875**: 188501 [PMID: 33400969 DOI: 10.1016/j.bbcan.2020.188501]

16 **Toden S**, Zumwalt TJ, Goel A. Non-coding RNAs and potential therapeutic targeting in cancer. *Biochim Biophys Acta Rev Cancer* 2021; **1875**: 188491 [PMID: 33316377 DOI: 10.1016/j.bbcan.2020.188491]

17 **Morgan E**, Arnold M, Gini A, Lorenzoni V, Cabasag CJ, Laversanne M, Vignat J, Ferlay J, Murphy N, Bray F. Global burden of colorectal cancer in 2020 and 2040: incidence and mortality estimates from GLOBOCAN. *Gut* 2023; **72**: 338-344 [PMID: 36604116 DOI: 10.1136/gutjnl-2022-327736]

18 **Siegel RL**, Miller KD, Wagle NS, Jemal A. Cancer statistics, 2023. *CA Cancer J Clin* 2023; **73**: 17-48 [PMID: 36633525 DOI: 10.3322/caac.21763]

19 **Dekker E**, Tanis PJ, Vleugels JLA, Kasi PM, Wallace MB. Colorectal cancer. *Lancet* 2019; **394**: 1467-1480 [PMID: 31631858 DOI: 10.1016/S0140-6736(19)32319-0]

20 **Miller KD**, Nogueira L, Devasia T, Mariotto AB, Yabroff KR, Jemal A, Kramer J, Siegel RL. Cancer treatment and survivorship statistics, 2022. *CA Cancer J Clin* 2022; **72**: 409-436 [PMID: 35736631 DOI: 10.3322/caac.21731]

21 **Biller LH**, Schrag D. Diagnosis and Treatment of Metastatic Colorectal Cancer: A Review. *JAMA* 2021; **325**: 669-685 [PMID: 33591350 DOI: 10.1001/jama.2021.0106]

22 **Vatandoust S**, Price TJ, Karapetis CS. Colorectal cancer: Metastases to a single organ. *World J Gastroenterol* 2015; **21**: 11767-11776 [PMID: 26557001 DOI: 10.3748/wjg.v21.i41.11767]

23 **Beniwal SS**, Lamo P, Kaushik A, Lorenzo-Villegas DL, Liu Y, MohanaSundaram A. Current Status and Emerging Trends in Colorectal Cancer Screening and Diagnostics. *Biosensors (Basel)* 2023; **13** [PMID: 37887119 DOI: 10.3390/bios13100926]

24 **Yao T**, Sun Q, Xiong K, Su Y, Zhao Q, Zhang C, Zhang L, Li X, Fang H. Optimization of screening strategies for colorectal cancer based on fecal DNA and occult blood testing. *Eur J Public Health* 2023; **33**: 336-341 [PMID: 36905607 DOI: 10.1093/eurpub/ckad032]

25 **Chan SCH**, Liang JQ. Advances in tests for colorectal cancer screening and diagnosis. *Expert Rev Mol Diagn* 2022; **22**: 449-460 [PMID: 35400293 DOI: 10.1080/14737159.2022.2065197]

26 **Ferrari A**, Neefs I, Hoeck S, Peeters M, Van Hal G. Towards Novel Non-Invasive Colorectal Cancer Screening Methods: A Comprehensive Review. *Cancers (Basel)* 2021; **13** [PMID: 33920293 DOI: 10.3390/cancers13081820]

27 **Issa IA**, Noureddine M. Colorectal cancer screening: An updated review of the available options. *World J Gastroenterol* 2017; **23**: 5086-5096 [PMID: 28811705 DOI: 10.3748/wjg.v23.i28.5086]

28 **Binefa G**, Rodríguez-Moranta F, Teule A, Medina-Hayas M. Colorectal cancer: from prevention to personalized medicine. *World J Gastroenterol* 2014; **20**: 6786-6808 [PMID: 24944469 DOI: 10.3748/wjg.v20.i22.6786]

29 **Wang QQ**, Zhou L, Qin G, Tan C, Zhou YC, Yao SK. Leukocyte immunoglobulin-like receptor B2 overexpression as a promising therapeutic target and noninvasive screening biomarker for colorectal cancer. *World J Gastroenterol* 2023; **29**: 5313-5326 [PMID: 37899785 DOI: 10.3748/wjg.v29.i37.5313]

30 **Li Y**, Li B, Jiang R, Liao L, Zheng C, Yuan J, Zeng L, Hu K, Zhang Y, Mei W, Hong Z, Xiao B, Kong L, Han K, Tang J, Jiang W, Pan Z, Zhang S, Ding P. A novel screening method of DNA methylation biomarkers helps to improve the detection of colorectal cancer and precancerous lesions. *Cancer Med* 2023; **12**: 20626-20638 [PMID: 37881109 DOI: 10.1002/cam4.6511]

31 **Okugawa Y**, Toiyama Y, Toden S, Mitoma H, Nagasaka T, Tanaka K, Inoue Y, Kusunoki M, Boland CR, Goel A. Clinical significance of SNORA42 as an oncogene and a prognostic biomarker in colorectal cancer. *Gut* 2017; **66**: 107-117 [PMID: 26475630 DOI:

10.1136/gutjnl-2015-309359]
32 **Weng M**, Wu D, Yang C, Peng H, Wang G, Wang T, Li X. Noncoding RNAs in the development, diagnosis, and prognosis of colorectal cancer. *Transl Res* 2017; **181**: 108-120 [PMID: 27810413 DOI: 10.1016/j.trsl.2016.10.001]
33 **Esteller M**. Non-coding RNAs in human disease. *Nat Rev Genet* 2011; **12**: 861-874 [PMID: 22094949 DOI: 10.1038/nrg3074]
34 **Balakin AG**, Smith L, Fournier MJ. The RNA world of the nucleolus: two major families of small RNAs defined by different box elements with related functions. *Cell* 1996; **86**: 823-834 [PMID: 8797828 DOI: 10.1016/s0092-8674(00)80156-7]
35 **Henras AK**, Dez C, Henry Y. RNA structure and function in C/D and H/ACA s(no)RNPs. *Curr Opin Struct Biol* 2004; **14**: 335-343 [PMID: 15193314 DOI: 10.1016/j.sbi.2004.05.006]
36 **Khoshnevis S**, Dreggors RE, Hoffmann TFR, Ghalei H. A conserved Bcd1 interaction essential for box C/D snoRNP biogenesis. *J Biol Chem* 2019; **294**: 18360-18371 [PMID: 31537647 DOI: 10.1074/jbc.RA119.010222]
37 **Paul A**, Tiotiu D, Bragantini B, Marty H, Charpentier B, Massenet S, Labialle S. Bcd1p controls RNA loading of the core protein Nop58 during C/D box snoRNP biogenesis. *RNA* 2019; **25**: 496-506 [PMID: 30700579 DOI: 10.1261/rna.067967.118]
38 **Filipowicz W**, Pogacić V. Biogenesis of small nucleolar ribonucleoproteins. *Curr Opin Cell Biol* 2002; **14**: 319-327 [PMID: 12067654 DOI: 10.1016/s0955-0674(02)00334-4]
39 **Watkins NJ**, Bohnsack MT. The box C/D and H/ACA snoRNPs: key players in the modification, processing and the dynamic folding of ribosomal RNA. *Wiley Interdiscip Rev RNA* 2012; **3**: 397-414 [PMID: 22065625 DOI: 10.1002/wrna.117]
40 **Samarsky DA**, Fournier MJ, Singer RH, Bertrand E. The snoRNA box C/D motif directs nucleolar targeting and also couples snoRNA synthesis and localization. *EMBO J* 1998; **17**: 3747-3757 [PMID: 9649444 DOI: 10.1093/emboj/17.13.3747]
41 **Kiss-László Z**, Henry Y, Bachellerie JP, Caizergues-Ferrer M, Kiss T. Site-specific ribose methylation of preribosomal RNA: a novel function for small nucleolar RNAs. *Cell* 1996; **85**: 1077-1088 [PMID: 8674114 DOI: 10.1016/s0092-8674(00)81308-2]
42 **Bachellerie JP**, Michot B, Nicoloso M, Balakin A, Ni J, Fournier MJ. Antisense snoRNAs: a family of nucleolar RNAs with long complementarities to rRNA. *Trends Biochem Sci* 1995; **20**: 261-264 [PMID: 7667877 DOI: 10.1016/s0968-0004(00)89039-8]
43 **Kiss T**. Small nucleolar RNAs: an abundant group of noncoding RNAs with diverse cellular functions. *Cell* 2002; **109**: 145-148 [PMID: 12007400 DOI: 10.1016/s0092-8674(02)00718-3]
44 **Watkins NJ**, Gottschalk A, Neubauer G, Kastner B, Fabrizio P, Mann M, Lührmann R. Cbf5p, a potential pseudouridine synthase, and Nhp2p, a putative RNA-binding protein, are present together with Gar1p in all H BOX/ACA-motif snoRNPs and constitute a common bipartite structure. *RNA* 1998; **4**: 1549-1568 [PMID: 9848653 DOI: 10.1017/s1355838298980761]
45 **Hamma T**, Reichow SL, Varani G, Ferré-D'Amaré AR. The Cbf5-Nop10 complex is a molecular bracket that organizes box H/ACA RNPs. *Nat Struct Mol Biol* 2005; **12**: 1101-1107 [PMID: 16286935 DOI: 10.1038/nsmb1036]
46 **Yu YT**, Meier UT. RNA-guided isomerization of uridine to pseudouridine--pseudouridylation. *RNA Biol* 2014; **11**: 1483-1494 [PMID: 25590339 DOI: 10.4161/15476286.2014.972855]
47 **Ganot P**, Bortolin ML, Kiss T. Site-specific pseudouridine formation in preribosomal RNA is guided by small nucleolar RNAs. *Cell* 1997; **89**: 799-809 [PMID: 9182768 DOI: 10.1016/s0092-8674(00)80263-9]
48 **Kiss T**, Fayet-Lebaron E, Jády BE. Box H/ACA small ribonucleoproteins. *Mol Cell* 2010; **37**: 597-606 [PMID: 20227365 DOI: 10.1016/j.molcel.2010.01.032]
49 **Pogacić V**, Dragon F, Filipowicz W. Human H/ACA small nucleolar RNPs and telomerase share evolutionarily conserved proteins NHP2 and NOP10. *Mol Cell Biol* 2000; **20**: 9028-9040 [PMID: 11074001 DOI: 10.1128/MCB.20.23.9028-9040.2000]
50 **MacNeil DE**, Bensoussan HJ, Autexier C. Telomerase Regulation from Beginning to the End. *Genes (Basel)* 2016; **7** [PMID: 27649246 DOI: 10.3390/genes7090064]
51 **Deryusheva S**, Gall JG. scaRNAs and snoRNAs: Are they limited to specific classes of substrate RNAs? *RNA* 2019; **25**: 17-22 [PMID: 30301832 DOI: 10.1261/rna.068593.118]
52 **Marnef A**, Richard P, Pinzón N, Kiss T. Targeting vertebrate intron-encoded box C/D 2'-O-methylation guide RNAs into the Cajal body. *Nucleic Acids Res* 2014; **42**: 6616-6629 [PMID: 24753405 DOI: 10.1093/nar/gku287]
53 **Zhang H**, Liu X, Zhang W, Deng J, Lin C, Qi Z, Li Y, Gu Y, Wang Q, Shen L, Wang Z. Oncogene SCARNA12 as a potential diagnostic biomarker for colorectal cancer. *Mol Biomed* 2023; **4**: 37 [PMID: 37907779 DOI: 10.1186/s43556-023-00147-x]
54 **Zhang Z**, Tao Y, Hua Q, Cai J, Ye X, Li H. SNORA71A Promotes Colorectal Cancer Cell Proliferation, Migration, and Invasion. *Biomed Res Int* 2020; **2020**: 8284576 [PMID: 33083486 DOI: 10.1155/2020/8284576]
55 **Allmang C**, Kufel J, Chanfreau G, Mitchell P, Petfalski E, Tollervey D. Functions of the exosome in rRNA, snoRNA and snRNA synthesis. *EMBO J* 1999; **18**: 5399-5410 [PMID: 10508172 DOI: 10.1093/emboj/18.19.5399]
56 **Huang C**, Shi J, Guo Y, Huang W, Huang S, Ming S, Wu X, Zhang R, Ding J, Zhao W, Jia J, Huang X, Xiang AP, Shi Y, Yao C. A snoRNA modulates mRNA 3' end processing and regulates the expression of a subset of mRNAs. *Nucleic Acids Res* 2017; **45**: 8647-8660 [PMID: 28911119 DOI: 10.1093/nar/gkx651]
57 **Li S**, Yang Q, Zhou Z, Fu M, Yang X, Hao K, Liu Y. SNHG3 cooperates with ELAVL2 to modulate cell apoptosis and extracellular matrix accumulation by stabilizing SNAI2 in human trabecular meshwork cells under oxidative stress. *Environ Toxicol* 2021; **36**: 1070-1079 [PMID: 33522089 DOI: 10.1002/tox.23106]
58 **Decatur WA**, Fournier MJ. rRNA modifications and ribosome function. *Trends Biochem Sci* 2002; **27**: 344-351 [PMID: 12114023 DOI: 10.1016/s0968-0004(02)02109-6]
59 **Zhong F**, Zhou N, Wu K, Guo Y, Tan W, Zhang H, Zhang X, Geng G, Pan T, Luo H, Zhang Y, Xu Z, Liu J, Liu B, Gao W, Liu C, Ren L, Li J, Zhou J. A SnoRNA-derived piRNA interacts with human interleukin-4 pre-mRNA and induces its decay in nuclear exosomes. *Nucleic Acids Res* 2015; **43**: 10474-10491 [PMID: 26405199 DOI: 10.1093/nar/gkv954]
60 **Scott MS**, Ono M. From snoRNA to miRNA: Dual function regulatory non-coding RNAs. *Biochimie* 2011; **93**: 1987-1992 [PMID: 21664409 DOI: 10.1016/j.biochi.2011.05.026]
61 **Brameier M**, Herwig A, Reinhardt R, Walter L, Gruber J. Human box C/D snoRNAs with miRNA like functions: expanding the range of regulatory RNAs. *Nucleic Acids Res* 2011; **39**: 675-686 [PMID: 20846955 DOI: 10.1093/nar/gkq776]
62 **Bergeron D**, Laforest C, Carpentier S, Calvé A, Fafard-Couture É, Deschamps-Francoeur G, Scott MS. SnoRNA copy regulation affects family size, genomic location and family abundance levels. *BMC Genomics* 2021; **22**: 414 [PMID: 34090325 DOI: 10.1186/s12864-021-07757-1]
63 **Bratkovič T**, Božič J, Rogelj B. Functional diversity of small nucleolar RNAs. *Nucleic Acids Res* 2020; **48**: 1627-1651 [PMID: 31828325

DOI: 10.1093/nar/gkz1140]
64 **Bratkovič T**, Rogelj B. The many faces of small nucleolar RNAs. *Biochim Biophys Acta* 2014; **1839**: 438-443 [PMID: 24735946 DOI: 10.1016/j.bbagrm.2014.04.009]
65 **Fang X**, Yang D, Luo H, Wu S, Dong W, Xiao J, Yuan S, Ni A, Zhang KJ, Liu XY, Chu L. SNORD126 promotes HCC and CRC cell growth by activating the PI3K-AKT pathway through FGFR2. *J Mol Cell Biol* 2017; **9**: 243-255 [PMID: 27913571 DOI: 10.1093/jmcb/mjw048]
66 **Sahoo T**, del Gaudio D, German JR, Shinawi M, Peters SU, Person RE, Garnica A, Cheung SW, Beaudet AL. Prader-Willi phenotype caused by paternal deficiency for the HBII-85 C/D box small nucleolar RNA cluster. *Nat Genet* 2008; **40**: 719-721 [PMID: 18500341 DOI: 10.1038/ng.158]
67 **Gallagher RC**, Pils B, Albalwi M, Francke U. Evidence for the role of PWCR1/HBII-85 C/D box small nucleolar RNAs in Prader-Willi syndrome. *Am J Hum Genet* 2002; **71**: 669-678 [PMID: 12154412 DOI: 10.1086/342408]
68 **O'Brien JE Jr**, Kibiryeva N, Zhou XG, Marshall JA, Lofland GK, Artman M, Chen J, Bittel DC. Noncoding RNA expression in myocardium from infants with tetralogy of Fallot. *Circ Cardiovasc Genet* 2012; **5**: 279-286 [PMID: 22528145 DOI: 10.1161/CIRCGENETICS.111.961474]
69 **Lester E**, Ooi FK, Bakkar N, Ayers J, Woerman AL, Wheeler J, Bowser R, Carlson GA, Prusiner SB, Parker R. Tau aggregates are RNA-protein assemblies that mislocalize multiple nuclear speckle components. *Neuron* 2021; **109**: 1675-1691.e9 [PMID: 33848474 DOI: 10.1016/j.neuron.2021.03.026]
70 **Romano G**, Veneziano D, Acunzo M, Croce CM. Small non-coding RNA and cancer. *Carcinogenesis* 2017; **38**: 485-491 [PMID: 28449079 DOI: 10.1093/carcin/bgx026]
71 **Tycowski KT**, Shu MD, Steitz JA. A mammalian gene with introns instead of exons generating stable RNA products. *Nature* 1996; **379**: 464-466 [PMID: 8559254 DOI: 10.1038/379464a0]
72 **Xu G**, Yang F, Ding CL, Zhao LJ, Ren H, Zhao P, Wang W, Qi ZT. Small nucleolar RNA 113-1 suppresses tumorigenesis in hepatocellular carcinoma. *Mol Cancer* 2014; **13**: 216 [PMID: 25217841 DOI: 10.1186/1476-4598-13-216]
73 **Mei YP**, Liao JP, Shen J, Yu L, Liu BL, Liu L, Li RY, Ji L, Dorsey SG, Jiang ZR, Katz RL, Wang JY, Jiang F. Small nucleolar RNA 42 acts as an oncogene in lung tumorigenesis. *Oncogene* 2012; **31**: 2794-2804 [PMID: 21986946 DOI: 10.1038/onc.2011.449]
74 **Su H**, Xu T, Ganapathy S, Shadfan M, Long M, Huang TH, Thompson I, Yuan ZM. Elevated snoRNA biogenesis is essential in breast cancer. *Oncogene* 2014; **33**: 1348-1358 [PMID: 23542174 DOI: 10.1038/onc.2013.89]
75 **Wang B**, Zhao Y, Li Y, Xu Y, Chen Y, Jiang Q, Yao D, Zhang L, Hu X, Fu C, Zhang S, Chen S. A plasma SNORD33 signature predicts platinum benefit in metastatic triple-negative breast cancer patients. *Mol Cancer* 2022; **21**: 22 [PMID: 35042534 DOI: 10.1186/s12943-022-01504-0]
76 **Li C**, Wu L, Liu P, Li K, Zhang Z, He Y, Liu Q, Jiang P, Yang Z, Liu Z, Yuan Y, Chang L. The C/D box small nucleolar RNA SNORD52 regulated by Upf1 facilitates Hepatocarcinogenesis by stabilizing CDK1. *Theranostics* 2020; **10**: 9348-9363 [PMID: 32802196 DOI: 10.7150/thno.47677]
77 **Zhuo Y**, Li S, Hu W, Zhang Y, Shi Y, Zhang F, Zhang J, Wang J, Liao M, Chen J, Qian H, Li D, Sun C. Targeting SNORA38B attenuates tumorigenesis and sensitizes immune checkpoint blockade in non-small cell lung cancer by remodeling the tumor microenvironment *via* regulation of GAB2/AKT/mTOR signaling pathway. *J Immunother Cancer* 2022; **10** [PMID: 35577506 DOI: 10.1136/jitc-2021-004113]
78 **Welch HG**, Robertson DJ. Colorectal Cancer on the Decline--Why Screening Can't Explain It All. *N Engl J Med* 2016; **374**: 1605-1607 [PMID: 27119236 DOI: 10.1056/NEJMp1600448]
79 **Fearon ER**. Molecular genetics of colorectal cancer. *Annu Rev Pathol* 2011; **6**: 479-507 [PMID: 21090969 DOI: 10.1146/annurev-pathol-011110-130235]
80 **Jiang MC**, Ni JJ, Cui WY, Wang BY, Zhuo W. Emerging roles of lncRNA in cancer and therapeutic opportunities. *Am J Cancer Res* 2019; **9**: 1354-1366 [PMID: 31392074]
81 **Liang J**, Wen J, Huang Z, Chen XP, Zhang BX, Chu L. Small Nucleolar RNAs: Insight Into Their Function in Cancer. *Front Oncol* 2019; **9**: 587 [PMID: 31338327 DOI: 10.3389/fonc.2019.00587]
82 **Shen L**, Lu W, Huang Y, He J, Wang Q, Zheng X, Wang Z. SNORD15B and SNORA5C: Novel Diagnostic and Prognostic Biomarkers for Colorectal Cancer. *Biomed Res Int* 2022; **2022**: 8260800 [PMID: 35586811 DOI: 10.1155/2022/8260800]
83 **Yang X**, Li Y, Li L, Liu J, Wu M, Ye M. SnoRNAs are involved in the progression of ulcerative colitis and colorectal cancer. *Dig Liver Dis* 2017; **49**: 545-551 [PMID: 28110922 DOI: 10.1016/j.dld.2016.12.029]
84 **Yoshida K**, Toden S, Weng W, Shigeyasu K, Miyoshi J, Turner J, Nagasaka T, Ma Y, Takayama T, Fujiwara T, Goel A. SNORA21 - An Oncogenic Small Nucleolar RNA, with a Prognostic Biomarker Potential in Human Colorectal Cancer. *EBioMedicine* 2017; **22**: 68-77 [PMID: 28734806 DOI: 10.1016/j.ebiom.2017.07.009]
85 **Shen L**, Lin C, Lu W, He J, Wang Q, Huang Y, Zheng X, Wang Z. Involvement of the oncogenic small nucleolar RNA SNORA24 in regulation of p53 stability in colorectal cancer. *Cell Biol Toxicol* 2023; **39**: 1377-1394 [PMID: 36087186 DOI: 10.1007/s10565-022-09765-7]
86 **Liu Y**, Zhao C, Sun J, Wang G, Ju S, Qian C, Wang X. Overexpression of small nucleolar RNA SNORD1C is associated with unfavorable outcome in colorectal cancer. *Bioengineered* 2021; **12**: 8943-8952 [PMID: 34702132 DOI: 10.1080/21655979.2021.1990194]
87 **Liu Y**, Zhao C, Wang G, Chen J, Ju S, Huang J, Wang X. SNORD1C maintains stemness and 5-FU resistance by activation of Wnt signaling pathway in colorectal cancer. *Cell Death Discov* 2022; **8**: 200 [PMID: 35422067 DOI: 10.1038/s41420-022-00996-5]
88 **Xu L**, Ziegelbauer J, Wang R, Wu WW, Shen RF, Juhl H, Zhang Y, Rosenberg A. Distinct Profiles for Mitochondrial t-RNAs and Small Nucleolar RNAs in Locally Invasive and Metastatic Colorectal Cancer. *Clin Cancer Res* 2016; **22**: 773-784 [PMID: 26384739 DOI: 10.1158/1078-0432.CCR-15-0737]
89 **Huang L**, Liang XZ, Deng Y, Liang YB, Zhu X, Liang XY, Luo DZ, Chen G, Fang YY, Lan HH, Zeng JH. Prognostic value of small nucleolar RNAs (snoRNAs) for colon adenocarcinoma based on RNA sequencing data. *Pathol Res Pract* 2020; **216**: 152937 [PMID: 32312483 DOI: 10.1016/j.prp.2020.152937]
90 **Yuan S**, Wu Y, Wang Y, Chen J, Chu L. An Oncolytic Adenovirus Expressing SNORD44 and GAS5 Exhibits Antitumor Effect in Colorectal Cancer Cells. *Hum Gene Ther* 2017; **28**: 690-700 [PMID: 28530127 DOI: 10.1089/hum.2017.041]
91 **Siprashvili Z**, Webster DE, Johnston D, Shenoy RM, Ungewickell AJ, Bhaduri A, Flockhart R, Zarnegar BJ, Che Y, Meschi F, Puglisi JD, Khavari PA. The noncoding RNAs SNORD50A and SNORD50B bind K-Ras and are recurrently deleted in human cancer. *Nat Genet* 2016; **48**: 53-58 [PMID: 26595770 DOI: 10.1038/ng.3452]
92 **Tosar JP**, García-Silva MR, Cayota A. Circulating SNORD57 rather than piR-54265 is a promising biomarker for colorectal cancer: common pitfalls in the study of somatic piRNAs in cancer. *RNA* 2021; **27**: 403-410 [PMID: 33376191 DOI: 10.1261/rna.078444.120]
93 **Gao L**, Ma J, Mannoor K, Guarnera MA, Shetty A, Zhan M, Xing L, Stass SA, Jiang F. Genome-wide small nucleolar RNA expression

analysis of lung cancer by next-generation deep sequencing. *Int J Cancer* 2015; **136**: E623-E629 [PMID: 25159866 DOI: 10.1002/ijc.29169]

94 **McMahon M**, Contreras A, Holm M, Uechi T, Forester CM, Pang X, Jackson C, Calvert ME, Chen B, Quigley DA, Luk JM, Kelley RK, Gordan JD, Gill RM, Blanchard SC, Ruggero D. A single H/ACA small nucleolar RNA mediates tumor suppression downstream of oncogenic RAS. *Elife* 2019; **8** [PMID: 31478838 DOI: 10.7554/eLife.48847]

95 **Zhang D**, Zhou J, Gao J, Wu RY, Huang YL, Jin QW, Chen JS, Tang WZ, Yan LH. Targeting snoRNAs as an emerging method of therapeutic development for cancer. *Am J Cancer Res* 2019; **9**: 1504-1516 [PMID: 31497339]

96 **Bian Z**, Zhou M, Cui K, Yang F, Cao Y, Sun S, Liu B, Gong L, Li J, Wang X, Li C, Yao S, Yin Y, Huang S, Fei B, Huang Z. SNHG17 promotes colorectal tumorigenesis and metastasis *via* regulating Trim23-PES1 axis and miR-339-5p-FOSL2-SNHG17 positive feedback loop. *J Exp Clin Cancer Res* 2021; **40**: 360 [PMID: 34782005 DOI: 10.1186/s13046-021-02162-8]

97 **Mannoor K**, Shen J, Liao J, Liu Z, Jiang F. Small nucleolar RNA signatures of lung tumor-initiating cells. *Mol Cancer* 2014; **13**: 104 [PMID: 24886050 DOI: 10.1186/1476-4598-13-104]

98 **Jiang F**, Qiu Q, Khanna A, Todd NW, Deepak J, Xing L, Wang H, Liu Z, Su Y, Stass SA, Katz RL. Aldehyde dehydrogenase 1 is a tumor stem cell-associated marker in lung cancer. *Mol Cancer Res* 2009; **7**: 330-338 [PMID: 19276181 DOI: 10.1158/1541-7786.MCR-08-0393]

99 **Jiang X**, Yang Z, Li Z. Zinc finger antisense 1: A long noncoding RNA with complex roles in human cancers. *Gene* 2019; **688**: 26-33 [PMID: 30503395 DOI: 10.1016/j.gene.2018.11.075]

100 **Bai B**, Yegnasubramanian S, Wheelan SJ, Laiho M. RNA-Seq of the nucleolus reveals abundant SNORD44-derived small RNAs. *PLoS One* 2014; **9**: e107519 [PMID: 25203660 DOI: 10.1371/journal.pone.0107519]

101 **Mai D**, Ding P, Tan L, Zhang J, Pan Z, Bai R, Li C, Li M, Zhou Y, Tan W, Zhou Z, Li Y, Zhou A, Ye Y, Pan L, Zheng Y, Su J, Zuo Z, Liu Z, Zhao Q, Li X, Huang X, Li W, Wu S, Jia W, Zou S, Wu C, Xu RH, Zheng J, Lin D. PIWI-interacting RNA-54265 is oncogenic and a potential therapeutic target in colorectal adenocarcinoma. *Theranostics* 2018; **8**: 5213-5230 [PMID: 30555542 DOI: 10.7150/thno.28001]

102 **Mai D**, Zheng Y, Guo H, Ding P, Bai R, Li M, Ye Y, Zhang J, Huang X, Liu D, Sui Q, Pan L, Su J, Deng J, Wu G, Li R, Deng S, Bai Y, Ligu Y, Tan W, Wu C, Wu T, Zheng J, Lin D. Serum piRNA-54265 is a New Biomarker for early detection and clinical surveillance of Human Colorectal Cancer. *Theranostics* 2020; **10**: 8468-8478 [PMID: 32754257 DOI: 10.7150/thno.46241]

103 **Su X**, Feng C, Wang S, Shi L, Gu Q, Zhang H, Lan X, Zhao Y, Qiang W, Ji M, Hou P. The noncoding RNAs SNORD50A and SNORD50B-mediated TRIM21-GMPS interaction promotes the growth of p53 wild-type breast cancers by degrading p53. *Cell Death Differ* 2021; **28**: 2450-2464 [PMID: 33742136 DOI: 10.1038/s41418-021-00762-7]

104 **Krens LL**, Baas JM, Gelderblom H, Guchelaar HJ. Therapeutic modulation of k-ras signaling in colorectal cancer. *Drug Discov Today* 2010; **15**: 502-516 [PMID: 20594936 DOI: 10.1016/j.drudis.2010.05.012]

105 **Jung G**, Hernández-Illán E, Moreira L, Balaguer F, Goel A. Epigenetics of colorectal cancer: biomarker and therapeutic potential. *Nat Rev Gastroenterol Hepatol* 2020; **17**: 111-130 [PMID: 31900466 DOI: 10.1038/s41575-019-0230-y]

106 **Puccini A**, Berger MD, Naseem M, Tokunaga R, Battaglin F, Cao S, Hanna DL, McSkane M, Soni S, Zhang W, Lenz HJ. Colorectal cancer: epigenetic alterations and their clinical implications. *Biochim Biophys Acta Rev Cancer* 2017; **1868**: 439-448 [PMID: 28939182 DOI: 10.1016/j.bbcan.2017.09.003]

107 **Lichtenstern CR**, Ngu RK, Shalapour S, Karin M. Immunotherapy, Inflammation and Colorectal Cancer. *Cells* 2020; **9** [PMID: 32143413 DOI: 10.3390/cells9030618]

108 **Dienstmann R**, Vermeulen L, Guinney J, Kopetz S, Tejpar S, Tabernero J. Consensus molecular subtypes and the evolution of precision medicine in colorectal cancer. *Nat Rev Cancer* 2017; **17**: 79-92 [PMID: 28050011 DOI: 10.1038/nrc.2016.126]

109 **Herman JG**, Umar A, Polyak K, Graff JR, Ahuja N, Issa JP, Markowitz S, Willson JK, Hamilton SR, Kinzler KW, Kane MF, Kolodner RD, Vogelstein B, Kunkel TA, Baylin SB. Incidence and functional consequences of hMLH1 promoter hypermethylation in colorectal carcinoma. *Proc Natl Acad Sci U S A* 1998; **95**: 6870-6875 [PMID: 9618505 DOI: 10.1073/pnas.95.12.6870]

110 **Vacante M**, Ciuni R, Basile F, Biondi A. The Liquid Biopsy in the Management of Colorectal Cancer: An Overview. *Biomedicines* 2020; **8** [PMID: 32858879 DOI: 10.3390/biomedicines8090308]

111 **Marcuello M**, Vymetalkova V, Neves RPL, Duran-Sanchon S, Vedeld HM, Tham E, van Dalum G, Flügen G, Garcia-Barberan V, Fijneman RJ, Castells A, Vodicka P, Lind GE, Stoecklein NH, Heitzer E, Gironella M. Circulating biomarkers for early detection and clinical management of colorectal cancer. *Mol Aspects Med* 2019; **69**: 107-122 [PMID: 31189073 DOI: 10.1016/j.mam.2019.06.002]

112 **Zhang Z**, Zhang J, Diao L, Han L. Small non-coding RNAs in human cancer: function, clinical utility, and characterization. *Oncogene* 2021; **40**: 1570-1577 [PMID: 33452456 DOI: 10.1038/s41388-020-01630-3]

113 **Zygulska AL**, Pierzchalski P. Novel Diagnostic Biomarkers in Colorectal Cancer. *Int J Mol Sci* 2022; **23** [PMID: 35055034 DOI: 10.3390/ijms23020852]

114 **Abel Y**, Rederstorff M. SnoRNAs and the emerging class of sdRNAs: Multifaceted players in oncogenesis. *Biochimie* 2019; **164**: 17-21 [PMID: 31078583 DOI: 10.1016/j.biochi.2019.05.006]

115 **Mannoor K**, Liao J, Jiang F. Small nucleolar RNAs in cancer. *Biochim Biophys Acta* 2012; **1826**: 121-128 [PMID: 22498252 DOI: 10.1016/j.bbcan.2012.03.005]

116 **Li Q**, Xie B, Chen X, Lu B, Chen S, Sheng X, Zhao Y. SNORD6 promotes cervical cancer progression by accelerating E6-mediated p53 degradation. *Cell Death Discov* 2023; **9**: 192 [PMID: 37369687 DOI: 10.1038/s41420-023-01488-w]

117 **Toth K**, Doronin K, Tollefson AE, Wold WS. A multitasking oncolytic adenovirus vector. *Mol Ther* 2003; **7**: 435-437 [PMID: 12727104 DOI: 10.1016/s1525-0016(03)00071-6]

118 **Xu HN**, Huang WD, Cai Y, Ding M, Gu JF, Wei N, Sun LY, Cao X, Li HG, Zhang KJ, Liu XR, Liu XY. HCCS1-armed, quadruple-regulated oncolytic adenovirus specific for liver cancer as a cancer targeting gene-viro-therapy strategy. *Mol Cancer* 2011; **10**: 133 [PMID: 22040050 DOI: 10.1186/1476-4598-10-133]

119 **Zhao L**, Gu J, Dong A, Zhang Y, Zhong L, He L, Wang Y, Zhang J, Zhang Z, Huiwang J, Qian Q, Qian C, Liu X. Potent antitumor activity of oncolytic adenovirus expressing mda-7/IL-24 for colorectal cancer. *Hum Gene Ther* 2005; **16**: 845-858 [PMID: 16000066 DOI: 10.1089/hum.2005.16.845]

World Journal of Gastroenterology

Submit a Manuscript: https://www.f6publishing.com

World J Gastroenterol 2024 January 14; 30(2): 128-136

DOI: 10.3748/wjg.v30.i2.128

ISSN 1007-9327 (print) ISSN 2219-2840 (online)

MINIREVIEWS

Hepatocardiorenal syndrome in liver cirrhosis: Recognition of a new entity?

Henry H L Wu, Amina Rakisheva, Arvind Ponnusamy, Rajkumar Chinnadurai

Specialty type: Gastroenterology and hepatology

Provenance and peer review: Invited article; Externally peer reviewed.

Peer-review model: Single blind

Peer-review report's scientific quality classification

Grade A (Excellent): 0
Grade B (Very good): B
Grade C (Good): C
Grade D (Fair): 0
Grade E (Poor): 0

P-Reviewer: El-Nakeep S, Egypt; Zhao P, China

Received: November 6, 2023
Peer-review started: November 6, 2023
First decision: November 30, 2023
Revised: December 5, 2023
Accepted: December 28, 2023
Article in press: December 28, 2023
Published online: January 14, 2024

Henry H L Wu, Renal Research, Kolling Institute of Medical Research, Royal North Shore Hospital & The University of Sydney, St. Leonards (Sydney) 2065, New South Wales, Australia

Amina Rakisheva, Department of Cardiology, City Cardiological Center, Almaty 050000, Kazakhstan

Arvind Ponnusamy, Department of Renal Medicine, Royal Preston Hospital, Preston PR2 9HT, United Kingdom

Rajkumar Chinnadurai, Donal O'Donoghue Renal Research Centre & Department of Renal Medicine, Northern Care Alliance National Health Service Foundation Trust, Salford M6 8HD, United Kingdom

Corresponding author: Henry H L Wu, MBChB, Academic Editor, Academic Fellow, Doctor, Honorary Research Fellow, Renal Research, Kolling Institute of Medical Research, Royal North Shore Hospital & The University of Sydney, Reserve Road, St. Leonards (Sydney) 2065, New South Wales, Australia. henrywu96@yahoo.com

Abstract

Emerging evidence and perspectives have pointed towards the heart playing an important role in hepatorenal syndrome (HRS), outside of conventional understanding that liver cirrhosis is traditionally considered the sole origin of a cascade of pathophysiological mechanisms directly affecting the kidneys in this context. In the absence of established heart disease, cirrhotic cardiomyopathy may occur more frequently in those with liver cirrhosis and kidney disease. It is a specific form of cardiac dysfunction characterized by blunted contractile responsiveness to stress stimuli and altered diastolic relaxation with electrophysiological abnormalities. Despite the clinical description of these potential cardiac-related complications of the liver, the role of the heart has traditionally been an overlooked aspect of circulatory dysfunction in HRS. Yet from a physiological sense, temporality (prior onset) of cardiorenal interactions in HRS and positive effects stemming from portosystemic shunting demonstrated an important role of the heart in the development and progression of kidney dysfunction in cirrhotic patients. In this review, we discuss current concepts surrounding how the heart may influence the development and progression of HRS, and the role of systemic inflammation and endothelial dysfunction causing circulatory dysfunction within this setting. The temporality of heart and kidney dysfunction in HRS will be

discussed. For a subgroup of patients who receive portosystemic shunting, the dynamics of cardiorenal interactions following treatment is reviewed. Continued research to determine the unknowns in this topic is anticipated, hopefully to further clarify the intricacies surrounding the liver-heart-kidney connection and improve strategies for management.

Key Words: Hepatorenal syndrome; Cardiorenal syndrome; Cirrhosis; Cardiac dysfunction; Circulatory dysfunction

Core Tip: There is emerging evidence to suggest that the heart plays an important role in advanced liver disease and contributes significantly to hepatorenal syndrome (HRS) progression. It is now increasingly agreed upon that circulatory dysfunction in HRS is at least in part due to cardiac impairment, which can exist prior to kidney dysfunction in cirrhotic patients who develop HRS. There are numerous pathophysiological mechanisms which may co-exist in both hepatorenal and cardiorenal syndrome pathways, and treatments which ameliorate kidney dysfunction in HRS are likely to also address the mechanisms which lie within this intricate hepatocardiorenal syndrome entity that is being postulated.

Citation: Wu HHL, Rakisheva A, Ponnusamy A, Chinnadurai R. Hepatocardiorenal syndrome in liver cirrhosis: Recognition of a new entity? *World J Gastroenterol* 2024; 30(2): 128-136
URL: https://www.wjgnet.com/1007-9327/full/v30/i2/128.htm
DOI: https://dx.doi.org/10.3748/wjg.v30.i2.128

INTRODUCTION

Hepatorenal syndrome (HRS) is a condition that occurs during decompensated liver disease defined by volume-unresponsive kidney dysfunction in the absence of circulatory shock, identified structural kidney disease, and nephrotoxins[1]. Our current understanding of the condition recognizes the liver as the centerpiece of various pathophysiological processes which leads to multisystem failure[2,3]. A major characteristic feature of HRS which represents the liver-kidney connection is functional kidney failure due to portal hypertension and splanchnic arterial vasodilation, triggering a cascade of pathophysiologic events including maladaptive neurohormonal activation, which leads to intense renal vasoconstriction and subsequently urine sodium excretion[1-5]. This results in progressive kidney function decline and fluid overload.

Whilst there has been recognition on the negative impact of liver dysfunction upon the cardiovascular system, understanding the exact mechanisms which lead to this have not been fully established[6-8]. Ongoing advancement of laboratory technology and discovery of biomarkers certainly allowed for a more precise and closer monitoring of cardiac and circulatory function in HRS[9]. It is thought that cirrhotic cardiomyopathy occurs in HRS settings in the absence of previous cardiac co-morbidities because of blunted contractile responsiveness to stress stimuli and altered diastolic relaxation with electrophysiological abnormalities[10].

The former mainstream opinion in medicine views HRS and cardiorenal syndrome (CRS) as two separate conditions with distinct pathophysiological pathways. One with acute or chronic liver disease and the other with acute or chronic heart failure leading to kidney complications (in the case of CRS, acute or chronic kidney disease may also result in cardiac dysfunction)[11]. Evidence building from previous clinical observations is gradually pointing towards a significant relationship which connects between the liver, heart, and kidneys mechanistically in disease[12].

Throughout this review, we aim to explore the cardiac contribution towards circulatory changes and dysfunction in HRS, and whether there is indeed an undervalued element of CRS within the HRS pathway. We will also specifically explore the role of inflammation and endothelial dysfunction in the HRS pathway, given previous suggestions of its significance towards cardiorenal interactions in HRS. The temporality (prior onset) of cardiorenal interactions in HRS will be reviewed. With a substantial number of patients who may receive portosystemic shunting in advanced liver disease, we will also discuss the dynamics of cardiorenal interaction following treatment. Advancing our understanding in the intertwined relationship across the liver-heart-kidney connection is important to inform clinicians on the diagnostic and therapeutic implications within this complex setting.

The heart and its role in circulatory dysfunction in cirrhosis and HRS

Circulatory function in the early stages of cirrhotic liver disease is characterized by maintenance of its homeostasis through development of a hyperdynamic circulation[13]. This involves an increased cardiac output, heart rate and plasma volume. Because there is a normal or increased cardiac output in the initial phase of cirrhosis, general opinion considers the heart to be largely intact throughout the early disease processes[11,14]. The progression of circulatory dysfunction in cirrhosis is thought to be mainly led by systemic vascular resistance and arterial underfilling in the form of central hypovolemia[15]. It is now increasingly acknowledged that hemodynamic derangement typically occurs in later stages of cirrhosis because progressive decline in hemodynamic status in cardiac afterload is no longer responded to by an increase in cardiac output[11,14,15]. Previous longitudinal studies have demonstrated that baseline cardiac function

markers such as cardiac output and stroke volume were significantly lower in cirrhotic patients who subsequently developed HRS, and these markers further decreased with HRS progression[16].

What is significant in linking the pathophysiology that exist between the heart and liver and kidney dysfunction here is that neurohormonal activation is the cornerstone pathway which result in the development of both CRS and HRS[17,18]. In the case of CRS, numerous factors in cardiac dysfunction from a low cardiac output to diuretic treatment may result in heightened neurohormone levels and adverse consequences for the kidneys with their downstream[18]. Decline in estimated glomerular filtration rate and impairment in sodium and water excretion would be expected[19]. Furthermore, deterioration in the hemodynamics and function of the kidneys may occur with elevated right-sided cardiac pressure, leading to increased congestion in the kidney venous system[20]. The heart is a key driving factor for higher neurohormonal activity in later stages of cirrhosis progressing to HRS, considering abnormal cardiac output in the face of unaltered systemic vascular resistance[21,22]. This is supported by seminal results from a study by Krag *et al*[23], which found patients with cirrhosis who developed kidney failure during spontaneous bacterial peritonitis had a reduced cardiac output compared to those without kidney failure. Following treatment and resolution of spontaneous bacterial peritonitis, an even lower cardiac output was observed amongst patients with kidney failure. This is important to support the claim that abnormalities in cardiac inotropic and chronotropic function is an instrumental component of circulatory dysfunction in HRS, given current evidence point out irregulated neurohormonal activation as a key mechanism in HRS-related cardiac dysfunction[17,18,23].

Nevertheless, there have been more recent observations that it is an increased cardiac output, rather than low cardiac output, that is the instigator for progression to HRS[9,24-26]. Using dobutamine stress echocardiography to monitor patients with cirrhosis, Koshy *et al*[25] indicated that it is not the hyperdynamic cardiac output at rest, but rather an inability to increment this cardiac output during periods of physiological stress such as where there is infection and hemodynamic stress, that predisposes to the development of HRS. They noted that an impaired cardiac reserve (defined by a change in cardiac reserve < 25% with low-dose dobutamine), was associated with a 4-fold risk of progressing to HRS [25]. The investigators ultimately concluded that a hyperdynamic resting cardiac function may in fact represent patients encroaching on their resting state cardiac reserve[25]. This may have therapeutic implications because the use of β-blockers in this patient group can be harmful. Further study is required before we can verify the pathophysiological claims from this stance more confidently.

Impact of inflammation and endothelial dysfunction towards hepatocardiorenal interactions

Whilst hemodynamic and neurohormonal dysregulation has been primarily thought of as the main pathways of HRS manifestation and circulatory dysfunction in HRS, there is increasing evidence to suggest that systemic inflammation and endothelial dysfunction have a major role in this scenario by triggering splanchnic arterial vasodilation and other pathways[11,27,28]. Inflammatory response and endothelial dysfunction also lead to derangements of other organs such as the heart in decompensated liver disease and HRS[18,27]. The pathophysiological hallmarks of liver cirrhosis are associated with inflammation. Increased macrophage activation, pro-inflammatory cytokines, systemic oxidative stress and activated circulating monocytes and neutrophils are observed in cirrhotic disease[18,27]. In decompensated liver disease, such as when spontaneous bacterial peritonitis is present, it has been described that the degree of inflammation and endothelial dysfunction correlates with the severity of hepatic, cardiac and kidney dysfunction[29]. Commonly it is bacterial infections which precipitate the progression to HRS. The development of an aggressive inflammatory response is stimulated by translocation of bacteria and pathogen-associated molecular patterns from the intestine[30]. Animal models of cirrhosis suggest these profound inflammatory responses, especially the build-up of oxidative stress and tumor necrosis factor-α, may result in β-receptor signaling alterations and cardiac systolic function impairment[31]. It has been demonstrated that serum levels of lipopolysaccharide-binding protein are independently associated with the severity of left ventricular diastolic dysfunction (LVDD)[32,33]. Lipopolysaccharide-binding protein is a marker of bacterial endotoxin exposure[32]. Coupled with convincing evidence demonstrating the instrumental role played by endothelial dysfunction in CRS, such observations are important to indicate that inflammation is a very plausible pathophysiological process linking the liver-heart-kidney connection together in HRS.

Temporality of heart and kidney dysfunction in HRS

It is logical to assume that cardiac dysfunction would precede the manifestations of HRS in cirrhosis here given the postulations of how cardiac dysfunction may mechanistically contribute towards kidney dysfunction in cirrhosis. The original observational study by Ruiz-del-Arbol *et al*[34] have found that cirrhotic patients who develop HRS already presented with clinical features of cardiac dysfunction in the form of low stroke volume, for example, prior to kidney function decline. In their cohort of patients, Ruiz-del-Arbol *et al*[34] noted that a low cardiac output and increased plasma-renin activity at baseline appeared to be the only independent predictors for HRS development. Krag *et al*[23] found that there were more patients with low cardiac index at baseline (defined as < 1.5 L/min/m^2 measured by gated myocardial perfusion imaging) who developed HRS compared to those with higher cardiac index levels. Albeit significant additional cardiovascular stress during the procedure, the general direction of evidence have pointed towards liver transplantation reversing these aspects of cardiac dysfunction which are commonly observed in HRS, resulting in improved cardiac performance and restored hemodynamics post-transplantation[35,36]. These observations highlighted a temporal pattern of cardiac and kidney dysfunction in HRS, suggesting perhaps there is pathophysiological involvement of the heart in the manifestation of HRS and cardiac dysfunction is not simply just the consequence of a HRS-associated complication[23,37].

Clinical and therapeutic implications of hepatocardiorenal interactions in HRS

Given there could be cardiac contribution towards a myriad of pathophysiological effects in HRS as outlined from our review, it would be prudent to systematically evaluate and monitor cardiac function in advanced liver disease patients, including for those without previously known cardiac impairment. In cirrhotic disease and early HRS, abnormalities in left ventricular systolic function is usually identified late and often only diagnosed when individuals display a blunted response during hemodynamic or pharmacologic stress[38]. Therefore, an abnormal left ventricular systolic function may be clinically utilized as a specific prognostic indicator to determine at-risk subgroups of cirrhotic patients who are at higher risk of developing HRS[16]. The advent of more recently developed imaging methods may allow for better identification of subclinical cardiac dysfunction in HRS. For one, 2-dimensional speckle-tracking echocardiography assesses left ventricular regional myocardial function and global longitudinal strain (GLS) through tracking natural acoustic markers such as speckles[39,40]. This technique is likely to be less dependent on cardiac preload or afterload in comparison to standard echocardiography. A previous study by Altekin *et al*[41] using 2-dimensional speckle-tracking echocardiography has revealed that a reduced longitudinal systolic function is common amongst cirrhosis patients despite a normal ejection fraction.

A very recent study by Danielsen *et al*[9] utilized magnetic resonance imaging to assess cardiac function and peripheral blood flow in patients across a spectrum of liver disease, including those with HRS. The investigators characterized renal blood flow in their study where despite a high cardiac output in patients with HRS, they demonstrated lower renal artery flow compared to non-HRS groups[9]. These findings indicate that even with a hyperdynamic resting cardiac output there was inadequate kidney perfusion in early stages of HRS triggered by activation of the renin-angiotensin-aldosterone system[9]. It confirms the pathophysiological link of cardiac dysfunction being manifested during periods of physiological stress in cirrhosis resulting in progression to HRS. Moreover, contrary to updated consensus guidance that GLS is a prognostically accurate marker of systolic dysfunction in subclinical myocardial dysfunction in HRS, this study by Danielsen *et al*[9] concluded no significant differences were found in GLS in HRS patients with different levels of cardiac output.

Although it remains debatable, diastolic dysfunction could be a useful marker for prognostication in cirrhotic cardiomyopathy and HRS, which is often overlooked compared to systolic dysfunction within the clinical setting[42-44]. Ruíz-del-Árbol *et al*[43] investigated LVDD and its relationship with circulatory function and prognosis in cirrhotic patients with portal hypertension and normal serum creatinine levels. Monitoring 80 patients prospectively with conventional and tissue Doppler echocardiography as well as their systemic and hepatic hemodynamics and the activity of endogenous vasoactive systems, Ruíz-del-Árbol *et al*[43] noted 37 patients out of the 80 presenting with LVDD in which 14 of these 37 patients went on to develop HRS. They concluded that patient survival was associated with the extent of LVDD, and LVDD occurs simultaneously with changes in cardiac structure and function and is associated with an impairment of effective arterial blood volume in cirrhosis. Ultimately, LVDD demonstrated to be a sensitive marker for progression from cirrhosis to HRS and mortality[43]. These conclusions were concurred in the study from Premkumar *et al*[44], where their group additionally found that the degree of LVDD is significantly associated with health-related quality of life outcomes in cirrhotic patients.

Whilst guidelines are constantly revised and optimized focusing on the utilization of serum pro-brain natriuretic peptide (pro-BNP) as a screening marker for acute and chronic heart failure, there is emerging discussions over the past decade on its clinical utility to project cirrhosis severity, the presence of cirrhotic cardiomyopathy, and HRS[45,46]. Kapoor *et al*[47] performed a prospective observational study for 53 cirrhosis patients who underwent 2-dimensional Doppler echocardiography, and had their serum pro-BNP and troponin T levels measured. This study showed that diastolic dysfunction is highly prevalent in cirrhotic patients (56.6% of cohort), and that serum pro-BNP as well as QTc intervals were also significantly raised in those with diastolic dysfunction[47]. Moreover, this group of patients were also more likely to progress to HRS, as well as developing other complications of cirrhosis such as spontaneous bacterial peritonitis and hepatic encephalopathy compared to those without cardiac dysfunction[47]. Overall, despite encouraging developments in research and updated findings, further studies are imperative to inform clinicians on which cardiac testing and imaging methods are cost-effective and clinically reliable to reflect cardiac function in cirrhosis and HRS.

Many patients with decompensated liver disease may receive transjugular intrahepatic shunting (TIPS) to treat portal hypertension[48,49]. The changes in hepatocardiorenal interactions following TIPS are of interest as immediately after the procedure, blood from the splanchnic bed and portal system is unloaded into the systemic circulation[48,49]. The kidney's hemodynamic status is typically not affected unless there is change in the state of kidney perfusion with renal veins draining directly into the systemic circulation[50]. TIPS have shown efficacy on improving kidney function in patients across all stages of kidney status, where there is evidence of increased urinary sodium excretion indicative of improved kidney perfusion, and improved creatinine clearance[51]. Better kidney perfusion following TIPS is thought to be due to the mediating effects from cardiorenal interplay, which enhances cardiac inotropic function resulting in increased central blood volume and subsequently kidney perfusion[52]. Another positive effect which can result from TIPS to improve kidney function is its ability to improve endothelial function which follows the amelioration of systemic inflammation[53-55]. This is achieved from lowering pressures and shear stress in the portal system and preventing the intestinal translocation of bacteria[55]. More studies are needed to further distinguish the hepatocardiorenal interactions before TIPS and following TIPS in advanced liver disease.

In terms of other medical treatments, beyond its utility as a potent plasma and volume expander, the anti-inflammatory properties of albumin and its role in improving endothelial dysfunction during decompensated liver disease and HRS has further supported the notion that inflammation and endothelial dysfunction are key pathophysiological processes in the proposed hepatocardiorenal syndrome entity[56]. Rat studies have shown the infusion of albumin increases cardiac contractility through counteracting myocardial oxidative stress and inflammation[31]. It has been found that in spontaneous bacterial peritonitis, albumin instead of hydroxyethyl starch increased systemic vascular resistance

and the left ventricular stroke work index[57]. The incidence of HRS and mortality rate more than halved in cirrhotic patients with spontaneous bacterial peritonitis if albumin is added to antibiotic treatment[58].

The use of cardiac inotropes to reverse cardiac and kidney dysfunction in HRS have been considered. There are reports of successful use to reverse kidney dysfunction in refractory HRS, which indicates the contributive role of cardiorenal pathways within the HRS setting[59,60]. Otherwise, β-agonists have been thought of as being unsuitable in this setting, given there is downregulation of β-adrenergic receptors in cirrhosis[61,62]. It remains to be clarified what is the optimized strategy in prescribing cardiac inotrope therapy in HRS. There are other emerging treatment options with potential benefits in heart failure such as empagliflozin, urodilatin and urocortin which are currently investigated for use in HRS [63-67]. Serelaxin, which is a recombinant human relaxin-2 with cardioprotective effects in acute heart failure, has been evaluated in a phase II randomized-controlled trial[67]. The investigators noted significantly improved kidney perfusion in patients with decompensated liver disease who were prescribed serelaxin compared to the control group.

It is concurred from the majority of published evidence that there is a positive long-term cardiac outlook for patients with HRS following liver transplantation[36]. An important factor would be the individual's pre-existing cardiac status prior to transplantation, although cardiac dysfunction in cirrhosis does not appear to be linearly associated with severity of liver disease[43,68,69]. Whilst international consensus on an optimal strategy of assessing pre-transplant cardiac status remains desirable, it is now established that cirrhotic patients with cardiac risk factors selected for liver transplant should undergo a rigid evaluation for operative risk. There is significant cardiovascular stress associated with this major operation, particularly for those with pre-existing cardiac dysfunction due to cirrhosis, hence an accurate patient selection for liver transplantation and precise investigation for degree of cirrhotic cardiomyopathy is vital[70]. Pre-transplant screening for cirrhotic cardiomyopathy should be conducted independently of Child-Pugh or model for end-stage liver disease classifications. Results from electrocardiography may demonstrate early indications of cirrhotic cardiomyopathy in potential transplant candidates from the presence of QT interval prolongation. QT interval prolongation is considered the earliest sign of cirrhotic cardiomyopathy, with the prevalence of QT interval prolongation amongst cirrhotic patients shown to be reaching 60% in those with Child Pugh class C (compared with 25% in Child Pugh class A *vs* 51% in Child Pugh class B)[71,72]. Otherwise, the American Association for the Study of Liver Diseases currently recommends that it is mandatory for all liver transplant candidates to undergo transthoracic echocardiography as the minimum pre-transplant cardiac investigation[73].

Changes in cardiac preload and afterload due to fluid infusion and clamping of the hepatic vein would result in tremendous stress towards a post-transplant patient's cardiovascular homeostasis, irrespective of pre-existing cardiac status[74]. Meticulous management to ensure appropriate responses in myocardial contractility is important, and prompt fluid management with cardiac monitoring through transesophageal echocardiography and/or pulmonary artery catheterization are often required in the early post-transplant scenario[75]. There remains much uncertainty as to the optimal timing to restore to restore hemodynamics during the post-transplant phase, but it is expected that a progressive correction of portal hypertension and hyperdynamic status would ensue with a transplanted liver[76]. Previous studies have reported a high prevalence of post-transplant subtle, sub-clinical cardiac complications such as diastolic function deterioration and ventricular dysfunction[77,78]. Nevertheless, the prognostic ability of these events to predict short- and long-term cardiac and overall clinical outcomes remain in discussion due to a relative paucity of data currently. Further work to address this is needed.

CONCLUSION

Our historical understanding of HRS and the mechanisms affecting circulatory dysfunction is being challenged, with the emergence of data and hypotheses which consider the extent of the heart's involvement and contributory role in cirrhosis and HRS. Although the impact of the heart in HRS may result in varying levels of disease severity and clinical presentations, it is now increasingly established that circulatory dysfunction in HRS is at least in part due to cardiac impairment; that cardiac dysfunction commonly exist prior to kidney dysfunction in cirrhotic patients who develop HRS; that numerous cardinal pathophysiological pathways such as neurohormonal activation, inflammation and endothelial dysfunction are interlinked between HRS and CRS; and that treatments which are known to improve kidney dysfunction in HRS may also address pathophysiological mechanisms within the liver-heart-kidney connection (Figure 1).

Despite our increased knowledge, insight and appreciation into the existence of a hepatocardiorenal syndrome entity, there are still many unknowns in this novel model that requires further investigation (Table 1). We are still not at a stage where there is clarity on defining the criteria of hepatocardiorenal syndrome or even cirrhotic cardiomyopathy itself. The cardiac and circulatory disturbances within the HRS definition which are discussed in our review could instead represent a hepatic form of CRS, for example. In this scenario, the liver affects the kidneys primarily *via* cardiorenal pathways. Addressing the unknowns in this topic would be challenging due to the current scarcity of data and importantly, given the pathophysiological interactions which occur in HRS and CRS are still not entirely understood. There should also be consideration on how other metabolic pathways (*i.e.*, lipid and cholesterol metabolism) could potentially affect the liver-heart-kidney connection, given prior evidence of these being risk factors for disease in each organ[79,80]. We anticipate research efforts to hopefully provide further answers on current knowledge gaps, and to optimize the diagnostic and treatment approach for this patient population.

Table 1 Summary of current knowledge and remaining knowledge gaps within the liver-heart-kidney connection

What is currently known	Remaining knowledge gaps
Pathophysiological mechanisms behind the onset and progression of HRS[1-5]	Exact timing and sequelae of cirrhotic cardiomyopathy in the setting of HRS[10-25]
Targeted prevention and interventional strategies to prevent the onset and terminate the progression of HRS[1-5]	Potential pathophysiological mechanisms that interlink the onset and progression of cardiac dysfunction in HRS[11,18,23,27-34,37]
	Optimal screening markers and imaging modalities in the clinical setting to diagnose cardiac disease in cirrhosis and HRS, and to prognosticate outcomes[9,38-47]
	How can specific interventions like volume expansion using albumin and TIPS improve HRS-associated cardiac dysfunctions?[31,48-58]

HRS: Hepatorenal syndrome; TIPS: Transjugular intrahepatic portosystemic shunt.

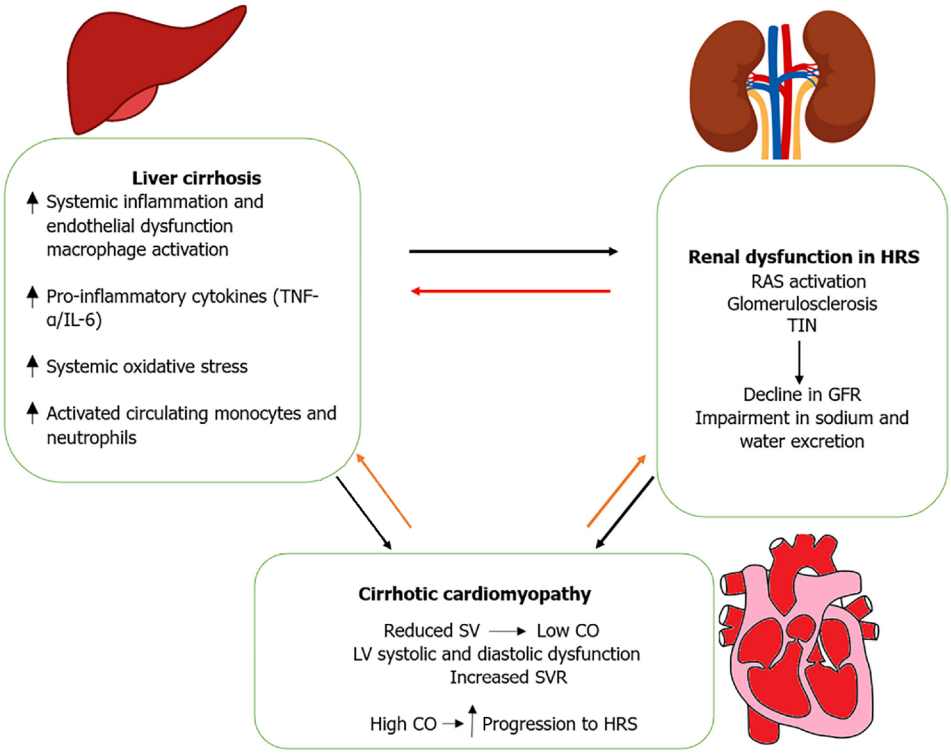

DOI: 10.3748/wjg.v30.i2.128

Figure 1 Potential pathophysiological mechanisms within the liver-heart-kidney connection. CO: Cardiac output; GFR: Glomerular filtration rate; LV: Left ventricle; RAS: Renin-angiotensin system; SV: Stroke volume; SVR: Systemic vascular resistance; TIN: Tubulointerstitial nephritis; HRS: Hepatorenal syndrome; TNF: Tumor necrosis factor; IL: Interleukin.

FOOTNOTES

Author contributions: Wu HHL and Chinnadurai R designed the outline and coordinated the writing of the paper; Wu HHL performed majority of the writing; Chinnadurai R prepared the figures and tables; Rakisheva A and Ponnusamy A provided review of the draft versions of the paper prior to submission of the final version; and all authors read and approved the final manuscript.

Conflict-of-interest statement: All the authors report no relevant conflicts of interest for this article.

Country/Territory of origin: Australia

ORCID number: Henry H L Wu 0000-0002-4561-0844; Arvind Ponnusamy 0000-0002-3882-9370; Rajkumar Chinnadurai 0000-0003-3973-6595.

S-Editor: Wang JJ
L-Editor: A
P-Editor: Yu HG

REFERENCES

1 **Francoz C**, Durand F, Kahn JA, Genyk YS, Nadim MK. Hepatorenal Syndrome. *Clin J Am Soc Nephrol* 2019; **14**: 774-781 [PMID: 30996046 DOI: 10.2215/CJN.12451018]
2 **Ginès P**, Solà E, Angeli P, Wong F, Nadim MK, Kamath PS. Hepatorenal syndrome. *Nat Rev Dis Primers* 2018; **4**: 23 [PMID: 30213943 DOI: 10.1038/s41572-018-0022-7]
3 **Simonetto DA**, Gines P, Kamath PS. Hepatorenal syndrome: pathophysiology, diagnosis, and management. *BMJ* 2020; **370**: m2687 [PMID: 32928750 DOI: 10.1136/bmj.m2687]
4 **Bloom S**, Kemp W, Lubel J. Portal hypertension: pathophysiology, diagnosis and management. *Intern Med J* 2015; **45**: 16-26 [PMID: 25230084 DOI: 10.1111/imj.12590]
5 **Arroyo V**, Guevara M, Ginès P. Hepatorenal syndrome in cirrhosis: pathogenesis and treatment. *Gastroenterology* 2002; **122**: 1658-1676 [PMID: 12016430 DOI: 10.1053/gast.2002.33575]
6 **Cogger VC**, Fraser R, Le Couteur DG. Liver dysfunction and heart failure. *Am J Cardiol* 2003; **91**: 1399 [PMID: 12767448 DOI: 10.1016/s0002-9149(03)00370-9]
7 **Lee H**, Lee YH, Kim SU, Kim HC. Metabolic Dysfunction-Associated Fatty Liver Disease and Incident Cardiovascular Disease Risk: A Nationwide Cohort Study. *Clin Gastroenterol Hepatol* 2021; **19**: 2138-2147.e10 [PMID: 33348045 DOI: 10.1016/j.cgh.2020.12.022]
8 **Ren Z**, Wesselius A, Stehouwer CDA, Brouwers MCGJ. Cardiovascular Implications of Metabolic Dysfunction-Associated Fatty Liver Disease. *Endocrinol Metab Clin North Am* 2023; **52**: 459-468 [PMID: 37495337 DOI: 10.1016/j.ecl.2023.01.002]
9 **Danielsen KV**, Wiese S, Busk T, Nabilou P, Kronborg TM, Petersen CL, Hove JD, Møller S, Bendtsen F. Cardiovascular Mapping in Cirrhosis From the Compensated Stage to Hepatorenal Syndrome: A Magnetic Resonance Study. *Am J Gastroenterol* 2022; **117**: 1269-1278 [PMID: 35916685 DOI: 10.14309/ajg.0000000000001847]
10 **Izzy M**, VanWagner LB, Lin G, Altieri M, Findlay JY, Oh JK, Watt KD, Lee SS; Cirrhotic Cardiomyopathy Consortium. Redefining Cirrhotic Cardiomyopathy for the Modern Era. *Hepatology* 2020; **71**: 334-345 [PMID: 31342529 DOI: 10.1002/hep.30875]
11 **Kazory A**, Ronco C. Hepatorenal Syndrome or Hepatocardiorenal Syndrome: Revisiting Basic Concepts in View of Emerging Data. *Cardiorenal Med* 2019; **9**: 1-7 [PMID: 30223273 DOI: 10.1159/000492791]
12 **Krag A**, Gluud LL. Cross-talk between the liver, heart and kidney - another piece in the puzzle. *J Gastrointestin Liver Dis* 2014; **23**: 119-121 [PMID: 24949601 DOI: 10.15403/jgld.2014.1121.ak1]
13 **Carvalho MVH**, Kroll PC, Kroll RTM, Carvalho VN. Cirrhotic cardiomyopathy: the liver affects the heart. *Braz J Med Biol Res* 2019; **52**: e7809 [PMID: 30785477 DOI: 10.1590/1414-431X20187809]
14 **Kaur H**, Premkumar M. Diagnosis and Management of Cirrhotic Cardiomyopathy. *J Clin Exp Hepatol* 2022; **12**: 186-199 [PMID: 35068798 DOI: 10.1016/j.jceh.2021.08.016]
15 **Dourakis SP**, Geladari E, Geladari C, Vallianou N. Cirrhotic Cardiomyopathy: The Interplay Between Liver and Cardiac Muscle. How Does the Cardiovascular System React When the Liver is Diseased? *Curr Cardiol Rev* 2021; **17**: 78-84 [PMID: 31072296 DOI: 10.2174/1573403X15666190509084519]
16 **Ruiz-del-Arbol L**, Monescillo A, Arocena C, Valer P, Ginès P, Moreira V, Milicua JM, Jiménez W, Arroyo V. Circulatory function and hepatorenal syndrome in cirrhosis. *Hepatology* 2005; **42**: 439-447 [PMID: 15977202 DOI: 10.1002/hep.20766]
17 **Wadei HM**, Mai ML, Ahsan N, Gonwa TA. Hepatorenal syndrome: pathophysiology and management. *Clin J Am Soc Nephrol* 2006; **1**: 1066-1079 [PMID: 17699328 DOI: 10.2215/CJN.01340406]
18 **Ronco C**, Cicoira M, McCullough PA. Cardiorenal syndrome type 1: pathophysiological crosstalk leading to combined heart and kidney dysfunction in the setting of acutely decompensated heart failure. *J Am Coll Cardiol* 2012; **60**: 1031-1042 [PMID: 22840531 DOI: 10.1016/j.jacc.2012.01.077]
19 **Ronco C**, McCullough PA, Anker SD, Anand I, Aspromonte N, Bagshaw SM, Bellomo R, Berl T, Bobek I, Cruz DN, Daliento L, Davenport A, Haapio M, Hillege H, House A, Katz NM, Maisel A, Mankad S, Zanco P, Mebazaa A, Palazzuoli A, Ronco F, Shaw A, Sheinfeld G, Soni S, Vescovo G, Zamperetti N, Ponikowski P. Cardiorenal syndromes: an executive summary from the consensus conference of the Acute Dialysis Quality Initiative (ADQI). *Contrib Nephrol* 2010; **165**: 54-67 [PMID: 20427956 DOI: 10.1159/000313745]
20 **Mukherjee M**, Sharma K, Madrazo JA, Tedford RJ, Russell SD, Hays AG. Right-Sided Cardiac Dysfunction in Heart Failure With Preserved Ejection Fraction and Worsening Renal Function. *Am J Cardiol* 2017; **120**: 274-278 [PMID: 28528661 DOI: 10.1016/j.amjcard.2017.04.019]
21 **Clementi A**, Virzì GM, Battaglia GG, Ronco C. Neurohormonal, Endocrine, and Immune Dysregulation and Inflammation in Cardiorenal Syndrome. *Cardiorenal Med* 2019; **9**: 265-273 [PMID: 31266023 DOI: 10.1159/000500715]
22 **Patel KP**, Katsurada K, Zheng H. Cardiorenal Syndrome: The Role of Neural Connections Between the Heart and the Kidneys. *Circ Res* 2022; **130**: 1601-1617 [PMID: 35549375 DOI: 10.1161/CIRCRESAHA.122.319989]
23 **Krag A**, Bendtsen F, Henriksen JH, Møller S. Low cardiac output predicts development of hepatorenal syndrome and survival in patients with cirrhosis and ascites. *Gut* 2010; **59**: 105-110 [PMID: 19837678 DOI: 10.1136/gut.2009.180570]
24 **Gaskari SA**, Honar H, Lee SS. Therapy insight: Cirrhotic cardiomyopathy. *Nat Clin Pract Gastroenterol Hepatol* 2006; **3**: 329-337 [PMID: 16741552 DOI: 10.1038/ncpgasthep0498]
25 **Koshy AN**, Farouque O, Cailes B, Testro A, Ramchand J, Sajeev JK, Han HC, Srivastava PM, Jones EF, Salehi H, Teh AW, Lim HS, Calafiore P, Gow PJ. Impaired Cardiac Reserve on Dobutamine Stress Echocardiography Predicts the Development of Hepatorenal Syndrome. *Am J Gastroenterol* 2020; **115**: 388-397 [PMID: 31738284 DOI: 10.14309/ajg.0000000000000462]
26 **Cailes B**, Farouque O, Majumdar A, Koshy AN. Cardiac Dysfunction in the Pathogenesis of Hepatorenal Syndrome. *Am J Gastroenterol* 2023; **118**: 179-180 [PMID: 36191281 DOI: 10.14309/ajg.0000000000002032]
27 **Matyas C**, Haskó G, Liaudet L, Trojnar E, Pacher P. Interplay of cardiovascular mediators, oxidative stress and inflammation in liver disease

and its complications. *Nat Rev Cardiol* 2021; **18**: 117-135 [PMID: 32999450 DOI: 10.1038/s41569-020-0433-5]

28 **Adebayo D**, Wong F. Pathophysiology of Hepatorenal Syndrome - Acute Kidney Injury. *Clin Gastroenterol Hepatol* 2023; **21**: S1-S10 [PMID: 37625861 DOI: 10.1016/j.cgh.2023.04.034]

29 **Navasa M**, Follo A, Filella X, Jiménez W, Francitorra A, Planas R, Rimola A, Arroyo V, Rodés J. Tumor necrosis factor and interleukin-6 in spontaneous bacterial peritonitis in cirrhosis: relationship with the development of renal impairment and mortality. *Hepatology* 1998; **27**: 1227-1232 [PMID: 9581675 DOI: 10.1002/hep.510270507]

30 **Fasolato S**, Angeli P, Dallagnese L, Maresio G, Zola E, Mazza E, Salinas F, Donà S, Fagiuoli S, Sticca A, Zanus G, Cillo U, Frasson I, Destro C, Gatta A. Renal failure and bacterial infections in patients with cirrhosis: epidemiology and clinical features. *Hepatology* 2007; **45**: 223-229 [PMID: 17187409 DOI: 10.1002/hep.21443]

31 **Bortoluzzi A**, Ceolotto G, Gola E, Sticca A, Bova S, Morando F, Piano S, Fasolato S, Rosi S, Gatta A, Angeli P. Positive cardiac inotropic effect of albumin infusion in rodents with cirrhosis and ascites: molecular mechanisms. *Hepatology* 2013; **57**: 266-276 [PMID: 22911662 DOI: 10.1002/hep.26021]

32 **Virzì GM**, Zhang J, Nalesso F, Ronco C, McCullough PA. The Role of Dendritic and Endothelial Cells in Cardiorenal Syndrome. *Cardiorenal Med* 2018; **8**: 92-104 [PMID: 29617002 DOI: 10.1159/000485937]

33 **Karagiannakis DS**, Vlachogiannakos J, Anastasiadis G, Vafiadis-Zouboulis I, Ladas SD. Frequency and severity of cirrhotic cardiomyopathy and its possible relationship with bacterial endotoxemia. *Dig Dis Sci* 2013; **58**: 3029-3036 [PMID: 23907333 DOI: 10.1007/s10620-013-2693-y]

34 **Ruiz-del-Arbol L**, Urman J, Fernández J, González M, Navasa M, Monescillo A, Albillos A, Jiménez W, Arroyo V. Systemic, renal, and hepatic hemodynamic derangement in cirrhotic patients with spontaneous bacterial peritonitis. *Hepatology* 2003; **38**: 1210-1218 [PMID: 14578859 DOI: 10.1053/jhep.2003.50447]

35 **Gadano A**, Hadengue A, Widmann JJ, Vachiery F, Moreau R, Yang S, Soupison T, Sogni P, Degott C, Durand F. Hemodynamics after orthotopic liver transplantation: study of associated factors and long-term effects. *Hepatology* 1995; **22**: 458-465 [PMID: 7635413]

36 **Zardi EM**, Zardi DM, Chin D, Sonnino C, Dobrina A, Abbate A. Cirrhotic cardiomyopathy in the pre- and post-liver transplantation phase. *J Cardiol* 2016; **67**: 125-130 [PMID: 26074443 DOI: 10.1016/j.jjcc.2015.04.016]

37 **Ronco C**, McCullough P, Anker SD, Anand I, Aspromonte N, Bagshaw SM, Bellomo R, Berl T, Bobek I, Cruz DN, Daliento L, Davenport A, Haapio M, Hillege H, House AA, Katz N, Maisel A, Mankad S, Zanco P, Mebazaa A, Palazzuoli A, Ronco F, Shaw A, Sheinfeld G, Soni S, Vescovo G, Zamperetti N, Ponikowski P; Acute Dialysis Quality Initiative (ADQI) consensus group. Cardio-renal syndromes: report from the consensus conference of the acute dialysis quality initiative. *Eur Heart J* 2010; **31**: 703-711 [PMID: 20037146 DOI: 10.1093/eurheartj/ehp507]

38 **Arroyo V**, Fernandez J, Ginès P. Pathogenesis and treatment of hepatorenal syndrome. *Semin Liver Dis* 2008; **28**: 81-95 [PMID: 18293279 DOI: 10.1055/s-2008-1040323]

39 **Marwick TH**, Leano RL, Brown J, Sun JP, Hoffmann R, Lysyansky P, Becker M, Thomas JD. Myocardial strain measurement with 2-dimensional speckle-tracking echocardiography: definition of normal range. *JACC Cardiovasc Imaging* 2009; **2**: 80-84 [PMID: 19356538 DOI: 10.1016/j.jcmg.2007.12.007]

40 **Jansen C**, Nordmann P, Cremonese C, Praktiknjo M, Chang J, Lehmann J, Thomas D, Nickenig G, Weber M, Stöhr E, Öztürk C, Zachoval C, Hammersting C, Strassburg CP, Meyer C, Trebicka J. Change of Left Ventricular Myocardial Contractility in Speckle Tracking Echocardiography After Transjugular Intrahepatic Portosystemic Shunt Predicts Survival. *Front Gastroenterol* 2022; **1**: 860800 [DOI: 10.3389/fgstr.2022.860800]

41 **Altekin RE**, Caglar B, Karakas MS, Ozel D, Deger N, Demir I. Evaluation of subclinical left ventricular systolic dysfunction using two-dimensional speckle-tracking echocardiography in patients with non-alcoholic cirrhosis. *Hellenic J Cardiol* 2014; **55**: 402-410 [PMID: 25243439]

42 **Somani PO**, Contractor Q, Chaurasia AS, Rathi PM. Diastolic dysfunction characterizes cirrhotic cardiomyopathy. *Indian Heart J* 2014; **66**: 649-655 [PMID: 25634400 DOI: 10.1016/j.ihj.2014.06.001]

43 **Ruíz-del-Árbol L**, Achécar L, Serradilla R, Rodríguez-Gandía MÁ, Rivero M, Garrido E, Natcher JJ. Diastolic dysfunction is a predictor of poor outcomes in patients with cirrhosis, portal hypertension, and a normal creatinine. *Hepatology* 2013; **58**: 1732-1741 [PMID: 23703953 DOI: 10.1002/hep.26509]

44 **Premkumar M**, Devurgowda D, Vyas T, Shasthry SM, Khumuckham JS, Goyal R, Thomas SS, Kumar G. Left Ventricular Diastolic Dysfunction is Associated with Renal Dysfunction, Poor Survival and Low Health Related Quality of Life in Cirrhosis. *J Clin Exp Hepatol* 2019; **9**: 324-333 [PMID: 31360025 DOI: 10.1016/j.jceh.2018.08.008]

45 **Bayes-Genis A**, Docherty KF, Petrie MC, Januzzi JL, Mueller C, Anderson L, Bozkurt B, Butler J, Chioncel O, Cleland JGF, Christodorescu R, Del Prato S, Gustafsson F, Lam CSP, Moura B, Pop-Busui R, Seferovic P, Volterrani M, Vaduganathan M, Metra M, Rosano G. Practical algorithms for early diagnosis of heart failure and heart stress using NT-proBNP: A clinical consensus statement from the Heart Failure Association of the ESC. *Eur J Heart Fail* 2023; **25**: 1891-1898 [PMID: 37712339 DOI: 10.1002/ejhf.3036]

46 **Ge PS**, Runyon BA. Role of plasma BNP in patients with ascites: advantages and pitfalls. *Hepatology* 2014; **59**: 751-753 [PMID: 23959954 DOI: 10.1002/hep.26689]

47 **Kapoor N**, Mehta V, Singh B, Karna R, Kumar S, Kar P. Prevalence of cirrhotic cardiomyopathy and its relationship with serum pro-brain natriuretic peptide, hepatorenal syndrome, spontaneous bacterial peritonitis, and mortality. *Indian J Gastroenterol* 2020; **39**: 481-486 [PMID: 33188455 DOI: 10.1007/s12664-020-01083-2]

48 **Han G**, Qi X, He C, Yin Z, Wang J, Xia J, Yang Z, Bai M, Meng X, Niu J, Wu K, Fan D. Transjugular intrahepatic portosystemic shunt for portal vein thrombosis with symptomatic portal hypertension in liver cirrhosis. *J Hepatol* 2011; **54**: 78-88 [PMID: 20932597 DOI: 10.1016/j.jhep.2010.06.029]

49 **Rajesh S**, George T, Philips CA, Ahamed R, Kumbar S, Mohan N, Mohanan M, Augustine P. Transjugular intrahepatic portosystemic shunt in cirrhosis: An exhaustive critical update. *World J Gastroenterol* 2020; **26**: 5561-5596 [PMID: 33088154 DOI: 10.3748/wjg.v26.i37.5561]

50 **Lotterer E**, Wengert A, Fleig WE. Transjugular intrahepatic portosystemic shunt: short-term and long-term effects on hepatic and systemic hemodynamics in patients with cirrhosis. *Hepatology* 1999; **29**: 632-639 [PMID: 10051460 DOI: 10.1002/hep.510290302]

51 **Ponzo P**, Campion D, Rizzo M, Roma M, Caviglia GP, Giovo I, Rizzi F, Bonetto S, Saracco GM, Alessandria C. Transjugular intrahepatic porto-systemic shunt in cirrhotic patients with hepatorenal syndrome - chronic kidney disease: Impact on renal function. *Dig Liver Dis* 2022; **54**: 1101-1108 [PMID: 34625366 DOI: 10.1016/j.dld.2021.09.008]

52 **Busk TM**, Bendtsen F, Poulsen JH, Clemmesen JO, Larsen FS, Goetze JP, Iversen JS, Jensen MT, Møgelvang R, Pedersen EB, Bech JN, Møller S. Transjugular intrahepatic portosystemic shunt: impact on systemic hemodynamics and renal and cardiac function in patients with

cirrhosis. *Am J Physiol Gastrointest Liver Physiol* 2018; **314**: G275-G286 [PMID: 29074483 DOI: 10.1152/ajpgi.00094.2017]
53 **Deltenre P**, Zanetto A, Saltini D, Moreno C, Schepis F. The role of transjugular intrahepatic portosystemic shunt in patients with cirrhosis and ascites: Recent evolution and open questions. *Hepatology* 2023; **77**: 640-658 [PMID: 35665949 DOI: 10.1002/hep.32596]
54 **Hartl L**, Rumpf B, Domenig O, Simbrunner B, Paternostro R, Jachs M, Poglitsch M, Marculescu R, Trauner M, Reindl-Schwaighofer R, Hecking M, Mandorfer M, Reiberger T. The systemic and hepatic alternative renin-angiotensin system is activated in liver cirrhosis, linked to endothelial dysfunction and inflammation. *Sci Rep* 2023; **13**: 953 [PMID: 36653504 DOI: 10.1038/s41598-023-28239-2]
55 **Fakhritdinovna JM**. Hepatocardiorenal Syndrome. *Asian J Pharm Bio Res* 2022; **11**: 82-97
56 **Garcia-Martinez R**, Andreola F, Mehta G, Poulton K, Oria M, Jover M, Soeda J, Macnaughtan J, De Chiara F, Habtesion A, Mookerjee RP, Davies N, Jalan R. Immunomodulatory and antioxidant function of albumin stabilises the endothelium and improves survival in a rodent model of chronic liver failure. *J Hepatol* 2015; **62**: 799-806 [PMID: 25450713 DOI: 10.1016/j.jhep.2014.10.031]
57 **Fernández J**, Monteagudo J, Bargallo X, Jiménez W, Bosch J, Arroyo V, Navasa M. A randomized unblinded pilot study comparing albumin versus hydroxyethyl starch in spontaneous bacterial peritonitis. *Hepatology* 2005; **42**: 627-634 [PMID: 16108036 DOI: 10.1002/hep.20829]
58 **Sort P**, Navasa M, Arroyo V, Aldeguer X, Planas R, Ruiz-del-Arbol L, Castells L, Vargas V, Soriano G, Guevara M, Ginès P, Rodés J. Effect of intravenous albumin on renal impairment and mortality in patients with cirrhosis and spontaneous bacterial peritonitis. *N Engl J Med* 1999; **341**: 403-409 [PMID: 10432325 DOI: 10.1056/NEJM199908053410603]
59 **Mocarzel L**, Lanzieri P, Nascimento J, Peixoto C, Ribeiro M, Mesquita E. Hepatorenal syndrome with cirrhotic cardiomyopathy: case report and literature review. *Case Reports Hepatol* 2015; **2015**: 573513 [PMID: 25874140 DOI: 10.1155/2015/573513]
60 **Mocarzel LO**, Bicca J, Jarske L, Oliveira T, Lanzieri P, Gismondi R, Ribeiro ML. Cirrhotic Cardiomyopathy: Another Case of a Successful Approach to Treatment of Hepatorenal Syndrome. *Case Rep Gastroenterol* 2016; **10**: 531-537 [PMID: 27843430 DOI: 10.1159/000448885]
61 **Theocharidou E**, Krag A, Bendtsen F, Møller S, Burroughs AK. Cardiac dysfunction in cirrhosis - does adrenal function play a role? A hypothesis. *Liver Int* 2012; **32**: 1327-1332 [PMID: 22292920 DOI: 10.1111/j.1478-3231.2011.02751.x]
62 **Muciño-Bermejo MJ**. Mechanisms of kidney dysfunction in the cirrhotic patient: Non-hepatorenal acute-on-chronic kidney damage considerations. *Ann Hepatol* 2020; **19**: 145-152 [PMID: 31594758 DOI: 10.1016/j.aohep.2019.06.022]
63 **Gao Y**, Wei L, Zhang DD, Chen Y, Hou B. SGLT2 Inhibitors: A New Dawn for Recurrent/Refractory Cirrhotic Ascites. *J Clin Transl Hepatol* 2021; **9**: 795-797 [PMID: 34966642 DOI: 10.14218/JCTH.2021.00418]
64 **ElBaset MA**, Salem RS, Ayman F, Ayman N, Shaban N, Afifi SM, Esatbeyoglu T, Abdelaziz M, Elalfy ZS. Effect of Empagliflozin on Thioacetamide-Induced Liver Injury in Rats: Role of AMPK/SIRT-1/HIF-1α Pathway in Halting Liver Fibrosis. *Antioxidants (Basel)* 2022; **11** [PMID: 36358524 DOI: 10.3390/antiox11112152]
65 **Carstens J**, Grønbaek H, Larsen HK, Pedersen EB, Vilstrup H. Effects of urodilatin on natriuresis in cirrhosis patients with sodium retention. *BMC Gastroenterol* 2007; **7**: 1 [PMID: 17257428 DOI: 10.1186/1471-230X-7-1]
66 **Hey P**, Sinclair M. Upcoming pharmacological and interventional therapies for the treatment of physical frailty and sarcopenia. In: Tandon P, Montano-Loza A. Frailty and Sarcopenia in Cirrhosis. Switzerland: Springer, 2020: 211-232
67 **Snowdon VK**, Lachlan NJ, Hoy AM, Hadoke PW, Semple SI, Patel D, Mungall W, Kendall TJ, Thomson A, Lennen RJ, Jansen MA, Moran CM, Pellicoro A, Ramachandran P, Shaw I, Aucott RL, Severin T, Saini R, Pak J, Yates D, Dongre N, Duffield JS, Webb DJ, Iredale JP, Hayes PC, Fallowfield JA. Serelaxin as a potential treatment for renal dysfunction in cirrhosis: Preclinical evaluation and results of a randomized phase 2 trial. *PLoS Med* 2017; **14**: e1002248 [PMID: 28245243 DOI: 10.1371/journal.pmed.1002248]
68 **Merli M**, Calicchia A, Ruffa A, Pellicori P, Riggio O, Giusto M, Gaudio C, Torromeo C. Cardiac dysfunction in cirrhosis is not associated with the severity of liver disease. *Eur J Intern Med* 2013; **24**: 172-176 [PMID: 22958907 DOI: 10.1016/j.ejim.2012.08.007]
69 **Darstein F**, König C, Hoppe-Lotichius M, Grimm D, Knapstein J, Mittler J, Zimmermann A, Otto G, Lang H, Galle PR, Zimmermann T. Preoperative left ventricular hypertrophy is associated with reduced patient survival after liver transplantation. *Clin Transplant* 2014; **28**: 236-242 [PMID: 24372847 DOI: 10.1111/ctr.12304]
70 **Torregrosa M**, Aguadé S, Dos L, Segura R, Gónzalez A, Evangelista A, Castell J, Margarit C, Esteban R, Guardia J, Genescà J. Cardiac alterations in cirrhosis: reversibility after liver transplantation. *J Hepatol* 2005; **42**: 68-74 [PMID: 15629509 DOI: 10.1016/j.jhep.2004.09.008]
71 **Zardi EM**, Abbate A, Zardi DM, Dobrina A, Margiotta D, Van Tassell BW, Afeltra A, Sanyal AJ. Cirrhotic cardiomyopathy. *J Am Coll Cardiol* 2010; **56**: 539-549 [PMID: 20688208 DOI: 10.1016/j.jacc.2009.12.075]
72 **Bernardi M**, Maggioli C, Dibra V, Zaccherini G. QT interval prolongation in liver cirrhosis: innocent bystander or serious threat? *Expert Rev Gastroenterol Hepatol* 2012; **6**: 57-66 [PMID: 22149582 DOI: 10.1586/egh.11.86]
73 **American Association for the Study of Liver Diseases**. Evaluation for Liver Transplantation in Adults. [cited 15 September 2023]. Available from: https://www.aasld.org/practice-guidelines/evaluation-adult-liver-transplant-patient
74 **Aggarwal S**, Kang Y, Freeman JA, Fortunato FL Jr, Pinsky MR. Postreperfusion syndrome: hypotension after reperfusion of the transplanted liver. *J Crit Care* 1993; **8**: 154-160 [PMID: 8275160 DOI: 10.1016/0883-9441(93)90021-c]
75 **Izzy M**, Fortune BE, Serper M, Bhave N, deLemos A, Gallegos-Orozco JF, Guerrero-Miranda C, Hall S, Harinstein ME, Karas MG, Kriss M, Lim N, Palardy M, Sawinski D, Schonfeld E, Seetharam A, Sharma P, Tallaj J, Dadhania DM, VanWagner LB. Management of cardiac diseases in liver transplant recipients: Comprehensive review and multidisciplinary practice-based recommendations. *Am J Transplant* 2022; **22**: 2740-2758 [PMID: 35359027 DOI: 10.1111/ajt.17049]
76 **Manning MW**, Kumar PA, Maheshwari K, Arora H. Post-Reperfusion Syndrome in Liver Transplantation-An Overview. *J Cardiothorac Vasc Anesth* 2020; **34**: 501-511 [PMID: 31084991 DOI: 10.1053/j.jvca.2019.02.050]
77 **Koshy AN**, Gow PJ, Han HC, Teh AW, Jones R, Testro A, Lim HS, McCaughan G, Jeffrey GP, Crawford M, Macdonald G, Fawcett J, Wigg A, Chen JWC, Gane EJ, Munn SR, Clark DJ, Yudi MB, Farouque O. Cardiovascular mortality following liver transplantation: predictors and temporal trends over 30 years. *Eur Heart J Qual Care Clin Outcomes* 2020; **6**: 243-253 [PMID: 32011663 DOI: 10.1093/ehjqcco/qcaa009]
78 **Altieri MH**, Liu H, Lee SS. Cardiovascular events after liver transplantation: MACE hurts. *Rev Cardiovasc Med* 2022; **23**: 91 [PMID: 35345258 DOI: 10.31083/j.rcm2303091]
79 **Tauseef A**, Zafar M, Rashid B, Thirumalareddy J, Chalfant V, Farooque U, Mirza M. Correlation of Fasting Lipid Profile in Patients With Chronic Liver Disease: A Descriptive Cross-Sectional Study in Tertiary Care Hospital. *Cureus* 2020; **12**: e11019 [PMID: 33214947 DOI: 10.7759/cureus.11019]
80 **Liu H**, Naser JA, Lin G, Lee SS. Cardiomyopathy in cirrhosis: From pathophysiology to clinical care. *JHEP Rep* 2024; **6**: 100911 [PMID: 38089549 DOI: 10.1016/j.jhepr.2023.100911]

World Journal of Gastroenterology

Submit a Manuscript: https://www.f6publishing.com

World J Gastroenterol 2024 January 14; 30(2): 137-145

DOI: 10.3748/wjg.v30.i2.137

ISSN 1007-9327 (print) ISSN 2219-2840 (online)

MINIREVIEWS

Esophageal intramural pseudodiverticulosis

Masako Shintaku

Specialty type: Gastroenterology and hepatology

Provenance and peer review: Unsolicited article; Externally peer reviewed.

Peer-review model: Single blind

Peer-review report's scientific quality classification

Grade A (Excellent): A
Grade B (Very good): 0
Grade C (Good): C
Grade D (Fair): 0
Grade E (Poor): 0

P-Reviewer: Liu YC, China; Pavlidis TE, Greece

Received: November 19, 2023
Peer-review started: November 19, 2023
First decision: December 15, 2023
Revised: December 21, 2023
Accepted: December 28, 2023
Article in press: December 28, 2023
Published online: January 14, 2024

Masako Shintaku, Department of Gastroenterology, Japan Community Healthcare Organization Hoshigaoka Medical Center, Hirakata 573-8511, Osaka, Japan

Corresponding author: Masako Shintaku, MD, Doctor, Department of Gastroenterology, Japan Community Healthcare Organization Hoshigaoka Medical Center, 4-8-1 Hoshigaoka, Hirakata 573-8511, Osaka, Japan. shintakumahoshi@gmail.com

Abstract

Esophageal intramural pseudodiverticulosis (EIPD) is a disease of unknown pathogenesis characterized by usually systemic, cystic dilatation of the excretory ducts of esophageal submucosal glands. In this article, I review the epidemiology, clinical manifestations, endoscopic findings, esophagographic findings, and histopathology of EIPD. I also discuss the etiology and possible pathogenesis of EIPD based on my experiences with this disease and a review of the literature. EIPD usually presents with dysphagia in middle-aged individuals. It is often complicated with secondary infections, most commonly candidiasis. On esophagography, EIPD is delineated as small, multiple, flask-shaped outward projections within the esophageal wall. In recent years, EIPD has been mainly diagnosed by endoscopic findings of multiple, localized, small mucosal depressions. The orifices of the "pseudodiverticula" periodically open and close, and excrete mucus onto the mucosal surface. On histopathological examination, the luminal surface of dilated ducts in EIPD is covered by multilayered, hyperplastic epithelial cells, but myoepithelial cells in the glandular acini are well preserved. Treatment of EIPD is usually symptomatic therapy, and prevention of the infectious complications is important. The etiology and pathogenesis of EIPD are largely unknown, but functional abnormalities of autonomic nerve fibers innervating the esophageal glands likely play an important role, since the structures of the glands are basically preserved in this disease.

Key Words: Esophageal endoscopy; Esophageal intramural pseudodiverticulosis; Esophagography; Dysphagia

Core Tip: Esophageal intramural pseudodiverticulosis (EIPD) is a rare disease in which the ducts of the esophageal glands become cystically dilated. Prolonged chronic inflammation can lead to esophageal stenosis, perforation, mediastinitis, and lung abscess. EIPD needs to be diagnosed at an early stage, and patients should be carefully observed and treated appropriately.

Citation: Shintaku M. Esophageal intramural pseudodiverticulosis. *World J Gastroenterol* 2024; 30(2): 137-145
URL: https://www.wjgnet.com/1007-9327/full/v30/i2/137.htm
DOI: https://dx.doi.org/10.3748/wjg.v30.i2.137

INTRODUCTION

Esophageal intramural pseudodiverticulosis (EIPD) is a disease in which the excretory ducts of esophageal submucosal glands show systemic, cystic dilatation. On endoscopic examination, the orifices of the dilated ducts appear as multiple, small mucosal depressions resembling diverticula[1-4]. Chronic inflammation is a frequent complication, and prolonged inflammation results in esophageal stricture with impaired peristaltic movements, which leads to difficulty swallowing or impaction of food[2].

Although EIPD is a rare disease, it can have serious complications, such as esophageal perforation, mediastinitis, and lung abscess, if not adequately treated[5-8]. In this article, I review the epidemiology, clinical manifestations, characteristic endoscopic findings, radiological findings, complications, and medical treatment of EIPD. I also discuss some hypotheses concerning its etiology and pathogenesis, based on my own experience and a review of the literature.

EPIDEMIOLOGY

Since the first clinicopathological report by Mendl *et al*[9], approximately 320 cases of EIPD have been recorded to date, mainly in Europe and the United States. EIPD affects men more commonly than women and occurs in all age groups, the peak incidence being between 50 and 70 years of age[10-12]. About 20 cases have also been reported in the pediatric population, the youngest patient being diagnosed at 37 d after birth[13]. In a survey of the literature, excluding conference proceeding abstracts, less than 60 cases of EIPD have been reported in Japan.

Many asymptomatic patients are incidentally found to have EIPD by endoscopic examination, and, even if detected, some patients do not wish to undergo treatment or observation because the subjective symptoms are usually mild or, in some cases, absent.

CLINICAL MANIFESTATIONS

The main symptom of EIPD is dysphagia of solid food, which is intermittent and unremarkable in the incipient stages. In many cases, dysphagia progresses slowly, and patients occasionally present for emergency endoscopy due to impaction of food or consult for a thorough endoscopic examination seeking the cause of their weight loss[14-18]. Other symptoms such as a feeling of congestion in the esophagus, chest pain, and hematemesis have been reported[5,19-21]. EIPD is usually diagnosed in individuals of middle age or older, and many patients have a history of heavy drinking or smoking [7,22-25]. Some disorders, such as diabetes mellitus, gastroesophageal reflux disease (GERD), chronic lung diseases, alcoholic liver cirrhosis, esophageal cancer, and collagen-vascular diseases, have been reported as conditions predisposing patients to EIPD[1,23,26].

In pediatric cases, EIPD may manifest several years after surgery for esophageal atresia or tracheoesophageal fistula [27,28]. There are also some reports of cases with underlying asthmatic bronchitis[29] and pediatric patients with siblings suffering from the same disease[30]. In some cases, EIPD presents with vomiting soon after birth and is followed by dysphagia of solid food and growth retardation. The symptoms are aggravated by disturbance of esophageal peristalsis or GERD in the period from approximately 5 years of age to adolescence[31-35]. In some pediatric patients, EIPD becomes apparent after repeated surgical interventions for esophageal hiatal hernia or GERD[36]. Cases of young patients diagnosed with EIPD after ingestion of corrosive substances have also been reported[28,37].

CLINICAL EXAMINATIONS

Endoscopic examination

Endoscopy of the esophagus has markedly advanced in recent years, and nowadays most cases of EIPD are diagnosed by endoscopic examination[23]. On endoscopy, EIPD is usually observed as multiple, diverticulum-like, small, localized mucosal depressions measuring approximately 1 mm to 4 mm in diameter (Figure 1A). Narrow band imaging (NBI) or

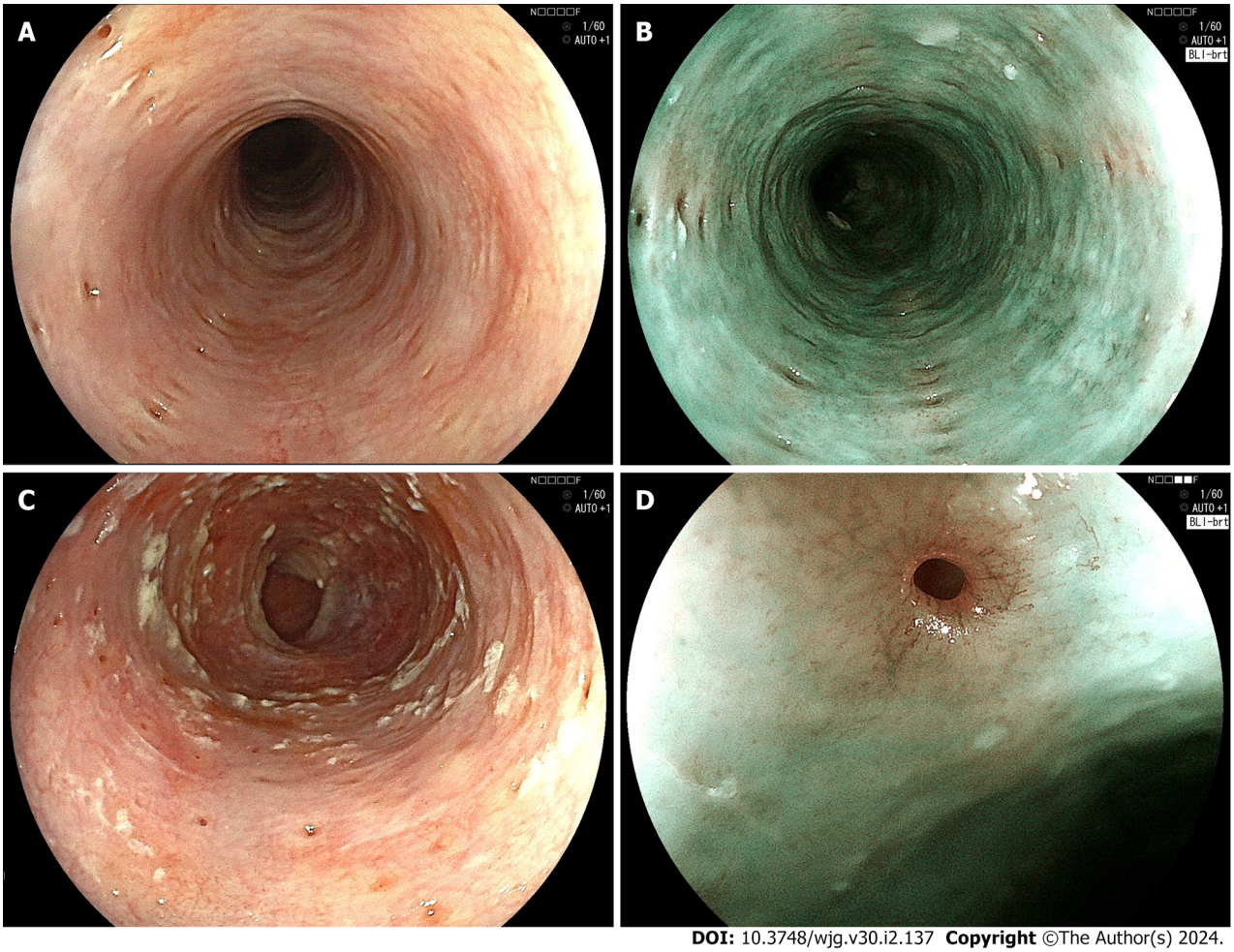

DOI: 10.3748/wjg.v30.i2.137

Figure 1 Endoscopic examination. A: White-light endoscopic image. Multiple small diverticulum-like depressions of the mucosa with a diameter of 1-4 mm are seen. Fujifilm EG-L600ZW; B: Blue laser imaging (BLI)-bright image. The light-brown depressions are longitudinally aligned on the green-colored mucosa. Fujifilm EG-L600ZW; C: White-light endoscopic image. The orifices of pseudodiverticula are covered with whitish, plaque-like material. Fujifilm EG-L600ZW; D: BLI-bright, medium magnifying image. The orifice of the pseudodiverticulum is surrounded by blood vessels arranged in an eyelash-like pattern. Fujifilm EG-L600ZW.

blue laser imaging (BLI) shows multiple small, light-brown spots that tend to be arranged longitudinally on the background mucosa, which is green (Figure 1B). Although the orifices of EIPD are often covered by inflammatory exudate produced by infection with *Candida* spp., the orifices become more clearly visible after washing away the adherent exudate (Figure 1C). In magnified images, the orifices of the dilated ducts of esophageal glands can be seen in the center of small depressions as pinhole-like, minute spots surrounded by an intraepithelial papillary loop of capillaries that resemble eyelashes[38] (Figure 1D).

Among the cases of EIPD, those in which many small "pseudodiverticula" are distributed along the entire length of the esophagus are called "diffuse EIPD". In contrast, when the occurrence of multiple "pseudodiverticula" is limited to only a part of the esophagus, it is called "segmental EIPD". Segmental EIPD can be easily overlooked, especially when it is not associated with esophageal stricture and the subjective symptoms are mild, but endoscopy with NBI or BLI improves the detection rate of the orifices of dilated ducts due to differences in the colors of the mucosa[23].

In 2011, the present author and colleagues reported for the first time that the mucosal orifices of dilated ducts in EIPD periodically open and close asynchronously with respiratory or peristaltic movements[19]. These movements were observed at intervals of approximately 2 min, and clear or white-colored mucus was discharged from the orifices onto the mucosal surface[19,38]. The opening and closing of the mucosal orifices typically starts a few minutes after insertion of the endoscope or after stimulation with air or water.

In EIPD patients complicated with severe *Candida* esophagitis, EIPD may be overlooked because the orifices of dilated ducts are covered by white plaques or inspissated mucus[11]. There are a few reports of EIPD complicated with severe candidiasis in which cystically dilated ducts coalesced to form a "sinus tract"-like structure in the submucosa[25,39,40]. In many cases of EIPD, inflammation involving the esophageal wall is prolonged, the mucosa is thickened by edema, and the mucosal vascular pattern becomes hardly discernible. Web-like constriction of the esophagus due to inflammatory changes may be occasionally observed[23]. Further progression of inflammation leads to esophageal stricture or disorders of peristaltic movements[10]. In one of our own cases, in which the patient suffered from GERD with Barrett esophagus, the lower portion of the esophagus was constricted[38]. However, according to many previously reported cases of EIPD, stenosis is mostly noted in the upper portion of the esophagus[1,23,41].

Esophagography

A barium esophagogram shows characteristic, numerous, tiny, flask-shaped outpouching within the esophageal wall, when contrast medium flows into the "pseudodiverticula"[19,42]. These outpouchings correspond to cystic dilatation of the ducts of esophageal glands. When the esophagus is regionally narrowed, these outpouchings are often seen in the vicinity of the narrowed portion. Since the quality of endoscopic images was suboptimal in the past and magnifying endoscopes were not widely used until about 10 years ago, EIPD was mainly diagnosed by esophagography. However, infusion of contrast medium into the "pseudodiverticula" is difficult when the dilated ducts are filled with inflammatory exudates, desquamated epithelial cells, or inspissated mucus, or when the orifices of EIPD are very small[28,32,43]. EIPD that was not detected by esophagography is occasionally found at autopsy[3]. It takes time and sufficient knowledge of EIPD to obtain clear esophagographic images of the disease[21].

Computed tomography and esophageal manometry

When the inflammatory process complicating EIPD is prolonged, computed tomography (CT) shows thickening of the esophageal wall due to inflammatory exudation and fibrosis. Intramural air images reflecting dilatation of ducts are also observed[25,40,44,45]. Esophageal manometry may demonstrate decreased peristaltic movements, abnormal motility, and abnormal intraluminal pressure of the esophagus[46,47]. There are several reports of EIPD co-existing with motility disorders, such as achalasia[48,49] or "jackhammer esophagus"[50,51]. To select an appropriate treatment for EIPD, high-resolution manometry is useful for evaluating esophageal peristalsis and sphincter function at the proximal and distal ends of the esophagus[46,47].

PATHOLOGICAL FINDINGS

Since EIPD is a disorder that is rarely treated surgically, pathological findings of the esophagus are often obtained only for autopsied cases or for patients who underwent surgical treatment due to complications or co-existing disorders, such as esophageal cancer. There are very few reports dealing with pathological findings of the esophagus in EIPD, especially in recent years[52].

The present author and colleagues reported the results of a histopathological and immunohistochemical study of ductal epithelial cells of the esophageal glands and their pathological changes in two operated cases of EIPD[52]. In the normal esophagus used as a control, the inner surface of the excretory ducts of esophageal gland was lined by simple cuboidal or columnar epithelium, and a single layer of cuboidal, basal cells was seen in the underlying layer. In EIPD, both the surface epithelial cells and basal cells of the ducts showed hyperplasia and stratification of varying degrees, and the ductal walls were thickened (Figure 2A). On immunohistochemical examination, whereas the surface epithelial cells were immunoreactive for cytokeratin 7 (CK7) and negative for CK5/6, basal cells showed the reverse pattern (CK7-negative and CK5/6-positive). The nuclei of basal cells were immunoreactive for p63. The stratified squamous epithelium covering the mucosa of the esophagus was CK7-negative and clearly distinguished from the CK7-positive surface epithelium of the ducts[52]. The immunohistochemical profiles of epithelial cells described above were essentially unchanged in EIPD (Figure 2B). In the acinar portion of esophageal glands located in the submucosa, myoepithelial cells surrounding each acinus were well preserved. This finding supported the endoscopic findings that the orifices of ducts in EIPD periodically opened and closed, thereby discharging mucus onto the mucosal surface.

In the cases of EIPD with a long clinical course, inflammatory cells infiltrated into the periductal and periacinar regions of esophageal glands, and the ductal lumina were filled with inflammatory cells, desquamated epithelial cells, and mucus. Extensive periglandular fibrosis was often observed[3,21,28]. Acinar cells were infrequently replaced by squamous cells, thus forming a lesion analogous to the "necrotizing sialometaplasia" of minor salivary glands[52,53].

Esophageal biopsies usually reveal only non-specific, chronic inflammation, edema, and acanthosis of the surface epithelium[10,14]. Although EIPD cannot be diagnosed by biopsy, biopsy is performed to exclude candidiasis, eosinophilic esophagitis, lymphocytic esophagitis, or esophageal cancer, and also to evaluate the degree of inflammatory changes[10].

ETIOLOGY AND PATHOGENESIS

Looking back at the history of the development of the disease concept of EIPD, a pathological condition in which the orifices of esophageal gland ducts are obstructed by inflammation, resulting in the formation of retention cysts that protrude into the esophageal lumen, had been described using the term "cystic esophagitis" in 1899 (according to Piazza and Palma[54]). The first description of EIPD was published in 1960 by Mendl *et al*[9], who detected an esophageal disease with a radiographic appearance resembling the Rokitansky-Aschoff's sinus of the gallbladder. They described it as "intramural diverticulosis"[9]. Boyd *et al*[2], by examining autopsied cases, demonstrated that the disease was not "diverticulosis" but a cystic dilatation of the esophageal gland ducts and termed it "pseudodiverticulosis". As mentioned previously, EIPD is not a mucosal prolapse or depression, such as seen in pseudodiverticulosis of the large intestine, but a dilatation of the esophageal gland ducts that disturbs mucus excretion. The term "EIPD" therefore does not reflect the true nature of the disease, and a more appropriate term may be needed, such as "systemic dilatation of esophageal gland ducts".

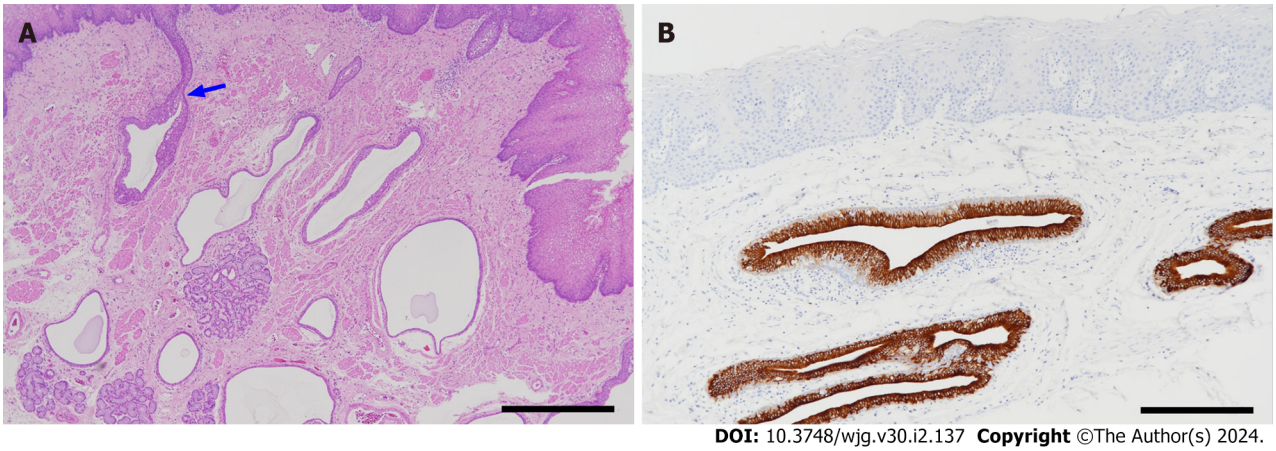

DOI: 10.3748/wjg.v30.i2.137

Figure 2 Pathological findings. A: Histology of esophageal intramural pseudodiverticulosis (hematoxylin-eosin stain). Many cystically dilated ducts of the esophageal glands are seen in the lamina propria mucosae and submucosa. Some of them are continuous with the superficial epithelium (arrow) (scale bar: 1 mm); B: Cytokeratin 7 (CK7) immunostaining. Epithelial cells lining the ducts are positive for CK7. The epithelium of the duct shows hyperplasia and stratification. The esophageal mucosal epithelium (upper part of the figure) is negative for CK7 (scale bar: 200 μm).

The etiology and pathogenesis of EIPD remain unknown. It has been generally assumed that the disease is an acquired condition and the neck portion of the ducts is obstructed by inflammatory changes, resulting in cystic dilatation due to an increased internal pressure[1,2]. However, Umlas and Sakhuja[3] found that the ducts are also slightly dilated in autopsy cases used as a normal control, and they stated that it is difficult to determine whether inflammation elicited the dilatation of ducts or the inflammation was only a secondary change caused by EIPD. They considered the esophageal stricture and *Candida* infection seen in EIPD patients to be secondary changes[3]. *Candida* infection of the oral cavity and pharynx is a common phenomenon that is found in 30% of normal individuals[55], and *Candida* infection frequently seen in EIPD patients is now considered a secondary infection rather than a causative agent of EIPD. Medeiros *et al*[4] found that the number of esophageal glands increased with aging and considered that periglandular chronic inflammation dilates the ducts and leads to the formation of a pseudodiverticulum. Kataoka *et al*[56] found that, among 27 autopsied cases, 15 cases (56%) showed slight dilatation of esophageal gland ducts. The two-thirds of the cases showing ductal dilatation had chronic inflammatory changes surrounding the glands, and the authors concluded that the changes that had been regarded to be an incipient change of EIPD were commonly seen in the general population[56]. They stated that EIPD is caused by chronic inflammation of the esophageal glands due to various causes, such as infection, GERD, and erosion, and that diabetes mellitus and an excessive ingestion of alcohol might accelerate the inflammation[56].

Candida, bacteria, and refluxing gastric juice or bile easily flow into the pseudodiverticula in EIPD through their dilated orifices. Excessive ingestion of alcohol, smoking, and diabetes mellitus accelerate inflammatory changes. Inflammatory changes cause retention and concentration of secreted mucus within the dilated ducts and further increase dilatation of the ducts[3,21,28].

The etiology and pathogenesis of EIPD remain obscure, but, as mentioned previously, the ducts and acini of esophageal glands in EIPD do not show significant structural differences in comparison with those of normal glands. I suspect that functional abnormalities of the autonomic nerve (vagal nerve) innervating the esophageal glands and regulating their function might play a role in the pathogenesis of EIPD. The functional disturbance of the autonomic nerve caused by inflammation or aging may affect the function of myoepithelial cells in the acini of esophageal glands and aggravate the pathological condition of EIPD.

Regarding pediatric cases of EIPD, Peters *et al*[57] observed the clinical course of a 5-year-old girl with EIPD for 16 years and found that whereas the pseudodiverticula increased in number and became more pronounced, the patient did not develop any serious complications. Freud *et al*[36] compared the esophagographic findings obtained from one month after birth to 3 years of a male infant who developed severe vomiting immediately after birth and underwent repeated cardioplasty and dilatation of the esophagus, and stated that his EIPD gradually progressed. Solomon *et al*[13] reported a female infant who was born with pulmonary dysplasia and was diagnosed with EIPD on day 37 after birth, and presumed that her EIPD was a congenital disorder. A retrospective review of esophagograms from pediatric cases indicated that the number of pseudodiverticula and the sizes of their orifices increased as the children aged[34,57]. In recent years, the number of reported cases of pediatric EIPD has markedly decreased, making comparisons between EIPD in adults and that in the pediatric population more difficult. I suspect that EIPD in pediatric patients may have a different etiopathogenesis from that in adults, and they could actually be distinct entities.

COMPLICATIONS

EIPD, if not treated adequately, can lead to fibrosis of the esophageal mucosa and submucosa as a result of long-lasting, chronic esophagitis caused by infection or gastroesophageal reflux. The fibrosis subsequently causes esophageal stenosis or disturbance of the esophageal motility. Delay of diagnosis can lead to serious complications, such as intra-mediastinal

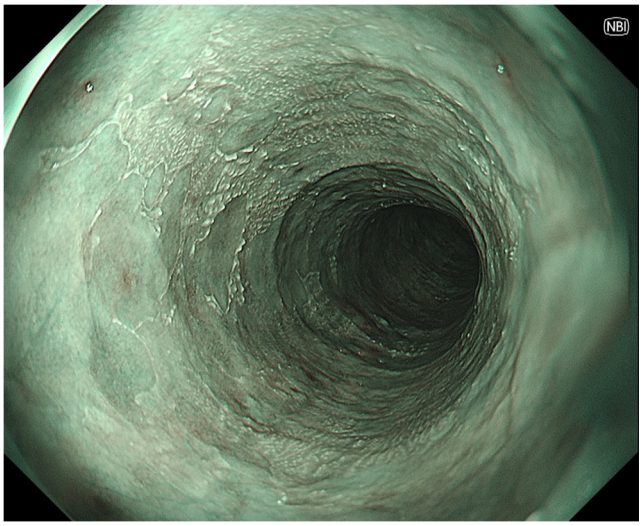

DOI: 10.3748/wjg.v30.i2.137

Figure 3 Narrow band imaging shows "epidermization", which was widely spread in the middle esophagus 2.5 years after the first endoscopic examination. The extent of epidermization has not markedly changed over a 3-year period. Olympus GIF-XZ1200.

fistula due to progression of the inflammatory changes[26]. There are several reported cases of serious complications of EIPD as follows. For example, a case was reported in which the diagnosis of EIPD was not rendered despite the typical clinical findings, and the patient underwent unnecessary subtotal esophagectomy[58]. In another case, the patient underwent emergency operation because of esophageal perforation due to severe vomiting associated with EIPD[5]. Other cases include EIPD brought about esophageal perforation with mediastinal emphysema or abscess[6], EIPD associated with Mallory-Weiss syndrome[20], and a case in which the patient underwent esophagectomy due to esophageal stenosis[59]. Fatal cases of perforation due to EIPD[60] and the association of EIPD with esophageal cancer[61] have also been reported. Prolongation of the inflammatory changes, excessive intake of alcohol or smoking, and the presence of various underlying disorders are considered risk factors for the complications associated with EIPD[10,23].

During the observation period of a case of EIPD, my colleagues and I found "epidermization" of the mucosal squamous epithelium of the esophagus[62] (Figure 3). Although the etiology and pathogenesis of "epidermization" have not yet been clarified, it may arise during the repair of damage caused by inflammation[63-65]. *Candida* esophagitis had persisted for a long time in that case, and we considered that the "epidermization" occurred during the healing process [62]. Since a few cases of esophageal cancer associated with "epidermization" have been reported[65,66], we are carefully following the patient. No significant changes have been found during the 3-year observation period.

TREATMENTS

EIPD is a benign condition, and its treatment is basically conservative, symptomatic therapy. However, to prevent prolongation of the clinical course of EIPD, inflammation associated with EIPD, which can be caused by various factors, including *Candida* infection and GERD, should be treated. It is also important to be aware of esophageal strictures, perforations, mediastinitis, and lung abscesses that can result from long-term chronic inflammation. Thus, EIPD requires early diagnosis, careful observation, and appropriate treatment. The following factors are worth noting regarding treatment for EIPD: (1) The weaning from the habit of heavy alcohol drinking or smoking is important; (2) For the complication of *Candida* infection, anti-fungal agents are effective[18,40,44,67,68]; (3) Endoscopic ballooning dilatation is effective when difficulty swallowing due to fibrosis of the esophageal wall develops, but multiple dilatation procedures are often required[17,24,45,69,70]. When the esophageal stenosis is mild, an endoscopic "bougie" procedure is effective and often improves symptoms[16,71]; (4) When EIPD is complicated with GERD, administration of drugs inhibiting the secretion of gastric acid, such as proton pump inhibitors or H2-receptor antagonists, is effective[18,22,24,45]. However, there are no established opinions regarding the dosage or duration of use for these drugs. If the patients are allergic to acid-secretion inhibitors, agents that increase the mucosal protective function are also effective[72]; (5) Isosorbide dinitrate, a smooth muscle relaxant, has been reported to improve symptoms due to strong contraction of the lower esophagus[47]. Inhalation of amyl nitrite is reported to have improved the symptoms in EIPD patients with the complication of esophageal achalasia[48]; (6) Corticosteroids may also alleviate the subjective symptoms of EIPD[56]; and (7) In Europe and the United States, swallowing therapy using inhaled corticosteroids has been studied in EIPD associated with eosinophilic esophagitis[73-75].

CONCLUSION

The etiopathogenesis and natural course of EIPD have not yet been elucidated, and only conservative treatments focusing on symptom management have been employed for patients. In the modern era, EIPD is mainly diagnosed *via* esophageal endoscopy. A better understanding of EIPD will improve differential diagnoses of this and other disorders, such as dysphagia or a feeling of congestion in the esophagus, and ultimately bring about the early diagnosis and appropriate treatment of EIPD, thereby preventing the development of serious complications.

FOOTNOTES

Author contributions: Shintaku M wrote the manuscript.

Conflict-of-interest statement: The author declares no conflict of interest related to this article.

Country/Territory of origin: Japan

ORCID number: Masako Shintaku 0009-0005-0624-9901.

S-Editor: Chen YL
L-Editor: A
P-Editor: Yu HG

REFERENCES

1 **Sabanathan S**, Salama FD, Morgan WE. Oesophageal intramural pseudodiverticulosis. *Thorax* 1985; **40**: 849-857 [PMID: 3934782 DOI: 10.1136/thx.40.11.849]
2 **Boyd RM**, Bogoch A, Greig JH, Trites AE. Esophageal intramural pseudodiverticulosis. *Radiology* 1974; **113**: 267-270 [PMID: 4213918 DOI: 10.1148/113.2.267]
3 **Umlas J**, Sakhuja R. The pathology of esophageal intramural pseudodiverticulosis. *Am J Clin Pathol* 1976; **65**: 314-320 [PMID: 816192 DOI: 10.1093/ajcp/65.3.314]
4 **Medeiros LJ**, Doos WG, Balogh K. Esophageal intramural pseudodiverticulosis: a report of two cases with analysis of similar, less extensive changes in "normal" autopsy esophagi. *Hum Pathol* 1988; **19**: 928-931 [PMID: 3136073 DOI: 10.1016/s0046-8177(88)80008-x]
5 **Murakami M**, Tsuchiya K, Ichikawa H, Kawaguchi K, Sugiyama A, Ishida K, Chisuwa H, Kawasaki S. Esophageal intramural pseudodiverticulosis associated with esophageal perforation. *J Gastroenterol* 2000; **35**: 702-705 [PMID: 11023042 DOI: 10.1007/s005350070050]
6 **Struyve M**, Langemans C, Robaeys G. Pneumomediastinum as a complication of esophageal intramural pseudodiverticulosis. *Acta Gastroenterol Belg* 2018; **81**: 433-435 [PMID: 30350535]
7 **Thibodeau MP**, Brigand C, Ferraro P, Martin J, Duranceau A. Esophagectomy for complications of esophageal intramural pseudodiverticulosis. *Dis Esophagus* 2007; **20**: 178-182 [PMID: 17439604 DOI: 10.1111/j.1442-2050.2007.00666.x]
8 **Liechty J**, Wood R. Operative management of pulmonary abscess due to spontaneous perforation of diffuse intramural esophageal pseudodiverticulosis. *Proc (Bayl Univ Med Cent)* 2011; **24**: 216-219 [PMID: 21738294 DOI: 10.1080/08998280.2011.11928718]
9 **Mendl K**, McKay JM, Tanner CH. Intramural diverticulosis of the oesophagus and Rokitansky-Aschoff sinuses in the gall-bladder. *Br J Radiol* 1960; **33**: 496-501 [DOI: 10.1259/0007-1285-33-392-496]
10 **Hentschel F**, Lüth S. Clinical and endoscopic characteristics of diffuse esophageal intramural pseudo-diverticulosis. *Esophagus* 2020; **17**: 492-501 [PMID: 32162106 DOI: 10.1007/s10388-020-00729-6]
11 **Frieling T**, Kreysel C, Blank M, Mülle D, Euler P, Melchior I. Not always eosinophilic esophagitis - intramural pseudodiverticulosis of the esophagus - a case report and literature review. *Z Gastroenterol* 2020; **58**: 1201-1207 [PMID: 33152792 DOI: 10.1055/a-1288-1521]
12 **Hentschel F**. Chronic fibrosing esophagitis with diffuse esophageal intramural pseudo-diverticulosis. *JGH Open* 2022; **6**: 287-291 [PMID: 35601128 DOI: 10.1002/jgh3.12750]
13 **Solomon NS**, Berseth CL, Braverman RM, Munden MM, Ferry GD. Infantile esophageal intramural pseudodiverticulosis. *J Pediatr Gastroenterol Nutr* 2000; **31**: 76-79 [PMID: 10896076 DOI: 10.1097/00005176-200007000-00017]
14 **Chino O**, Makuuchi H, Kondo Y, Nakamura T, Tanaka Y, Hanashi T, Yokoyama D, Kajiwara H. Esophageal intramural pseudodiverticulosis treated by endoscopic balloon dilatation. *Tokai J Exp Clin Med* 2014; **39**: 137-140 [PMID: 25248429]
15 **Attila T**, Marcon NE. Esophageal intramural pseudodiverticulosis with food impaction. *Can J Gastroenterol* 2006; **20**: 37-38 [PMID: 16432558 DOI: 10.1155/2006/373264]
16 **Shapiro MJ**, Sloan WC. Intramural pseudodiverticulosis of the esophagus. *Ann Otol Rhinol Laryngol* 1977; **86**: 594-597 [PMID: 410348 DOI: 10.1177/000348947708600505]
17 **Tatsumi N**, Mitsufuji S, Tatsumi Y, Wakabayashi N, Konishi H, Kataoka K, Okanoue T. Esophageal intramural pseudodiverticulosis: a case of a young woman. *Dig Dis Sci* 2004; **49**: 1556-1559 [PMID: 15481337 DOI: 10.1023/b:ddas.0000042264.56178.fe]

18 **Siba Y**, Gorantla S, Gupta A, Lung E, Culpepper-Morgan J. Esophageal intramural pseudodiverticulosis, a rare cause of food impaction: case report and review of the literature. *Gastroenterol Rep (Oxf)* 2015; **3**: 175-178 [PMID: 24951515 DOI: 10.1093/gastro/gou035]

19 **Shintaku M**, Nishida T, Shiomi K, Shintaku M. Active opening and closing movements of the orifices of esophageal intramural pseudodiverticulosis. *Gastrointest Endosc* 2011; **74**: 1420-1422 [PMID: 21295301 DOI: 10.1016/j.gie.2010.12.002]

20 **Yamamoto N**, Nakamura M, Tachibana S, Konno H, Nakamura S, Nishino N. Esophageal intramural pseudodiverticulosis with Mallory-Weiss syndrome: report of a case. *Surg Today* 2002; **32**: 519-522 [PMID: 12107778 DOI: 10.1007/s005950200089]

21 **Brühlmann WF**, Zollikofer CL, Maranta E, Hefti ML, Bivetti J, Giger M, Wellauer J, Blum AL. Intramural pseudodiverticulosis of the esophagus: report of seven cases and literature review. *Gastrointest Radiol* 1981; **6**: 199-208 [PMID: 6796452 DOI: 10.1007/BF01890250]

22 **Chon YE**, Hwang S, Jung KS, Lee HJ, Lee SG, Shin SK, Lee YC. A case of esophageal intramural pseudodiverticulosis. *Gut Liver* 2011; **5**: 93-95 [PMID: 21461080 DOI: 10.5009/gnl.2011.5.1.93]

23 **Halm U**, Lamberts R, Knigge I, Mössner J, Zachäus M. Esophageal intramural pseudodiverticulosis: endoscopic diagnosis and therapy. *Dis Esophagus* 2014; **27**: 230-234 [PMID: 23834490 DOI: 10.1111/dote.12104]

24 **Ali O**, Asumu H, Kaur T, Mathew A, Kim R. A rare cause of dysphagia due to esophageal intramural pseudodiverticulosis: a case report and review of literature. *BMC Gastroenterol* 2020; **20**: 72 [PMID: 32178627 DOI: 10.1186/s12876-020-01209-y]

25 **Akkari I**, Jazia EB, Mrabet S, Jemni I. Candida albicans: a cause or a consequence of esophageal intramural pseudo-diverticulosis. *Pan Afr Med J* 2019; **33**: 280 [PMID: 31692736 DOI: 10.11604/pamj.2019.33.280.19601]

26 **Herter B**, Dittler HJ, Wuttge-Hannig A, Siewert JR. Intramural pseudodiverticulosis of the esophagus: a case series. *Endoscopy* 1997; **29**: 109-113 [PMID: 9101148 DOI: 10.1055/s-2007-1004084]

27 **Markle BM**, Hanson K. Esophageal pseudodiverticulosis: two new cases in children. *Pediatr Radiol* 1992; **22**: 194-195 [PMID: 1508587 DOI: 10.1007/BF02012493]

28 **Muhletaler CA**, Lams PM, Johnson AC. Occurrence of oesophageal intramural pseudodiverticulosis in patients with pre-existing benign oesophageal stricture. *Br J Radiol* 1980; **53**: 299-303 [PMID: 6769530 DOI: 10.1259/0007-1285-53-628-299]

29 **Starinsky R**, Manor A, Pajewsky M, Varsano D. Intramural esophageal diverticulosis in an infant. *Isr J Med Sci* 1980; **16**: 604-606 [PMID: 6774955]

30 **Braun P**, Nussle D, Roy CC, Cuendet A. Intramural diverticulosis of the esophagus in an eight-year-old boy. *Pediatr Radiol* 1978; **6**: 235-237 [PMID: 417285 DOI: 10.1007/BF00975544]

31 **Weller MH**. Intramural diverticulosis of the esophagus: report of a case in a child. *J Pediatr* 1972; **80**: 281-285 [PMID: 4621514 DOI: 10.1016/s0022-3476(72)80592-4]

32 **Hammon JW Jr**, Rice RP, Postlethwait RW, Young WG Jr. Esophageal intramural diverticulosis: a clinical and pathological survey. *Ann Thorac Surg* 1974; **17**: 260-267 [PMID: 4204944 DOI: 10.1016/s0003-4975(10)65646-9]

33 **Daud AS**, O'Connor F. Oesophageal intramural pseudodiverticulosis: a cause of dysphagia in a 10-year-old boy. *Eur J Pediatr* 1997; **156**: 530-532 [PMID: 9243234 DOI: 10.1007/s004310050655]

34 **Lingaraj K**, Prabhakaran K, Quak SH. Esophageal intramural pseudodiverticulosis associated with a web in a 12-year-old boy. *J Pediatr Surg* 1999; **34**: 1573-1574 [PMID: 10549779 DOI: 10.1016/s0022-3468(99)90135-5]

35 **van der Pol RJ**, Benninga MA, Bredenoord AJ, Kindermann A. Intramural pseudodiverticulosis of the esophagus: a case report. *Eur J Pediatr* 2013; **172**: 1697-1699 [PMID: 23604394 DOI: 10.1007/s00431-013-2000-0]

36 **Freud E**, Golinsky D, Ziv N, Mor C, Zahavi I, Zer M. Esophageal intramural pseudodiverticulosis: a congenital or acquired condition? *J Pediatr Gastroenterol Nutr* 1997; **24**: 602-607 [PMID: 9161959 DOI: 10.1097/00005176-199705000-00020]

37 **Kochhar R**, Mehta SK, Nagi B, Goenka MK. Corrosive acid-induced esophageal intramural pseudodiverticulosis. A study of 14 patients. *J Clin Gastroenterol* 1991; **13**: 371-375 [PMID: 1918840 DOI: 10.1097/00004836-199108000-00002]

38 **Shintaku M**, Tokuhara M, Aoi M. A case of pseudodiverticulosis within the esophageal wall with endoscopically characteristic findings. *Gastroenterol Endosc* 2018; **60**: 1208-1212 [DOI: 10.11280/gee.60.1208]

39 **Tsuboi J**, Tajika M, Nakamura T, Kawai H, Bhatia V, Takayama R, Kitamura J, Yatabe Y, Hatooka S, Shinoda M, Yamao K, Ogura Y. Endoscopic features of short-term progression of esophageal intramural pseudodiverticulosis. *Endoscopy* 2010; **42** Suppl 2: E92-E93 [PMID: 20195983 DOI: 10.1055/s-0029-1243915]

40 **Chiba T**, Iijima K, Koike T, Uno K, Asano N, Shimosegawa T. A case of severe esophageal intramural pseudodiverticulosis whose symptoms were ameliorated by oral administration of anti-fungal medicine. *Case Rep Gastroenterol* 2012; **6**: 103-110 [PMID: 22619654 DOI: 10.1159/000336846]

41 **Bechtler M**, Vollmer H, Vetter S, Fuchs ES, Weickert U, Jakobs R. Long-term follow-up after dilation in symptomatic esophageal intramural pseudodiverticulosis: an observational study in 22 cases. *Endoscopy* 2014; **46**: 795-797 [PMID: 24977396 DOI: 10.1055/s-0034-1377304]

42 **Levine MS**, Moolten DN, Herlinger H, Laufer I. Esophageal intramural pseudodiverticulosis: a reevaluation. *AJR Am J Roentgenol* 1986; **147**: 1165-1170 [PMID: 3096096 DOI: 10.2214/ajr.147.6.1165]

43 **Canon CL**, Levine MS, Cherukuri R, Johnson LF, Smith JK, Koehler RE. Intramural tracking: a feature of esophageal intramural pseudodiverticulosis. *AJR Am J Roentgenol* 2000; **175**: 371-374 [PMID: 10915677 DOI: 10.2214/ajr.175.2.1750371]

44 **Pearlberg JL**, Sandler MA, Madrazo BL. Computed tomographic features of esophageal intramural pseudodiverticulosis. *Radiology* 1983; **147**: 189-190 [PMID: 6402805 DOI: 10.1148/radiology.147.1.6402805]

45 **Teraishi F**, Fujiwara T, Jikuhara A, Kamitani S, Morino Y, Sato K, Tanaka N. Esophageal intramural pseudodiverticulosis with esophageal strictures successfully treated with dilation therapy. *Ann Thorac Surg* 2006; **82**: 1119-1121 [PMID: 16928560 DOI: 10.1016/j.athoracsur.2006.01.062]

46 **Murney RG Jr**, Linne JH, Curtis J. High-amplitude peristaltic contractions in a patient with esophageal intramural pseudodiverticulosis. *Dig Dis Sci* 1983; **28**: 843-847 [PMID: 6411438 DOI: 10.1007/BF01296908]

47 **Aimi M**, Mikami H, Izumi D, Okimoto E, Tada Y, Mishiro T, Ishimura N, Ishihara S, Kinoshita Y. Evaluation of esophageal intramural pseudo-diverticulosis using high-resolution manometry. *Clin J Gastroenterol* 2016; **9**: 281-284 [PMID: 27412025 DOI: 10.1007/s12328-016-0672-5]

48 **Dua KS**, Stewart E, Arndorfer R, Shaker R. Esophageal intramural pseudodiverticulosis associated with achalasia. *Am J Gastroenterol* 1996; **91**: 1859-1860 [PMID: 8792718]

49 **Turan I**, Ozen E, Bor S, Ozutemiz O. Esophageal intramural pseudodiverticulosis associated with achalasia: an unusual endoscopic appearance. *Endoscopy* 2009; **41** Suppl 2: E23-E24 [PMID: 19221981 DOI: 10.1055/s-0028-1103473]

50 **Takahashi K**, Ikarashi S, Yokoyama J, Terai S. Jackhammer Esophagus Accompanied by Esophageal Intramural Pseudodiverticulosis. *Intern Med* 2018; **57**: 1051-1052 [PMID: 29225275 DOI: 10.2169/internalmedicine.9734-17]

51 **Veria S**, Glosser LD, Lombardi CV, Javaid T, Ramadugu A. Symptomatic esophageal intramural pseudodiverticulosis without stricture: A case report. *SAGE Open Med Case Rep* 2023; **11**: 2050313X221140244 [PMID: 36814679 DOI: 10.1177/2050313X221140244]

52 **Shintaku M**, Ohta M, Noguchi A, Shintaku M. Esophageal Intramural Pseudodiverticulosis: A Histopathological and Immunohistochemical Study of 2 Cases. *Case Rep Gastroenterol* 2022; **16**: 270-277 [PMID: 35702443 DOI: 10.1159/000524496]

53 **Braxton DR**, Nickleach DC, Liu Y, Farris AB 3rd. Necrotizing sialometaplasia-like change of the esophageal submucosal glands is associated with Barrett's esophagus. *Virchows Arch* 2014; **465**: 135-143 [PMID: 24863247 DOI: 10.1007/s00428-014-1590-x]

54 **Piazza M**, Dalla Palma P. Polycystic "dystrophy" of the esophagus. *Am J Clin Pathol* 1977; **67**: 307-308 [PMID: 402810 DOI: 10.1093/ajcp/67.3.307]

55 **Cohen R**, Roth FJ, Delgado E, Ahearn DG, Kalser MH. Fungal flora of the normal human small and large intestine. *N Engl J Med* 1969; **280**: 638-641 [PMID: 5764842 DOI: 10.1056/NEJM196903202801204]

56 **Kataoka H**, Higa T, Koono M. An autopsy case report of diffuse esophageal intramural pseudodiverticulosis. *Acta Pathol Jpn* 1992; **42**: 837-840 [PMID: 1471532 DOI: 10.1111/j.1440-1827.1992.tb01886.x]

57 **Peters ME**, Crummy AB, Wojtowycz MM, Toussaint JB. Intramural esophageal pseudodiverticulosis: a report in a child with a 16-year follow up. *Pediatr Radiol* 1983; **13**: 229-230 [PMID: 6412202 DOI: 10.1007/BF00973162]

58 **Liu SM**, Wu HH, Chang KK, Tseng LJ, Han SC, Mo LR. Esophageal intramural pseudodiverticulosis complicated with stricture. *J Formos Med Assoc* 2010; **109**: 241-244 [PMID: 20434033 DOI: 10.1016/S0929-6646(10)60048-4]

59 **Onozato Y**, Sasaki Y, Abe Y, Yaoita T, Yagi M, Mizumoto N, Shoji M, Kon T, Nishise S, Ueno Y. Esophageal intramural pseudodiverticulosis complicated with severe stricture requiring surgical resection. *Clin J Gastroenterol* 2019; **12**: 292-295 [PMID: 30697669 DOI: 10.1007/s12328-019-00940-8]

60 **Rahlf G**, Wilbert L, Lankisch PG, Hüttemann U. Intramural esophageal diverticulosis. *Acta Hepatogastroenterol (Stuttg)* 1977; **24**: 110-115 [PMID: 404817]

61 **Plavsic BM**, Chen MY, Gelfand DW, Drnovsek VH, Williams JP 3rd, Kogutt MS, Terry JA, Plenkovich D. Intramural pseudodiverticulosis of the esophagus detected on barium esophagograms: increased prevalence in patients with esophageal carcinoma. *AJR Am J Roentgenol* 1995; **165**: 1381-1385 [PMID: 7484570 DOI: 10.2214/ajr.165.6.7484570]

62 **Shintaku M**, Shintaku M, Torii I. Development of Epidermoid Metaplasia of the Mucosa in Association with Esophageal Intramural Pseudodiverticulosis and Candidiasis. *Case Rep Gastroenterol* 2021; **15**: 709-714 [PMID: 34594170 DOI: 10.1159/000518023]

63 **Ezoe Y**, Fujii S, Muto M, Ochiai A, Ohtsu A. Epidermoid metaplasia of the esophagus: endoscopic feature and differential diagnosis. *Hepatogastroenterology* 2011; **58**: 809-813 [PMID: 21830395]

64 **Singhi AD**, Arnold CA, Crowder CD, Lam-Himlin DM, Voltaggio L, Montgomery EA. Esophageal leukoplakia or epidermoid metaplasia: a clinicopathological study of 18 patients. *Mod Pathol* 2014; **27**: 38-43 [PMID: 23765246 DOI: 10.1038/modpathol.2013.100]

65 **Yamanouchi S**, Sako Y, Suemitsu S, Tsukano K, Kotani S, Kusunoki R, Miyaoka Y, Miyake T, Fujishiro H, Kohge N, Yamamoto T, Ohnuma H. Early esophageal cancer with epidermization diagnosed and treated with endoscopic resection. *Clin J Gastroenterol* 2018; **11**: 29-33 [PMID: 29079895 DOI: 10.1007/s12328-017-0792-6]

66 **Nakanishi Y**, Ochiai A, Shimoda T, Yamaguchi H, Tachimori Y, Kato H, Watanabe H, Hirohashi S. Epidermization in the esophageal mucosa: unusual epithelial changes clearly detected by Lugol's staining. *Am J Surg Pathol* 1997; **21**: 605-609 [PMID: 9158687 DOI: 10.1097/00000478-199705000-00015]

67 **Takeshita N**, Kanda N, Fukunaga T, Kimura M, Sugamoto Y, Tasaki K, Uesato M, Sazuka T, Maruyama T, Aida N, Tamachi T, Hosokawa T, Asai Y, Matsubara H. Esophageal intramural pseudodiverticulosis of the residual esophagus after esophagectomy for esophageal cancer. *World J Gastroenterol* 2015; **21**: 9223-9227 [PMID: 26290650 DOI: 10.3748/wjg.v21.i30.9223]

68 **Kunimitsu A**, Ujiie N, Sato C, Taniyama Y, Okamoto H, Fukutomi T, Ozawa Y, Ohnuma S, Unno M, Kamei T. Esophageal Intramural Pseudodiverticulosis Diagnosed by Combining Esophagogastroduodenoscopy, Esophagography, and High-resolution Manometry. *Intern Med* 2023; **62**: 1495-1499 [PMID: 36223924 DOI: 10.2169/internalmedicine.0337-22]

69 **Yoneyama F**, Kobayashi Y, Miyata K, Ohta H, Takeuchi E, Yamada T, Hattori T. Esophageal intramural pseudodiverticulosis treated by balloon dilatation: report of a case. *Surg Today* 2004; **34**: 62-64 [PMID: 14714231 DOI: 10.1007/s00595-003-2629-9]

70 **Naqvi H**, Yousaf MN, Sandhu G, Bhansali D, Farooqi R. Recurrent Dysphagia Associated with Esophageal Intramural Pseudodiverticulosis. *Case Rep Gastroenterol* 2021; **15**: 551-556 [PMID: 34616255 DOI: 10.1159/000517093]

71 **Koyama S**, Watanabe M, Iijima T. Esophageal intramural pseudodiverticulosis (diffuse type). *J Gastroenterol* 2002; **37**: 644-648 [PMID: 12203081 DOI: 10.1007/s005350200102]

72 **Tyberg A**, Jodorkovsky D. A Treatment Option for Esophageal Intramural Pseudodiverticulosis. *ACG Case Rep J* 2014; **1**: 134-136 [PMID: 26157852 DOI: 10.14309/crj.2014.28]

73 **Engel MA**, Raithel M, Amann K, Greess H, Hahn EG, Konturek PC. Rare coincidence of eosinophilic esophagitis with esophageal stenosis and intramural pseudodiverticulosis. *Dig Liver Dis* 2008; **40**: 700-706 [PMID: 17643358 DOI: 10.1016/j.dld.2007.04.011]

74 **Tsai CM**, Butler J, Cash BD. Pseudodiverticulosis with eosinophilic esophagitis: first reported case. *Gastrointest Endosc* 2007; **66**: 1223-4; discussion 1224 [PMID: 18061722 DOI: 10.1016/j.gie.2007.06.049]

75 **Müller M**, Will RC, Eckardt AJ. Eosinophilic esophagitis with pseudodiverticulosis: a rare coincidence. *Endoscopy* 2012; **44** Suppl 2 UCTN: E71 [PMID: 22396287 DOI: 10.1055/s-0031-1291588]

World Journal of Gastroenterology

Submit a Manuscript: https://www.f6publishing.com

World J Gastroenterol 2024 January 14; 30(2): 146-157

DOI: 10.3748/wjg.v30.i2.146

ISSN 1007-9327 (print) ISSN 2219-2840 (online)

ORIGINAL ARTICLE

Retrospective Cohort Study

Long-term prognosis and its associated predictive factors in patients with eosinophilic gastroenteritis

Kai-Wen Li, Ge-Chong Ruan, Shuang Liu, Tian-Ming Xu, Ye Ma, Wei-Xun Zhou, Wei Liu, Peng-Yu Zhao, Zhi-Rong Du, Ji Li, Jing-Nan Li

Specialty type: Gastroenterology and hepatology

Provenance and peer review: Unsolicited article; Externally peer reviewed.

Peer-review model: Single blind

Peer-review report's scientific quality classification

Grade A (Excellent): 0
Grade B (Very good): 0
Grade C (Good): C
Grade D (Fair): 0
Grade E (Poor): 0

P-Reviewer: Caboclo JLF, Brazil

Received: August 22, 2023
Peer-review started: August 22, 2023
First decision: November 20, 2023
Revised: November 28, 2023
Accepted: December 25, 2023
Article in press: December 25, 2023
Published online: January 14, 2024

Kai-Wen Li, Ge-Chong Ruan, Tian-Ming Xu, Ye Ma, Ji Li, Jing-Nan Li, Department of Gastroenterology, Chinese Academy of Medical Sciences and Peking Union Medical College Hospital, Beijing 100730, China

Shuang Liu, Zhi-Rong Du, Department of Allergy, Chinese Academy of Medical Sciences and Peking Union Medical College Hospital, Beijing 100730, China

Wei-Xun Zhou, Department of Pathology, Chinese Academy of Medical Sciences and Peking Union Medical College Hospital, Beijing 100730, China

Wei Liu, Department of Radiology, Chinese Academy of Medical Sciences and Peking Union Medical College Hospital, Beijing 100730, China

Peng-Yu Zhao, Affairs Office, Chinese Academy of Medical Sciences and Peking Union Medical College Hospital (West campus), Beijing 100032, China

Corresponding author: Ji Li, MD, Doctor, Department of Gastroenterology, Chinese Academy of Medical Sciences and Peking Union Medical College Hospital, No. 1 Shuaifuyuan, Wangfujing, Beijing 100730, China. liji0235@pumch.cn

Abstract

BACKGROUND

Eosinophilic gastroenteritis (EGE) is a chronic recurrent disease with abnormal eosinophilic infiltration in the gastrointestinal tract. Glucocorticoids remain the most common treatment method. However, disease relapse and glucocorticoid dependence remain notable problems. To date, few studies have illuminated the prognosis of EGE and risk factors for disease relapse.

AIM

To describe the clinical characteristics of EGE and possible predictive factors for disease relapse based on long-term follow-up.

METHODS

This was a retrospective cohort study of 55 patients diagnosed with EGE admitted to one medical center between 2013 and 2022. Clinical records were collected and analyzed. Kaplan-Meier curves and log-rank tests were conducted to reveal the risk factors for long-term relapse-free survival (RFS).

RESULTS

EGE showed a median onset age of 38 years and a slight female predominance (56.4%). The main clinical symptoms were abdominal pain (89.1%), diarrhea (61.8%), nausea (52.7%), distension (49.1%) and vomiting (47.3%). Forty-three (78.2%) patients received glucocorticoid treatment, and compared with patients without glucocorticoid treatments, they were more likely to have elevated serum immunoglobin E (IgE) (86.8% *vs* 50.0%, P = 0.022) and descending duodenal involvement (62.8% *vs* 27.3%, P = 0.046) at diagnosis. With a median follow-up of 67 mo, all patients survived, and 56.4% had at least one relapse. Six variables at baseline might have been associated with the overall RFS rate, including age at diagnosis < 40 years [hazard ratio (HR) 2.0408, 95% confidence interval (CI): 1.0082–4.1312, P = 0.044], body mass index (BMI) > 24 kg/m^2 (HR 0.3922, 95%CI: 0.1916-0.8027, P = 0.014), disease duration from symptom onset to diagnosis > 3.5 mo (HR 2.4725, 95%CI: 1.220-5.0110, P = 0.011), vomiting (HR 3.1259, 95%CI: 1.5246-6.4093, P = 0.001), total serum IgE > 300 KU/L at diagnosis (HR 0.2773, 95%CI: 0.1204-0.6384, P = 0.022) and glucocorticoid treatment (HR 6.1434, 95%CI: 2.8446-13.2676, P = 0.003).

CONCLUSION

In patients with EGE, younger onset age, longer disease course, vomiting and glucocorticoid treatment were risk factors for disease relapse, whereas higher BMI and total IgE level at baseline were protective.

Key Words: Eosinophilic gastroenteritis; Prognosis; Relapse; Glucocorticoid; Glucocorticoid dependence

Core Tip: Disease relapse has been a long-standing concern for patients with eosinophilic gastroenteritis (EGE). Limited evidence has shown that predicting the course of EGE is complex and related to many factors. There is an urgent need to understand the long-term prognosis of EGE. Therefore, we aimed to describe the features of Chinese EGE patients and construct a model to predict disease relapse based on baseline clinical characteristics.

Citation: Li KW, Ruan GC, Liu S, Xu TM, Ma Y, Zhou WX, Liu W, Zhao PY, Du ZR, Li J, Li JN. Long-term prognosis and its associated predictive factors in patients with eosinophilic gastroenteritis. *World J Gastroenterol* 2024; 30(2): 146-157
URL: https://www.wjgnet.com/1007-9327/full/v30/i2/146.htm
DOI: https://dx.doi.org/10.3748/wjg.v30.i2.146

INTRODUCTION

Eosinophilic gastroenteritis (EGE) is a rare chronic disease characterized by eosinophilic infiltration in the gastrointestinal (GI) tract. EGE was first described by Kaijser in 1937 and, in 1970 by Klein *et al*[1], was classified as mucosal, muscular and serosal types based on the depth of eosinophilic infiltration in the GI tract. The prevalence of EGE reported in Western countries is 5.1-8.4/100000[2,3]. However, racial differences have been found, and EGE is more commonly seen in Asians than in Caucasians[4]. Although the overall pathogenesis of EGE is complicated and still not fully understood, it is widely considered to be related to a Th2-mediated allergic response, in which several molecules are involved, such as interleukin (IL)-4, IL-5, IL-13 and eotaxin[5-7].

Glucocorticoid and diet therapy remain the classical treatments for EGE. A considerable number of patients can achieve clinical remission after initial treatment, although more have recurrent disease or even develop glucocorticoid dependence. However, there are few studies about the long-term prognosis of EGE, most of which were case reports or case series. Some studies have suggested that EGE is related to the Klein classification[8,9]. However, there is more evidence that predicting the course of EGE is complicated and attributed to many factors. To meet this urgent need, this study aimed to clarify the long-term prognosis of EGE patients and to explore the predictive factors for disease relapse.

MATERIALS AND METHODS

Patient selection

We retrospectively enrolled 55 patients with EGE who were diagnosed and hospitalized at Peking Union Medical College Hospital (PUMCH) between 2013 and 2022. EGE was defined by the criteria proposed by Talley *et al*[8], including GI symptoms, eosinophilic infiltration in one or more areas of GI biopsy specimens or ascites, and no evidence of other diseases that may lead to elevated eosinophils. Eosinophilic infiltration is defined as an eosinophil count > 20 per high-power field (HPF) in gastric and/or duodenal biopsies or an eosinophil count > 10% of the total white blood cells in ascites. The inclusion criteria were as follows: (1) Age ≥ 18 years; (2) comprehensive evaluation of clinical features, endoscopic findings and histological examinations confirming the diagnosis of EGE; (3) at least 6 mo of follow-up; and (4) signed informed consent. Exclusion criteria included: (1) Age < 18 years; and (2) clear evidence of parasite infections,

inflammatory bowel diseases, high eosinophilia syndrome, connective tissue disease, malignant tumors, drug allergies and other diseases that could cause elevated eosinophil levels. Two experienced gastroenterologists (Li J and Li JN) reviewed the data and verified the EGE diagnosis.

The following baseline clinical data were collected from medical records: Age; sex; body mass index (BMI); duration from symptom onset to diagnosis; initial symptoms (*e.g.*, abdominal pain, diarrhea, nausea, vomiting, distension, GI bleeding, weight loss, fever, and rash); complications (*e.g.*, ascites and intestinal obstruction); comorbidities (*e.g.*, *Helicobacter pylori* infection, hypertension, diabetes, and hepatitis B virus infection); allergic history (*e.g.*, allergic rhinitis, asthma, and urticaria); laboratory test results (*e.g.* peripheral eosinophil count, hemoglobin, platelets, total serum immunoglobin E (IgE), high sensitivity C-reactive protein, erythrocyte sedimentation rate, antinuclear autoantibodies, antineutrophil cytoplasmic antibodies, and specific allergen tests); computed tomography features; and endoscopic findings.

All patients gave signed informed consent or oral consent, and the study was approved by the Institutional Review Board of Peking Union Medical College Hospital (Ethics approval number: I-23PJ1227).

Follow-up and classification

The treatment and outcome of each patient were reviewed from medical records and updated *via* outpatient services or telephone calls. During follow-up, disease relapse was defined as recurrence of GI symptoms with elevated peripheral blood eosinophil levels. Adverse outcomes include GI surgery or death due to EGE or its complications. Loss of follow-up was defined as failing to contact patients by telephone > 3 times on different days in a week. According to follow-up, patients were divided into two groups based on the status of disease relapse. In addition, according to the efficacy of glucocorticoid treatment, the cohort was classified into glucocorticoid-dependent and non-glucocorticoid-dependent groups. Glucocorticoid dependence was defined as the failure to reduce glucocorticoids to the equivalent dose of prednisone of 10 mg/d within 3 mo after moderate or full doses of glucocorticoid use or a relapse within 3 mo of drug withdrawal.

Statistical analysis

Continuous variables were expressed as the mean and standard deviation for those fitting a normal distribution and were tested by Student's *t* test for the comparison analysis between groups. Medians and quartiles [M (Q1, Q3)] were used for those not fitting a normal distribution, and the comparison analysis was conducted by the Mann-Whitney *U* test. Categorical variables were reported as numbers and percentages and compared by Fisher's exact test between the groups. Relapse-free survival (RFS) was calculated from the date when the patient was first diagnosed with EGE at PUMCH until the date of disease relapse or the last follow-up. We plotted the survival curves by the Kaplan-Meier method and further explored possible risk factors by log-rank analysis. Receiver operating characteristic curves were used to find proper cutoff values and transform continuous variables to categorical variables. A Cox proportional hazards model was used to assess the association of clinical variables with RFS. Only variables with significance ($P < 0.05$) in the univariate analysis were included in the multivariate model. A forest plot was used to show the hazard ratios (HRs) of predictive variables in the Cox regression model. A two-tailed $P < 0.05$ was considered significant. All analyses were performed with R (version 4.1.2).

RESULTS

Clinical characteristics

This study enrolled 55 patients with long-term follow-up. Clinical characteristics are shown in Table 1. Patients had a median age of 38 years at diagnosis, and females (56.4%) were slightly predominant. The median time interval from symptom onset to diagnosis was 5 mo. The most common GI symptom was abdominal pain (89.1%), followed by diarrhea (61.8%), nausea (52.7%), distension (49.1%) and vomiting (47.3%). Weight loss was commonly seen (65.5%). Eighteen patients (32.7%) had a history of allergic diseases, including allergic rhinitis (18.2%), asthma (20.0%) and urticaria (3.6%). Nine (16.4%) and 15 (27.3%) patients complained of a history of food and drug allergies, respectively. The most common complications were ascites (30.2%) and intestinal obstruction (14.5%). Sixteen patients (16/50, 32.0%) had *Helicobacter pylori* infection simultaneously. Elevated initial eosinophil levels were observed in 47 patients (85.5%) at diagnosis [1.16 (0.67–3.91) eosinophils/μL]. Additionally, 38 patients (79.2%) had increased total IgE.

The most commonly affected site of the GI tract under endoscopy was the duodenum (74.1%), which mainly presented as hyperemia (57.4%), erosion (24.1%) and ulceration (9.3%). The descending duodenum (55.6%) was more commonly involved than the duodenal bulb (50.0%) and retrobulbar duodenum (29.6%). In upper GI tissue biopsies, more than 20 eosinophils/HPF was considered to represent significant infiltration. In our cohort, 14 patients (25.5%) showed eosinophil infiltration in the stomach, and 30 (54.5%) showed eosinophil infiltration in the duodenum. Eight patients had a normal appearance on endoscopy examinations. Another important diagnostic procedure was the eosinophil count in ascites. Of the 17 patients complicated with ascites, 13 had accepted abdominocentesis and 10 (76.9%) of them had elevated eosinophils in ascites. However, three patients with elevated eosinophils in ascites had no elevated eosinophil infiltration in the gastric and duodenal biopsies, suggesting the need for increased ascites eosinophil counts to be included in the diagnostic criteria.

Twenty-eight patients (50.9%) were categorized into the mucosal type, nine (16.4%) into the muscular type and 18 (32.7%) into the serosal type based on the Klein classification.

Table 1 Clinical characteristics of eosinophilic gastroenteritis patients in this cohort, *n* (%)

All patients (*N* = 55)					
Demographic characteristics		Complications		ESR (mm/h)[2]	4.00 [2.00, 8.00]
Sex, female	31 (56.4)	Ascite	17 (30.9)	Elevated ESR (> 15)	7 (7/49, 14.3)
Age (yr)[2]	38.00 [25.50, 50.00]	Intestinal obstruction	8 (14.5)	CRP (mg/L)[2]	1.62 [0.84, 4.38]
BMI (kg/m^2)[1]	23.28 ± 3.96	Comorbidities		Elevated hsCRP (> 3)	11 (11/53, 20.8)
BMI > 24	21 (38.9)	Hp infection	16 (16/50, 32.0)	ANA (+)	8 (8/47, 17.0)
Clinical manifestations		HTN	8 (14.5)	ANCA (+)	4 (4/46, 8.7)
Disease duration (mo)[2]	5.00 [1.00, 30.00]	DM	3 (5.5)	Allergen test (+)	14 (14/28, 50.0)
Allergic history	18 (32.7)	HBV infection	4 (7.3)	Inhalant allergen	8 (8/25, 32.0)
Allergic rhinitis	10 (18.2)	Klein classification		Food allergen	8 (8/27, 29.6)
Asthma	11 (20.0)	Mucosal type	28 (50.9)	Endoscopy findings	
Urticaria	2 (3.6)	Muscular type	9 (16.4)	Duodenum involvement	40 (40/54, 74.1)
Symptoms, *n* (%)		Serosal type	18 (32.7)	Bulb	27 (27/54, 50.0)
Abdominal pain	49 (89.1)	Laboratory tests		Post-bulb	16 (16/54, 29.6)
Diarrhea	34 (61.8)	EOS (× 10^9/L)[2]	1.16 [0.67, 3.91]	Descending part	29 (29/54, 55.6)
Nausea	29 (52.7)	Hb (g/L)[1]	138.36 ± 14.81	Hyperaemia	31 (31/54, 57.4)
Vomiting	26 (47.3)	PLT (× 10^9/L)[1]	279.29 ± 81.84	Erosion	13 (13/54, 24.1)
Distension	27 (49.1)	Alb (g/L)[2]	40.00 [37.00, 42.00]	Ulcer	5 (5/54, 9.3)
GI bleeding	3 (5.5)	IgE (KU/L)[2]	152.00 [66.55, 335.50]	Therapy	
Weight loss	36 (65.5)	> 60	38 (79.2)	Diet therapy	7 (12.7)
Fever	4 (7.3)	> 300	13 (27.1)	Anti-allergic agents	7 (12.7)
Rash	6 (10.9)			Immunosuppressors	3 (5.5)

[1]mean ± SD.
[2]Mean[Q1, Q3].
EGE: Eosinophilic gastroenteritis; BMI: Body mass index; GI: Bleeding: gastrointestinal bleeding; Hp: *Helicobacter pylori*; HTN: Hypertension; DM: Diabetes mellitus; HBV: Hepatitis B virus; EOS: Eosinophil count; Hb: Hemoglobin; PLT: Platelet; T-IgE: Total serum immunoglobin E; hsCRP: High sensitivity C reactive protein; ESR: Erythrocyte sedimentation rate; ANA: Antinuclear autoantibodies; ANCA: Anti-neutrophil cytoplasmic antibodies.

Treatments and outcomes

Forty-three patients (78.2%) were treated with glucocorticoids, and all showed a clinical response. Glucocorticoids were used for the initial therapy in 35 patients (81.4%), while the remaining eight initiated glucocorticoids during follow-up. Other treatments included dietary therapy (12.7%), antiallergic drugs (13.2%) and immunosuppressants (5.5%). Patients receiving glucocorticoid treatment, compared with those who did not, had a significantly higher proportion with elevated IgE (86.8% *vs* 50.0%, P = 0.022) at diagnosis and were more likely to have descending duodenal involvement (62.8% *vs* 27.3%, P = 0.046) (Table 2, Supplementary Table 1). There were no significant differences observed between the two groups with regards to sex, disease duration, symptoms, Klein classification or the degree of eosinophil elevation and infiltration. Twenty-one patients (48.8%) were glucocorticoid dependent and had a significantly lower BMI (21.85 *vs* 24.51, P = 0.041). Additionally, duodenal ulcers were more frequently noted by endoscopy in glucocorticoid-dependent patients (19.0% *vs* 0.0%, P = 0.048).

Long-term prognosis and its predictive factors

With a median follow-up of 67 (21.5-89.0) mo, all patients survived, and disease relapse after diagnosis was observed in 56.4% (31/55) of all patients and in 67.4% (29/43) of patients who were treated with glucocorticoids at diagnosis. The median RFS was 12 mo in EGE patients, and the incidences of RFS at 6, 12 and 24 mo were 63.4%, 48.4% and 46.1%, respectively (Figure 1). Patients with onset age < 40 years (HR 2.0408, 95%CI: 1.0082-4.1312, P = 0.044), a disease duration from symptom onset to diagnosis > 3.5 mo (HR 2.4725, 95%CI: 1.220-5.0110, P = 0.011), vomiting (HR 3.1259, 95%CI: 1.5246-6.4093, P = 0.001) and glucocorticoid treatment (HR 6.1434, 95%CI: 2.8446-13.2676, P = 0.003) were observed to be more likely to suffer from disease relapse during follow-up, while BMI > 24 kg/m^2 (HR 0.3922, 95%CI: 0.1916-0.8027, P = 0.014) and baseline IgE level > 300 KU/L (HR 0.2773, 95%CI: 0.1204-0.6384, P = 0.022) tended to be protective factors for disease relapse (Figure 2). Multivariate analysis showed that higher BMI (HR 0.3206, 95%CI: 0.11-0.9347, P = 0.037) was

Table 2 Clinical characteristics and intergroup comparisons

	Non glucocorticoid treatment (*n* = 12)	Glucocorticoid treatment (*n* = 43)	*P* value	Non-glucocorticoid dependent (*n* = 22)	Glucocorticoid dependent (*n* = 21)	*P* value
Sex (female)	8 (66.7)	23 (53.5)	0.519	10 (45.5)	13 (61.9)	0.364
Age (yr)[2]	44.00 [27.75, 48.75]	36.00 [25.00, 50.00]	0.838	36.00 [26.00, 53.25]	36.00 [25.00, 48.00]	0.780
BMI (kg/m^2)[1]	23.43 ± 2.84	23.24 (4.25)	0.888	24.51 (4.55)	21.85 (3.50)	0.041[a]
Disease duration (mo)	2.00 [1.00, 10.00]	7.00 [1.00, 41.00]	0.223	3.00 [1.00, 15.75]	11.00 [4.00, 60.00]	0.056[b]
Allergic history	2 (16.7)	16 (37.2)	0.298	8 (36.4)	8 (38.1)	1.000
Symptoms						
Abdominal pain	11 (91.7)	38 (88.4)	1.000	19 (86.4)	19 (90.5)	1.000
Diarrhea	8 (66.7)	26 (60.5)	0.750	12 (54.5)	14 (66.7)	0.537
Vomiting	3 (25.0)	23 (53.5)	0.108	12 (54.5)	11 (52.4)	1.000
Weight loss	10 (83.3)	26 (60.5)	0.183	14 (63.6)	12 (57.1)	0.760
Hp infection	5 (5/11, 45.5)	11 (11/39, 28.2)	0.297	6 (6/20, 30.0)	5 (5/19, 26.3)	1.000
Klein classification						
Mucosal type	6 (50.0)	22 (51.2)	1.000	11 (50.0)	11 (52.4)	0.298
Muscular type	2 (16.7)	7 (16.3)		2 (9.1)	5 (23.8)	
Serosal type	4 (33.3)	14 (32.6)		9 (40.9)	5 (23.8)	
EOS (× 10^9/L)[2]	0.76 [0.51, 2.32]	1.48 [0.95, 4.00]	0.124	2.46 [1.13, 3.96]	1.01 [0.48, 3.99]	0.065[b]
IgE (KU/L)[2]	54.50 [23.77, 629.75]	166.00 [72.90, 298.00]	0.406	234.00 [118.00, 343.25]	118.00 [67.10,191.00]	0.082[b]
Elevated IgE (> 60)	5 (5/10, 50.0)	33 (33/36, 86.8)	0.022[a]	17 (17/20, 85.0)	16 (16/18, 88.9)	1.000
Duodenum involvement	7 (7/11, 63.6)	33 (33/43, 76.7)	0.448	15 (68.2)	18 (85.7)	0.281
Bulb	5 (5/11, 45.5)	21 (21/43, 48.8)	1.000	9 (40.9)	13 (61.9)	0.227
Post-bulb	1 (1/11, 9.1)	15 (15/43, 34.9)	0.144	11 (50.0)	4 (19.0)	0.055[b]
Descending part	3 (3/11, 27.3)	27 (27/43, 62.8)	0.046[a]	12 (54.5)	15 (71.4)	0.347
Duodenum endoscopic features						
Hyperaemia	6 (6/11, 54.5)	25 (25/43, 58.1)	1.000	14 (63.6)	11 (52.4)	0.543
Erosion	3 (3/11, 27.3)	10 (10/43, 23.3)	1.000	4 (18.2)	6 (28.6)	0.488
Ulcer	1 (1/11, 9.1)	4 (4/43, 9.3)	1.000	0 (0.0)	4 (19.0)	0.048[a]

[1]mean ± SD.
[2]Mean[Q1, Q3].
[a]$P < 0.05$.
[b]$P < 0.10$.
Hp: *Helicobacter pylori*; EOS: Eosinophil count; IgE: Serum immunoglobin E; BMI: Body mass index.

independently significant for the prediction of less disease relapse (Table 3, Figure 3, Supplementary Table 2).

DISCUSSION

Establishing the long-term prognosis and predictive factors is valuable for clinical practice in EGE patients. This study conducted a median 67-mo follow-up and found that the median RFS was 12 mo, and the rates of RFS were quite high. Age at onset, BMI, disease duration from symptom onset to diagnosis, vomiting symptoms, serum level of IgE, and glucocorticoid treatment helped to predict disease prognosis. Higher BMI was independently significant for the prediction of less disease relapse based on multivariate analysis. These findings could facilitate the categorization of EGE patients into groups with different prognoses.

Table 3 Univariate and multivariate Cox analysis for disease relapse

	Univariate analysis		Multivariate analysis		
	HR (95%CI)	*P* value	Coef	HR (95%CI)	*P* value
Age (yr)					
> 40	1	0.044[a]		1	0.330
≤ 40	2.0408 (1.0082-4.1312)		0.6827	1.9791 (0.5013-7.8140)	
BMI (kg/m^2)					
≤ 24	1	0.014[a]		1	0.037[a]
> 24	0.3922 (0.1916-0.8027)		-1.1375	0.3206 (0.11-0.9347)	
Disease duration (mo)					
≤ 3.5	1	0.011[a]		1	0.106
> 3.5	2.4725 (1.2200-5.0110)		0.7447	2.1058 (0.8533-5.1968)	
Vomiting					
No	1	0.001[a]		1	0.695
Yes	3.1259 (1.5246-6.4093)		0.2677	1.3069 (0.3423-4.9904)	
T-IgE (KU/L)					
≤ 300	1	0.022[a]		1	0.233
> 300	0.2773 (0.1204-0.6384)		-0.7995	0.4496 (0.121-1.6699)	
Glucocorticoid treatment					
No	1	0.003[a]		1	0.065[b]
Yes	6.1434 (2.8446-13.2676)		1.4038	4.0705 (0.917-18.0689)	

[a]$P < 0.05$.
[b]$P < 0.10$.
HR: Hazard ratio; coef: Coefficient; T-IgE: Total serum immunoglobin E; BMI: Body mass index.

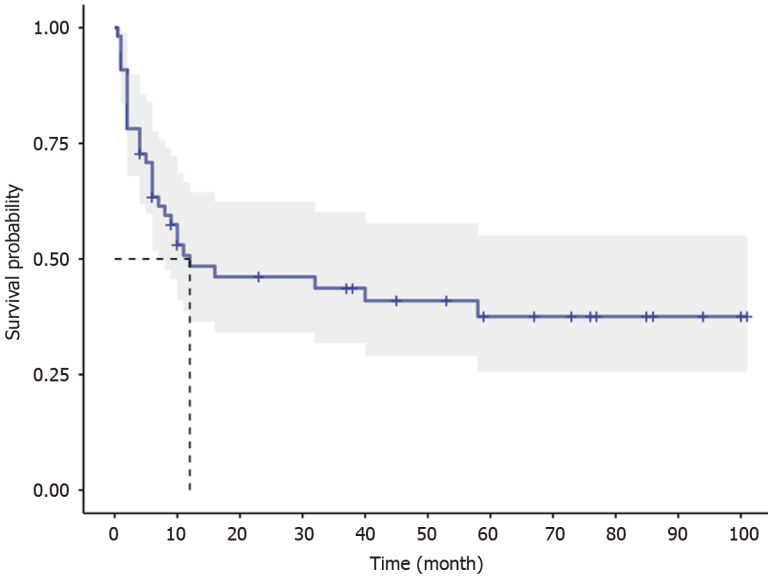

DOI: 10.3748/wjg.v30.i2.146

Figure 1 Kaplan-Meier survival curve of the recurrence-free survival for all eosinophilic gastroenteritis patients (median relapse-free survival time: 12 mo). 6-mo, 1-year and 2-year relapse-free survival rate were 63.4%, 48.4% and 46.1% respectively.

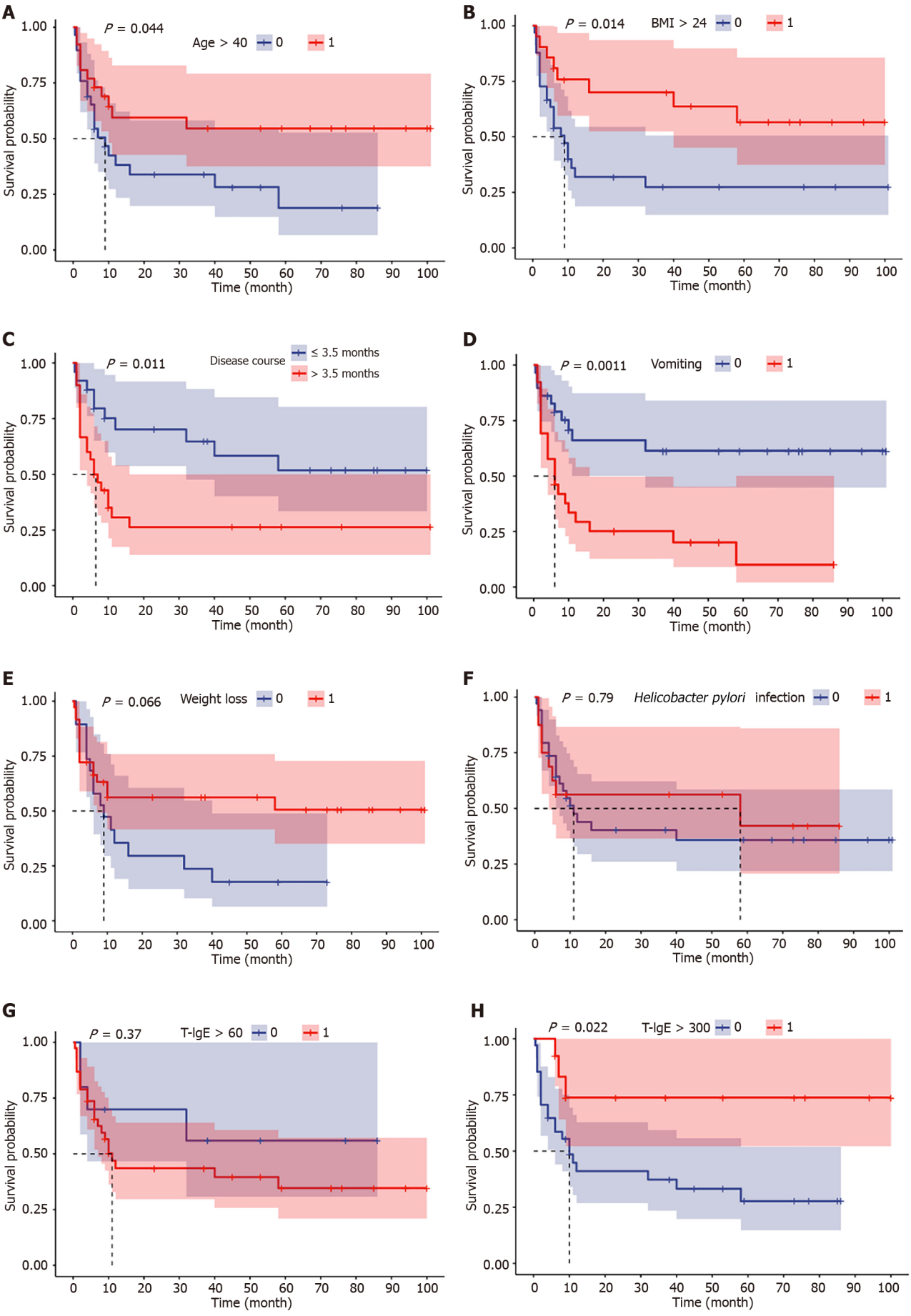
A
P = 0.044
Age > 40 0 1
B
P = 0.014
BMI > 24 0 1
C
P = 0.011
Disease course ≤ 3.5 months > 3.5 months
D
P = 0.0011
Vomiting 0 1
E
P = 0.066
Weight loss 0 1
F
P = 0.79
Helicobacter pylori infection 0 1
G
P = 0.37
T-IgE > 60 0 1
H
P = 0.022
T-IgE > 300 0 1
Survival probability
Time (month)

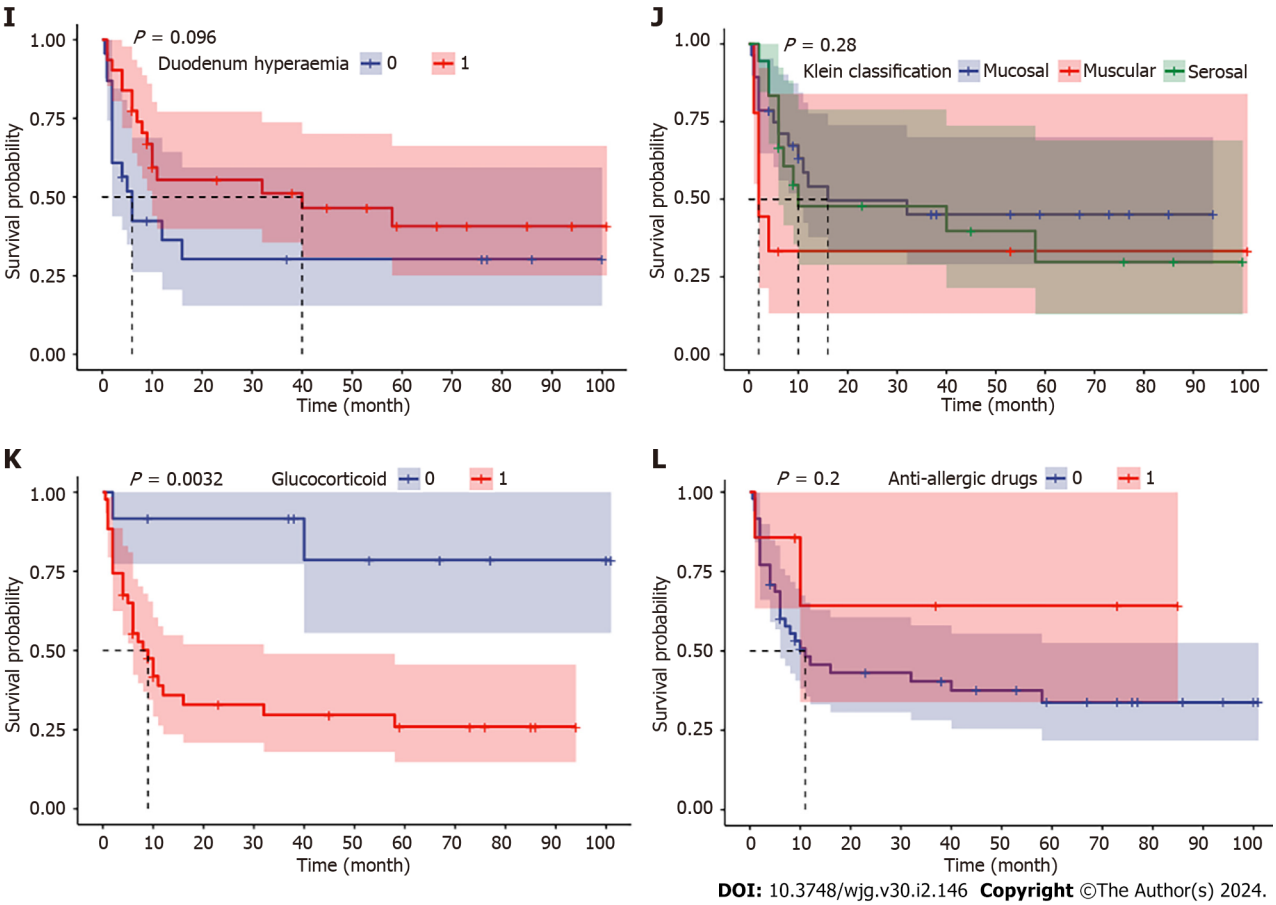

DOI: 10.3748/wjg.v30.i2.146

Figure 2 Kaplan-Meier survival curves according to different prognostic factors for disease relapse. Age < 40, body mass index (BMI) < 24, disease duration > 3.5 mo, vomiting, immunoglobin E (IgE) level < 300 KU/L, and glucocorticoid treatment showed a statistical difference between the relapse group and relapse-free group. Other variables included weight loss, Hp infection, IgE level > 60 KU/L, duodenal hyperaemia, Klein classification and anti-allergic drugs. A: Age, $P = 0.044$; B: BMI, $P = 0.014$; C: Disease duration, $P = 0.011$; D: Vomiting, $P = 0.0011$; E: Weight loss, $P = 0.066$; F: *Helicobacter pylori* infection, $P = 0.790$; G: T-IgE > 60, $P = 0.370$; H: T-IgE > 300, $P = 0.022$; I: Duodenal hyperaemia, $P = 0.096$; J: Klein classification, $P = 0.280$; K: Glucocorticoid, $P = 0.0032$; L: Anti-allergic drugs, $P = 0.200$.

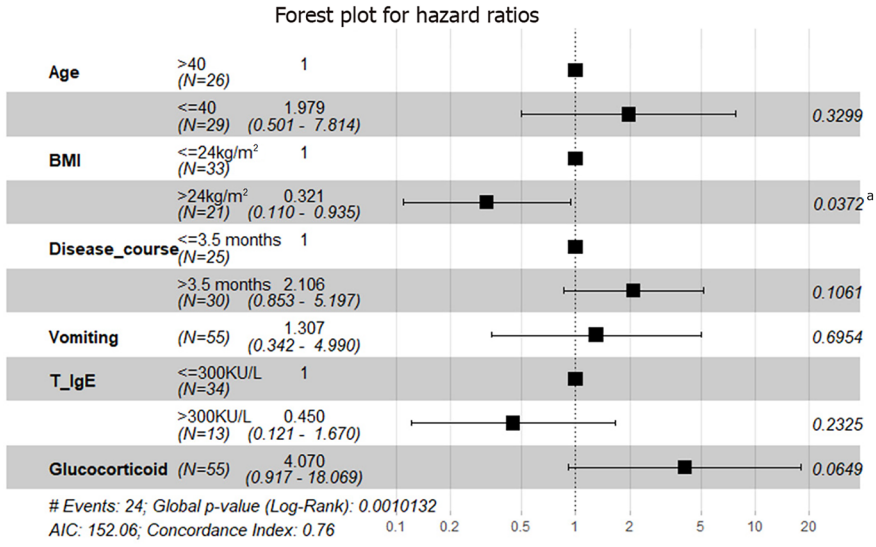

DOI: 10.3748/wjg.v30.i2.146

Figure 3 Forest plot for hazard ratios for predictors included in the Cox regression model. BMI: Body mass index; T_IgE: Total serum immunoglobin E. [a]$P < 0.05$.

Consistent with previous studies[2,10], our patients showed a median onset in the third decade of life and a slight predominance in women. The diagnosis of EGE has long been considered difficult. In 2021, the United States Food and Drug Administration indicated a prolonged diagnosis delay of 4-9 years, which was probably due to delays in referral, endoscopic procedures, and the absence of biopsy[11,12]. However, the median duration from symptom onset to diagnosis in our study was only 5 mo. The physician's knowledge of EGE might have contributed to the earlier diagnosis of EGE in our medical center, which is a tertiary medical center and the national medical center for refractory and rare diseases.

A significant percentage of patients had a history of allergic diseases or positive results in allergen tests, which is also comparable with previous studies from 23.8% to 63%[9,13-15], indicating the association between allergy and EGE pathogenesis. Nonspecific GI symptoms, such as abdominal pain, diarrhea and vomiting, are the main manifestations of EGE. However, in our cohort, weight loss was another dominant symptom, with a frequency of 65.5%. Extraintestinal manifestations such as pancreatitis, cholecystitis or splenic hypofunction[16-18] were not observed in our study. Peripheral eosinophil count elevation was observed in 85.6% of our patients but was neither necessary for diagnosis nor significant for disease severity. The proportion reported varied from 10.9% to 85.7%[9,10,19,20].

Endoscopy is one of the most important measures for EGE diagnosis. As research has described, EGE can affect any part of the GI tract, from the esophagus to the colon and rectum, but the small intestine and antrum are commonly affected[8,14,15]. This also agrees with our observations, and in our cohort, the duodenum was mostly involved. Previous studies reported that 62%-92.2% of patients showed a normal endoscopic appearance due to the patchy distribution of EGE[14,19,21]. In our study, only 14.5% of the patients had normal endoscopies. However, this does not deny the necessity for biopsies because eosinophilic infiltration was also frequently seen in endoscopically normal parts during routine biopsies from the antrum and descending duodenum in our cohort. Meanwhile, the endoscopic features of the stomach were not used for further analysis because > 30% of patients had *Helicobacter pylori* infection, which resulted in unavoidable bias for the interpretation of the endoscopic findings in the stomach.

In 1990, Talley *et al*[8] reported a 40-patient cohort in the Mayo Clinic with distributions of 44%, 12% and 39% for the mucosal, muscular and serosal types, respectively, by the Klein classification. In 2010, Chang *et al*[13] reported 59 new cases in the Mayo Clinic and suggested a shifting trend toward the mucosal type (52/59). However, muscular and serosal types made up almost half of the cohort (16.4% and 32.7%) in our study. Following an inward–outward pathway, EGE is considered to start in the mucosal layer; thus, the serosal type represents a more advanced stage. This may reflect the selection bias of our study in that patients with more severe symptoms were more commonly seen and treated in our center.

By suppressing the transcription of chemokines and eosinophilic growth factors, such as IL-3, IL-5, and granulocyte–macrophage colony-stimulating factor, glucocorticoids remain the most commonly used treatment for EGE. In our center, most patients received an equivalent prednisone dose of 0.5-1.0 mg/kg/d as the initial medication, with dose tapering, and nearly all our patients treated with glucocorticoids showed a rapid clinical response. Alternative therapies include dietary therapy, antiallergic agents and immunosuppressants. Among them, dietary therapy and antiallergic therapy are often used together with glucocorticoids if patients have definite food allergies or are complicated with allergic diseases. Immunosuppressants are rarely used and are mainly used in cases of glucocorticoid dependence. Currently, the use of biologic agents, such as the anti-Siglec-8 antibody AK002[22], the anti-IL-5 antibody mepolizumab [23] and the anti-IgE antibody omalizumab (OmAb)[24], is under investigation and has a partially positive effect in reducing GI symptoms and eosinophilic infiltration. These data may provide more options for treating EGE in the future.

Only a few studies have reported the long-term outcomes of EGE, and small sample sizes and short follow-up times limit the conclusions that can be drawn from these studies. Between 42% and 50% of patients had spontaneous remission and remained asymptomatic without specific treatment in previous studies[9,14]. Chambrun *et al* identified three different courses of EGE after a 15-year follow-up: single flare (42%), recurring course (37%) and continuous course (21%). They found that more patients with the serosal type had a single flare, and predominant mucosal disease presented mostly a continuous course[9]. Sato *et al*[25] proposed that the chronicity of coexisting allergic disorders may be associated with the chronicity of EGE. However, in our study, the Klein classification and history of allergic diseases did not present a significant difference for disease relapse or glucocorticoid dependence. In 2021, Havlichek *et al*[10] divided patients into two groups by four clinical characteristics at diagnosis: weight loss, hypoalbuminemia, serosa involvement, and anemia. Patients in the severe group, who had one of the four characteristics, had a higher risk of chronic disease. However, we did not observe these characteristics to be significant prognostic factors for EGE relapse, probably because they grouped patients with preidentified risk factors and then validated them, while we directly filtered baseline variables by log-rank tests and had a longer follow-up time. Grandinetti *et al*[26] also reported that an increasing number of involved GI segments was associated with disease relapse, indicating the importance of multiple biopsies regardless of endoscopic manifestations in suspected EGE patients.

Notably, we identified six possible prognostic factors for disease relapse in EGE. As expected by clinical experience, patients with a younger onset age are more likely to have disease relapse, and a longer delay of diagnosis may contribute to the recurrent course, which emphasizes the importance of early recognition and diagnosis of EGE. In our previous work, we suggested a diagnostic flowchart for patients suspected of having EGE, including several key steps for a quicker and more accurate diagnosis[27]. Vomiting is a newly identified factor for EGE prognosis in our study. It may be a nonspecific GI symptom caused by muscular involvement. Our study indicates that if a patient has vomiting as one of the initial symptoms, he may be at higher risk for disease relapse. Consistent with observations in clinical practice, elevated total serum IgE is a protective prognostic factor for EGE relapse. The cutoff value (300 KU/L) is four times higher than the upper limit of normal (60 KU/L) in our center. IgE is produced by activated B cells and binds to the Fcε receptor I (FcεRI) on eosinophils and mast cells, inducing their degranulation. It can be hypothesized that in patients with a markedly elevated baseline IgE level, their FcεRIs on eosinophils and mast cells may be saturated and thus unable to

function upon re-exposure to allergens. Glucocorticoid treatment is also a significant factor for disease relapse. Patients treated with glucocorticoids had a greater possibility of at least one relapse during our follow-up, which might be partially explained by their own greater disease burden with more involvement of the descending duodenum compared with patients without glucocorticoid treatment. The exact clinical value or pathogenesis needs to be validated and clarified in future studies.

For multivariate analysis, higher BMI was an independent protective factor for disease relapse in our study. However, from the survival analysis, we noticed that patients without weight loss were more likely to have a recurrent course, although the *P* value was not significant (0.066). This seems contradictory. Given the large proportion of patients with serosal involvement in our cohort, the measurement of BMI might have been affected by the large amount of ascites. While the effect of obesity on EGE has not been previously studied, several studies have pointed out that lower BMI in patients with eosinophilic esophagitis (EoE) might indicate more severe disease[28,29]. In addition to the possible association with EoE-induced dysphagia and thus malnutrition, studies found that this may be associated with tumor necrosis factor-α release from adipose tissue, which promotes a shifting trend from Th-2 to Th-1 responses[30]. The exact clinical value of obesity in EGE still needs further investigation.

Beyond the abovementioned limitations, there were some other limitations in our study. First, the findings were based on 55 patients from one medical center, which makes generalization difficult. Second, selection bias was also unavoidable because the patients were all hospitalized in one medical center. For example, there was a higher percentage of serosal type in this study. Third, the knowledge and clinical experience among different physicians during the long study period were variable, which directly affected the treatment decisions. Finally, the definition of disease relapse was mainly based on symptoms and did not include endoscopic and histological diagnostic criteria, which might have overestimated the relapse rate. Future prospective multicenter studies of EGE with confirmed and validated criteria of disease relapse should be conducted to fully address the clinical manifestations and long-term prognosis.

CONCLUSION

We have described the general clinical characteristics of Chinese EGE patients and their long-term outcomes and identified six baseline clinical variables that could predict prognosis.

ARTICLE HIGHLIGHTS

Research background

Eosinophilic gastroenteritis (EGE) is a rare, chronic and recurrent disease with abnormal eosinophilic infiltration in gastrointestinal tract. Disease relapse and glucocorticoid dependence remain notable problems.

Research motivation

Few studies had illuminated the prognosis of EGE and risk factors for disease relapse. By exploring prognostic factors by baseline clinical data, we may identify patients who are more vulnerable for disease relapse at diagnosis and offer them individualized treatment.

Research objectives

To describe the clinical characteristics of EGE and possible predictive factors for disease relapse based on long-term follow-up.

Research methods

This retrospective cohort study enrolled 55 EGE patients (2013-2022, Peking Union Medical College Hospital) and analyzed their clinical records. Kaplan-Meier analysis, Log-Rank test and Cox regression analysis were conducted to reveal the risk factors for long-term prognosis.

Research results

In our cohort, EGE showed a female predominance (56.4%) and its median onset age was 38 years old. Abdominal pain (89.1%) was most commonly seen. 78.2% of patients received glucocorticoid treatment in whom elevated serum immunoglobin E (IgE) at diagnosis (86.8% *vs* 50.0%, *P* = 0.022) and descending duodenum involvement (62.8% *vs* 27.3%, *P* = 0.046) were more frequently seen. The median follow-up time was 67 mo, during which 31 patients (56.4%) suffered from at least one flares of disease relapse. Six prognostic factors were figured out, including age at diagnosis < 40 years (hazard ratio (HR) 2.0408, 95% confidence interval (CI): 1.0082-4.1312, *P* = 0.044), body mass index > 24 kg/m^2 (HR 0.3922, 95%CI: 0.1916-0.8027, *P* = 0.014), disease duration from symptom onset to diagnosis > 3.5 mo (HR 2.4725, 95%CI: 1.220-5.0110, *P* = 0.011), vomiting (HR 3.1259, 95%CI: 1.5246-6.4093, *P* = 0.001), total serum IgE > 300 KU/L at diagnosis (HR 0.2773, 95%CI: 0.1204-0.6384, *P* = 0.022) and glucocorticoid treatment (HR 6.1434, 95%CI: 2.8446-13.2676, *P* = 0.003).

Research conclusions

We identified younger onset age, longer disease course, vomiting and glucocorticoid treatment to be risk factors for

disease relapse, whereas higher body mass index and total-IgE level at baseline to be protective.

Research perspectives

In future research, we tend to conduct multi-center prospective study to verify and improve our prognostic model and further explore more accurate biomarkers for disease relapse based on serum proteomics and intestinal microbiomes.

FOOTNOTES

Co-first authors: Kai-Wen Li and Ge-Chong Ruan.

Co-corresponding authors: Ji Li and Jing-Nan Li.

Author contributions: Li KW, Ruan GC, Li J and Li JN designed the study; Li KW, Ruan GC, Zhou WX and Liu W acquired and analyzed the data; Liu S, Xu TM, Ma Y and Du ZR helped with patient follow-up; Zhao PY contributed to the statistical methodology; Li J and Li JN provided resources and acquired funding; Li KW, Ruan GC, Li J and Li JN wrote the paper. During the course of this study, Li KW and Ruan GC made equal contributions across various stage. Their involvement encompassed the design of the study, selection of patients, collection of baseline data, follow-up *via* telephone calls and outpatient services, as well as data analysis and the drafting of the article, thus leading to shared first authorship. Furthermore, the study also benefited from the substantial contributions of Li J and Li JN. They played equally vital roles in the process of study design, funding support, article writing and reviewing, thereby sharing co-correspondence authorship. These collaborative efforts have been instrumental in shaping the final outcome of this work.

Supported by National High Level Hospital Clinical Research Funding, No. 2022-PUMCH-B-022; CAMS Innovation Fund for Medical Sciences, No. CIFMS 2021-1-I2M-003; and Undergraduate Innovation Program, No. 2023zglc06076.

Institutional review board statement: The study was reviewed and approved by the Chinese Academy of Medical Sciences and Peking Union Medical College Hospital Institutional Review Board (Approval No. I-23PJ1227).

Informed consent statement: All study participants or their legal guardian provided informed written consent about personal and medical data collection prior to study enrolment.

Conflict-of-interest statement: All the Authors have no conflict of interest related to the manuscript.

Data sharing statement: No additional data are available.

STROBE statement: The authors have read the STROBE Statement-checklist of items, and the manuscript was prepared and revised according to the STROBE Statement-checklist of items.

Country/Territory of origin: China

ORCID number: Shuang Liu 0000-0003-2099-5140; Tian-Ming Xu 0000-0003-3868-9205; Wei-Xun Zhou 0000-0002-7459-7343; Ji Li 0000-0002-0285-2966; Jing-Nan Li 0000-0003-0098-8429.

S-Editor: Qu XL
L-Editor: A
P-Editor: Yu HG

REFERENCES

1 **Klein NC**, Hargrove RL, Sleisenger MH, Jeffries GH. Eosinophilic gastroenteritis. *Medicine (Baltimore)* 1970; **49**: 299-319 [PMID: 5426746 DOI: 10.1097/00005792-197007000-00003]

2 **Mansoor E**, Saleh MA, Cooper GS. Prevalence of Eosinophilic Gastroenteritis and Colitis in a Population-Based Study, From 2012 to 2017. *Clin Gastroenterol Hepatol* 2017; **15**: 1733-1741 [PMID: 28603057 DOI: 10.1016/j.cgh.2017.05.050]

3 **Jensen ET**, Martin CF, Kappelman MD, Dellon ES. Prevalence of Eosinophilic Gastritis, Gastroenteritis, and Colitis: Estimates From a National Administrative Database. *J Pediatr Gastroenterol Nutr* 2016; **62**: 36-42 [PMID: 25988554 DOI: 10.1097/MPG.0000000000000865]

4 **Ito J**, Fujiwara T, Kojima R, Nomura I. Racial differences in eosinophilic gastrointestinal disorders among Caucasian and Asian. *Allergol Int* 2015; **64**: 253-259 [PMID: 26117257 DOI: 10.1016/j.alit.2015.02.003]

5 **Hogan SP**, Rosenberg HF, Moqbel R, Phipps S, Foster PS, Lacy P, Kay AB, Rothenberg ME. Eosinophils: biological properties and role in health and disease. *Clin Exp Allergy* 2008; **38**: 709-750 [PMID: 18384431 DOI: 10.1111/j.1365-2222.2008.02958.x]

6 **Stone KD**, Prussin C. Immunomodulatory therapy of eosinophil-associated gastrointestinal diseases. *Clin Exp Allergy* 2008; **38**: 1858-1865 [PMID: 19037962 DOI: 10.1111/j.1365-2222.2008.03122.x]

7 **Rothenberg ME**. Eosinophilia. *N Engl J Med* 1998; **338**: 1592-1600 [PMID: 9603798 DOI: 10.1056/NEJM199805283382206]

8 **Talley NJ**, Shorter RG, Phillips SF, Zinsmeister AR. Eosinophilic gastroenteritis: a clinicopathological study of patients with disease of the mucosa, muscle layer, and subserosal tissues. *Gut* 1990; **31**: 54-58 [PMID: 2318432 DOI: 10.1136/gut.31.1.54]

9 **Pineton de Chambrun G**, Gonzalez F, Canva JY, Gonzalez S, Houssin L, Desreumaux P, Cortot A, Colombel JF. Natural history of eosinophilic gastroenteritis. *Clin Gastroenterol Hepatol* 2011; **9**: 950-956.e1 [PMID: 21806952 DOI: 10.1016/j.cgh.2011.07.017]

10 **Havlichek D 3rd**, Choung RS, Murray JA. Eosinophilic Gastroenteritis: Using Presenting Findings to Predict Disease Course. *Clin Transl Gastroenterol* 2021; **12**: e00394 [PMID: 34620754 DOI: 10.14309/ctg.0000000000000394]

11 **Rothenberg ME**, Hottinger SKB, Gonsalves N, Furuta GT, Collins MH, Talley NJ, Peterson K, Menard-Katcher C, Smith M, Hirano I, Genta RM, Chehade M, Gupta SK, Spergel JM, Aceves SS, Dellon ES. Impressions and aspirations from the FDA GREAT VI Workshop on Eosinophilic Gastrointestinal Disorders Beyond Eosinophilic Esophagitis and Perspectives for Progress in the Field. *J Allergy Clin Immunol* 2022; **149**: 844-853 [PMID: 34953790 DOI: 10.1016/j.jaci.2021.12.768]

12 **Chehade M**, Kamboj AP, Atkins D, Gehman LT. Diagnostic Delay in Patients with Eosinophilic Gastritis and/or Duodenitis: A Population-Based Study. *J Allergy Clin Immunol Pract* 2021; **9**: 2050-2059.e20 [PMID: 33440255 DOI: 10.1016/j.jaip.2020.12.054]

13 **Chang JY**, Choung RS, Lee RM, Locke GR 3rd, Schleck CD, Zinsmeister AR, Smyrk TC, Talley NJ. A shift in the clinical spectrum of eosinophilic gastroenteritis toward the mucosal disease type. *Clin Gastroenterol Hepatol* 2010; **8**: 669-75; quiz e88 [PMID: 20451664 DOI: 10.1016/j.cgh.2010.04.022]

14 **Wong GW**, Lim KH, Wan WK, Low SC, Kong SC. Eosinophilic gastroenteritis: Clinical profiles and treatment outcomes, a retrospective study of 18 adult patients in a Singapore Tertiary Hospital. *Med J Malaysia* 2015; **70**: 232-237 [PMID: 26358020]

15 **Zhang L**, Duan L, Ding S, Lu J, Jin Z, Cui R, McNutt M, Wang A. Eosinophilic gastroenteritis: clinical manifestations and morphological characteristics, a retrospective study of 42 patients. *Scand J Gastroenterol* 2011; **46**: 1074-1080 [PMID: 21623674 DOI: 10.3109/00365521.2011.579998]

16 **Di Sabatino A**, Aronico N, Giuffrida P, Cococcia S, Lenti MV, Vanoli A, Guerci M, Di Stefano M, Corazza GR. Association between defective spleen function and primary eosinophilic gastrointestinal disorders. *J Allergy Clin Immunol Pract* 2018; **6**: 1056-1058.e1 [PMID: 29128338 DOI: 10.1016/j.jaip.2017.10.017]

17 **Hui CK**. Eosinophilic gastroenteritis complicating acute calculus eosinophilic cholecystitis 6 months after cholecystectomy. *J Dig Dis* 2018; **19**: 693-695 [PMID: 30370999 DOI: 10.1111/1751-2980.12683]

18 **Sheikh RA**, Prindiville TP, Pecha RE, Ruebner BH. Unusual presentations of eosinophilic gastroenteritis: case series and review of literature. *World J Gastroenterol* 2009; **15**: 2156-2161 [PMID: 19418590 DOI: 10.3748/wjg.15.2156]

19 **Hui CK**, Hui NK. A Prospective Study on the Prevalence, Extent of Disease and Outcome of Eosinophilic Gastroenteritis in Patients Presenting with Lower Abdominal Symptoms. *Gut Liver* 2018; **12**: 288-296 [PMID: 29212311 DOI: 10.5009/gnl17056]

20 **Yang XM**, He SQ, Yang H, Zheng HH, Zhu LH, Zhou SK, Zhang Y. Clinical features and treatment outcomes of eosinophilic gastroenteritis : an analysis of 28 cases. *Acta Gastroenterol Belg* 2019; **82**: 5-10 [PMID: 30888747]

21 **Pesek RD**, Reed CC, Collins MH, Muir AB, Fulkerson PC, Menard-Katcher C, Falk GW, Kuhl J, Magier AZ, Ahmed FN, Demarshall M, Gupta A, Gross J, Ashorobi T, Carpenter CL, Krischer JP, Gonsalves N, Hirano I, Spergel JM, Gupta SK, Furuta GT, Rothenberg ME, Dellon ES; Consortium of Eosinophilic Gastrointestinal Disease Researchers (CEGIR). Association Between Endoscopic and Histologic Findings in a Multicenter Retrospective Cohort of Patients with Non-esophageal Eosinophilic Gastrointestinal Disorders. *Dig Dis Sci* 2020; **65**: 2024-2035 [PMID: 31773359 DOI: 10.1007/s10620-019-05961-4]

22 **Dellon ES**, Peterson KA, Murray JA, Falk GW, Gonsalves N, Chehade M, Genta RM, Leung J, Khoury P, Klion AD, Hazan S, Vaezi M, Bledsoe AC, Durrani SR, Wang C, Shaw C, Chang AT, Singh B, Kamboj AP, Rasmussen HS, Rothenberg ME, Hirano I. Anti-Siglec-8 Antibody for Eosinophilic Gastritis and Duodenitis. *N Engl J Med* 2020; **383**: 1624-1634 [PMID: 33085861 DOI: 10.1056/NEJMoa2012047]

23 **Assa'ad AH**, Gupta SK, Collins MH, Thomson M, Heath AT, Smith DA, Perschy TL, Jurgensen CH, Ortega HG, Aceves SS. An antibody against IL-5 reduces numbers of esophageal intraepithelial eosinophils in children with eosinophilic esophagitis. *Gastroenterology* 2011; **141**: 1593-1604 [PMID: 21835135 DOI: 10.1053/j.gastro.2011.07.044]

24 **Foroughi S**, Foster B, Kim N, Bernardino LB, Scott LM, Hamilton RG, Metcalfe DD, Mannon PJ, Prussin C. Anti-IgE treatment of eosinophil-associated gastrointestinal disorders. *J Allergy Clin Immunol* 2007; **120**: 594-601 [PMID: 17765756 DOI: 10.1016/j.jaci.2007.06.015]

25 **Sato H**, Honma T, Owaki T, Tominaga K, Yokoyama J, Terai S. Clinical and pathological profile of eosinophilic gastroenteritis. *Eur J Gastroenterol Hepatol* 2019; **31**: 157-162 [PMID: 30113369 DOI: 10.1097/MEG.0000000000001241]

26 **Grandinetti T**, Biedermann L, Bussmann C, Straumann A, Hruz P. Eosinophilic Gastroenteritis: Clinical Manifestation, Natural Course, and Evaluation of Treatment with Corticosteroids and Vedolizumab. *Dig Dis Sci* 2019; **64**: 2231-2241 [PMID: 30982212 DOI: 10.1007/s10620-019-05617-3]

27 **Li K**, Ruan G, Liu S, Xu T, Guan K, Li J. Eosinophilic gastroenteritis: Pathogenesis, diagnosis, and treatment. *Chin Med J (Engl)* 2023; **136**: 899-909 [PMID: 37022943 DOI: 10.1097/CM9.0000000000002511]

28 **Trovato A**, Tsang T, Manem N, Donovan K, Gemoets DE, Ashley C, Dellon ES, Tadros M. The Impact of Obesity on the Fibrostenosis Progression of Eosinophilic Esophagitis in a U.S. Veterans Cohort. *Dysphagia* 2023; **38**: 866-873 [PMID: 36074175 DOI: 10.1007/s00455-022-10510-9]

29 **Wolf WA**, Piazza NA, Gebhart JH, Rusin S, Covey S, Higgins LL, Beitia R, Speck O, Woodward K, Cotton CC, Runge TM, Eluri S, Woosley JT, Shaheen NJ, Dellon ES. Association Between Body Mass Index and Clinical and Endoscopic Features of Eosinophilic Esophagitis. *Dig Dis Sci* 2017; **62**: 143-149 [PMID: 27778205 DOI: 10.1007/s10620-016-4357-1]

30 **McLaughlin T**, Ackerman SE, Shen L, Engleman E. Role of innate and adaptive immunity in obesity-associated metabolic disease. *J Clin Invest* 2017; **127**: 5-13 [PMID: 28045397 DOI: 10.1172/JCI88876]

World Journal of Gastroenterology

Submit a Manuscript: https://www.f6publishing.com

World J Gastroenterol 2024 January 14; 30(2): 158-169

DOI: 10.3748/wjg.v30.i2.158

ISSN 1007-9327 (print) ISSN 2219-2840 (online)

ORIGINAL ARTICLE

Retrospective Study

Association of tumor budding with clinicopathological features and prognostic value in stage III-IV colorectal cancer

Yue-Hao Luo, Zhe-Cheng Yan, Jia-Ying Liu, Xin-Yi Li, Ming Yang, Jun Fan, Bo Huang, Cheng-Gong Ma, Xiao-Na Chang, Xiu Nie

Specialty type: Gastroenterology and hepatology

Provenance and peer review: Unsolicited article; Externally peer reviewed.

Peer-review model: Single blind

Peer-review report's scientific quality classification

Grade A (Excellent): 0
Grade B (Very good): B
Grade C (Good): C, C
Grade D (Fair): 0
Grade E (Poor): 0

P-Reviewer: Jeong KY, South Korea; Lim YC, Brunei Darussalam

Received: October 25, 2023
Peer-review started: October 25, 2023
First decision: November 12, 2023
Revised: November 23, 2023
Accepted: December 14, 2023
Article in press: December 14, 2023
Published online: January 14, 2024

Yue-Hao Luo, Zhe-Cheng Yan, Jia-Ying Liu, Xin-Yi Li, Ming Yang, Jun Fan, Bo Huang, Cheng-Gong Ma, Xiao-Na Chang, Xiu Nie, Department of Pathology, Union Hospital, Tongji Medical College, Huazhong University of Science and Technology, Wuhan 430022, Hubei Province, China

Corresponding author: Xiu Nie, MD, Professor, Department of Pathology, Union Hospital, Tongji Medical College, Huazhong University of Science and Technology, No. 1277 Jiefang Avenue, Wuhan 430022, Hubei Province, China. niexiuyishi@126.com

Abstract

BACKGROUND

Tumor budding (TB) has emerged as a promising independent prognostic biomarker in colorectal cancer (CRC). The prognostic role of TB has been extensively studied and currently affects clinical decision making in patients with stage I and II CRC. However, existing prognostic studies on TB in stage III CRC have been confined to small retrospective cohort studies. Consequently, this study investigated the correlation among TB categories, clinicopathological features, and prognosis in stage III-IV CRC to further enhance the precision and individualization of treatment through refined prognostic risk stratification.

AIM

To analyze the relationship between TB categories and clinicopathological characteristics and assess their prognostic value in stage III-IV CRC to further refine the prognostic risk stratification of stage III-IV CRC.

METHODS

The clinical data of 547 CRC patients were collected for this retrospective study. Infiltration at the front edge of the tumor buds was counted according to the 2016 International Tumor Budding Consensus Conference guidelines.

RESULTS

Multivariate Cox proportional hazards regression analysis demonstrated that chemotherapy ($P = 0.004$), clinical stage IV ($P < 0.001$), ≥ 4 regional lymph node metastases ($P = 0.004$), left-sided colonic cancer ($P = 0.040$), and Bd 2-3 ($P = 0.002$) were independent prognostic factors in patients with stage III-IV CRC. Moreover, the density of tumor infiltrating lymphocytes was higher in Bd 1 than in Bd 2-3, both in the tumor stroma and its invasive margin.

CONCLUSION
TB has an independent predictive prognostic value in patients with stage III-IV CRC. It is recommended to complete the TB report of stage III-IV CRC cases in the standardized pathological report to further refine risk stratification.

Key Words: Tumor budding; Tumor infiltrating lymphocytes; Colorectal cancer; Survival analysis; Prognosis

Core Tip: This study included 547 colorectal cancer (CRC) patients. Tumor budding (TB) was evaluated independently by two pathologists and re-evaluated by a third pathologist when the results were inconsistent, ensuring a high level of reliability. The 2016 International Tumor Budding Consensus Conference recommendations were followed to evaluate TB in patients with stage III-IV CRC, thereby investigating its impact on patient prognosis. TB has predictive prognostic value for progression-free survival and overall survival in patients with stage III-IV CRC. It is recommended to complete the TB report of stage III-IV CRC cases in the standardized pathological report to further refine risk stratification.

Citation: Luo YH, Yan ZC, Liu JY, Li XY, Yang M, Fan J, Huang B, Ma CG, Chang XN, Nie X. Association of tumor budding with clinicopathological features and prognostic value in stage III-IV colorectal cancer. *World J Gastroenterol* 2024; 30(2): 158-169
URL: https://www.wjgnet.com/1007-9327/full/v30/i2/158.htm
DOI: https://dx.doi.org/10.3748/wjg.v30.i2.158

INTRODUCTION

Colorectal cancer (CRC) is the third most common malignant tumor in the world[1]. The occurrence and development of CRC represent a complex multifactorial process[2]. Despite significant advancements in medical technology both domestically and internationally, the incidence of CRC has continued to rise in recent years. This trend can be attributed to improvements in people's living standards as well as changes in lifestyle and dietary habits. There were an estimated 1.93 million new CRC cases diagnosed, and 0.94 million CRC-related deaths in 2020 worldwide. China is expected to have the highest estimated number of new CRC cases over the next 20 years. The number of new CRC cases is expected to increase from 0.56 million (2020) to 0.91 million (2040) in China[3].The tumor-node-metastasis (TNM) staging system published simultaneously by the Union for International Cancer Control and The American Joint Committee on Cancer (AJCC) remains a widely accepted standard for classifying malignant tumors[4]. The prognosis of patients with CRC is often influenced by the time gap between cancer detection and treatment initiation. Notably, even patients with identical stage of disease may exhibit diverse clinical outcomes, suggesting the limited predictive value of TNM stage in estimating CRC prognosis. Tumor budding (TB), defined as a single cancer cell of up to four cancer cells at the tumor invasive margin, has emerged as a promising independent prognostic biomarker in CRC[5].

TB reflects an invasive growth pattern with metastatic potential that plays a key role in the tumor microenvironment (TME) and epithelial-mesenchymal transition (EMT). The prognostic role of TB has been extensively studied and currently affects clinical decision making in patients with stage I and II CRC[6,7]. However, existing prognostic studies on TB in stage III CRC have been confined to small retrospective cohort studies. Consequently, this study investigated the correlation among TB categories, clinicopathological features, and prognosis in stage III-IV CRC to further enhance the precision and individualization of treatment through refined prognostic risk stratification.

Tumor-infiltrating lymphocytes (TILs) are a heterogeneous group of cells that leave the blood and migrate to the tumor regions with antigenic effects. They are also an important part of the TME and are generally considered to protect the host against tumor development. It also plays a vital role in inhibiting cancer cell invasion and distant metastasis[8]. The interaction between TB and the immune system is known as the attack-defense model[9]. TB reflects an aggressive disease phenotype; however, TILs can regulate immune function and improve the body's ability to kill tumors. Therefore, in our study, we also discussed the relationship between TB and TILs based on the idea that the combination of TB and TILs can effectively predict the prognosis of stage III-IV CRC patients and analyzed the changes in TILs in cases of different TB levels to preliminarily explore the correlation between TB and the immune microenvironment.

MATERIALS AND METHODS

We retrospectively analyzed the medical records and clinical data of 838 patients with stage III-IV resectable CRC pathologically diagnosed at Union Hospital, Tongji Medical College of Huazhong University of Science and Technology (Wuhan City, Hubei Province, China) from January 1, 2015, to December 31, 2018 (Figure 1). A total of 547 patients with CRC were enrolled, and their TB categories and clinicopathological features were analyzed.

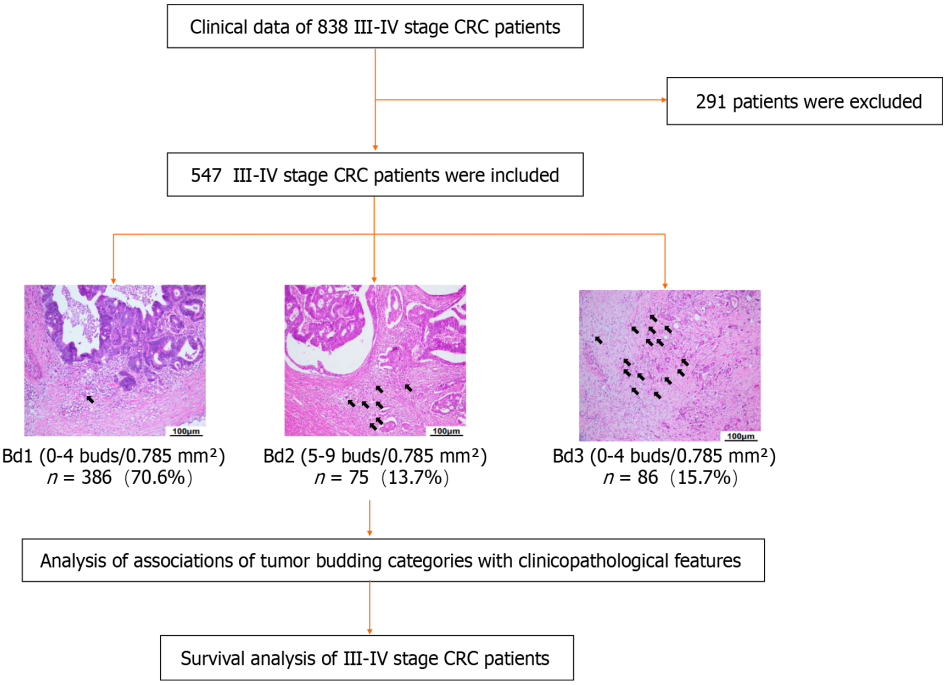

DOI: 10.3748/wjg.v30.i2.158

Figure 1 Study design and flow diagram. CRC: Colorectal cancer.

The primary objective of this study was to investigate the relationship between TB and progression-free survival (PFS), defined as the time from the beginning of radical surgery to relapse or death, whichever occurred first. The secondary objective was to determine the association between TB and overall survival (OS), defined as the time from the start of radical surgery until death from any cause. The survival time and prognosis of the patients were followed up until the end of the study. The follow-up period was 61 mo. This study was approved by the review committee of the affiliated institution of Tongji Medical College of Huazhong University of Science and Technology (2018-S377), and consent was obtained from all patients participating in the study.

TB assessment

TB was assessed on scanned hematoxylin and eosin (H&E)-stained tissue sample slides (Union Hospital, Wuhan, China) and scored at medium power (10 × to 20 × magnification) in a single hotspot field area normalized to 0.785 mm² at the invasive front according to the 2016 International TB Consensus Conference (ITBCC 2016). TB was defined as a single tumor cell or a cell cluster of up to four tumor cells at the invasive margin. Tumor buds were counted independently by two pathologists (Yue-Hao Luo and Zhe-Cheng Yan), and any discrepancies were resolved by a third expert (Xiao-Na Chang). The TB scoring categories were Bd 1 (0-4 buds: Low), Bd 2 (5-9 buds: Intermediate), and Bd 3 (≥ 10 buds: High).

Statistical analysis

All statistical analyses were performed using the statistical software SPSS version 27.0, with two-sided statistical testing, and $P < 0.05$ was considered statistically significant. Clinicopathological features and *KRAS, NRAS, BRAF* mutation status of the patients were descriptively analyzed. The χ^2 test (or Fisher's exact test, if appropriate) was used to evaluate the relationship between the TB categories and clinicopathological features. Spearman correlation analysis was used to evaluate the consistency between the TB categories evaluated by the two pathologists (Figure 2). Kaplan-Meier survival analysis was used to compare PFS and OS between patients with TB and those with other clinicopathological features. Cox proportional hazard regression models were used to estimate hazard ratios (HRs) and 95% confidence interval (CI). The association of baseline parameters with PFS and OS was first examined using univariate Cox analysis, and variables with $P < 0.05$ were entered into a Cox regression multivariate model. After normal distribution detection of TILs in the tumor stroma and at the TB of the tumor invasion front was conducted, it was found that both groups of data were biased. The Mann-Whitney *U* test was used to evaluate the relationship between TILs in the tumor stroma and TILs at TB of the tumor invasion front with Bd 1 and Bd 2-3, respectively.

RESULTS

Patient characteristics

The clinical data of 838 CRC patients were retrospectively collected. The TB of 547 CRC patients was assessed. The frequency of Bd 1, Bd 2, and Bd 3 were 70.6%, 13.7%, and 15.7%, respectively. The clinicopathological characteristics are

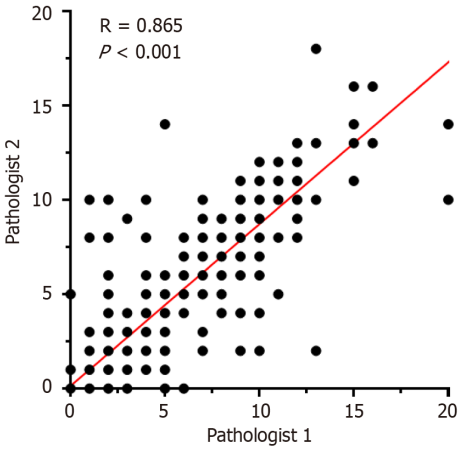

DOI: 10.3748/wjg.v30.i2.158

Figure 2 Spearman correlation analysis was used to evaluate the consistency between tumor budding categories evaluated by two pathologists. $R = 0.865$, $P < 0.001$.

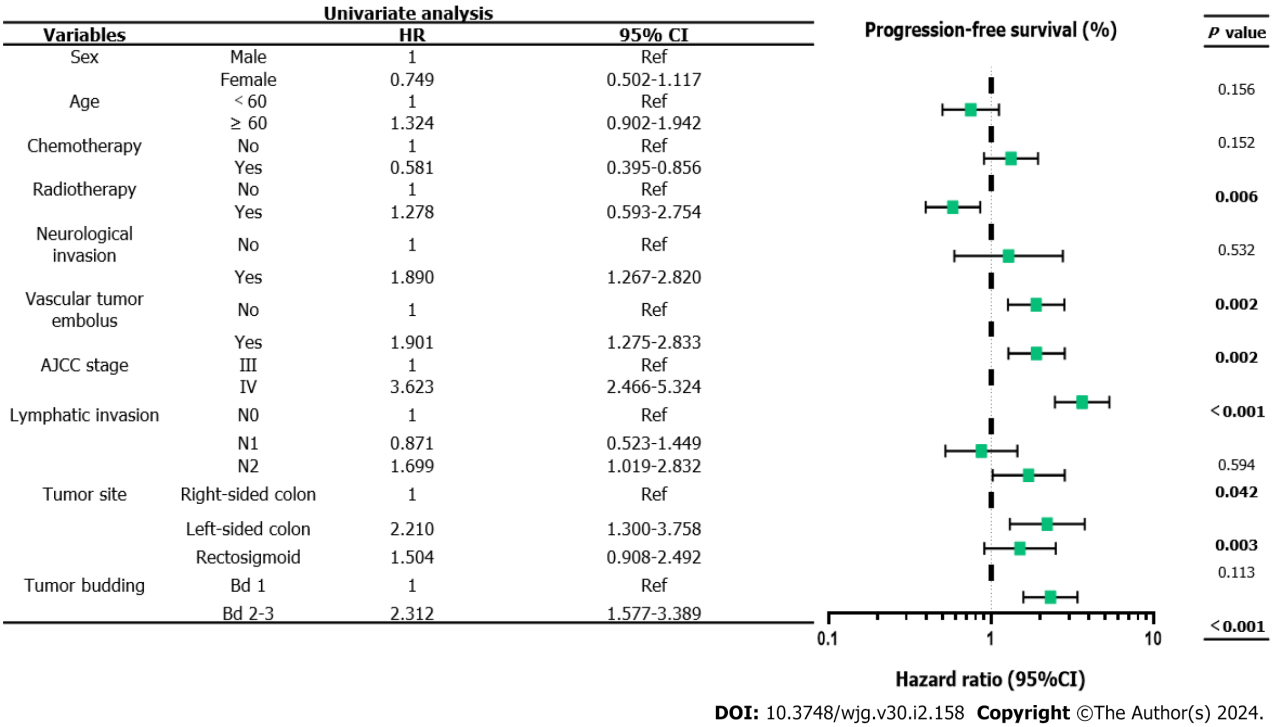

DOI: 10.3748/wjg.v30.i2.158

Figure 3 Univariable analysis of progression-free survival in colorectal cancer patients. AJCC: American Joint Committee on Cancer; HR: Hazard ratio.

listed in Table 1. Patients with *KRAS, NRAS, BRAF* mutations are listed in Table 2. TB categories were correlated with vascular tumor embolus ($P = 0.004$), neurological invasion ($P < 0.001$), AJCC stage III-IV ($P = 0.006$), and lymph node metastasis (LNM) ($P = 0.019$), but they were not significantly correlated with age, sex, chemotherapy, radiotherapy or tumor site ($P > 0.05$).

TB and survival

The 5-year PFS and 5-year OS rates of Bd 1 *vs* Bd 2-3 were 72% *vs* 45% ($P < 0.001$) and 49% *vs* 17% ($P < 0.001$), respectively. In univariable analysis, Bd 2-3 was associated with shorter PFS (HR: 2.312; 95%CI: 1.577 to 3.389; $P < 0.001$) (Figure 3) and OS (HR: 2.024, 95%CI: 1.378 to 2.972; $P = 0.002$) (Figure 4). Moreover, neurological invasion (HR: 1.890, 95%CI: 1.267 to 2.820; $P = 0.002$), vascular tumor embolus (HR: 1.901, 95%CI: 1.275 to 2.833; $P = 0.002$), AJCC stage IV (HR: 3.623, 95%CI: 2.466 to 5.324; $P < 0.001$), N2 (number of lymph node metastases ≥ 4) (HR: 1.699, 95%CI: 1.019 to 2.832; $P = 0.042$), and left-sided colon cancer (HR: 2.210, 95%CI: 1.300 to 3.758; $P = 0.003$) were associated with shorter PFS, and the prognosis of patients with chemotherapy was better (HR: 0.581, 95%CI: 0.395 to 0.856; $P = 0.006$). The other clinicopathological variables were not correlated with PFS ($P > 0.05$). Multivariate Cox proportional hazards regression analysis

Table 1 Patient population characteristics according to tumor budding

Characteristics	Total, *n* = 547	Bd 1, *n* = 386	Bd 2-3, *n* = 161	*P* value
Sex				0.514
Male	317 (58.0)	224 (58.0)	93 (57.8)	
Female	230 (42.0)	162 (42.0)	68 (42.2)	
Age in yr				0.141
< 60	276 (50.5)	201 (52.1)	75 (46.6)	
≥ 60	271 (49.5)	185 (47.9)	86 (53.4)	
Chemotherapy				0.055
Yes	319 (58.3)	234 (60.6)	85 (52.8)	
No	228 (41.7)	152 (39.4)	76 (47.2)	
Radiotherapy				0.119
Yes	32 (5.9)	26 (6.7)	6 (3.7)	
No	515 (94.1)	360 (93.3)	155 (96.3)	
Perineural invasion				< 0.001
Yes	171 (31.3)	100 (25.9)	71 (44.1)	
No	376 (68.7)	286 (74.1)	90 (55.9)	
Vascular invasion				0.004
Yes	152 (27.8)	94 (24.4)	58 (36.0)	
No	395 (72.2)	292 (75.6)	103 (64.0)	
Clinical stages				0.006
3	436 (79.7)	319 (82.6)	117 (72.7)	
4	111 (20.3)	67 (17.4)	44 (27.3)	
Lymphatic invasion				0.019
N0	134 (24.5)	105 (27.2)	29 (18.0)	
N1	258 (47.2)	183 (47.4)	75 (46.6)	
N2	155 (28.3)	98 (25.4)	57 (35.4)	
Tumor location				0.458
Right-sided colon	167 (30.5)	124 (32.1)	43 (26.7)	
Left-sided colon	136 (24.9)	93 (24.1)	43 (26.7)	
Rectosigmoid	244 (44.6)	169 (43.8)	75 (46.6)	

Data are *n* (%).

demonstrated that AJCC stage IV, N2 (number of lymph node metastases ≥ 4), left-sided colon cancer, and Bd 2-3 were independent risk factors for stage III-IV CRC. Similarly, chemotherapy (P = 0.004) was an independent protective factor (Figures 5 and 6). Kaplan-Meier survival analysis (Figure 7) showed that patients with Bd 1 had a better prognosis than those with Bd 2-3. Meanwhile, when further grouping, we found that patients with Bd 1 had longer PFS and OS than those with Bd 2-3 in the invasion area (perineural and vascular invasions), and the difference was statistically significant (Figures 8 and 9). The density of TILs was higher in Bd 1 than in Bd 2-3, both in the stromal area and invasive margin (Figure 10).

DISCUSSION

As early as 1954, Imai first reported the phenomenon of TB in various solid tumors and its correlation with prognosis of disease[10]. Subsequent studies have further demonstrated that TB serves as an independent prognostic biomarker in CRC and is observed in a variety of solid tumors, including tongue, larynx, esophagus, stomach, breast, and intrahepatic

Table 2 Patients with *KRAS, NRAS, BRAF* mutations according to tumor budding

Characteristics	Total, *n* = 112	Bd 1, *n* = 87	Bd 2-3, *n* = 25	*P* value
KRAS				0.064
Wild	53 (47.3)	45 (51.7)	8 (32.0)	
Mutant	59 (52.7)	42 (48.3)	17 (68.0)	
NRAS				0.275
Wild	107 (95.5)	82 (94.3)	25 (100.0)	
Mutant	5 (4.5)	5 (5.7)	0 (0.0)	
BRAF				0.597
Wild	106 (94.6)	82 (94.3)	24 (96.0)	
Mutant	6 (5.4)	5 (5.7)	1 (4.0)	

Data are *n* (%).

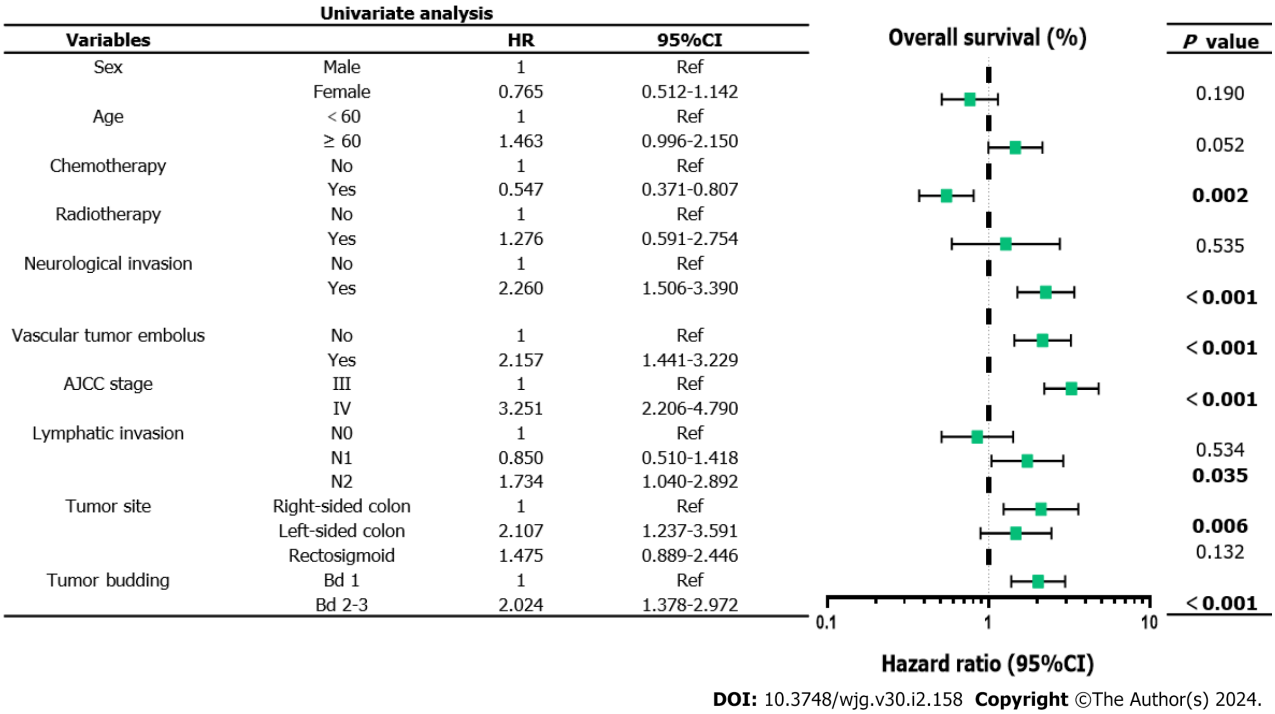

DOI: 10.3748/wjg.v30.i2.158

Figure 4 Univariable analysis of overall survival in colorectal cancer patients. AJCC: American Joint Committee on Cancer; HR: Hazard ratio.

cholangiocarcinomas. It has been shown to be predictive of cancer progression[11-14].

Currently, high-grade TB is an independent predictor of LNM to determine subsequent surgical treatment for stage I CRC[6,15]. In particular, Bd 3 is a strong adverse prognostic factor used to identify those stage II CRC patients with high recurrence rates and high mortality to guide adjuvant treatment[16]. In the new 2017 TNM and 2019 World Health Organization classifications, TB is regarded as an important complementary biological marker for predicting the prognosis of CRC[17]. Although the prognostic impact of TB on stage I and II CRC is clear, the application of this criterion in clinical practice for treatment decision-making in stage III-IV CRC is limited. This is mainly due to the lack of relevant research data in this context[18]. In this study, 547 patients with stage III-IV CRC were evaluated for TB and TILs according to the ITBCC 2016 scoring system. Combined with patient history, clinicopathological data and patient prognosis, the association between TB and various clinicopathological features and TILs, as well as the prognostic significance, were analyzed. These results suggest that TB independently affects the prognostic outcome of stage III-IV CRC.

The results of our study are consistent with the conclusion reached by Akabane *et al*[18] who retrospectively collected clinicopathological data from 237 patients with stage III CRC in a single center. This study showed that Bd 1 patients showed significantly better disease-free survival. The importance of TB in adjuvant treatment decision-making for stage III CRC has been emphasized. Notably, our study showed that TB was an independent adverse prognostic biomarker for

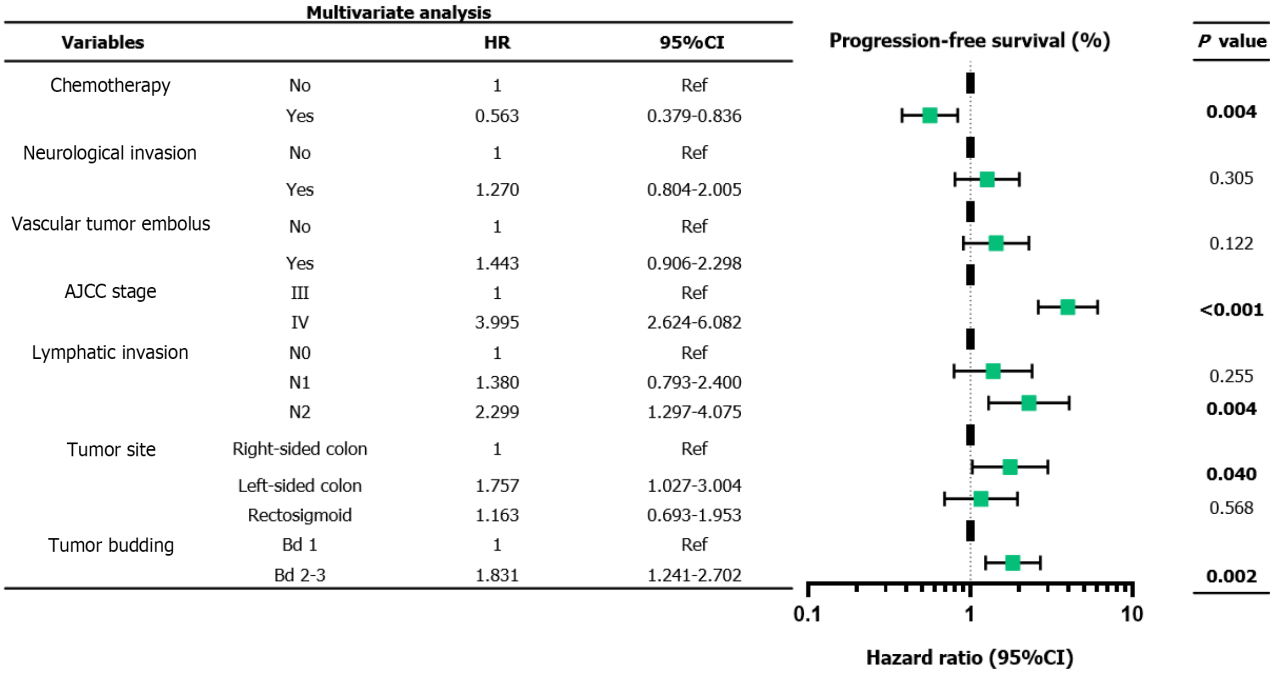

DOI: 10.3748/wjg.v30.i2.158

Figure 5 Multivariable Cox hazards model analysis on progression-free survival in colorectal cancer patients. AJCC: American Joint Committee on Cancer; HR: Hazard ratio.

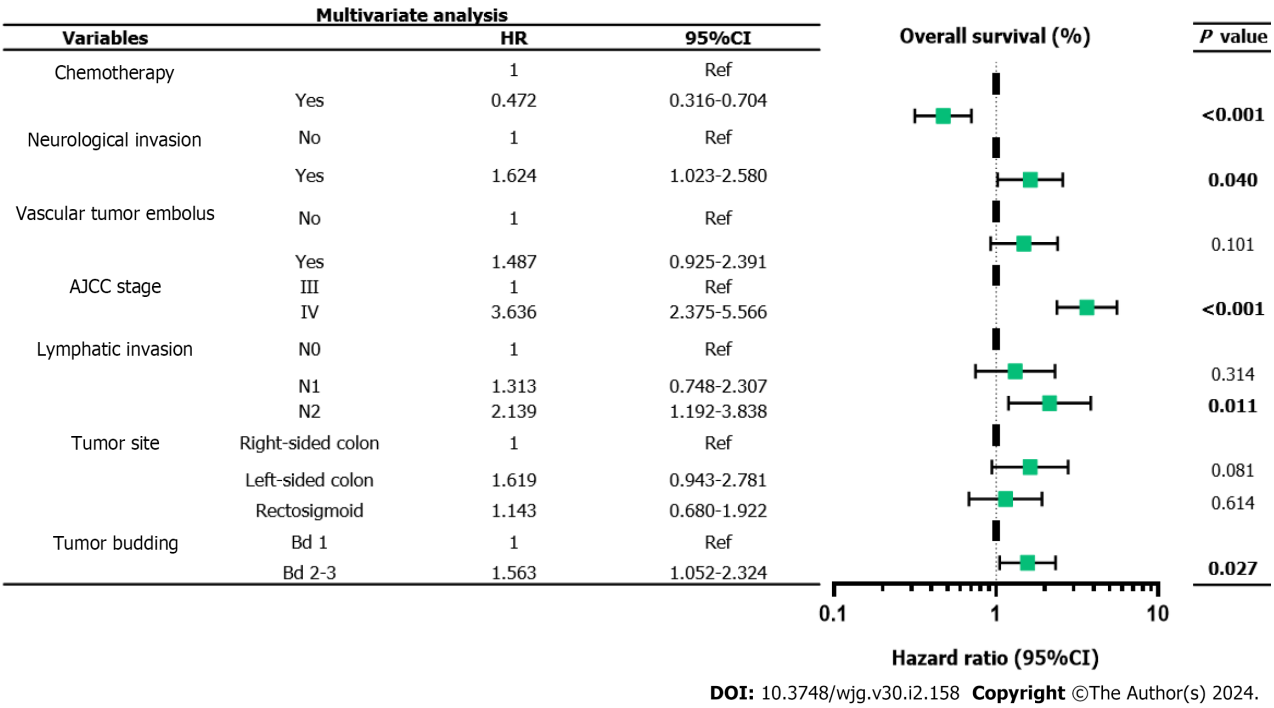

DOI: 10.3748/wjg.v30.i2.158

Figure 6 Multivariable Cox hazards model analysis on overall survival in colorectal cancer patients. AJCC: American Joint Committee on Cancer; HR: Hazard ratio.

PFS and OS in stage III-IV CRC. A single-center retrospective study of 589 patients with stage III CRC reported by Yamadera *et al*[19] used a binary classification system similar to that of Akabane *et al*[18] but the cut-off value was different (0-9 buds: Low; ≥ 10 buds: High). The results showed that among patients with stage III CRC, the Bd1 group had better survival after adjuvant chemotherapy. Rogers *et al*[16] conducted a meta-analysis of 34 studies with a total of 7821 CRC patients at various stages, and found that TB was significantly correlated with LNM (odds ratio [OR]: 4.94, 95%CI: 3.96-6.17; $P < 0.00001$), 5-year PFS (OR: 5.50, 95%CI: 3.64-8.29; $P < 0.00001$) and 5-year OS (OR: 4.51, 95%CI: 2.55-7.99; $P < 0.0001$) . It was concluded that TB was a risk factor for predicting LNM at 5 years, PFS at 5 years, and OS at 5 years in

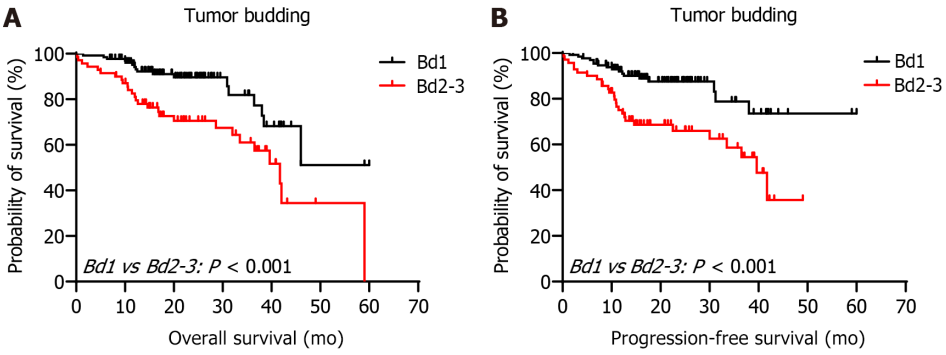

DOI: 10.3748/wjg.v30.i2.158

Figure 7 Kaplan–Meier survival analysis of survival in patients with Stage III-IV colorectal cancer according to grade of tumor budding. A: Overall survival in patients with Bd 1 and Bd 2-3; B: Progression-free survival in patients with Bd 1 and Bd 2-3.

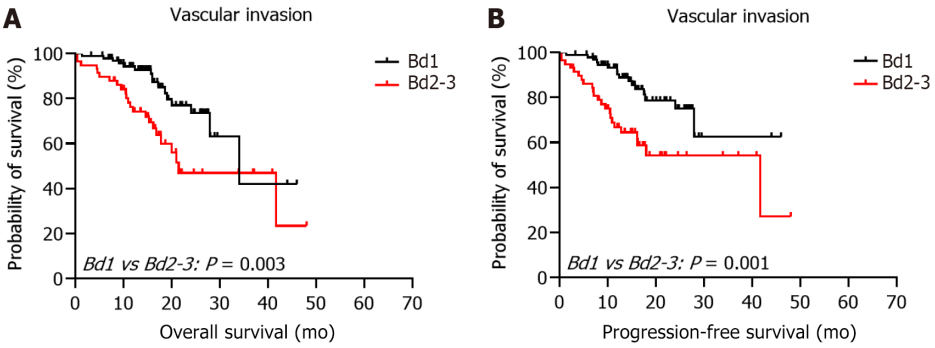

DOI: 10.3748/wjg.v30.i2.158

Figure 8 Kaplan–Meier survival analysis of survival in patients with Stage III-IV colorectal cancer according to grade of tumor budding. A: Overall survival in the vascular invasion group; B: Progression-free survival in the vascular invasion group.

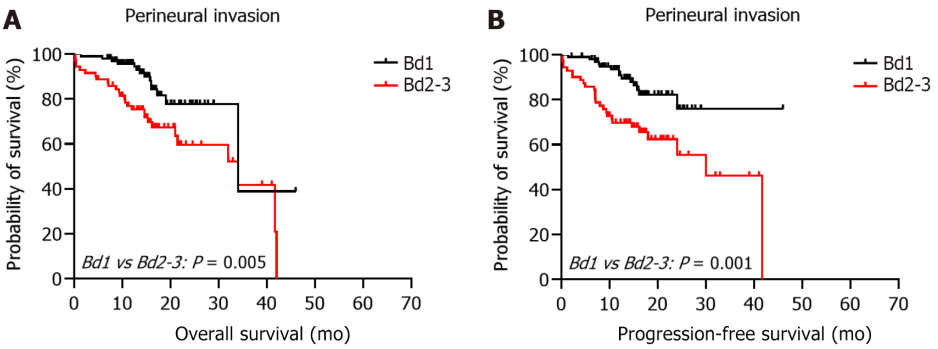

DOI: 10.3748/wjg.v30.i2.158

Figure 9 Kaplan–Meier survival analysis of survival in patients with Stage III-IV colorectal cancer according to grade of tumor budding. A: Overall survival in the perineural invasion group; B: Progression-free survival in the perineural invasion group.

CRC patients, and its inclusion in CRC staging facilitated further risk stratification; however, there was a lack of studies on stage III-IV CRC in a meta-analysis by Rogers *et al*[16] and the definition and evaluation criteria of TB varied greatly between different studies. Similarly, Graham *et al*[20] evaluated 553 CRC patients at various stages and found that high-grade TB was an independent predictor of poor disease-specific Survival. Therefore, TB could also be a pathological marker that is clinically practical to further refine risk classification and guide decision-making in stage III-IV CRC.

Interestingly, our study also found that the Bd 1 group had a higher proportion of TILs at the tumor invasive margin, which may be associated with better prognosis. This is consistent with the findings of Nearchou *et al*[21], who found the deletion of TILs in high-grade TB by exploring the effects of different lymphocyte distribution patterns and TB quantity and density on prognosis in stage II CRC through automatic imaging analysis and machine learning workflow.

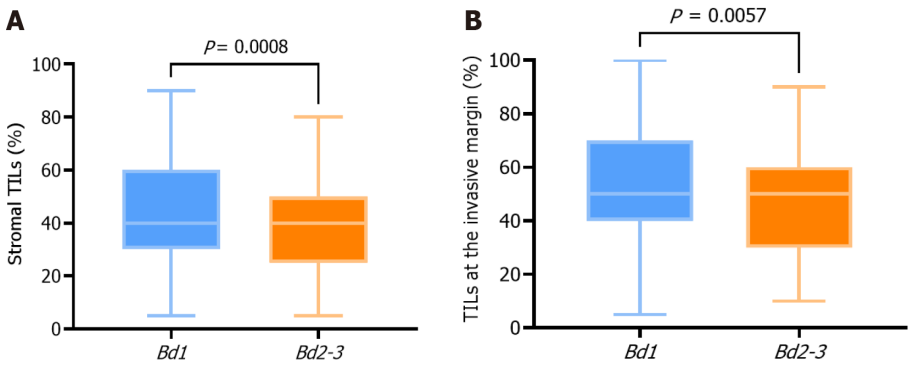

DOI: 10.3748/wjg.v30.i2.158

Figure 10 Relationship between grade of tumor budding and tumor infiltrating lymphocytes. A: Bd 1 and Bd 2-3 with stromal tumor-infiltrating lymphocytes (TILs); B: Bd 1 and Bd 2-3 with TILs at the invasive margin.

During the development of cancer, EMT promotes cancer development by empowering mesenchymal phenotypes associated with highly aggressive tumor cells[22]. TB demonstrates the dynamic process of EMT; that is, tumor cells in the aggressive front acquire an interstitial phenotype. This increases the malignant potential of vascular invasion and distant metastasis, and consequently, metastases to lymph nodes or distant parenchymal organs through the vasculature[23-25].

E-cadherin is an intercellular adhesion protein and pivotal regulatory factor in this process[26,27]. Numerous studies have claimed that in different solid tumors, the expression of E-cadherin is reduced or absent on the cell surface of the tumor invasion front, especially in TB[28-31]. This loss is usually accompanied by a decrease in β-catenin expression, indicating that the WNT pathway in cells may be activated. Hence, budding tumor cells can degrade the extracellular matrix (ECM) and invade and migrate through the surrounding stroma. In addition, it has been found that the expression of laminin 5γ2 is usually increased in response to tumor invasion[32]. In the gene ontology study, RNA sequencing data from the TB region and the corresponding central tumor region were compared and analyzed. The expression of genes involved in integrin-mediated cell adhesion, migration, cytoskeleton rearrangement and ECM degradation were found to be significantly different between the two regions[33]. Koelzer *et al*[34] found that there is an immune escape mechanism in EMT, in which tumor cells lose the expression of their major histocompatibility complex, allowing them to evade recognition and attack by the immune system.

Finally, our study included a substantial number of 547 CRC patients. TB was evaluated independently by two pathologists and re-evaluated by a third pathologist when the results were inconsistent, ensuring a high level of reliability in the TB assessment. Furthermore, the ITBCC 2016 recommendations were followed to evaluate TB specifically in patients with stage III-IV CRC, thereby investigating its impact on patient prognosis.

However, this study had some limitations. First, this study was a retrospective analysis conducted at a single center, which may introduce some degree of bias as the study population may not represent all CRC patients in China. Second, using a single index as a risk factor still has some drawbacks, which can be solved by constructing a prognosis model with a multi-index multidimensional association algorithm. Furthermore, the accuracy of the assessment results based on TILs on H&E slides must be improved to provide better medical strategies and achieve individualized precision treatment for patients with CRC. Future efforts should focus on utilizing artificial intelligence techniques, such as digital pathology methods, to enhance the accuracy and reproducibility of TB and TIL assessments. Additionally, integrating TB with the immunoscore could refine the risk stratification of stage III-IV CRC.

CONCLUSION

TB has an independent predictive prognostic value for PFS and OS in patients with stage III-IV CRC. It is recommended to complete the TB report of stage III-IV CRC cases in the standardized pathological report to further refine risk stratification.

ARTICLE HIGHLIGHTS

Research background

Tumor budding (TB) is a novel prognostic biomarker that may influence clinical treatment decisions in stage I-II colorectal cancer (CRC) patients. This study analyzed the relationship between TB categories and clinicopathological characteristics and assess their prognostic value in stage III-IV CRC to further refine the prognostic risk stratification of stage III-IV CRC. Additionally, we analyzed changes in tumor-infiltrating lymphocytes (TILs) in patients with different TB categories and initially explored the correlation between TB and the tumor immune microenvironment.

Research motivation

To explore the association of TB with clinicopathological features and prognostic value in stage III-IV CRC.

Research objectives

This study analyzed the relationship between TB categories and clinicopathological characteristics and assess their prognostic value in stage III-IV CRC to further refine the prognostic risk stratification of stage III-IV CRC.

Research methods

This study included a substantial number of 547 CRC patients. TB was evaluated independently by two pathologists and re-evaluated by a third pathologist when the results were inconsistent, ensuring a high level of reliability in the TB assessment. Furthermore, the 2016 International TB Consensus Conference recommendations were followed to evaluate TB specifically in patients with stage III-IV CRC, thereby investigating its impact on patient prognosis.

Research results

Multivariate Cox proportional hazards regression analysis demonstrated that chemotherapy, clinical stage IV, ≥ 4 regional lymph node metastases, left-sided colonic cancer, and Bd 2-3 were independent prognostic factors in patients with stage III-IV CRC. Moreover, the density of TILs was higher in Bd 1 than in Bd 2-3, both in the tumor stroma and its invasive margin.

Research conclusions

TB has an independent predictive prognostic value for progression-free survival and overall survival in patients with stage III-IV CRC. It is recommended to complete the TB report of stage III-IV CRC cases in the standardized pathological report to further refine risk stratification.

Research perspectives

A multicenter prospective study with large samples should be conducted in the future, and constructing a prognosis model with a multi-index multidimensional association algorithm with other prediction models is needed to further verify its reliability.

ACKNOWLEDGEMENTS

We thank all the patients and their family members involved in the study without which the advancements described herein would have not been made possible.

FOOTNOTES

Co-first authors: Yue-Hao Luo and Zhe-Cheng Yan.

Co-corresponding authors: Xiao-Na Chang and Xiu Nie.

Author contributions: Luo YH and Yan ZC contributed equally to this work; Luo YH, Yan ZC, Liu JY, Li XY, Yang M, and Fan J designed the research study; Luo YH, Huang B, and Ma CG performed the research; Luo YH, Chang XN, and Niu X analyzed the data and wrote the manuscript; All authors have read and approve the final manuscript.

Supported by National Key R&D Program of China, No. 2022YFF1203300.

Institutional review board statement: This study was approved by the review committee of the affiliated institution of Tongji Medical College of Huazhong University of Science and Technology (2018-S377).

Informed consent statement: Consent was obtained from all patients participating in the study.

Conflict-of-interest statement: The authors have no conflicts of interest to declare.

Data sharing statement: No additional data are available.

Country/Territory of origin: China

ORCID number: Yue-Hao Luo 0009-0000-6774-888X; Jun Fan 0000-0003-0221-5451; Xiu Nie 0000-0003-0221-5000.

S-Editor: Li L
L-Editor: Filipodia
P-Editor: Zhao S

REFERENCES

1 **Siegel RL**, Miller KD, Fedewa SA, Ahnen DJ, Meester RGS, Barzi A, Jemal A. Colorectal cancer statistics, 2017. *CA Cancer J Clin* 2017; **67**: 177-193 [PMID: 28248415 DOI: 10.3322/caac.21395]
2 **Murphy N**, Moreno V, Hughes DJ, Vodicka L, Vodicka P, Aglago EK, Gunter MJ, Jenab M. Lifestyle and dietary environmental factors in colorectal cancer susceptibility. *Mol Aspects Med* 2019; **69**: 2-9 [PMID: 31233770 DOI: 10.1016/j.mam.2019.06.005]
3 **Xi Y**, Xu P. Global colorectal cancer burden in 2020 and projections to 2040. *Transl Oncol* 2021; **14**: 101174 [PMID: 34243011 DOI: 10.1016/j.tranon.2021.101174]
4 **Basile D**, Broudin C, Emile JF, Falcoz A, Pagès F, Mineur L, Bennouna J, Louvet C, Artru P, Fratte S, Ghiringhelli F, André T, Derangère V, Vernerey D, Taieb J, Svrcek M; for PRODIGE investigators, GERCOR, Fédération Française de Cancerologie Digestive, and UNICANCER. Tumor budding is an independent prognostic factor in stage III colon cancer patients: a post-hoc analysis of the IDEA-France phase III trial (PRODIGE-GERCOR). *Ann Oncol* 2022; **33**: 628-637 [PMID: 35306156 DOI: 10.1016/j.annonc.2022.03.002]
5 **Lugli A**, Kirsch R, Ajioka Y, Bosman F, Cathomas G, Dawson H, El Zimaity H, Fléjou JF, Hansen TP, Hartmann A, Kakar S, Langner C, Nagtegaal I, Puppa G, Riddell R, Ristimäki A, Sheahan K, Smyrk T, Sugihara K, Terris B, Ueno H, Vieth M, Zlobec I, Quirke P. Recommendations for reporting tumor budding in colorectal cancer based on the International Tumor Budding Consensus Conference (ITBCC) 2016. *Mod Pathol* 2017; **30**: 1299-1311 [PMID: 28548122 DOI: 10.1038/modpathol.2017.46]
6 **Cappellesso R**, Luchini C, Veronese N, Lo Mele M, Rosa-Rizzotto E, Guido E, De Lazzari F, Pilati P, Farinati F, Realdon S, Solmi M, Fassan M, Rugge M. Tumor budding as a risk factor for nodal metastasis in pT1 colorectal cancers: a meta-analysis. *Hum Pathol* 2017; **65**: 62-70 [PMID: 28438617 DOI: 10.1016/j.humpath.2017.04.013]
7 **Ueno H**, Ishiguro M, Nakatani E, Ishikawa T, Uetake H, Matsuda C, Nakamoto Y, Kotake M, Kurachi K, Egawa T, Yasumasa K, Murata K, Ikawa O, Shinji S, Murotani K, Matsui S, Teramukai S, Tomita N, Sugihara K; SACURA Study Group. Prospective Multicenter Study on the Prognostic and Predictive Impact of Tumor Budding in Stage II Colon Cancer: Results From the SACURA Trial. *J Clin Oncol* 2019; **37**: 1886-1894 [PMID: 31180819 DOI: 10.1200/JCO.18.02059]
8 **Lugli A**, Karamitopoulou E, Panayiotides I, Karakitsos P, Rallis G, Peros G, Iezzi G, Spagnoli G, Bihl M, Terracciano L, Zlobec I. CD8+ lymphocytes/ tumour-budding index: an independent prognostic factor representing a 'pro-/anti-tumour' approach to tumour host interaction in colorectal cancer. *Br J Cancer* 2009; **101**: 1382-1392 [PMID: 19755986 DOI: 10.1038/sj.bjc.6605318]
9 **Lugli A**, Zlobec I, Berger MD, Kirsch R, Nagtegaal ID. Tumour budding in solid cancers. *Nat Rev Clin Oncol* 2021; **18**: 101-115 [PMID: 32901132 DOI: 10.1038/s41571-020-0422-y]
10 **IMAI T**. Growth patterns in human carcinoma. Their classification and relation to prognosis. *Obstet Gynecol* 1960; **16**: 296-308 [PMID: 13717558]
11 **Berg KB**, Schaeffer DF. Tumor budding as a standardized parameter in gastrointestinal carcinomas: more than just the colon. *Mod Pathol* 2018; **31**: 862-872 [PMID: 29403085 DOI: 10.1038/s41379-018-0028-4]
12 **Voutsadakis IA**. Prognostic role of tumor budding in breast cancer. *World J Exp Med* 2018; **8**: 12-17 [PMID: 30211020 DOI: 10.5493/wjem.v8.i2.12]
13 **Beer A**, Reber A, Paireder M, Schoppmann SF, Heber S, Schiefer AI. Tumor cell budding in preoperative biopsies of esophageal and gastroesophageal junction carcinoma independently predicts survival in a grade-dependent manner. *Surgery* 2022; **172**: 567-574 [PMID: 35422326 DOI: 10.1016/j.surg.2022.02.020]
14 **Kosaka H**, Ishida M, Ueno M, Komeda K, Hokutou D, Iida H, Hirokawa F, Matsui K, Sekimoto M, Kaibori M. Tumor budding may be a promising prognostic indicator in intrahepatic cholangiocarcinoma: A multicenter retrospective study. *Ann Gastroenterol Surg* 2023; **7**: 138-146 [PMID: 36643363 DOI: 10.1002/ags3.12605]
15 **Bosch SL**, Teerenstra S, de Wilt JH, Cunningham C, Nagtegaal ID. Predicting lymph node metastasis in pT1 colorectal cancer: a systematic review of risk factors providing rationale for therapy decisions. *Endoscopy* 2013; **45**: 827-834 [PMID: 23884793 DOI: 10.1055/s-0033-1344238]
16 **Rogers AC**, Winter DC, Heeney A, Gibbons D, Lugli A, Puppa G, Sheahan K. Systematic review and meta-analysis of the impact of tumour budding in colorectal cancer. *Br J Cancer* 2016; **115**: 831-840 [PMID: 27599041 DOI: 10.1038/bjc.2016.274]
17 **Nagtegaal ID**, Odze RD, Klimstra D, Paradis V, Rugge M, Schirmacher P, Washington KM, Carneiro F, Cree IA; WHO Classification of Tumours Editorial Board. The 2019 WHO classification of tumours of the digestive system. *Histopathology* 2020; **76**: 182-188 [PMID: 31433515 DOI: 10.1111/his.13975]
18 **Akabane S**, Shimizu W, Takakura Y, Kochi M, Taguchi K, Nakashima I, Sato K, Hattori M, Egi H, Sentani K, Yasui W, Ohdan H. Tumor budding as a predictive marker for 5-fluorouracil response in adjuvant-treated stage III colorectal cancer. *Int J Clin Oncol* 2021; **26**: 1285-1292 [PMID: 33881678 DOI: 10.1007/s10147-021-01917-9]
19 **Yamadera M**, Shinto E, Kajiwara Y, Mochizuki S, Okamoto K, Hase K, Yamamoto J, Ueno H. Differential Survival Benefits of 5-Fluorouracil-Based Adjuvant Chemotherapy for Patients With Microsatellite-Stable Stage III Colorectal Cancer According to the Tumor Budding Status: A Retrospective Analysis. *Dis Colon Rectum* 2019; **62**: 1316-1325 [PMID: 31567925 DOI: 10.1097/DCR.0000000000001480]
20 **Graham RP**, Vierkant RA, Tillmans LS, Wang AH, Laird PW, Weisenberger DJ, Lynch CF, French AJ, Slager SL, Raissian Y, Garcia JJ, Kerr SE, Lee HE, Thibodeau SN, Cerhan JR, Limburg PJ, Smyrk TC. Tumor Budding in Colorectal Carcinoma: Confirmation of Prognostic Significance and Histologic Cutoff in a Population-based Cohort. *Am J Surg Pathol* 2015; **39**: 1340-1346 [PMID: 26200097 DOI: 10.1097/PAS.0000000000000504]
21 **Nearchou IP**, Lillard K, Gavriel CG, Ueno H, Harrison DJ, Caie PD. Automated Analysis of Lymphocytic Infiltration, Tumor Budding, and Their Spatial Relationship Improves Prognostic Accuracy in Colorectal Cancer. *Cancer Immunol Res* 2019; **7**: 609-620 [PMID: 30846441 DOI: 10.1158/2326-6066.CIR-18-0377]

22 **Derynck R**, Weinberg RA. EMT and Cancer: More Than Meets the Eye. *Dev Cell* 2019; **49**: 313-316 [PMID: 31063750 DOI: 10.1016/j.devcel.2019.04.026]

23 **Klymkowsky MW**, Savagner P. Epithelial-mesenchymal transition: a cancer researcher's conceptual friend and foe. *Am J Pathol* 2009; **174**: 1588-1593 [PMID: 19342369 DOI: 10.2353/ajpath.2009.080545]

24 **Yilmaz M**, Christofori G. EMT, the cytoskeleton, and cancer cell invasion. *Cancer Metastasis Rev* 2009; **28**: 15-33 [PMID: 19169796 DOI: 10.1007/s10555-008-9169-0]

25 **Polyak K**, Weinberg RA. Transitions between epithelial and mesenchymal states: acquisition of malignant and stem cell traits. *Nat Rev Cancer* 2009; **9**: 265-273 [PMID: 19262571 DOI: 10.1038/nrc2620]

26 **Zlobec I**, Lugli A, Baker K, Roth S, Minoo P, Hayashi S, Terracciano L, Jass JR. Role of APAF-1, E-cadherin and peritumoral lymphocytic infiltration in tumour budding in colorectal cancer. *J Pathol* 2007; **212**: 260-268 [PMID: 17516584 DOI: 10.1002/path.2164]

27 **Kohler I**, Bronsert P, Timme S, Werner M, Brabletz T, Hopt UT, Schilling O, Bausch D, Keck T, Wellner UF. Detailed analysis of epithelial-mesenchymal transition and tumor budding identifies predictors of long-term survival in pancreatic ductal adenocarcinoma. *J Gastroenterol Hepatol* 2015; **30** Suppl 1: 78-84 [PMID: 25827809 DOI: 10.1111/jgh.12752]

28 **Jensen DH**, Dabelsteen E, Specht L, Fiehn AM, Therkildsen MH, Jønson L, Vikesaa J, Nielsen FC, von Buchwald C. Molecular profiling of tumour budding implicates TGFβ-mediated epithelial-mesenchymal transition as a therapeutic target in oral squamous cell carcinoma. *J Pathol* 2015; **236**: 505-516 [PMID: 25925492 DOI: 10.1002/path.4550]

29 **Attramadal CG**, Kumar S, Boysen ME, Dhakal HP, Nesland JM, Bryne M. Tumor Budding, EMT and Cancer Stem Cells in T1-2/N0 Oral Squamous Cell Carcinomas. *Anticancer Res* 2015; **35**: 6111-6120 [PMID: 26504037]

30 **Lee SJ**, Choi SY, Kim WJ, Ji M, Lee TG, Son BR, Yoon SM, Sung R, Lee EJ, Youn SJ, Park SM. Combined aberrant expression of E-cadherin and S100A4, but not β-catenin is associated with disease-free survival and overall survival in colorectal cancer patients. *Diagn Pathol* 2013; **8**: 99 [PMID: 23783026 DOI: 10.1186/1746-1596-8-99]

31 **Nakagawa Y**, Ohira M, Kubo N, Yamashita Y, Sakurai K, Toyokawa T, Tanaka H, Muguruma K, Shibutani M, Yamazoe S, Kimura K, Nagahara H, Amano R, Ohtani H, Yashiro M, Maeda K, Hirakawa K. Tumor budding and E-cadherin expression are useful predictors of nodal involvement in T1 esophageal squamous cell carcinoma. *Anticancer Res* 2013; **33**: 5023-5029 [PMID: 24222146]

32 **Katayama M**, Sekiguchi K. Laminin-5 in epithelial tumour invasion. *J Mol Histol* 2004; **35**: 277-286 [PMID: 15339047 DOI: 10.1023/b:hijo.0000032359.35698.fe]

33 **Zhou B**, Zong S, Zhong W, Tian Y, Wang L, Zhang Q, Zhang R, Li L, Wang W, Zhao J, Chen X, Feng Y, Zhai B, Sun T, Liu Y. Interaction between laminin-5γ2 and integrin β1 promotes the tumor budding of colorectal cancer *via* the activation of Yes-associated proteins. *Oncogene* 2020; **39**: 1527-1542 [PMID: 31676872 DOI: 10.1038/s41388-019-1082-1]

34 **Koelzer VH**, Herrmann P, Zlobec I, Karamitopoulou E, Lugli A, Stein U. Heterogeneity analysis of Metastasis Associated in Colon Cancer 1 (MACC1) for survival prognosis of colorectal cancer patients: a retrospective cohort study. *BMC Cancer* 2015; **15**: 160 [PMID: 25884643 DOI: 10.1186/s12885-015-1150-z]

World Journal of Gastroenterology

Submit a Manuscript: https://www.f6publishing.com

World J Gastroenterol 2024 January 14; 30(2): 170-183

DOI: 10.3748/wjg.v30.i2.170

ISSN 1007-9327 (print) ISSN 2219-2840 (online)

ORIGINAL ARTICLE

Retrospective Study

Automatic detection of small bowel lesions with different bleeding risks based on deep learning models

Rui-Ya Zhang, Peng-Peng Qiang, Ling-Jun Cai, Tao Li, Yan Qin, Yu Zhang, Yi-Qing Zhao, Jun-Ping Wang

Specialty type: Gastroenterology and hepatology

Provenance and peer review: Unsolicited article; Externally peer reviewed.

Peer-review model: Single blind

Peer-review report's scientific quality classification

Grade A (Excellent): 0
Grade B (Very good): B
Grade C (Good): C
Grade D (Fair): 0
Grade E (Poor): 0

P-Reviewer: Mijwil MM, Iraq

Received: November 8, 2023
Peer-review started: November 8, 2023
First decision: December 7, 2023
Revised: December 15, 2023
Accepted: December 26, 2023
Article in press: December 26, 2023
Published online: January 14, 2024

Rui-Ya Zhang, Ling-Jun Cai, Yan Qin, Yu Zhang, Yi-Qing Zhao, Jun-Ping Wang, Department of Gastroenterology, The Fifth Clinical Medical College of Shanxi Medical University, Taiyuan 030012, Shanxi Province, China

Peng-Peng Qiang, School of Computer and Information Technology, Shanxi University, Taiyuan 030006, Shanxi Province, China

Tao Li, School of Life Sciences and Technology, Mudanjiang Normal University, Mudanjiang 157011, Heilongjiang Province, China

Corresponding author: Jun-Ping Wang, MD, PhD, Chief Physician, Professor, Department of Gastroenterology, The Fifth Clinical Medical College of Shanxi Medical University, No. 29 Shuangtasi Street, Taiyuan 030012, Shanxi Province, China. wangjp8396@sxmu.edu.cn

Abstract

BACKGROUND

Deep learning provides an efficient automatic image recognition method for small bowel (SB) capsule endoscopy (CE) that can assist physicians in diagnosis. However, the existing deep learning models present some unresolved challenges.

AIM

To propose a novel and effective classification and detection model to automatically identify various SB lesions and their bleeding risks, and label the lesions accurately so as to enhance the diagnostic efficiency of physicians and the ability to identify high-risk bleeding groups.

METHODS

The proposed model represents a two-stage method that combined image classification with object detection. First, we utilized the improved ResNet-50 classification model to classify endoscopic images into SB lesion images, normal SB mucosa images, and invalid images. Then, the improved YOLO-V5 detection model was utilized to detect the type of lesion and its risk of bleeding, and the location of the lesion was marked. We constructed training and testing sets and compared model-assisted reading with physician reading.

RESULTS

The accuracy of the model constructed in this study reached 98.96%, which was higher than the accuracy of other systems using only a single module. The sen-

sitivity, specificity, and accuracy of the model-assisted reading detection of all images were 99.17%, 99.92%, and 99.86%, which were significantly higher than those of the endoscopists' diagnoses. The image processing time of the model was 48 ms/image, and the image processing time of the physicians was 0.40 ± 0.24 s/image ($P < 0.001$).

CONCLUSION

The deep learning model of image classification combined with object detection exhibits a satisfactory diagnostic effect on a variety of SB lesions and their bleeding risks in CE images, which enhances the diagnostic efficiency of physicians and improves the ability of physicians to identify high-risk bleeding groups.

Key Words: Artificial intelligence; Deep learning; Capsule endoscopy; Image classification; Object detection; Bleeding risk

Core Tip: In clinical practice, capsule endoscopy is often used to detect small bowel (SB) lesions and find the cause of bleeding. Here, we have proposed a classification and detection model to automatically identify various SB lesions and their bleeding risks, and label the lesions accurately. This model can enhance the diagnostic efficiency of physicians and improve the ability of physicians to identify high-risk bleeding groups.

Citation: Zhang RY, Qiang PP, Cai LJ, Li T, Qin Y, Zhang Y, Zhao YQ, Wang JP. Automatic detection of small bowel lesions with different bleeding risks based on deep learning models. *World J Gastroenterol* 2024; 30(2): 170-183
URL: https://www.wjgnet.com/1007-9327/full/v30/i2/170.htm
DOI: https://dx.doi.org/10.3748/wjg.v30.i2.170

INTRODUCTION

Capsule endoscopy (CE), introduced in 2000, has successfully solved the problem pertaining to visualizing the small intestine and revolutionized the medical field. CE can be utilized as the preferred method for the diagnosis of small bowel (SB) diseases[1-3]. At present, obscure gastrointestinal bleeding is the most common indication for CE[4,5]. Therefore, physicians dedicate more attention to the bleeding risks of SB lesions in CE examination. However, CE reading is time-consuming and complicated[6-9], and abnormal parts account for only a small proportion. Thus, it is easy to miss the diagnosis, which affects the detection of lesions and assessment of bleeding risks. In addition, when there is a large amount of bile, food debris or air bubbles in the gastrointestinal tract, numerous invalid pictures will appear which will seriously affect the diagnostic efficiency[10].

In recent years, deep learning models have been widely utilized in automatic recognition of digestive endoscopic images[11,12]. Deep learning is characterized by processing large amounts of data with better experience and high performance, thus competing with the human mind[13,14]. Feature extraction using multilayer networks for classification and feedback can facilitate the identification of lesions[15-17], which significantly increases the sensitivity and specificity of lesion detection. Simultaneously, it effectively saves the time cost required for detection[18]. In the past few years, convolutional neural networks (CNNs) have advanced endoscopic image analysis. Several classical CNNs such as LeNet, AlexNet, GoogLeNet, and VGG-Net have exhibited strong performance in identifying SB lesions[19].

Although CNNs achieve excellent performance, they still have some limitations. First, a CNN cannot effectively focus on the important part of the image, which is easily affected by the organs and tissues around the area to be detected, resulting in limited accuracy of the model. Second, most of the existing research is related to the development of the classification model, while the image classification diagnosis system only adopts the binary classification method, which cannot distinguish two or more types of lesions in the image. Moreover, image classification cannot determine the specific location of the lesion. Therefore, its practicability still needs to be further improved. Third, most of the existing methods utilize spatial pyramid pooling (SPP), which has a lightweight characteristic of the backbone network and reduces the parameters. Although SPP improves the detection speed, it consequently suffers from a reduction in detection accuracy. It is worth emphasizing that existing studies have not evaluated the bleeding risks of SB lesions, but in clinical work, we urgently need to pay attention to the bleeding risks of lesions and try to find the cause of bleeding.

To solve the aforementioned problems, we have made the following efforts. We first added a multi-head self-attention (MHSA) mechanism to increase efficacy of the model's focus on important regions, improving the overall performance of the model. We next utilized a two-stage method to classify and detect various SB lesions. This two-stage method combined the classification model with the detection model, which allowed for distinguishment of multiple lesions in the image and accurate labeling of their location. We then replaced the SPP module with the "Atrous Spatial Pyramid Pooling" (ASPP) module. ASPP can effectively strengthen the feature extraction ability of the backbone network and improve the accuracy of diagnosis. At the same time, our model also increases the ability to assess the bleeding risks of lesions and is able to provide a more comprehensive understanding of the lesions being investigated.

Specifically, ResNet-50 utilizes a deep residual network to solve the gradient disappearance problem, and the increased number of network layers further enhances the image representation ability. Therefore, ResNet-50 was selected as the backbone of the classification model. On this basis, we added an MHSA mechanism, allowing the model to effectively focus on lesions and facilitating image classification. Meanwhile, we also combined YOLO-V5 as the detection model backbone to allow for identification of multiple lesions in the image simultaneously. The accuracy of YOLO exceeds that of general object detection algorithms while maintaining a fast speed, and it is currently one of the most popular algorithms[20]. Meanwhile, we utilized three branches to learn the features of the three RGB channels, respectively. The correlation between the three branches was considered, and the features were extracted from the three branches of the same image. Subsequently, the extracted features were fused. The independence and correlation were realized using a parallel network. To better focus on the bleeding risks of lesions, the MHSA mechanism and ASPP module were added to the detection model. Ablation experiments were performed to remove each mechanism and module in a one-by-one stepwise manner to evaluate their effects on the model performance. We finally proposed a two-stage approach for the classification and detection. On the RGB multi-channel, the ResNet-50 classification network with MHSA mechanism combined with the YOLO-V5 detection model, which added an RGB parallel network, the feature erase module, ASPP, and MHSA mechanism, was utilized.

In summary, the contributions from our work are as follows: (1) To the best of our knowledge, this is the first time that image classification combined with an object detection model is used to automatically identify a variety of SB lesions and evaluate their bleeding risks; and (2) The model based on deep learning has high accuracy, high sensitivity and high specificity, which improves the diagnostic efficiency of doctors and the ability to identify high-risk bleeding populations. Its diagnostic performance has good potential for clinical application.

MATERIALS AND METHODS

Materials

A total of 701 patients who underwent SB CE in Shanxi Provincial People's Hospital and Shanxi Provincial Hospital of Traditional Chinese Medicine from 2013 to 2023 were included in this study. Two different capsule types were used at our two centers: PillCam SB2 and SB3 systems (Medtronic, Minneapolis, MN, United States) and MiroCam system (Intromedic, Seoul, South Korea). All patient-generated videos were reviewed, collected, screened, and labeled by three expert gastroenterologists (who had read more than 200 CE studies). The inclusion and final labeling of images were contingent on the agreement of at least two of the three experts.

The lesions included in the pictures were divided into three bleeding risk levels according to Saurin classification[21]: No bleeding risk (P0); Uncertain bleeding risk (P1); And high bleeding risk (P2). We finally divided the included images into the following 12 types: N (normal); P0Lk (lymphangiectasia); P0Lz (lymphoid follicular hyperplasia); Xanthomatosis (P0X); Erosion (P1E); Ulcer smaller than 2 cm (P1U); Protruding lesion smaller than 1 cm (P1P); Ulcer larger than 2 cm (P2U); Protruding lesion larger than 1 cm (P2P); Vascular lesion (P2V); Blood (B); And invalid picture (I).

We selected a total of 111861 images, and randomly divided the training set and test set images into 74574 and 37287 images, respectively, according to the 2:1 ratio. Written informed consent was obtained from all patients. Patient data were anonymized, and any personal identifying information was omitted. This study was approved by the Ethics Committee of Shanxi Provincial People's Hospital.

Experimental setup

All image preprocessing algorithms were run on a standard computer using a 64-bit Windows 10 operating system and a Python laboratory environment provided by Anaconda 2.5.0. All experiments using deep learning for model training were conducted on an RTX 3060(GPU) and i7 processor, and the computational resources and computer-aided tools met the experimental requirements. The deep learning models applied in the experiments were provided by the Pytorch framework, which offers a variety of deep learning algorithms and pretrained models.

Data preprocessing

The collected visible light images were decomposed into R, G, and B channels as the network's input (representative example is depicted in Figure 1).

Model building

Herein, two stages were utilized to identify and label SB lesions and their bleeding risks. In the first stage (Stage 1), all input images were entered into the improved ResNet-50 classification model, and the images were divided into small intestinal lesion images, normal small intestinal mucosa images, and invalid images according to whether lesions existed. The main purpose of this stage was to filter invalid images. In the second stage (Stage 2), the images of normal small intestinal mucosa and lesions classified in Stage 1 were entered into the improved YOLO-V5 model, and the lesions were detected, assessed for bleeding risk, and labeled for location. This task can be formally defined as follows: For a given data set $\{x_i, y_i | 1 \ll i \ll N\}$, the research goal was to create a mapping function $F_{class}: x_i \to y_i$, where $x_i \in \{x_1, x_2, ..., x_n\}$ denotes the endoscopic image, and output image x_i corresponds to the disease category $y_i \in \{y_1, y_2, ..., y_m\}$. The model diagram is depicted in Figure 2. Ablation experiments were performed to remove specific modules in a one-by-one stepwise manner to investigate their individual impact on improving the performance of our model.

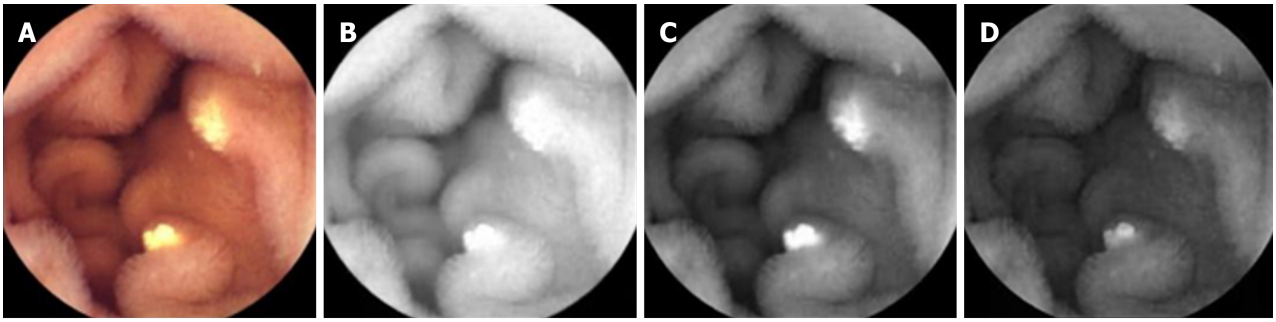

DOI: 10.3748/wjg.v30.i2.170

Figure 1 Visible light image decomposed into R, G, and B channels. A: Visible light image (original image); B: R channel image; C: G channel image; D: B channel image.

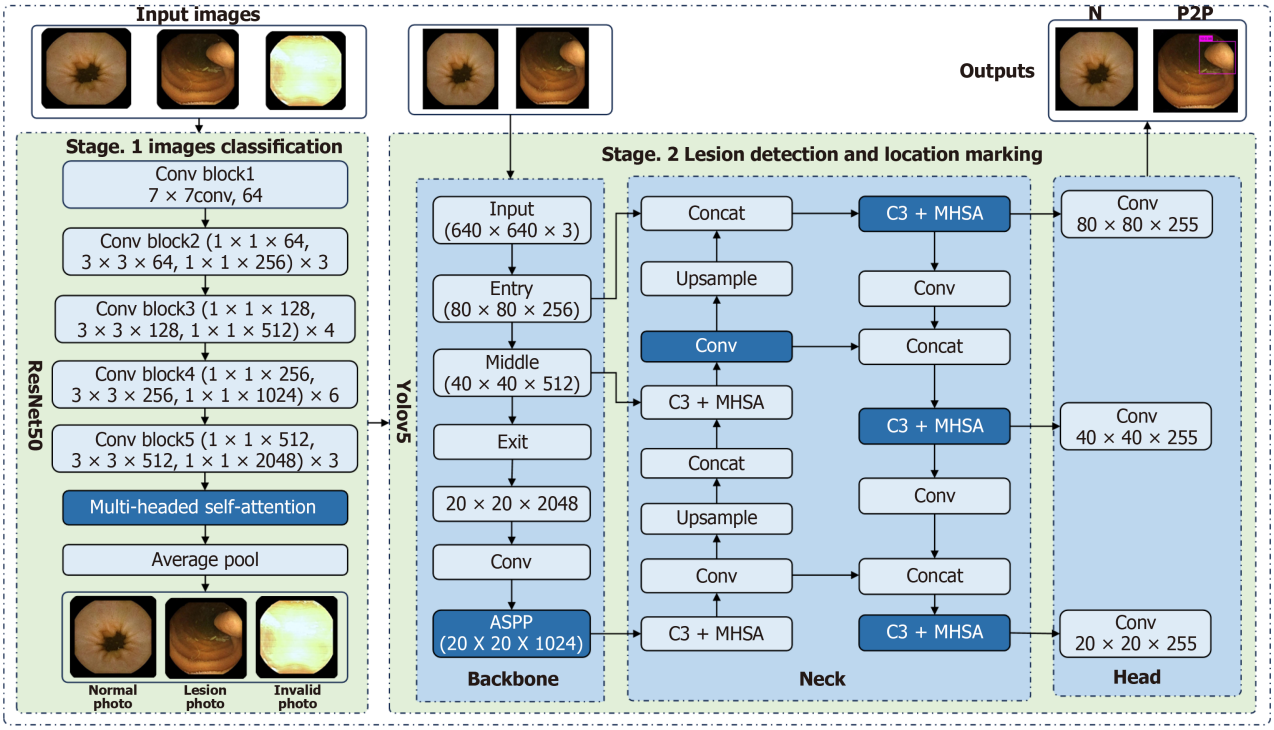

DOI: 10.3748/wjg.v30.i2.170

Figure 2 Overview of the proposed framework. ASPP: Atrous Spatial Pyramid Pooling; MHSA: Multi-head self-attention; N: Normal; P2P: Protruding lesion larger than 1 cm.

Building the Stage 1 classification model: Stage 1 utilized ResNet-50 as the network backbone and incorporated three branches to learn the features of the three RGB channels. The global average pooling layer was connected into the network, which can reduce the number and complexity of the neural network and simultaneously extract the global information of image features. Thus, the classification task was performed optimally. In addition, after the network's fifth convolutional block, we introduced a MHSA mechanism to fuse features at different levels, which can automatically capture the relationship between different locations or features. Thus, we captured the context information and crucial features in the image in an optimal manner. Finally, the fused features were fed into a softmax layer, which received a vector of scores from each category of the model and transformed these scores into a probability distribution representing the probabilities of each category. Specifically, the softmax function normalized the raw scores to a value between 0 and 1 and ensured that the sum was 1.

The ResNet-50 network model included one convolutional block, four residual blocks, and one output layer. $F_{class}: x_i \rightarrow y_i$ comprised two components: A nonlinear feature mapping structure and a classifier. During training, a two-dimensional image was mapped into a one-dimensional vector, which was then entered into the classifier for judgment: $\hat{x} = ResNet50(x_i)$. Here, x_i represents the input image, and $\hat{x}$ represents the image vector after ResNet-50 feature extraction.

In addition, the attention module was a simulation of the attention module associated with the human brain. Since individuals' eyes move to the place of interest and subsequently focus on a certain place, when the attention module was introduced, the proposed model focused on the place of feature focus distribution during training, as depicted:

$Attention(Q,K,V) = \sum_{i=1}^{l_x} Similarity(Q,K) * V$, where Q, K and V are the feature vectors $\hat{x}$ of the input x, respectively. Given Q, the correlation between Q and its different K values can be calculated, *i.e.* the weight coefficients of different V values in K. The weighted average result of V can be used as the attention value. The specific calculation process is shown.

$$DocproductSim(Q,K) = Q \cdot K$$

$$a_i = softmax(DocproductSim_i) = \frac{e^{Sim_i}}{\sum_{j=1}^{Lx} e^{Sim_i}}$$

$$Attention(Q,k) = \sum_{i=1}^{l_x} a_i \cdot V$$

Specifically, the correlation between Q and different K was calculated by dot product, *i.e.* the weight system of each part in the image was calculated. The output of the previous stage was then normalized to map the range of values between 0 and 1. Finally, the results of multiplication of the value and the corresponding weight of each value were accumulated to obtain the attention value.

The loss function of the model was the cross-entropy loss function, and the calculation process is shown.

$Loss = -(y \cdot log(\hat{y}) + (1-y) \cdot log(1-\hat{y}))$

Here, y is the actual category, and $\hat{y}$ is the predicted category.

Building the stage 2 lesion detection model: Stage 2 adopted YOLO-V5 as the network backbone, adopted three branches to learn the features of three RGB channels respectively, and introduced a parallel network, the feature erase module, ASPP, and MHSA mechanism for detection. YOLO-V5 is composed of the following four components: Input layer; backbone network; middle layer; and prediction layer. In the input layer, the input image was scaled, the data were enhanced, and the optimal anchor value was calculated. The backbone network was composed of a convolutional network to extract the main features. In the middle layer, the feature pyramid network and path aggregation network were utilized to extract more complex features. The prediction layer was utilized to predict the location and category of the target.

YOLO-V5 adopted the SPP module. To enhance the feature extraction capability of the backbone network, we replaced the SPP module with the ASPP module. The dilated convolution adopted by ASPP differs from the ordinary convolution in that it introduces the "rate" parameter, which represents the number of intervals between points in the convolution kernel. By adjusting the expansion rate, the receptive field size of the convolution operation can be controlled without having to reduce the resolution of the feature map. This enabled the ASPP module to effectively capture information in a wider range while maintaining a high resolution, thereby enhancing the feature extraction performance of the backbone network.

Considering the correlation between the three channels, features were extracted from three channels of the same image, followed by the fusion of these extracted features that was achieved through a parallel network to capture both independence and interdependence. The feature erase module was utilized to generate 000-111 random numbers using a computer. Thus, the existence of overfitting and underfitting in the feature fusion process was prevented. Researchers can determine whether the features of the corresponding branch are fused. If a bit of the binary number is 0, it represents the branch features of the branch to be erased (*i.e.* set to zero); if the bit is 1, it represents the branch features of the branch to be fused.

Meanwhile, to enable the model to focus on the crucial image components and enhance the ability of the model to extract features, we fused the MHSA mechanism in the C3 module of Neck to enhance the detection accuracy, and finally performed the detection in the Head layer.

The model's loss function was complete intersection over union loss, and the calculation process is shown:

$$F_{CIOU\_loss} = 1 - (F_{IOU_{loss}} - \frac{d_0^2}{d_c^2} - \frac{v^2}{1 - F_{IOU_{loss}} + v})$$

$F_{IOU_{loss}}$ is the intersection over union loss function, d_0 is the Euclidean distance between the target box and the center point of the prediction box, d_c is the diagonal distance of the target box, and v is the parameter measuring the aspect ratio.

Experimental procedure

The images in the test set were read by three physicians (gastroenterologists who read less than 10 CE examinations) through physician reading (A) and model-assisted reading (B). Process A randomly assigned 37287 images to the three physicians for reading. In process B, 37287 CE images were first entered into the model. After model classification and detection, the new image package was randomly assigned to the three physicians for a secondary review. Stage 1 of the model divided images into small intestinal lesion images, normal small intestinal mucosa images, and invalid images, and filtered out many invalid images. Figure 3 depicts a representative example of invalid images and normal small intestinal mucosa images. Then, Stage 2 detected the images of 11 types (normal SB mucosa, lymphangiectasia, lymphoid follicular hyperplasia, xanthoma, erosion, ulcer smaller than 2 cm, protruding lesion smaller than 1 cm, ulcer larger than 2 cm, protruding lesion larger than 1 cm, vascular lesions, and blood), assessed their risk of bleeding, and labeled the lesions. The effect of the proposed model structure on CE recognition is depicted in Figure 4. All the physicians determined a diagnosis of each frame of the picture through independent reading and model-assisted reading. If the diagnosis of physician reading was consistent with model-assisted reading, no further evaluation was conducted. If the final diagnosis was inconsistent and/or different lesions were observed, the diagnosis of three experts was assumed to be the gold standard.

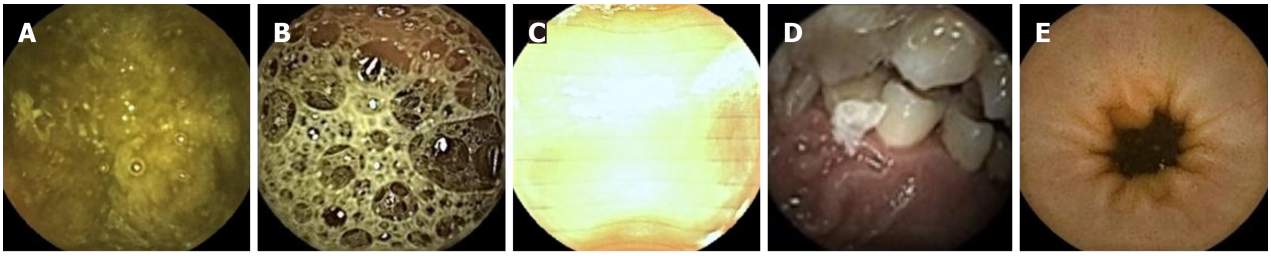

DOI: 10.3748/wjg.v30.i2.170

Figure 3 Representative examples of invalid images and normal small bowel mucosa images. A: Bowel contents; B: Air bubbles; C: Overexposure; D: Oral cavity; E: Normal small bowel mucosa.

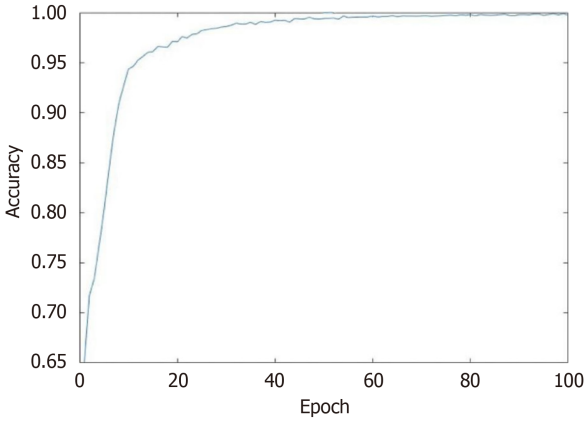

DOI: 10.3748/wjg.v30.i2.170

Figure 4 Trend plot of accuracy *vs* epoch.

RESULTS

Data

In the image pool (n = 74574) of the training dataset, there were 52310 negative pictures (normal small intestinal mucosa pictures and invalid pictures) and 22264 positive pictures. In the image pool of the test dataset (n = 37287), there were 26155 negative pictures and 11132 positive pictures. The distribution of specific types of images is depicted in Table 1.

Result analysis

The test set of pictures were respectively passed through the two processes of physician reading and model-assisted reading, and the final diagnosis was compared with the diagnosis provided by the expert analysis, which was the gold standard. The primary outcome measures included sensitivity, specificity, and accuracy.

Qualitative analysis: Representative examples of the heat maps generated by the model for 10 lesion types and of the results of the model system are depicted in Figures 5 and 6.

Quantitative analysis: (1) Physician reading. The sensitivity, specificity, and accuracy of physician reading for all pictures were 93.80%, 99.38%, and 98.92%, respectively. The sensitivity, specificity, and accuracy of physician reading for positive pictures were 89.95%, 99.80%, and 99.51%, respectively. The sensitivity, specificity, and accuracy for different types of image recognition are depicted in Table 2.

(2) Performance of the model. In Stage 1 we utilized ablation experiments, and the results indicated (Tables 3 and 4) that the accuracy, sensitivity, and specificity of the multimodal system model with three-channel RGB were more optimal than those of the R channel, G channel, and B channel. The accuracy, sensitivity, and specificity of the MHSA mechanism were more optimal than those of the spatial attention mechanism and the channel attention mechanism. The RGB multimodal channel and MHSA mechanism were more conducive to enhancing the performance of the overall diagnostic model. Therefore, the RGB multi-channel and MHSA mechanism access classification model backbone was utilized.

In Stage 2, we also utilized ablation experiments, and the results indicated (Tables 5 and 6) that the accuracy and AUC of the model with a parallel network were further enhanced and that the equal error rate was reduced. After the parallel network, the feature erase module was used to find that the RGB multimodal model was more conducive to enhancing the performance of the overall diagnostic model. The addition of ASPP and MHSA mechanism was more conducive to improving the performance of the overall diagnostic model. Therefore, RGB multi-channel, parallel network, feature erase module, ASPP and the MHSA mechanism were used to access the detection model backbone.

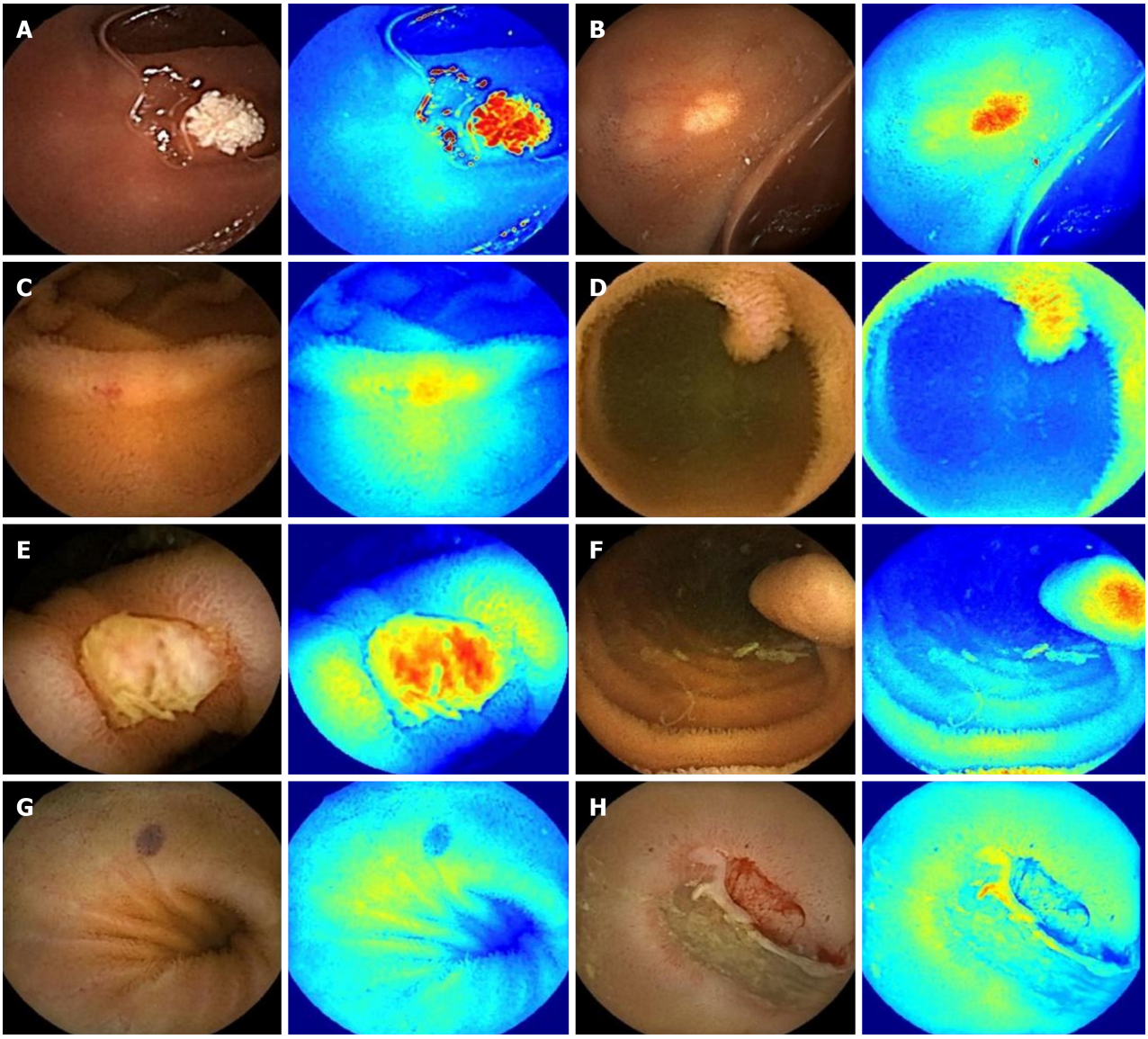

DOI: 10.3748/wjg.v30.i2.170

Figure 5 Software-generated image representation of the heat map. A: P0Lk (lymphangiectasia); B: P0X (xanthoma); C: P1E (erosion); D: P1P (protruding lesion smaller than 1 cm); E: P2U (ulcer larger than 2 cm); F: P2P (protruding lesion larger than 1 cm); G: P2V (vascular lesion); H: B (bleeding).

(3) Model auxiliary reading. We utilized the optimal model to assist physician reading. The study indicated that the sensitivity, specificity, and accuracy of model-assisted reading for all pictures were 99.17%, 99.92%, and 99.86%, respectively. The sensitivity, specificity, and accuracy of model-assisted reading for positive pictures were 98.81%, 99.96%, and 99.93%, respectively. The sensitivity and accuracy of model-assisted reading for various types of SB lesions were higher than those of physician reading (Table 2).

(4) Comparison with existing models. The proposed model was compared with the existing research models, and the experimental results are depicted in Table 7. Generally, the specificity and accuracy of the proposed model for the recognition of ulcers, protruding lesions, vascular lesions, and bleeding pictures and the sensitivity for the recognition of ulcers and bleeding pictures were higher than those of the other three methods. The sensitivity of the proposed algorithm in identifying protruding lesions and vascular lesions is slightly lower than that of Ding *et al*[22].

(5) Time calculation. The average processing time of physicians was 0.40 ± 0.24 s/image, and the image processing time of the improved model system was 48.00 ± 7.00 ms/image. The processing time of the system was significantly different from that of the clinicians ($P < 0.001$).

DISCUSSION

After 20 years of development, CE has continuously expanded its application depth and breadth and has become a crucial examination method for gastrointestinal diseases[23-25]. However, CE examination is a tedious task in clinical work due to its long reading time. With the wide application of artificial intelligence (AI)[26], the reading time of CE has

Table 1 Training and test sets image classification and the number of each classification

Set	Type of CE	Type of pictures												
		N	P0Lk	P0Lz	P0X	P1E	P1U	P1P	P2U	P2P	P2V	B	I	Total
Training set	PillCam	14026	2086	1505	551	1851	3867	687	1564	689	930	1529	17935	47220
	MiroCam	13452	612	817	494	1091	2062	180	341	205	421	782	6897	27354
Test set	PillCam	9221	245	435	122	235	1261	119	2608	109	139	1703	8446	24643
	MiroCam	4518	112	418	153	68	415	68	1581	68	92	1181	3970	12644

B: Blood; CE: Capsule endoscopy; I: Invalid pictures; N: Normal pictures; P0Lk: Lymphangiectasia; P0Lz: Lymphoid follicular hyperplasia; P0X: Xanthoma; P1E: Erosion; P1P: Protruding lesion smaller than 1 cm; P1U: Ulcer smaller than 2 cm; P2P: Protruding lesion larger than 1 cm; P2U: Ulcer larger than 2 cm; P2V: Vasculopathy.

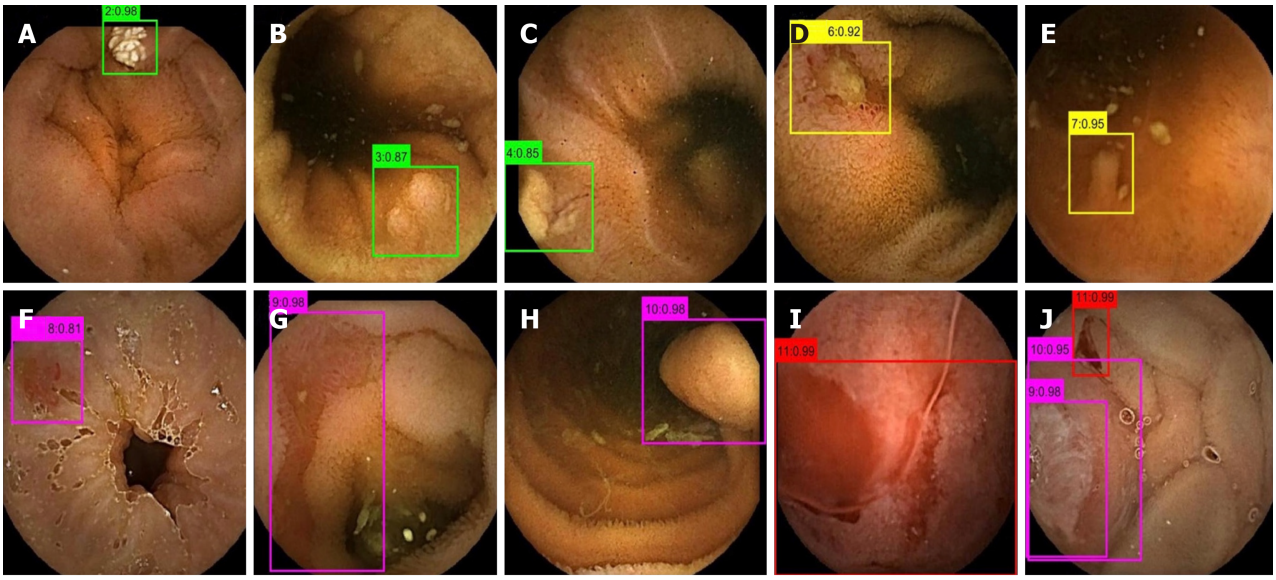

DOI: 10.3748/wjg.v30.i2.170

Figure 6 Output of YOLO-V5. Boxes with different colors in the output image represent different bleeding risks; Green represents no bleeding risk; Yellow represents uncertain risk of bleeding; Magenta represents high bleeding risk; Red represents bleeding. Different numbers in the output image represent different lesion types. A: P0Lk (lymphangiectasia); B: P0Lz (lymphoid follicular hyperplasia); C: P0X (xanthoma); D: P1U (ulcer smaller than 2 cm); E: P1P (protruding lesion smaller than 1 cm); F: P2V (vascular lesion); G: P2U (ulcer larger than 2 cm); H: P2P (protruding lesion larger than 1 cm); I: Bleeding (B); J: P2P (protruding lesion larger than 1 cm), P2U (ulcer larger than 2 cm), and B. Decimal point represents probability.

been immensely shortened. While reducing the reading time, it is more crucial to enhance the performance of the system. Initial research was limited to the identification of one lesion. For example, Tsuboi *et al*[27] developed a CNN model for the automatic identification of small intestinal vascular lesions and Ribeiro *et al*[28] developed a CNN model to automatically identify protruding lesions in the small intestine while Ferreira *et al*[16] developed a CNN system that can automatically identify ulcers and mucosal erosions. With continued research, CNNs have been developed to identify a variety of lesions. For example, Ding *et al*[22] conducted a multicenter retrospective study that included 77 medical centers and collected 6970 cases undergoing SB CE. A CNN model based on ResidualNet 152 that can automatically detect 10 small intestinal lesions (inflammation, ulcer, polyp, lymphangiectasia, hemorrhage, vascular disease, protrusion lesions, lymphoid follicular hyperplasia, diverticulum, and parasites) was developed[22]. Their system exhibited high-level performance, and this result indicates the potential of AI models for multi-lesion detection. However, CNN cannot effectively focus on the important part of the image, limiting the ability of the model to identify lesions. Moreover, the current research is based on the network model of image classification, which cannot distinguish two or more types of lesions in the image, let alone determine the specific location of the lesions, and its practicability is poor. More importantly, existing models do not identify the bleeding risks of SB lesions.

In this study, we explored the image classification and object detection model to facilitate the evaluation of CE images. Ablation experiments were also conducted on multiple modules to improve ResNet-50 and YOLO-V5, ultimately obtaining a high-precision model that can simultaneously detect a variety of SB lesions and assess the bleeding risks of lesions. We successfully tested the model using 37287 images. The results indicated that under the same hyperparameter and training round settings, the ResNet-50 classification system based on the three-channel RGB multimodal and MHSA mechanism combined with the YOLO-V5 detection system based on a parallel network, the feature erasures module,

Table 2 Comparison of sensitivity, specificity, and accuracy of physician and model-assisted reading for different types of image recognition

Type of CE	Mode of reading	Sensitivity, %	Specificity, %	Accuracy, %
I	P	95.96	98.10	97.39
	M	99.85	99.57	99.66
N	P	94.96	94.25	94.52
	M	98.84	99.77	99.43
P0Lk	P	84.31	99.89	99.75
	M	96.92	99.97	99.94
P0Lz	P	78.66	99.71	99.23
	M	97.30	99.90	99.83
P0X	P	65.45	99.87	99.62
	M	93.82	99.98	99.94
P1E	P	67.33	99.55	99.28
	M	91.75	99.96	99.90
P1U	P	74.88	99.68	98.57
	M	98.39	99.94	99.87
P1P	P	64.71	99.78	99.61
	M	94.12	99.94	99.91
P2U	P	98.35	99.94	99.76
	M	99.69	99.99	99.95
P2P	P	88.14	99.71	99.65
	M	100	99.96	99.96
P2V	P	52.38	99.92	99.62
	M	97.40	99.97	99.96
B	P	100	100	100
	M	100	100	100

The models in this table refer to the improved models (with modules added). B: Blood; CE: Capsule endoscopy; I: Invalid pictures; M: Model-assisted reading; N: Normal pictures; P: Physician reading; P0Lk: Lymphangiectasia; P0Lz: Lymphoid follicular hyperplasia; P0X: Xanthoma; P1E: Erosion; P1P: Protruding lesion smaller than 1 cm; P1U: Ulcer smaller than 2 cm; P2P: Protruding lesion larger than 1 cm; P2U: Ulcer larger than 2 cm; P2V: Vasculopathy.

Table 3 Effect of stage 1 multimodal module ablation experiments on the performance metrics of the algorithm

Method	Color channel module				Accuracy, %	Sensitivity, %	Specificity, %
	R	G	B	RGB			
Method 1	√	×	×	×	98.32	98.29	98.36
Method 2	×	√	×	×	96.97	96.99	96.93
Method 3	×	×	√	×	99.04	99.02	99.08
Method 4	×	×	×	√	99.08	99.05	99.12

ASPP, and MHSA mechanism had the highest diagnostic performance among all model combinations in our study. Moreover, the diagnostic performance of the model in assisting physician reading was higher than that in physician reading.

This study exhibited considerable novelty. First, this was based upon the pioneering AI diagnostic system for clinical CE to automatically detect SB lesions and their bleeding risks. Second, our model had high accuracy (98.96%) and high

Table 4 Effect of stage 1 attention module ablation experiments on the performance metrics of the algorithm

Method	Attention module			Accuracy, %	Sensitivity, %	Specificity, %
	SA	CA	MHSA			
Method 1	√	×	×	98.79	98.75	98.86
Method 2	×	√	×	98.82	98.66	99.06
Method 3	×	×	√	99.08	99.05	99.12

CA: Channel attention module; MHSA: Multi-head self-attention; SA: Spatial attention module.

Table 5 Effect of ablation experiments in stage 2 on algorithm performance metrics

Module	Accuracy, %	EER, %	AUC, %
PN, √	98.96	0.24	98.86
PN, ×	96.38	0.29	95.02
ASPP, √	98.96	0.24	98.86
ASPP, ×	96.01	0.28	96.47
MHSA, √	98.96	0.24	98.86
MHSA, ×	96.22	0.29	95.68

ASPP: Atrous spatial pyramid pooling; AUC: Area under the curve; EER: Equal error rate; MHSA: Multi-head self-attention mechanism; PN: Parallel network.

Table 6 Effect of random number experiment on algorithm performance index in stage 2 feature erase module

Random number	Accuracy, %	EER, %	AUC, %
001	97.91	0.29	98.49
010	97.92	0.28	98.47
100	97.91	0.29	98.50
011	98.58	0.24	98.63
101	98.37	0.25	98.66
110	98.27	0.25	98.67
111	98.96	0.24	98.86

AUC: Area under the curve; EER: Equal error rate.

sensitivity (99.17%) when assisting physician reading. Especially for SB vascular lesions, the sensitivity of physician reading was only 52.38%, which indicated that nearly half of the lesions will be missed, and SB vascular lesions exhibited a high risk of bleeding, which is a common causative factor for SB bleeding. The network model immensely enhanced the sensitivity for such lesions (97.40%), which bears immense significance for physicians tasked with enhancing the diagnosis of bleeding and identifying high-risk bleeding populations. Meanwhile, the model was time-efficient (48.00 ± 7.00 ms for each image compared with 0.40 ± 0.24 s for clinicians). Its diagnostic performance exhibited potential for clinical application.

In general, the proposed model outperforms the existing models in the identification of a variety of lesions (ulcers, luminal protrusion lesions, vascular lesions and bleeding), which can effectively improve the ability of physicians to identify lesions and evaluate bleeding. However, the sensitivity of the proposed algorithm for the recognition of intraluminal protruding lesions and vascular lesions was lower than that of Ding *et al*[22] (100/98.1, 98.9/97.4), which may be related to the following factors. First, the sample size of the dataset was small, and the model did not fully learn the relevant discriminative features. Second, other existing models only perform the task of picture classification, while the proposed model not only classifies and detects lesions, providing an the accurate location of the lesions, it also evaluates the bleeding risk of lesions. The effective completion of these tasks may affect the sensitivity of the model, however.

Table 7 Comparison of available models

Ref.	Year of publication	Application	Algorithm	Sensitivity, %	Specificity, %	Accuracy, %
Aoki *et al*[29]	2019	Erosion/ulcer	CNN system based on SSD	88.2	90.9	90.8
Ding *et al*[22]	2019	Ulcer	ResNet-152	99.7	99.9	99.8
		Bleeding		99.5	99.9	99.9
		Vascular lesion		98.9	99.9	99.2
Aoki *et al*[30]	2020	Protruding lesion	ResNet-50	100	99.9	99.9
		Bleeding		96.6	99.9	99.9
Current study	2023	Ulcer(P1U + P2U)	Improved ResNet-50 + YOLO-V5	99.7	99.9	99.9
		Vascular lesion		97.4	99.9	99.9
		Protruding lesion (P1P + P2P)		98.1	99.9	99.9
		Bleeding		100	100	100

CNN: Convolution neural network; P1U: Ulcer smaller than 2 cm; P1P: Protruding lesion smaller than 1 cm; P2P: Protruding lesion larger than 1 cm; P2U: Ulcer larger than 2 cm; SSD: Single shot multibox detector.

Several limitations of this study should be considered when interpreting the results. First, diverticulum and parasite images were not included in the study due to the limited number of images available for training. Future studies should be directed toward enrollment and multicenter collaboration so that the aforementioned issues can be effectively addressed. Second, as an experimental evaluation and first-step investigation, the system was developed and tested on still images; it failed to perform real-time detection and result interpretation on videos. Thus, future studies evaluating the real-time utilization of AI in CE are warranted.

CONCLUSION

The trained deep learning model based on image classification combined with object detection exhibited satisfactory performance in identifying SB lesions and their bleeding risk, which enhanced the diagnostic efficiency of physicians and improved the ability of physicians to identify high-risk bleeding groups. This system highlighted its future application potential as an AI diagnostic system.

ARTICLE HIGHLIGHTS

Research background

Deep learning provides an efficient automatic image recognition method for small bowel (SB) capsule endoscopy (CE) that can assist physicians in diagnosis. However, the existing deep learning models present some unresolved challenges.

Research motivation

CE reading is time-consuming and complicated. Abnormal parts account for only a small proportion of CE images. Therefore, it is easy to miss the diagnosis, which affects the detection of lesions and assessment of their bleeding risk. Also, both image classification and object detection have made significant progress in the field of deep learning.

Research objectives

To propose a novel and effective classification and detection model to automatically identify various SB lesions and their bleeding risks, and label the lesions accurately, so as to enhance the diagnostic efficiency of physicians and their ability to identify high-risk bleeding groups.

Research methods

The proposed model was a two-stage method that combined image classification with object detection. First, we utilized the improved ResNet-50 classification model to classify endoscopic images into SB lesion images, normal SB mucosa images, and invalid images. Then, the improved YOLO-V5 detection model was utilized to detect the type of lesion and the risk of bleeding, and the location of the lesion was marked. We constructed training and testing sets and compared

model-assisted readings with physician readings.

Research results

The accuracy of the model constructed in this study reached 98.96%, which was higher than the accuracy of other systems using only a single module. The sensitivity, specificity, and accuracy of the model-assisted reading detection of all images were 99.17%, 99.92%, and 99.86%, which were significantly higher than those of the endoscopists' diagnoses. The image processing time of the model was 48 ms/image, and the image processing time of the physicians was 0.40 ± 0.24 s/image ($P < 0.001$).

Research conclusions

The deep learning model of image classification combined with object detection exhibits a satisfactory diagnostic effect on a variety of SB lesions and their bleeding risks in CE images, which enhances the diagnostic efficiency of physicians and improves their ability to identify high-risk bleeding groups.

Research perspectives

We utilized a two-stage combination method and added multiple modules to identify normal SB mucosa images, invalid images, and various SB lesions (lymphangiectasia, lymphoid follicular hyperplasia, xanthoma, erosion, ulcer smaller than 2 cm, protruding lesion smaller than 1 cm, ulcer larger than 2 cm, protruding lesion larger than 1 cm, vascular lesions, and blood). The bleeding risk was evaluated and classified.

FOOTNOTES

Author contributions: Zhang RY collected the patients' clinical data and wrote the paper; Wang JP designed the report and revised the paper; Qiang PP and Cai LJ analyzed the data; Qiang PP, Cai LJ, and Li T revised the paper for important intellectual content; Qin Y, Zhang Y, and Zhao YQ collected the patients' clinical data.

Supported by The Shanxi Provincial Administration of Traditional Chinese Medicine, No. 2023ZYYDA2005.

Institutional review board statement: This study was approved by the Ethics Committee of the Shanxi Provincial People's Hospital [(2023)No.360].

Informed consent statement: Each patient provided written informed consent for inclusion in the study.

Conflict-of-interest statement: The authors declare having no conflicts of interest.

Data sharing statement: The datasets generated and/or analyzed during the current study are available from the corresponding author on reasonable request.

Country/Territory of origin: China

ORCID number: Rui-Ya Zhang 0000-0002-5925-8909; Ling-Jun Cai 0000-0002-1268-6703; Jun-Ping Wang 0000-0002-9360-4131.

S-Editor: Fan JR
L-Editor: A
P-Editor: Xu ZH

REFERENCES

1 **Sami SS**, Iyer PG, Pophali P, Halland M, di Pietro M, Ortiz-Fernandez-Sordo J, White JR, Johnson M, Guha IN, Fitzgerald RC, Ragunath K. Acceptability, Accuracy, and Safety of Disposable Transnasal Capsule Endoscopy for Barrett's Esophagus Screening. *Clin Gastroenterol Hepatol* 2019; **17**: 638-646.e1 [PMID: 30081223 DOI: 10.1016/j.cgh.2018.07.019]

2 **Kim SH**, Lim YJ. Artificial Intelligence in Capsule Endoscopy: A Practical Guide to Its Past and Future Challenges. *Diagnostics (Basel)* 2021; **11** [PMID: 34574063 DOI: 10.3390/diagnostics11091722]

3 **Jiang B**, Pan J, Qian YY, He C, Xia J, He SX, Sha WH, Feng ZJ, Wan J, Wang SS, Zhong L, Xu SC, Li XL, Huang XJ, Zou DW, Song DD, Zhang J, Ding WQ, Chen JY, Chu Y, Zhang HJ, Yu WF, Xu Y, He XQ, Tang JH, He L, Fan YH, Chen FL, Zhou YB, Zhang YY, Yu Y, Wang HH, Ge KK, Jin GH, Xiao YL, Fang J, Yan XM, Ye J, Yang CM, Li Z, Song Y, Wen MY, Zong Y, Han X, Wu LL, Ma JJ, Xie XP, Yu WH, You Y, Lu XH, Song YL, Ma XQ, Li SD, Zeng B, Gao YJ, Ma RJ, Ni XG, He CH, Liu YP, Wu JS, Liu J, Li AM, Chen BL, Cheng CS, Sun XM, Ge ZZ, Feng Y, Tang YJ, Li ZS, Linghu EQ, Liao Z; Capsule Endoscopy Group of the Chinese Society of Digestive Endoscopy. Clinical guideline on magnetically controlled capsule gastroscopy (2021 edition). *J Dig Dis* 2023; **24**: 70-84 [PMID: 37220999 DOI:

10.1111/1751-2980.13173]
4 **Nennstiel S**, Machanek A, von Delius S, Neu B, Haller B, Abdelhafez M, Schmid RM, Schlag C. Predictors and characteristics of angioectasias in patients with obscure gastrointestinal bleeding identified by video capsule endoscopy. *United European Gastroenterol J* 2017; **5**: 1129-1135 [PMID: 29238592 DOI: 10.1177/2050640617704366]
5 **Liao Z**, Gao R, Xu C, Li ZS. Indications and detection, completion, and retention rates of small-bowel capsule endoscopy: a systematic review. *Gastrointest Endosc* 2010; **71**: 280-286 [PMID: 20152309 DOI: 10.1016/j.gie.2009.09.031]
6 **Rondonotti E**, Pennazio M, Toth E, Koulaouzidis A. How to read small bowel capsule endoscopy: a practical guide for everyday use. *Endosc Int Open* 2020; **8**: E1220-E1224 [PMID: 33015322 DOI: 10.1055/a-1210-4830]
7 **Beg S**, Card T, Sidhu R, Wronska E, Ragunath K; UK capsule endoscopy users' group. The impact of reader fatigue on the accuracy of capsule endoscopy interpretation. *Dig Liver Dis* 2021; **53**: 1028-1033 [PMID: 34016545 DOI: 10.1016/j.dld.2021.04.024]
8 **Leenhardt R**, Koulaouzidis A, McNamara D, Keuchel M, Sidhu R, McAlindon ME, Saurin JC, Eliakim R, Fernandez-Urien Sainz I, Plevris JN, Rahmi G, Rondonotti E, Rosa B, Spada C, Toth E, Houdeville C, Li C, Robaszkiewicz M, Marteau P, Dray X. A guide for assessing the clinical relevance of findings in small bowel capsule endoscopy: analysis of 8064 answers of international experts to an illustrated script questionnaire. *Clin Res Hepatol Gastroenterol* 2021; **45**: 101637 [PMID: 33662785 DOI: 10.1016/j.clinre.2021.101637]
9 **ASGE Technology Committee**, Wang A, Banerjee S, Barth BA, Bhat YM, Chauhan S, Gottlieb KT, Konda V, Maple JT, Murad F, Pfau PR, Pleskow DK, Siddiqui UD, Tokar JL, Rodriguez SA. Wireless capsule endoscopy. *Gastrointest Endosc* 2013; **78**: 805-815 [PMID: 24119509 DOI: 10.1016/j.gie.2013.06.026]
10 **Chu Y**, Huang F, Gao M, Zou DW, Zhong J, Wu W, Wang Q, Shen XN, Gong TT, Li YY, Wang LF. Convolutional neural network-based segmentation network applied to image recognition of angiodysplasias lesion under capsule endoscopy. *World J Gastroenterol* 2023; **29**: 879-889 [PMID: 36816625 DOI: 10.3748/wjg.v29.i5.879]
11 **Esteva A**, Kuprel B, Novoa RA, Ko J, Swetter SM, Blau HM, Thrun S. Dermatologist-level classification of skin cancer with deep neural networks. *Nature* 2017; **542**: 115-118 [PMID: 28117445 DOI: 10.1038/nature21056]
12 **Hassan C**, Spadaccini M, Iannone A, Maselli R, Jovani M, Chandrasekar VT, Antonelli G, Yu H, Areia M, Dinis-Ribeiro M, Bhandari P, Sharma P, Rex DK, Rösch T, Wallace M, Repici A. Performance of artificial intelligence in colonoscopy for adenoma and polyp detection: a systematic review and meta-analysis. *Gastrointest Endosc* 2021; **93**: 77-85.e6 [PMID: 32598963 DOI: 10.1016/j.gie.2020.06.059]
13 **Mijwil MM**, Al-Mistarehi AH, Abotaleb M, El-kenawy EM, Ibrahim A, Abdelhamid6 AA, Eid MM. From Pixels to Diagnoses: Deep Learning's Impact on Medical Image Processing-A Survey. *Wasit J Comput Mathematics Sci* 2023; **2**: 9-15 [DOI: 10.31185/wjcms.178]
14 **Mijwil MM**. Deep Convolutional Neural Network Architecture to Detect COVID-19 from Chest X-Ray Images. *Iraqi J Sci* 2023; **64**: 2561-2574 [DOI: 10.24996/ijs.2023.64.5.38]
15 **Mascarenhas Saraiva MJ**, Afonso J, Ribeiro T, Ferreira J, Cardoso H, Andrade AP, Parente M, Natal R, Mascarenhas Saraiva M, Macedo G. Deep learning and capsule endoscopy: automatic identification and differentiation of small bowel lesions with distinct haemorrhagic potential using a convolutional neural network. *BMJ Open Gastroenterol* 2021; **8** [PMID: 34580155 DOI: 10.1136/bmjgast-2021-000753]
16 **Ferreira JPS**, de Mascarenhas Saraiva MJDQEC, Afonso JPL, Ribeiro TFC, Cardoso HMC, Ribeiro Andrade AP, de Mascarenhas Saraiva MNG, Parente MPL, Natal Jorge R, Lopes SIO, de Macedo GMG. Identification of Ulcers and Erosions by the Novel Pillcam™ Crohn's Capsule Using a Convolutional Neural Network: A Multicentre Pilot Study. *J Crohns Colitis* 2022; **16**: 169-172 [PMID: 34228113 DOI: 10.1093/ecco-jcc/jjab117]
17 **Mascarenhas Saraiva M**, Ribeiro T, Afonso J, Andrade P, Cardoso P, Ferreira J, Cardoso H, Macedo G. Deep Learning and Device-Assisted Enteroscopy: Automatic Detection of Gastrointestinal Angioectasia. *Medicina (Kaunas)* 2021; **57** [PMID: 34946323 DOI: 10.3390/medicina57121378]
18 **Zhou JX**, Yang Z, Xi DH, Dai SJ, Feng ZQ, Li JY, Xu W, Wang H. Enhanced segmentation of gastrointestinal polyps from capsule endoscopy images with artifacts using ensemble learning. *World J Gastroenterol* 2022; **28**: 5931-5943 [PMID: 36405108 DOI: 10.3748/wjg.v28.i41.5931]
19 **Li P**, Li Z, Gao F, Wan L, Yu J. Convolutional neural networks for intestinal hemorrhage detection in wireless capsule endoscopy images. Proceedings of the 2017 IEEE International Conference on Multimedia and Expo (ICME); 2017 Jul 10–14; Hong Kong, China. ICME, 2017: 1518–1523
20 **Jiang PY**, Ergu DJ, Liu FY, Cai Y, Ma B. A Review of Yolo Algorithm Developments. *Procedia Comput Sci* 2022; **199**: 1066-1073
21 **Saurin JC**, Delvaux M, Gaudin JL, Fassler I, Villarejo J, Vahedi K, Bitoun A, Canard JM, Souquet JC, Ponchon T, Florent C, Gay G. Diagnostic value of endoscopic capsule in patients with obscure digestive bleeding: blinded comparison with video push-enteroscopy. *Endoscopy* 2003; **35**: 576-584 [PMID: 12822092 DOI: 10.1055/s-2003-40244]
22 **Ding Z**, Shi H, Zhang H, Meng L, Fan M, Han C, Zhang K, Ming F, Xie X, Liu H, Liu J, Lin R, Hou X. Gastroenterologist-Level Identification of Small-Bowel Diseases and Normal Variants by Capsule Endoscopy Using a Deep-Learning Model. *Gastroenterology* 2019; **157**: 1044-1054.e5 [PMID: 31251929 DOI: 10.1053/j.gastro.2019.06.025]
23 **Ahmed I**, Ahmad A, Jeon G. An IoT-Based Deep Learning Framework for Early Assessment of Covid-19. *IEEE Internet Things J* 2021; **8**: 15855-15862 [PMID: 35782174 DOI: 10.1109/JIOT.2020.3034074]
24 **Xia J**, Xia T, Pan J, Gao F, Wang S, Qian YY, Wang H, Zhao J, Jiang X, Zou WB, Wang YC, Zhou W, Li ZS, Liao Z. Use of artificial intelligence for detection of gastric lesions by magnetically controlled capsule endoscopy. *Gastrointest Endosc* 2021; **93**: 133-139.e4 [PMID: 32470426 DOI: 10.1016/j.gie.2020.05.027]
25 **Konishi M**, Shibuya T, Mori H, Kurashita E, Takeda T, Nomura O, Fukuo Y, Matsumoto K, Sakamoto N, Osada T, Nagahara A, Ogihara T, Watanabe S. Usefulness of flexible spectral imaging color enhancement for the detection and diagnosis of small intestinal lesions found by capsule endoscopy. *Scand J Gastroenterol* 2014; **49**: 501-505 [PMID: 24417643 DOI: 10.3109/00365521.2013.873480]
26 **Maeda M**, Hiraishi H. Efficacy of video capsule endoscopy with flexible spectral imaging color enhancement at setting 3 for differential diagnosis of red spots in the small bowel. *Dig Endosc* 2014; **26**: 228-231 [PMID: 23730949 DOI: 10.1111/den.12124]
27 **Tsuboi A**, Oka S, Aoyama K, Saito H, Aoki T, Yamada A, Matsuda T, Fujishiro M, Ishihara S, Nakahori M, Koike K, Tanaka S, Tada T. Artificial intelligence using a convolutional neural network for automatic detection of small-bowel angioectasia in capsule endoscopy images. *Dig Endosc* 2020; **32**: 382-390 [PMID: 31392767 DOI: 10.1111/den.13507]
28 **Ribeiro T**, Saraiva MM, Ferreira JPS, Cardoso H, Afonso J, Andrade P, Parente M, Jorge RN, Macedo G. Artificial intelligence and capsule endoscopy: automatic detection of vascular lesions using a convolutional neural network. *Ann Gastroenterol* 2021; **34**: 820-828 [PMID: 34815648 DOI: 10.20524/aog.2021.0653]
29 **Aoki T**, Yamada A, Aoyama K, Saito H, Tsuboi A, Nakada A, Niikura R, Fujishiro M, Oka S, Ishihara S, Matsuda T, Tanaka S, Koike K, Tada

T. Automatic detection of erosions and ulcerations in wireless capsule endoscopy images based on a deep convolutional neural network. *Gastrointest Endosc* 2019; **89**: 357-363.e2 [PMID: 30670179 DOI: 10.1016/j.gie.2018.10.027]

30 **Aoki T**, Yamada A, Kato Y, Saito H, Tsuboi A, Nakada A, Niikura R, Fujishiro M, Oka S, Ishihara S, Matsuda T, Nakahori M, Tanaka S, Koike K, Tada T. Automatic detection of blood content in capsule endoscopy images based on a deep convolutional neural network. *J Gastroenterol Hepatol* 2020; **35**: 1196-1200 [PMID: 31758717 DOI: 10.1111/jgh.14941]

World Journal of Gastroenterology

Submit a Manuscript: https://www.f6publishing.com

World J Gastroenterol 2024 January 14; 30(2): 184-195

DOI: 10.3748/wjg.v30.i2.184

ISSN 1007-9327 (print) ISSN 2219-2840 (online)

ORIGINAL ARTICLE

Observational Study

Success of susceptibility-guided eradication of *Helicobacter pylori* in a region with high secondary clarithromycin and levofloxacin resistance rates

Yan-Meng Wang, Mo-Ye Chen, Jing Chen, Xin-He Zhang, Yan Feng, Yu-Xi Han, Yi-Ling Li

Specialty type: Gastroenterology and hepatology

Provenance and peer review: Unsolicited article; Externally peer reviewed.

Peer-review model: Single blind

Peer-review report's scientific quality classification

Grade A (Excellent): 0
Grade B (Very good): B
Grade C (Good): C
Grade D (Fair): 0
Grade E (Poor): 0

P-Reviewer: Sahin Y, Turkey; Ulasoglu C, Turkey

Received: October 30, 2023
Peer-review started: October 30, 2023
First decision: November 29, 2023
Revised: December 12, 2023
Accepted: December 28, 2023
Article in press: December 28, 2023
Published online: January 14, 2024

Yan-Meng Wang, Mo-Ye Chen, Xin-He Zhang, Yan Feng, Yu-Xi Han, Yi-Ling Li, Department of Gastroenterology, The First Affiliated Hospital of China Medical University, Shenyang 110000, Liaoning Province, China

Jing Chen, Key Laboratory of Cancer Etiology and Prevention in Liaoning Education Department, The First Hospital of China Medical University, Shenyang 110000, Liaoning Province, China

Corresponding author: Yi-Ling Li, MD, Chief Physician, Professor, Department of Gastroenterology, The First Affiliated Hospital of China Medical University, No. 92 North Second Road, Shenyang 110000, Liaoning Province, China. lyl-72@163.com

Abstract

BACKGROUND

Resistance to clarithromycin (CLA) and levofloxacin (LFX) of *Helicobacter pylori (H. pylori)* is increasing in severity, and successful eradication is essential. Presently, the eradication success rate has greatly declined, leaving a large number of patients with previous treatment histories.

AIM

To investigate secondary resistance rates, explore risk factors for antibiotic resistance, and assess the efficacy of susceptibility-guided therapy.

METHODS

We recruited 154 subjects positive for Urea Breath Test who attended The First Affiliated Hospital of China Medical University between July 2022 and April 2023. Participants underwent a string test after an overnight fast. The gastric juice was obtained and transferred to vials containing storage solution. Subsequently, DNA extraction and the specific DNA amplification were performed using quantitative polymerase chain reaction (qPCR). Demographic information was also analyzed as part of the study. Based on these results, the participants were administered susceptibility-guided treatment. Efficacy was compared with that of the empiric treatment group.

RESULTS

A total of 132 individuals tested positive for the *H. pylori ureA* gene by qPCR

technique. CLA resistance rate reached a high level of 82.6% (n = 109), LFX resistance rate was 69.7% (n = 92) and dual resistance was 62.1% (n = 82). Gastric symptoms [odds ratio (OR) = 2.782; 95% confidence interval (95%CI): 1.076-7.194; P = 0.035] and rural residence (OR = 5.152; 95%CI: 1.407-18.861; P = 0.013) were independent risk factors for secondary resistance to CLA and LFX, respectively. A total of 102 and 100 individuals received susceptibility-guided therapies and empiric treatment, respectively. The antibiotic susceptibility-guided treatment and empiric treatment groups achieved successful eradication rates of 75.5% (77/102) and 59.0% (59/411) by the intention-to-treat (ITT) analysis and 90.6% (77/85) and 70.2% (59/84) by the per-protocol (PP) analysis, respectively. The eradication rates of these two treatment strategies were significantly different in both ITT (P = 0.001) and PP (P = 0.012) analyses.

CONCLUSION

H. pylori presented high secondary resistance rates to CLA and LFX. For patients with previous treatment failures, treatments should be guided by antibiotic susceptibility tests or regional antibiotic resistance profile.

Key Words: *Helicobacter pylori*; Antibiotic resistance; Clarithromycin; Levofloxacin; String-test; Susceptibility-guided therapy; Eradication rate

Core Tip: Decreased success eradication rates of *Helicobacter pylori (H. pylori)* have received much attention in recent years, mainly due to the increasing resistance to antibiotics. Focus has begun to be placed on the efficacy of antibiotic susceptibility-guided eradication. This study revealed that the secondary resistance rate of *H. pylori* to clarithromycin and levofloxacin in Province Liaoning, was higher than the national average. Antibiotic susceptibility-guided eradication therapy is more effective than empiric treatment. It provided a reference for eradication therapy in regions in the northeast of China.

Citation: Wang YM, Chen MY, Chen J, Zhang XH, Feng Y, Han YX, Li YL. Success of susceptibility-guided eradication of *Helicobacter pylori* in a region with high secondary clarithromycin and levofloxacin resistance rates. *World J Gastroenterol* 2024; 30(2): 184-195

URL: https://www.wjgnet.com/1007-9327/full/v30/i2/184.htm

DOI: https://dx.doi.org/10.3748/wjg.v30.i2.184

INTRODUCTION

Approximately half of the world's population is infected with *Helicobacter pylori (H. pylori)*, a bacterium that contributes to various stomach disorders, such as atrophic gastritis, gastric carcinoma, and mucosa-associated lymphoid tissue lymphoma[1]. *H. pylori* has also been implicated in the development of extra-digestive disorders, such as iron deficiency anemia, idiopathic thrombocytopenic purpura, nonalcoholic fatty liver disease, and Alzheimer's disease (AD)[2-4]. *H. pylori* also elicits immune responses. Several researchers have investigated the association of *H. pylori* infection with mean platelet volume and neutrophil/lymphocyte ratio values in both adults and children[5,6]. *H. pylori*, classified as a group I carcinogen of gastric cancer (GC), could promote the development of precancerous gastric lesions[7,8]. Successful *H. pylori* eradication might serve as a long-term preventive measure against GC among populations at high risk of the disease[9-11]. Strategies for the effective *H. pylori* treatment are essential for the prevention of GC.

Recently, the eradication rates of standard triple therapies containing clarithromycin (CLA) and regimens based on levofloxacin (LFX) have declined substantially[12-14]. This marked reduction in eradication efficacy resulted mainly from the rising prevalence of antibiotic resistance[15]. Bismuth quadruple therapy was recommended by guidelines and used clinically, yet still with unsatisfactory eradication effects[16]. A rapid increase in the prevalence of *H. pylori* resistance to CLA and LFX has been observed[17], which might be closely related to previous treatment failure. It has been pointed out that with more than two previous histories of treatments, resistance to CLA and LFX could increase by more than 50% [18]. Current consensus recommended antibiotic susceptibility tests before prescriptions in populations with several treatment failures[19]. Besides, in areas characterized by high CLA and LFX resistance, it is essential to detect antibiotic resistance of *H. pylori* before prescription. Epidemiological data on secondary *H. pylori* resistance are crucial for decision-making within respective areas when local patients are unavailable for prior tests.

However, culturing and antibiotic susceptibility tests require significant investments in time and specialized laboratory equipment, limiting their wide clinical application, likewise[20]. Furthermore, molecular tests, such as quantitative polymerase chain reaction (qPCR), hold promise for clinical application in detecting *H. pylori* infection and antibiotic resistance in gastric mucosal specimens[21,22]. For focal distribution within the gastric mucosa, *H. pylori* is prone to false-negative results when biopsies are performed at several sites under gastroscopy. Conversely, the presence of bacteria and shed epithelial cells in gastric fluid achieved using the more available and less invasive string-test than the conventional method of extracting mucosal samples through endoscopic biopsies[21].

Moreover, the identification of risk factors for antibiotic resistance of *H. pylori* is valuable for identifying high-risk populations susceptible to antibiotic-resistant strains. This information holds value in clinical settings, enabling to provide prescriptions suitable for a specific region, thereby reducing the incidence of secondary antibiotic resistance. Several studies have investigated risk factors, such as age, gender, and previous antibiotic use[23-25]. However, conclusions remained contentious, displaying discrepancies across different geographical regions.

In the current study, we calculated the secondary CLA and LFX resistance rate of *H. pylori* strains in Liaoning Province, a region in the northeast of China, based on qPCR by string-test. Risk factors for antibiotic resistance were also evaluated. Besides, we assessed the eradication rate of susceptibility-guided therapy eradication and compared the outcomes with the empiric treatment eradication rate, in order to improve the eradication rate in Liaoning Province.

MATERIALS AND METHODS

Study design, participants and acquisition of basic information

This trial was conducted at the Department of Gastroenterology of the First Affiliated Hospital of China Medical University from July 2022 to April 2023. It was approved by the Human Ethics Review Committee of the First Affiliated Hospital of China Medical University (2021325). Written informed consent was obtained from all participants. Participants were drawn from various areas of Liaoning Province, and the study was conducted at a tertiary hospital. Subjects positive for *H. pylori* and aged ≥ 18 years were recruited. Exclusion criteria included administration of antibiotics in the past month, administration of proton pump inhibitors in the past half month, acute respiratory infections, recent gastrointestinal bleeding, esophageal and gastric varices, dysphagia, and esophageal cancer. Basic information on participants was obtained from the HIS Information System Technical Support Services, including gender, current smoking conditions, current drinking conditions, body mass index (BMI), hypertension, diabetes mellitus, gastrointestinal symptoms, family members with *H. pylori* infection, family histories of GC, and living area. The definition of current smoking and drinking in the present study was that participants engaged in smoking and/or drinking behavior in accordance with their personal smoking and/or drinking habits during the first 4 wk before conducting the string test. Gastrointestinal symptoms included abdominal pain, fullness, heartburn, dysphagia, and anorexia.

Determination of H. pylori infection and steps for string-test

Urea Breath Test (UBT) was performed with The Kit For 13C-Urea Breath Test (Haiderun Pharmaceutical Group Co. Ltd., Beijing, China). After the initial baseline breath samples were collected, participants fasting for at least two hours ingested 100-mg ^{13}C-labelled reagent. Breath samples exhaled after 30 min were analyzed by the WLD600C13C Analyzer (Haiderun Pharmaceutical Group Co. Ltd., Beijing, China).

A positive indicator of *H. pylori* infection was determined according to the manufacturer's instructions. Participants positive for UBT underwent the string-test. A gelatine capsule containing a 90-cm-long string of absorbent cotton (Shenzhen Hongmed-Infagen Co. Ltd., China) was swallowed by subjects after an overnight fast, along with 300 mL of water. One hour later, researchers withdrew the string, cut it at the designated position with a pair of sterile scissors, and discarded the proximal section to preclude oral contamination. The gastric-fluid-soaked portion was transferred into storage solution supplied in vials. All samples were sent to Shenzhen Hongmed-Infagen Co. Ltd. at ambient temperature for processing.

H. pylori infection and antibiotic resistance determination by qPCR

Genomic DNA was extracted by following the manufacturer's guidelines with *H. pylori* DNA extraction kit (Hongmed-Infagen Co. Ltd.). The Real-time PCR System Gentier 96R (Tianlong Technology Co. Ltd.) carried on the amplification to detect the presence of the specific *ureA* gene and the point mutations of 23S rRNA (A2142G, A2143G, and A2142C) and *gyrA* (260T, 261A, 261G, 271A, 271T, and 272G), which represented CLA and quinolone resistance, respectively. The cycling program included an initial cycle of 2 min at 42°C, then 2 min at 95°C, proceeded by 40 denaturation cycles of 10s at 95°C and 45s at 58°C for extension and annealing.

Susceptibility-guided treatment and empiric treatment

The susceptibility-guided treatment group enrolled participants with antibiotic susceptibility results. They received bismuth-based quadruple therapy based on The Fifth Chinese National Consensus Report on the management of *H. pylori* infection[19]. The quadruple therapy consisted of bismuth 200 mg bid, PPI (rabeprazole 20 mg or ilaprazole 5 mg) bid, and two types of antibiotics. Antibiotics were selected according to the antibiotic susceptibility outcomes, two of the following: Amoxicillin 1000 mg bid, CLA 500 mg bid, furazolidone 100 mg bid, LFX 500 mg qd, minocycline hydrochloride 100 mg bid. Bismuth and PPI were administered orally before meals and antibiotics after meals. The treatment course lasted 14 d and a follow-up UBT was performed at least 4 wk after treatment.

We retrospectively reviewed UBT and treatment records of the First Affiliated Hospital of China Medical University from October 2020 to June 2023 to assess the *H. pylori* eradication rates. Researchers reviewed treatment regimens and screened patients who received therapies at least once. Of the patients screened, those who met all the following criteria were recruited in the empiric treatment group: with both pre- and post-treatment UBT results, a complete course of bismuth quadruple therapy, and being prescribed a PPI of either rabeprazole or ilaprazole. Eradication rates of *H. pylori* were evaluated by intention-to-treat (ITT; including individuals enrolled in studies analyzing eradication therapies) and per-protocol (PP; eradication therapies) analyses.

Statistical analyses

The statistical software SPSS (version 18.0; SPSS Inc., Chicago, IL, United States) was used to perform all the statistical analyses. Categorical data were presented as numbers and percentages. Continuous data were presented as mean ± SD. The demographic data on participants were processed using descriptive statistical analysis. Chi-square test was applied to compare differences between groups. Fisher's exact test was applied when over 20% of the expected counts were below 5. The factors that could influence antibiotic resistance were analyzed by univariate analysis. A binary logistic regression model was used to calculate the odds ratios (ORs) and 95% confidence intervals (95%CIs) of different variables related to antibiotic resistance. *P* value less than 0.05 in two tails was considered statistically significant.

RESULTS

Baseline characteristics of participants

In total, 154 participants with positive UBT results were recruited in the present study. A total of 132 (85.7%) *H. pylori ureA*-positive subjects were evaluated, of which group baseline characteristics were summarized in Table 1. Most participants are from urban areas (103; 78.0%), and nearly half are females (71; 53.8%). The mean age and standard deviation of 132 adults was 52.7 ± 12.6, with a range from 18 to 78 years old. Most participants (83; 62.9%) have gastric symptoms, but only a minority of individuals whose family members were with *H. pylori* infection (41; 31.1%) and who had a family history of GC (16; 12.1%). Almost half (61; 46.2%) were overweight in terms of BMI. Besides, a small proportion of participants conducted current drinking, current smoking, were diagnosed with hypertension, and were diagnosed with diabetes, in descending order of 19.7%, 17.4%, 16.7%, and 11.4%, respectively.

Secondary antibiotic resistance rate and patterns of H. pylori

The secondary resistance rates to CLA and LFX were observed in 82.6% (n = 109) and 69.7% (n = 92) of the *ureA* positive subjects, respectively, which represented quite high levels (Figure 1). Of these, 82 isolates were resistant to both antibiotics, with a dual resistance rate of 62.1%. A total of 28.0% (n = 37) of the population was monoresistant, inferior to that of the dual-resistant population. Among these 37 subjects, the greatest number was resistant to CLA (27; 20.5%), leaving 10 subjects resistant to LFX. The least number of subjects were sensitive to both antibiotics, at 9.9% of 13 ones. Antibiotic resistance patterns of *H. pylori* are shown in Table 2.

Risk factors associated with antibiotic resistance of H. pylori

The chi-square results indicated that subjects with gastrointestinal symptoms and CLA-resistance differed significantly (P = 0.034). Another significant difference was observed between LFX-resistance and residential region (P = 0.008). As for the other factors, CLA-resistance differed from age and current smoking status, whereas LFX-resistance differed from age. However, these differences were not significant, with P values at 0.068, 0.076, and 0.060, respectively. No other associations were discovered between antibiotic resistance and patient characteristics, including gender, current drinking conditions, BMI, hypertension, diabetes mellitus, family members with *H. pylori* infection, and family histories of GC (P > 0.05; Table 3).

Furthermore, age, current smoking status, gastric symptoms, and residence region were included in the binary logistic regression analysis to assess their association with antibiotic resistance. The analysis revealed that patients with gastrointestinal symptoms were more likely to develop CLA-resistance (OR = 2.782; 95%CI: 1.076-7.194; P = 0.035). Patients living in rural areas were more likely to develop resistance to LFX than those living in urban areas (OR = 5.152; 95%CI: 1.407-18.861; P=0.013; Table 4).

Eradication rates of the susceptibility-guided and empiric treatments

A total of 102 and 100 individuals received susceptibility-guided therapies with antimicrobial susceptibility tests and empiric treatment, respectively. Demographic information of the two groups was summarized in Table 5. All of them were included in the ITT analysis. Among the 102 individuals with susceptibility-guided therapies, 13 were lost to follow-up and 4 did not retest UBT. Overall, 85 of them with follow-up UBT values were included in the PP analysis. Different bismuth-based quadruple therapies regimens were shown in Figure 2. For the empiric treatment group, we screened 100 records from the hospital database that met the aforementioned criteria. With 10 missing following-up and 6 Lacking UBT, 84 participants were finally included in the PP analysis. Therapy regimens were shown in Figure 3. For the antibiotic-susceptibility-guided treatment and empiric treatment groups, the eradication rates in the ITT analyses were 75.5% (77/102) and 59.0% (59/100), respectively. In the PP analyses, the eradication rates were 90.6% (77/85) and 70.2% (59/84), respectively (Table 6). In addition, a significantly difference was found between these two treatment strategies both in the ITT (P = 0.001) and PP analyses (P = 0.012).

DISCUSSION

CLA is the first-line antibiotic for *H. pylori* eradication[19]. When the efficacy of CLA-based regimens has been declining, LFX has been adopted as a second-line treatment option[26]. Unfortunately, *H. pylori* has exhibited growing resistances to both drugs, contributing to a global increase in treatment failure rates[27]. In recent years, the incidence of secondary resistance in China has increased due to the extensive use of antibiotics[28]. Limited studies estimated secondary

Table 1 The baseline information of *Helicobacter pylori* isolates (*n* = 132)

Factors	*n*	%
Sex (female)	71	53.8
Age (yr, ≥ 50)	85	64.4
BMI (kg/m^2, ≥ 25)	61	46.2
Current smoking	23	17.4
Current drinking	26	19.7
Hypertension (yes)	22	16.7
Diabetes (yes)	15	11.4
Gastrointestinal symptoms (yes)	83	62.9
Family members with *Helicobacter pylori* infection (yes)	41	31.1
Family histories of gastric cancer (yes)	16	12.1
Residence region (urban)	103	78.0

BMI: Body mass index.

Table 2 Antibiotic resistance patterns of *Helicobacter pylori* strains (*n* = 132)

Type of resistance	Overall (*n* = 132)	
	Number of strains	Resistance rate (%)
No resistance	13	9.9
Monoresistance	37	28.0
LFX	10	7.6
CLA	27	20.5
Double resistance	82	62.1
CLA + LFX	82	62.1

LFX: Levofloxacin; CLA: Clarithromycin.

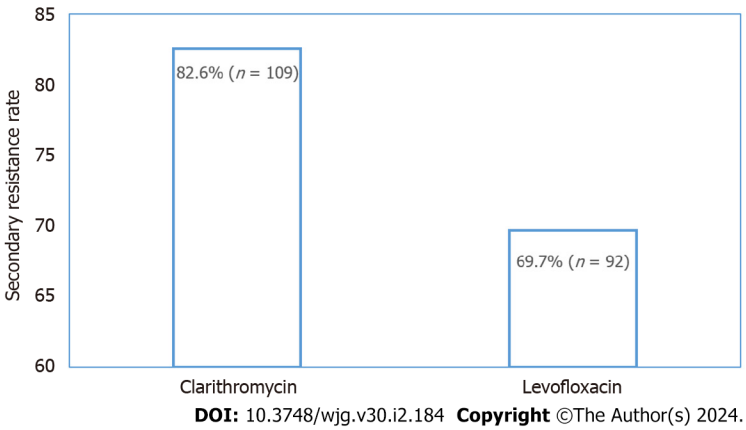

DOI: 10.3748/wjg.v30.i2.184

Figure 1 Secondary resistance rate of *Helicobacter pylori* strains to clarithromycin and levofloxacin.

Table 3 Rates of antimicrobial resistance stratified by patient characteristics

Characteristics	Clarithromycin		*P* value	Levofloxacin		*P* value
	Resistant	Sensitive		Resistant	Sensitive	
Age (yr)						
≥ 50	20	11	0.068	64	21	0.060
< 50	35	74		28	19	
Gender						
Male	48	13	0.275	43	18	0.854
Female	61	10		49	22	
Current smoking						
Yes	20	3	0.076	15	8	0.607
No	89	20		77	32	
Current drinking						
Yes	24	2	0.246	17	9	0.593
No	85	21		75	31	
BMI (kg/m^2)						
≥ 24	51	10	0.772	45	16	0.345
< 24	58	13		47	24	
Hypertension						
Yes	20	2	0.363	18	4	0.175
No	89	21		74	36	
Diabetes melllitus						
Yes	11	4	0.297	10	5	0.772
No	98	19		82	35	
Symptoms						
Yes	73	10	0.034	61	22	0.217
No	36	13		31	18	
Family members with *Helicobacter pylori* infection						
Yes	34	7	0.943	27	14	0.519
No	75	16		65	26	
Family histories of gastric cancer						
Yes	15	1	0.303	10	6	0.565
No	94	22		82	34	
Residence region						
Urban	83	20	0.255	66	37	0.008
Rural	26	3		26	3	

BMI: Body mass index.

resistance rates in Liaoning, a province in the northeast of China[29]. Owing to the easier and less invasive nature of the string-test and the more economical and simpler approaches of molecular biology methods, we detected the point mutations of 23S rRNA (A2142G, A2143G, and A2142C) and *gyrA* (260T, 261A, 261G, 271A, 271T, and 272G) by the above methods for *H. pylori* antibiotic susceptibility status determination. The results finally confirmed a pretty high rate of secondary resistance to CLA (82.6%) and LFX (69.7%) among the 132 *ureA* positive subjects (132/154; 85.7%).

The failure of the standard triple therapy eradication was mostly attributed to CLA resistance[16]. The eradication rate of first-line treatment in CLA-resistant cases was even as low as 59.4%, calculated by a meta-analysis, compared to 90.1%

Table 4 Correlations between *Helicobacter pylori* antibiotic resistance and characteristics of subjects

Variables	Clarithromycin		Levofloxacin	
	OR (95%CI)	*P* value	OR (95%CI)	*P* value
Age (yr)				
< 50	1		1	
≥ 50	2.379 (0.924-6.125)	0.072	1.972 (0.888-4.379)	0.095
Current smoking				
No	1		1	
Yes	1.151 (0.293-4.517)	0.841	0.546 (0.192-1.557)	0.258
Symptoms				
No	1		1	
Yes	2.782 (1.076-7.194)	0.035	1.851 (0.823-4.166)	0.137
Residence region				
Urban	1		1	
Rural	1.852 (0.489-7.010)	0.364	5.152 (1.407-18.861)	0.013

OR: Odds ratio; 95%CI: 95% confidence interval.

Table 5 Characteristics of the susceptibility-guided and empiric treatment groups

Characteristics	All (*n*, %)	Susceptibility-guided treatment (*n*, %)	Empiric treatment (*n*, %)	*P* value
Age (yr)				0.448
< 50	57 (33.7)	31 (54.4)	26 (45.6)	
≥ 50	112 (66.3)	54 (48.2)	58 (51.8)	
Gender				0.812
Male	78 (46.2)	40 (51.3)	38 (48.7)	
Female	91 (53.8)	45 (49.5)	46 (50.5)	

Table 6 Eradication rates of the susceptibility-guided and empiric treatment groups

	Susceptibility-guided treatment group	Empiric treatment group	*P* value
ITT analysis	75.5% (77/102)	59.0% (59/100)	0.001
PP analysis	90.6% (77/85)	70.2% (59/84)	0.012

ITT: Intention-to-treat analysis; PP: Per-protocol analysis.

in sensitive ones[30]. A secondary CLA-resistance rate of 76.9% has been recorded in China[28], but with variation across geographical regions. In this study, the secondary CLA-resistance rate was 82.6%, ranking second after Lanzhou (93.8%)[31], similar to Beijing (83.3%)[32] and Nanjing (77.8%)[33], while surpassing those in Shanghai (67.4%)[34], Nanchang (58.3%)[35], and Shenzhen (34.3%)[36]. The secondary resistance to CLA in China has demonstrated an increasing prevalence over time[32]. The significant upward trend in secondary resistance was observed after CLA-based treatments[32,33], indicating a correlation with the frequency of therapy[18]. The rate in Liaoning achieved a high level, probably attributed to the regional administration of CLA. CLA has been in frequent use in China since 1995, particularly for respiratory diseases prevalent in the colder regions, such as Liaoning and Beijing[37,38]. It provides a plausible explanation for the high rate of secondary CLA-resistance in the north of China. The Maastricht V consensus[16] suggest that if the CLA resistance rate exceeds 15% in a certain region, PPI-CLA-containing triple therapy without prior susceptibility tests should be abandoned[39]. Patients with previous CLA-containing therapy failure should not be readministered unless supported by confirmed susceptibility tests.

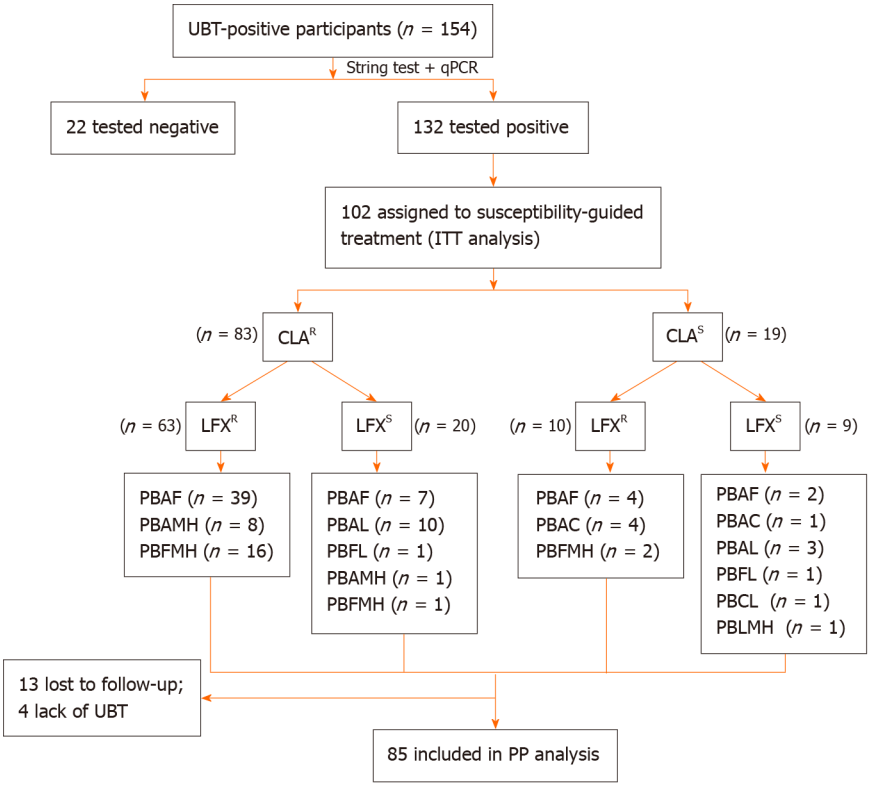

DOI: 10.3748/wjg.v30.i2.184

Figure 2 Flow diagram of antibiotic-susceptibility-guided therapy. qPCR: Quantitative polymerase chain reaction; UBT: Urea Breath Test; ITT: Intention-to-treat; PP: Per-protocol; A: Amoxicillin; B: Bismuth; C: Clarithromycin; F: Furazolidone; L: Levofloxacin; MH: Minocycline hydrochloride; P: Proton pump inhibitor; CLA^R: Clarithromycin-resistant; CLA^S: Clarithromycin-susceptible; LFX^R: Levofloxacin-resistant; LFX^S: Levofloxacin-susceptible.

The LFX-resistance rate reached up to 69.7%, similar to that in Beijing (73.3%)[32] and Lanzhou (64.6%)[31], all surpassing the average of 61.6% in China[28]. These high resistance rates might be attributed to the following reasons. LFX is widely used in China, with fewer restrictions than in western countries, is more frequently used for urogenital diseases and respiratory infection, and is widely used as a non-prescription drug, even in animal aquaculture and husbandry[40]. According to consensus recommendations, regimens containing LFX could be used as rescue treatments in regions with high CLA-resistance[16]. We observed such a high resistance rate to LFX that cautions should be taken when prescribing it in clinical settings. However, in Beijing, despite the high resistance rate to LFX, the final eradication rate after the LFX-based triple regimen still exceeded 80%[32]. This might demonstrate that the ultimate therapeutic effect does not depend solely on the resistance or susceptibility status *in vitro* of *H. pylori* to LFX.

In terms of resistance patterns, dual-resistant subjects accounted for the majority of the 132 participants (82; 62.1%), followed by mono-resistant subjects (28.0%). This indicated that in the studied area, the probability of eradication success might be improved if susceptibility tests have been confirmed.

Regarding the risk factors associated with antibiotic resistance in this study, binary logistic regression analyses revealed gastric symptoms as an independent risk predictor for CLA resistance. Patients with gastric symptoms, including abdominal pain, fullness, and heartburn, had a significantly higher probability of developing resistance to CLA than those without symptoms (OR = 2.782; 95%CI: 1.076-7.194; P = 0.035). Our findings were consistent with those of a trial conducted in Yangzhou, China[23]. Based on these results, we recommended that patients presenting with gastric discomfort undergo antibiotic susceptibility tests and receive precise treatments. If patients are unavailable for testing, gastric symptoms are an indication for physicians to avoid prescribing CLA-containing regimens. Additionally, rural residence was observed as an independent risk factor for LFX resistance. The LFX-resistance rate was significantly higher in rural residents than in urban residents (OR = 5.152; 95%CI: 1.407-18.861; P = 0.013). This might be explained by the casual and frequent use of LFX and the limited knowledge of *H. pylori* in rural areas. Thus, the administration of LFX to rural residents should be considered with caution. Physicians should preach to the public, especially rural residents, about preventing the misuse of antibiotics.

Among the risk factors investigated in the present study, age and current smoking status failed to exhibit significantly associations with CLA or LFX resistance. P values for age and CLA resistance, smoking and CLA resistance, and age and LFX resistance showed 0.068, 0.076, and 0.060, respectively, which were near critical values. Some articles reached the conclusion that age was an independent risk factor for antibiotic resistance[31,34,41]. In our study, the LFX resistance rate was higher in the age group above 50 (64/82), suggesting a potential age-related trend. However, in the CLA-resistant population, no age-related trends were observed, presumably associated with other variables, such as the method of classifying age groups. As for the association between smoking and CLA-resistance, it remained unclear and required further investigations.

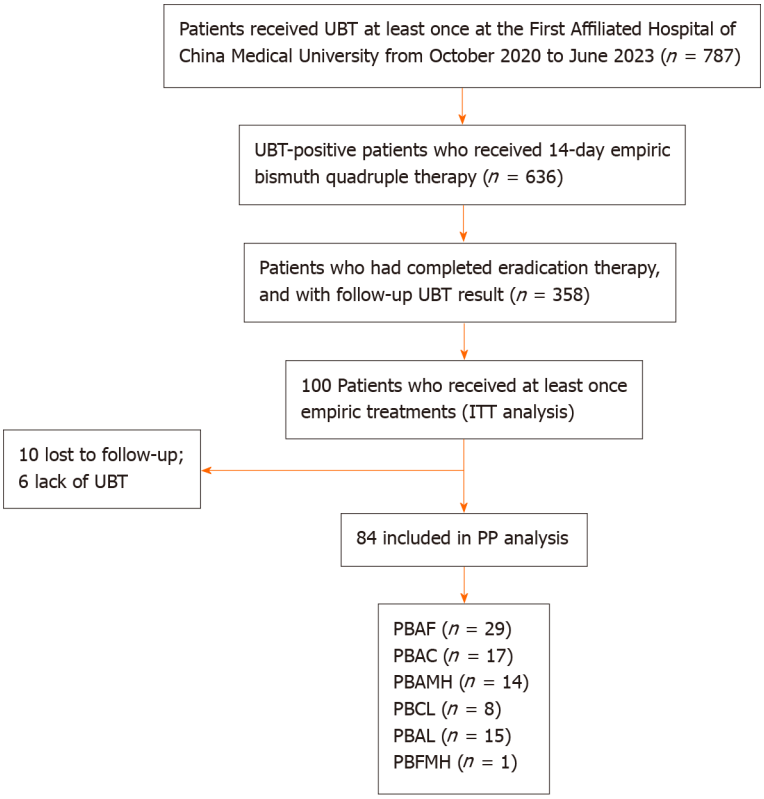

DOI: 10.3748/wjg.v30.i2.184

Figure 3 Empiric eradication treatment regimens of *Helicobacter pylori* infection. UBT: Urea Breath Test; ITT: Intention-to-treat; PP: Per-protocol; A: Amoxicillin; B: Bismuth; C: Clarithromycin; F: Furazolidone; L: Levofloxacin; MH: Minocycline hydrochloride; P: Proton pump inhibitor.

From the perspective of treatment efficacy, our study achieved acceptable eradication rates (90.6% by ITT and 75.5% by PP), similar to the results of other studies based on susceptibility-guided treatments[42,43]. These outcomes were significantly higher than those in the empiric treatment group (70.2% by ITT and 59.0% by PP) (P = 0.001 by ITT and P = 0.012 by PP). Achieving such a satisfactory result demonstrated that it is feasible for patients with previous eradication failures to perform antibiotic susceptibility tests based on qPCR by string-test.

The present study has limitations. Firstly, the analysis and derivation of antibiotic resistance data were based on data from a single hospital in Liaoning Province. A degree of bias might exist, although participants attending this large tertiary hospital come from across the province. Furthermore, certain risk factors approached critical values without reaching significance. Future studies should include larger sample sizes. In the future, we aim to conduct multicenter studies across various regions of the province to obtain a more comprehensive profile of antibiotic resistance in Liaoning. We will also endeavor to expand our sample size to provide more specific population characteristics. Nonetheless, as one of the few articles demonstrating secondary resistance in the northeast of China, this study still offered valuable insights into the possibility of eradication success in patients who had failed previous treatments once or more times.

CONCLUSION

Secondary resistance rates to CLA and LFX in Liaoning were high, both exceeding the average resistance rates in China. Patients with gastric symptoms and residing in rural areas were at higher risk of developing resistance to CLA and LFX, respectively. For patients who have failed previous eradications, antibiotic-guided treatments based on susceptibility results were more effective than empiric treatments. Therefore, it is crucial for clinicians to provide a regional treatment regimen based on regional antibiotic resistance patterns, combined with the patients' previous antibiotic exposure, the presence of gastric symptoms, and their region of residence.

ARTICLE HIGHLIGHTS

Research background

Decreased success eradication rates of *Helicobacter pylori (H. pylori)* have received much attention in recent years, mainly due to the increasing resistance to antibiotics. Hence, the rates and patterns of resistance of *H. pylori* to antibiotics need to be explored.

Research motivation
Susceptibility-guided therapy based on antibiotic susceptibility test improved *H. pylori* eradication rates. We evaluated the antibiotic resistance rate of *H. pylori*, performed precision treatment therapies, and compared the efficacy with empiric treatment therapies. It provided a reference for eradication therapy in regions in the northeast of China.

Research objectives
To investigate secondary resistance rates, explore risk factors for antibiotic resistance, and assess the efficacy of susceptibility-guided therapy.

Research methods
We observed antibiotic resistance rates of *H. pylori* and performed a single-center, clinical trial with the susceptibility-guided eradication regimen.

Research results
Clarithromycin (CLA) and levofloxacin (LFX) resistance rates were 82.6% and 69.7%, respectively. Gastric symptoms and rural residence were independent risk factors for secondary resistance to CLA and LFX, respectively. The overall susceptibility-guided eradication rates calculated using intention-to-treat and per-protocol analyses were 90.6% and 75.5%, respectively, both higher than rates with empiric treatment therapies.

Research conclusions
H. pylori presented high secondary resistance rates to CLA and LFX. For patients with previous treatment failures, treatments guided by antibiotic susceptibility tests showed good eradication efficacy.

Research perspectives
Large-scale, multi-center observed researches in various regions of the province are needed to obtain a more comprehensive profile of antibiotic resistance in Liaoning. It will be necessary to compare the safety, medication adherence and cost-effectiveness of the susceptibility-guided eradication regimen with the empiric eradication regimen in the future.

ACKNOWLEDGEMENTS

The authors are grateful to Professor Zhou BS for his help in the statistical analysis of this paper.

FOOTNOTES

Author contributions: Li YL conceived the study and carried out the experiments; Wang YM drafted the manuscript and completed data analysis; Chen MY suggested amendments to the manuscript; Chen J and Zhang XH provided assistance with data analysis; Feng Y and Han YX contributed to data collection; all authors approved the final version of the article.

Institutional review board statement: The study was reviewed and approved by the the Human Ethics Review Committee of the First Affiliated Hospital of China Medical University (Approval No. 2021325).

Informed consent statement: All study participants provided informed written consent prior to study.

Conflict-of-interest statement: The authors declare that they have no conflict of interest.

Data sharing statement: The data that support the findings of this study are available from the corresponding author upon reasonable request.

STROBE statement: The authors have read the STROBE Statement—checklist of items, and the manuscript was prepared and revised according to the STROBE Statement—checklist of items.

Country/Territory of origin: China

ORCID number: Yan-Meng Wang 0000-0002-9811-9098; Mo-Ye Chen 0000-0002-8192-4306; Xin-He Zhang 0000-0002-8773-2647; Yi-Ling Li 0000-0003-3209-8105.

S-Editor: Lin C
L-Editor: A

P-Editor: Yu HG

REFERENCES

1 **Hooi JKY**, Lai WY, Ng WK, Suen MMY, Underwood FE, Tanyingoh D, Malfertheiner P, Graham DY, Wong VWS, Wu JCY, Chan FKL, Sung JJY, Kaplan GG, Ng SC. Global Prevalence of Helicobacter pylori Infection: Systematic Review and Meta-Analysis. *Gastroenterology* 2017; **153**: 420-429 [PMID: 28456631 DOI: 10.1053/j.gastro.2017.04.022]

2 **Dogan A**, Ekinci O, Ebinc S. Effect of Helicobacter pylori infection on the first-line treatment outcomes in patients with immune thrombocytopenic purpura. *Eur Rev Med Pharmacol Sci* 2022; **26**: 3995-4000 [PMID: 35731071 DOI: 10.26355/eurrev_202206_28970]

3 **Mavilia-Scranton MG**, Wu GY, Dharan M. Impact of Helicobacter pylori Infection on the Pathogenesis and Management of Nonalcoholic Fatty Liver Disease. *J Clin Transl Hepatol* 2023; **11**: 670-674 [PMID: 36969902 DOI: 10.14218/JCTH.2022.00362]

4 **Xie J**, Cools L, Van Imschoot G, Van Wonterghem E, Pauwels MJ, Vlaeminck I, De Witte C, El Andaloussi S, Wierda K, De Groef L, Haesebrouck F, Van Hoecke L, Vandenbroucke RE. Helicobacter pylori-derived outer membrane vesicles contribute to Alzheimer's disease pathogenesis *via* C3-C3aR signalling. *J Extracell Vesicles* 2023; **12**: e12306 [PMID: 36792546 DOI: 10.1002/jev2.12306]

5 **Sahin Y**, Gubur O, Tekingunduz E. Relationship between the severity of Helicobacter pylori infection and neutrophil and lymphocyte ratio and mean platelet volume in children. *Arch Argent Pediatr* 2020; **118**: e241-e245 [PMID: 32470257 DOI: 10.5546/aap.2020.eng.e241]

6 **Guclu M**, Faruq Agan A. Association of Severity of Helicobacter pylori Infection with Peripheral Blood Neutrophil to Lymphocyte Ratio and Mean Platelet Volume. *Euroasian J Hepatogastroenterol* 2017; **7**: 11-16 [PMID: 29201765 DOI: 10.5005/jp-journals-10018-1204]

7 **Díaz P**, Valenzuela Valderrama M, Bravo J, Quest AFG. Helicobacter pylori and Gastric Cancer: Adaptive Cellular Mechanisms Involved in Disease Progression. *Front Microbiol* 2018; **9**: 5 [PMID: 29403459 DOI: 10.3389/fmicb.2018.00005]

8 **Kumar S**, Metz DC, Ellenberg S, Kaplan DE, Goldberg DS. Risk Factors and Incidence of Gastric Cancer After Detection of Helicobacter pylori Infection: A Large Cohort Study. *Gastroenterology* 2020; **158**: 527-536.e7 [PMID: 31654635 DOI: 10.1053/j.gastro.2019.10.019]

9 **Yan L**, Chen Y, Chen F, Tao T, Hu Z, Wang J, You J, Wong BCY, Chen J, Ye W. Effect of Helicobacter pylori Eradication on Gastric Cancer Prevention: Updated Report From a Randomized Controlled Trial With 26.5 Years of Follow-up. *Gastroenterology* 2022; **163**: 154-162.e3 [PMID: 35364066 DOI: 10.1053/j.gastro.2022.03.039]

10 **Chiang TH**, Chang WJ, Chen SL, Yen AM, Fann JC, Chiu SY, Chen YR, Chuang SL, Shieh CF, Liu CY, Chiu HM, Chiang H, Shun CT, Lin MW, Wu MS, Lin JT, Chan CC, Graham DY, Chen HH, Lee YC. Mass eradication of Helicobacter pylori to reduce gastric cancer incidence and mortality: a long-term cohort study on Matsu Islands. *Gut* 2021; **70**: 243-250 [PMID: 32792335 DOI: 10.1136/gutjnl-2020-322200]

11 **Ford AC**, Yuan Y, Moayyedi P. Helicobacter pylori eradication therapy to prevent gastric cancer: systematic review and meta-analysis. *Gut* 2020; **69**: 2113-2121 [PMID: 32205420 DOI: 10.1136/gutjnl-2020-320839]

12 **Malfertheiner P**, Megraud F, O'Morain CA, Atherton J, Axon AT, Bazzoli F, Gensini GF, Gisbert JP, Graham DY, Rokkas T, El-Omar EM, Kuipers EJ; European Helicobacter Study Group. Management of Helicobacter pylori infection--the Maastricht IV/ Florence Consensus Report. *Gut* 2012; **61**: 646-664 [PMID: 22491499 DOI: 10.1136/gutjnl-2012-302084]

13 **Graham DY**. Transitioning of Helicobacter pylori Therapy from Trial and Error to Antimicrobial Stewardship. *Antibiotics (Basel)* 2020; **9** [PMID: 33023041 DOI: 10.3390/antibiotics9100671]

14 **Xie Y**, Song C, Cheng H, Xu C, Zhang Z, Wang J, Huo L, Du Q, Xu J, Chen Y, Zhang X, Zhang G, Yang G, Zuo X, Guo T, Lu Y, Wang F, Wang X, Zhuang K, Chen S, Liu W, Lu N; Chinese Society of Gastroenterology, Chinese Study Group on Helicobacter pylori and Peptic Ulcer. Long-term follow-up of Helicobacter pylori reinfection and its risk factors after initial eradication: a large-scale multicentre, prospective open cohort, observational study. *Emerg Microbes Infect* 2020; **9**: 548-557 [PMID: 32160805 DOI: 10.1080/22221751.2020.1737579]

15 **Kim BJ**, Kim HS, Song HJ, Chung IK, Kim GH, Kim BW, Shim KN, Jeon SW, Jung YJ, Yang CH, Kim JH, Kim TH, Kim SG, Shin WG, Kim SM, Han SW, Lee JH, Kim KH, Park SK, Park BJ, Lee J, Kim JG; Korean College of Helicobacter and Upper Gastrointestinal Research. Online Registry for Nationwide Database of Current Trend of Helicobacter pylori Eradication in Korea: Interim Analysis. *J Korean Med Sci* 2016; **31**: 1246-1253 [PMID: 27478335 DOI: 10.3346/jkms.2016.31.8.1246]

16 **Malfertheiner P**, Megraud F, O'Morain CA, Gisbert JP, Kuipers EJ, Axon AT, Bazzoli F, Gasbarrini A, Atherton J, Graham DY, Hunt R, Moayyedi P, Rokkas T, Rugge M, Selgrad M, Suerbaum S, Sugano K, El-Omar EM; European Helicobacter and Microbiota Study Group and Consensus panel. Management of Helicobacter pylori infection-the Maastricht V/Florence Consensus Report. *Gut* 2017; **66**: 6-30 [PMID: 27707777 DOI: 10.1136/gutjnl-2016-312288]

17 **Graham DY**, Moss SF. Antimicrobial Susceptibility Testing for Helicobacter pylori Is Now Widely Available: When, How, Why. *Am J Gastroenterol* 2022; **117**: 524-528 [PMID: 35081545 DOI: 10.14309/ajg.0000000000001659]

18 **Jiang Z**, Qian X, Wang Z, Dong Y, Pan Y, Zhang Z, Wang S. Antibiotic resistance of Helicobacter pylori isolated from patients in Nanjing, China: A cross-section study from 2018 to 2021. *Front Cell Infect Microbiol* 2022; **12**: 970630 [PMID: 36159644 DOI: 10.3389/fcimb.2022.970630]

19 **Liu WZ**, Xie Y, Lu H, Cheng H, Zeng ZR, Zhou LY, Chen Y, Wang JB, Du YQ, Lu NH; Chinese Society of Gastroenterology, Chinese Study Group on Helicobacter pylori and Peptic Ulcer. Fifth Chinese National Consensus Report on the management of Helicobacter pylori infection. *Helicobacter* 2018; **23**: e12475 [PMID: 29512258 DOI: 10.1111/hel.12475]

20 **Li H**, Shen Y, Song X, Tang X, Hu R, Marshall BJ, Tang H, Benghezal M. Need for standardization and harmonization of Helicobacter pylori antimicrobial susceptibility testing. *Helicobacter* 2022; **27**: e12873 [PMID: 35151236 DOI: 10.1111/hel.12873]

21 **Han X**, Yu X, Gao X, Wang X, Tay CY, Wei X, Lai B, Marshall BJ, Zhang X, Chua EG. Quantitative PCR of string-test collected gastric material: A feasible approach to detect Helicobacter pylori and its resistance against clarithromycin and levofloxacin for susceptibility-guided therapy. *Helicobacter* 2023; **28**: e12985 [PMID: 37066609 DOI: 10.1111/hel.12985]

22 **Wang YH**, Li Z, Wang L, Zhu-Ge LY, Zhao RL, Wu S, Wang Y, An Y, Xie Y. A systematic review and meta-analysis of genotypic methods for detecting antibiotic resistance in Helicobacter pylori. *Helicobacter* 2018; **23**: e12467 [PMID: 29405526 DOI: 10.1111/hel.12467]

23 **Zhang Y**, Feng X, Bian L, Zhang Y, Li Q, Xu Y, She Q, Yan C, Lu G, Wu J, Xiao W, Ding Y, Deng B. Antibiotic Resistance of Helicobacter pylori and Related Risk Factors in Yangzhou, China: A Cross-Sectional Study. *J Clin Med* 2023; **12** [PMID: 36769465 DOI: 10.3390/jcm12030816]

24 **Huang JG**, Lim SYS, Aw MM, Quak SH. Antibiotic resistance patterns and therapeutic outcomes of pediatric Helicobacter pylori infection in

a high-migrant Singaporean cohort. *Helicobacter* 2022; **27**: e12868 [PMID: 34958710 DOI: 10.1111/hel.12868]

25 **Kwon YM**, Kim SJ, Lee JG, Lee SP. Effects of prior antibiotic use on clarithromycin resistance in Helicobacter pylori. *Helicobacter* 2023; **28**: e12974 [PMID: 36975018 DOI: 10.1111/hel.12974]

26 **Fallone CA**, Moss SF, Malfertheiner P. Reconciliation of Recent Helicobacter pylori Treatment Guidelines in a Time of Increasing Resistance to Antibiotics. *Gastroenterology* 2019; **157**: 44-53 [PMID: 30998990 DOI: 10.1053/j.gastro.2019.04.011]

27 **Tshibangu-Kabamba E**, Yamaoka Y. Helicobacter pylori infection and antibiotic resistance - from biology to clinical implications. *Nat Rev Gastroenterol Hepatol* 2021; **18**: 613-629 [PMID: 34002081 DOI: 10.1038/s41575-021-00449-x]

28 **Zhong Z**, Zhang Z, Wang J, Hu Y, Mi Y, He B, Zhang Y, Zhang X, Xia X, Huang H, Lai Y, Lin M, Su C, Wu Z, Lu L, Zhang B, Huang S, Zhong C, Zeng X, Peng Y, Chen G, Zhang H, Zhou G, Liu S, Yang C, Yan L, Chen A, Zhang G, Xu P, Wang S, Zheng P, Xu S, Gao H. A retrospective study of the antibiotic-resistant phenotypes and genotypes of Helicobacter pylori strains in China. *Am J Cancer Res* 2021; **11**: 5027-5037 [PMID: 34765309]

29 **Wang Y**, Li Y, Gong Y, Dong Y, Sun J, Chen M. Antibiotic resistance characteristics and risk factors analysis of Helicobacter pylori strains isolated from patients in Liaoning Province, an area in North China. *PeerJ* 2023; **11**: e15268 [PMID: 37214095 DOI: 10.7717/peerj.15268]

30 **Zou Y**, Qian X, Liu X, Song Y, Song C, Wu S, An Y, Yuan R, Wang Y, Xie Y. The effect of antibiotic resistance on Helicobacter pylori eradication efficacy: A systematic review and meta-analysis. *Helicobacter* 2020; **25**: e12714 [PMID: 32533599 DOI: 10.1111/hel.12714]

31 **Xu H**, Yun J, Li R, Ma X, Gou L, Che T, Zhang D. Antibiotics Resistance Prevalence of Helicobacter pylori Strains in Northwest China. *Infect Drug Resist* 2022; **15**: 5519-5528 [PMID: 36172620 DOI: 10.2147/IDR.S383444]

32 **Gao W**, Cheng H, Hu F, Li J, Wang L, Yang G, Xu L, Zheng X. The evolution of Helicobacter pylori antibiotics resistance over 10 years in Beijing, China. *Helicobacter* 2010; **15**: 460-466 [PMID: 21083752 DOI: 10.1111/j.1523-5378.2010.00788.x]

33 **Jiang ZD**, He BS, Zhang ZY, Wang SK, Ran D, Wang ZB. Analysis of the Primary and Post-Treatment Antibiotic Resistance of Helicobacter pylori in the Nanjing Area. *Curr Pharm Biotechnol* 2021; **22**: 682-685 [PMID: 32811409 DOI: 10.2174/1389201021666200722162613]

34 **Wang J**, Xie X, Zhong Z, Yuan H, Xu P, Gao H, Lai Y. Prevalence of antibiotic resistance of Helicobacter pylori isolates in Shanghai, China. *Am J Transl Res* 2022; **14**: 7831-7841 [PMID: 36505283]

35 **Liu DS**, Wang YH, Zhu ZH, Zhang SH, Zhu X, Wan JH, Lu NH, Xie Y. Characteristics of Helicobacter pylori antibiotic resistance: data from four different populations. *Antimicrob Resist Infect Control* 2019; **8**: 192 [PMID: 31798838 DOI: 10.1186/s13756-019-0632-1]

36 **Lyu T**, Cheung KS, Ni L, Guo J, Mu P, Li Y, Yang Q, Yu X, Lyu Z, Wu J, Guo H, Leung WK, Seto WK. High prevalence and risk factors of multiple antibiotic resistance in patients who fail first-line Helicobacter pylori therapy in southern China: a municipality-wide, multicentre, prospective cohort study. *J Antimicrob Chemother* 2020; **75**: 3391-3394 [PMID: 32785699 DOI: 10.1093/jac/dkaa315]

37 **Liu X**, Shen X, Chang H, Huang G, Fu Z, Zheng Y, Wang L, Li C, Liu L, Shen Y, Yang Y. High macrolide resistance in Streptococcus pyogenes strains isolated from children with pharyngitis in China. *Pediatr Pulmonol* 2009; **44**: 436-441 [PMID: 19360846 DOI: 10.1002/ppul.20976]

38 **Megraud F**, Bruyndonckx R, Coenen S, Wittkop L, Huang TD, Hoebeke M, Bénéjat L, Lehours P, Goossens H, Glupczynski Y; European Helicobacter pylori Antimicrobial Susceptibility Testing Working Group. Helicobacter pylori resistance to antibiotics in Europe in 2018 and its relationship to antibiotic consumption in the community. *Gut* 2021; **70**: 1815-1822 [PMID: 33837118 DOI: 10.1136/gutjnl-2021-324032]

39 **Graham DY**, Liou JM. Primer for Development of Guidelines for Helicobacter pylori Therapy Using Antimicrobial Stewardship. *Clin Gastroenterol Hepatol* 2022; **20**: 973-983.e1 [PMID: 33775895 DOI: 10.1016/j.cgh.2021.03.026]

40 **Chen J**, Li P, Huang Y, Guo Y, Ding Z, Lu H. Primary Antibiotic Resistance of Helicobacter pylori in Different Regions of China: A Systematic Review and Meta-Analysis. *Pathogens* 2022; **11** [PMID: 35890031 DOI: 10.3390/pathogens11070786]

41 **Dang NQH**, Ha TMT, Nguyen ST, Le NDK, Nguyen TMT, Nguyen TH, Pham TTH, Tran VH. High rates of clarithromycin and levofloxacin resistance of Helicobacter pylori in patients with chronic gastritis in the south east area of Vietnam. *J Glob Antimicrob Resist* 2020; **22**: 620-624 [PMID: 32590188 DOI: 10.1016/j.jgar.2020.06.007]

42 **Gao C**, Fan YH. Effect and Safety of Helicobacter pylori Eradication Treatment Based on Molecular Pathologic Antibiotic Resistance in Chinese Elderly People. *Infect Drug Resist* 2022; **15**: 3277-3286 [PMID: 35769552 DOI: 10.2147/IDR.S371113]

43 **Gao C**, Du SY, Fang L, Fan YH, Song AP, Chen H. Eradication Treatment of Helicobacter pylori Infection Based on Molecular Pathologic Antibiotic Resistance. *Infect Drug Resist* 2020; **13**: 69-79 [PMID: 32021321 DOI: 10.2147/IDR.S232169]

World Journal of Gastroenterology

Submit a Manuscript: https://www.f6publishing.com

World J Gastroenterol 2024 January 14; 30(2): 196-198

DOI: 10.3748/wjg.v30.i2.196

ISSN 1007-9327 (print) ISSN 2219-2840 (online)

LETTER TO THE EDITOR

Gastric cancer immunotherapy: A scientometric and clinical trial review

Qian-Cheng Du, Xin-Yu Wang, Hua Yu

Specialty type: Gastroenterology and hepatology

Provenance and peer review: Unsolicited article; Externally peer reviewed.

Peer-review model: Single blind

Peer-review report's scientific quality classification

Grade A (Excellent): 0
Grade B (Very good): 0
Grade C (Good): C
Grade D (Fair): 0
Grade E (Poor): 0

P-Reviewer: Kotelevets SM, Russia

Received: November 11, 2023
Peer-review started: November 11, 2023
First decision: December 20, 2023
Revised: December 21, 2023
Accepted: December 28, 2023
Article in press: December 28, 2023
Published online: January 14, 2024

Qian-Cheng Du, Thoracic Surgery, Shanghai Xuhui Central Hospital, Shanghai 200031, China

Xin-Yu Wang, Thyroid, Breast and Vascular Surgery, Shanghai Fourth People's Hospital Affiliated to Tongji University School of Medicine, Shanghai 200434, China

Hua Yu, Department of General Surgery, Shanghai Fourth People's Hospital Affiliated to Tongji University School of Medicine, Shanghai 200434, China

Corresponding author: Hua Yu, MM, Associate Chief Physician, Department of General Surgery, Shanghai Fourth People's Hospital Affiliated to Tongji University School of Medicine, No. 1279 Sanmen Road, Hongkou District, Shanghai 200434, China.
luckyyuhua@163.com

Abstract

This letter is intended to arouse your interest in a recent review of comprehensive scientometrics and clinical trials on immunotherapy for gastric cancer (GC). Our study reviews recent advances in immunotherapy in the field of GC and highlights its new prospects as a treatment for GC. Our research reveals China's leadership in this field, as well as new therapeutic strategies such as immune checkpoint inhibitors, cellular immunotherapy, and vaccines. The combined findings highlight the potential of immunotherapy to improve survival and quality of life in patients with stomach cancer. We believe that this study will provide important guidance for the future direction of the GC treatment field.

Key Words: Gastric cancer; Immunotherapy; Bibliometrics; Comment; Therapeutic strategies

Core Tip: The article is a comprehensive review of immunotherapy for gastric cancer (GC), emphasizing the leadership of immunotherapy in the field of GC. The paper focuses on new strategies such as immune checkpoint inhibitors, cellular immunotherapy, and vaccines, highlighting their potential in improving the survival and quality of life of GC patients. This study provides crucial guidance for the future development direction of GC treatment and valuable insights into emerging therapeutic approaches.

Citation: Du QC, Wang XY, Yu H. Gastric cancer immunotherapy: A scientometric and clinical trial review. *World J Gastroenterol* 2024; 30(2): 196-198
URL: https://www.wjgnet.com/1007-9327/full/v30/i2/196.htm
DOI: https://dx.doi.org/10.3748/wjg.v30.i2.196

TO THE EDITOR

I am writing to express my concern regarding the recently published paper titled "Advances and key focus areas in gastric cancer immunotherapy: A comprehensive scientometric and clinical trial review (1999-2023)" by Li *et al*[1] in the *World Journal of Gastroenterology*. The authors have done an exceptional job of providing a thorough analysis of the current status and emerging trends in the field of gastric cancer (GC) immunotherapy. Their findings offer valuable insights into significant advancements within this domain, underscoring its potential to revolutionize treatment approaches for patients with GC.

As a clinician and researcher in the field of gastroenterology, I am convinced that immunotherapy has great potential for GC patients. As the sixth most common cancer worldwide and the third leading cause of cancer-related death, GC highlights the urgent need for innovative treatments[2]. Current treatment modalities, mainly surgery and chemotherapy, have limitations, and the prognosis for advanced GC remains worrisome. The authors' bibliometric analysis reflects the rapid growth of GC immunotherapy research in recent years and the increasing dominance of China in the number of published articles, which indicates the global interest and commitment to advancing this field. The identification of keywords, such as "tumor microenvironment", "immunotherapy", "dendritic cell therapy", and "microsatellite instability", highlights the evolving focus areas of GC immunotherapy research.

In addition, I would like to emphasize that international cooperation and communication in this area is essential to accelerate progress in GC immunotherapy. As mentioned in the article, multiple countries and institutions worldwide have contributed to research in the field of GC immunotherapy[3]. Such collaboration helps to share best practices, drive innovation and advance global health. The good news is that combinations of immune checkpoint inhibitors (ICIs), chemotherapy, targeted therapies, and other immunotherapies are becoming major research directions in the future. The authors rightly point out that these new treatment options, including ICIs and chimeric antigen receptor T cells, hold promise for GC patients, with the potential to improve survival and quality of life.

In terms of looking to the future, I think as we develop a deeper understanding of the mechanisms of immunotherapy, we can expect to further increase the level of individualization of treatment. Based on the molecular characteristics of the tumor and individual differences in the immune system, we can predict how a patient will respond to a specific treatment and optimize the outcome by adjusting the treatment regimen. In addition, exploring new immunotherapy targets and strategies, such as tumor-associated antigens and immune cell therapies, will open new avenues for future GC therapies.

FOOTNOTES

Author contributions: Du QC and Wang XY contributed equally in analysis of the data and writing of the manuscript; Yu H designed the article and corrected the paper; and all authors have read and approved the final manuscript.

Supported by the Discipline Promotion Program of Shanghai Fourth People's Hospital, No. SY-XKZT-2020-1021.

Conflict-of-interest statement: The authors declare no conflicts of interest.

Country/Territory of origin: China

ORCID number: Qian-Cheng Du 0000-0002-0154-2210; Xin-Yu Wang 0000-0001-8488-7910; Hua Yu 0000-0002-1599-6192.

S-Editor: Chen YL
L-Editor: A
P-Editor: Yu HG

REFERENCES

1 **Li YN**, Xie B, Zhang Y, He MH, Xing Y, Mu DM, Wang H, Guo R. Advances and key focus areas in gastric cancer immunotherapy: A comprehensive scientometric and clinical trial review (1999-2023). *World J Gastroenterol* 2023; **29**: 5593-5617 [PMID: 37970478 DOI: 10.3748/wjg.v29.i40.5593]

2 **Sung H**, Ferlay J, Siegel RL, Laversanne M, Soerjomataram I, Jemal A, Bray F. Global Cancer Statistics 2020: GLOBOCAN Estimates of Incidence and Mortality Worldwide for 36 Cancers in 185 Countries. *CA Cancer J Clin* 2021; **71**: 209-249 [PMID: 33538338 DOI: 10.3322/caac.21660]

3 **Högner A**, Moehler M. Immunotherapy in Gastric Cancer. *Curr Oncol* 2022; **29**: 1559-1574 [PMID: 35323331 DOI: 10.3390/curroncol29030131]

Published by **Baishideng Publishing Group Inc**
7041 Koll Center Parkway, Suite 160, Pleasanton, CA 94566, USA
Telephone: +1-925-3991568
E-mail: office@baishideng.com
Help Desk: https://www.f6publishing.com/helpdesk
https://www.wjgnet.com